GAS VISCOSITY AT HIGH PRESSURE AND HIGH TEMPERATURE

A Dissertation

by

KEGANG LING

Submitted to the Office of Graduate Studies of
Texas A&M University
in partial fulfillment of the requirements for the degree of

DOCTOR OF PHILOSOPHY

December 2010

Major Subject: Petroleum Engineering

GAS VISCOSITY AT HIGH PRESSURE AND HIGH TEMPERATURE

A Dissertation

by

KEGANG LING

Submitted to the Office of Graduate Studies of
Texas A&M University
in partial fulfillment of the requirements for the degree of

DOCTOR OF PHILOSOPHY

Approved by:

Co-Chairs of Committee,	Gioia Falcone
	Catalin Teodoriu
Committee Members,	William D. McCain Jr.
	Yuefeng Sun
Head of Department,	Stephen A. Holditch

December 2010

Major Subject: Petroleum Engineering

ABSTRACT

Gas Viscosity at High Pressure and High Temperature. (December 2010)
Kegang Ling, B. S., University of Petroleum, China;
M. S., University of Louisiana at Lafayette
Chair of Advisory Committee: Dr. Gioia Falcone

Gas viscosity is one of the gas properties that is vital to petroleum engineering. Its role in the oil and gas production and transportation is indicated by its contribution in the resistance to the flow of a fluid both in porous media and pipes. Although viscosity of some pure components such as methane, ethane, propane, butane, nitrogen, carbon dioxide and binary mixtures of these components at low-intermediate pressure and temperature had been studied intensively and been understood thoroughly, very few investigations were performed on viscosity of naturally occurring gases, especially gas condensates at low-intermediate pressure and temperature, even fewer lab data were published. No gas viscosity data at high pressures and high temperatures (HPHT) is available. Therefore this gap in the oil industry still needs to be filled.

Gas viscosity at HPHT becomes crucial to modern oil industry as exploration and production move to deep formation or deep water where HPHT is not uncommon. Therefore, any hydrocarbon encountered there is more gas than oil due to the chemical reaction causing oil to transfer to gas as temperature increases. We need gas viscosity to optimize production rate for production system, estimate reserves, model gas injection, design drilling fluid, and monitor gas movement in well control. Current gas viscosity correlations are derived using measured data at low-moderate pressures and temperatures, and then extrapolated to HPHT. No measured gas viscosities at HPHT are

available so far. The validities of these correlations for gas viscosity at HPHT are doubted due to lack of experimental data.

In this study, four types of viscometers are evaluated and their advantages and disadvantages are listed. The falling body viscometer is used to measure gas viscosity at a pressure range of 3000 to 25000 psi and a temperature range of 100 to 415 ^{o}F. Nitrogen viscosity is measured to take into account of the fact that the concentration of nonhydrocarbons increase drastically in HPHT reservoir. More nitrogen is found as we move to HPHT reservoirs. High concentration nitrogen in natural gas affects not only the heat value of natural gas, but also gas viscosity which is critical to petroleum engineering. Nitrogen is also one of common inject gases in gas injection projects, thus an accurate estimation of its viscosity is vital to analyze reservoir performance. Then methane viscosity is measured to honor that hydrocarbon in HPHT which is almost pure methane. From our experiments, we found that while the Lee-Gonzalez-Eakin correlation estimates gas viscosity at a low-moderate pressure and temperature accurately, it cannot give good match of gas viscosity at HPHT. Apparently, current correlations need to be modified to predict gas viscosity at HPHT. New correlations constructed for HPHT conditions based on our experiment data give more confidence on gas viscosity.

DEDICATION

To my family for their love and support

ACKNOWLEDGMENTS

During these four years at Texas A&M University I have tried my best to adhere to the requirements of being a qualified graduate student. I got tons of help in the process of pursuing my Ph.D. degree. I want to acknowledge these people for their generosity and kindness.

First of all, my gratitude goes to my advisors, Dr. Gioia Falcone and Dr. Catalin Teodoriu, for their veritable academic advice to me in these years, and in years to come. Their inspiration, encouragement, guardianship, and patience were essential for my research and study.

I would also like to express my sincere appreciation to my committee member, Dr. William D. McCain Jr., for his advice, knowledge, and priceless assistance during these years.

Thanks are also extended to a member of my supervising committee, Dr. Yuefeng Sun, of the Department of Geology and Geophysics, for managing time out of his busy schedule to provide valuable comments and suggestions.

Furthermore, I appreciate Dr. Catalin Teodoriu, Dr. William D. McCain Jr., and Mr. Anup Viswanathan for setting up the High Pressure High Temperature laboratory for this project, and Mr. John Maldonado, Sr. for supplying gas resources. I am grateful to the sponsors of the Crisman Petroleum Research Institute at Texas A&M University for providing funding for this project.

I wish to express my appreciation to the faculty and staff of the Department of Petroleum

Engineering at Texas A&M University. I am indebted to my colleagues because they made the whole study more enjoyable. I truly appreciate my family, without their support I would not have realized my dream.

TABLE OF CONTENTS

Page

Page

LIST OF TABLES

Page

LIST OF FIGURES

Page

Page

Page

Page

Page

Page

Page

Page

CHAPTER I

INTRODUCTION

1.1 Viscosity

Viscosity is a fundamental characteristic property of fluids. Viscosity, which is also called a viscosity coefficient, is a measure of the resistance of a fluid to deform under shear stress resulting from the flow of fluid. It is commonly perceived as "thickness", or resistance to flow. Viscosity describes a fluid's internal resistance to flow and may be thought of as a measure of fluid friction, or sometime can also be termed as a drag force.

In general, in any flow, layers move at different velocities and the fluid's viscosity arises from the shear stress between the layers that ultimately oppose any applied force. To understand the definition of viscosity, we consider two plates closely spaced apart at a distance *y*, and separated by a homogeneous substance as illustrated in Figure 1-1.

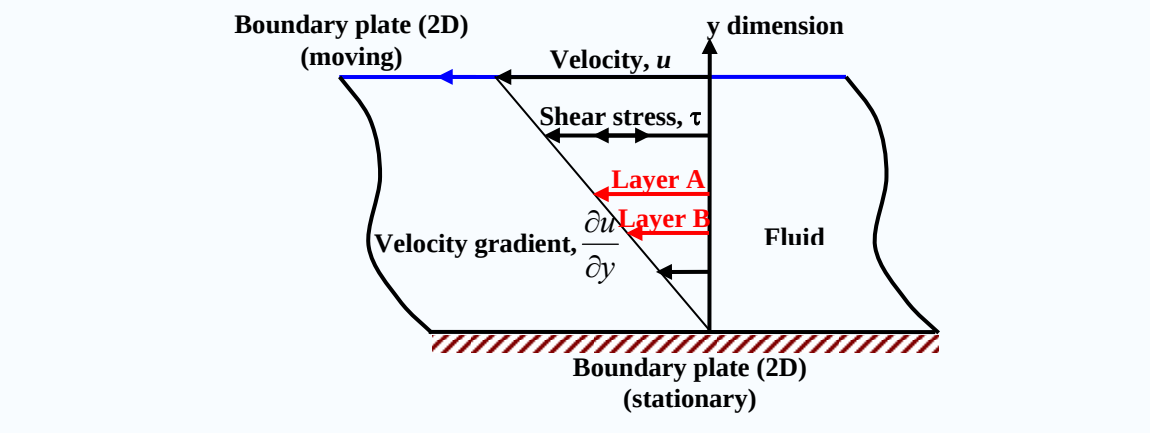

Figure 1-1. Laminar shear in fluids, after Wikipedia viscosity (2010)

Figure 1-2 is an amplification of the flow between layers *A* and *B* in Figure 1-1.

This dissertation follows the style and format of the *SPE Journal*.

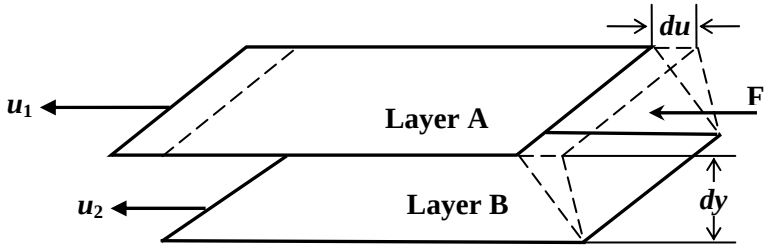

Figure 1-2. Laminar shear of a fluid film

Assuming that the plates are very large, with a large area A, such that edge effects may be ignored, and that the lower plate is fixed, let a force F be applied to the upper plate. Then dynamic viscosity is the tangential force per unit area required to slide one layer, A, against another layer, B, as shown in Figure 1-2. Employing Newton's law, if this force causes the substance between the plates to undergo shear flow, the applied force is proportional to the area and velocity of the plate and inversely proportional to the distance between the plates. Combining three relations results in the equation, $F / A = \mu(\partial u / \partial y)$, where μ is the proportionality factor called the absolute viscosity. The reciprocal of viscosity is the fluidity that is denoted as φ=1/μ.

The absolute viscosity is also known as the dynamic viscosity, and is often shortened to simply viscosity. The equation can be expressed in terms of shear stress, $\tau = F / A = \mu(\partial u / \partial y)$. The rate of shear deformation is $\partial u / \partial y$ and can be also written as a shear velocity or shear rate, γ. Hence, through this method, the relation between the shear stress and shear rate can be obtained, and viscosity, μ, is defined as the ratio of shear stress to shear rate and is expressed mathematically as follows:

$$\mu = \frac{\tau}{\gamma} = \frac{\tau}{\frac{\partial u}{\partial y}} \tag{1.1}$$

where

τ = Shear stress

γ = Shear rate

μ =Viscosity

Common units for viscosity are Poise (named after French physician, Jean Louis Poiseuille (1799 - 1869)), equivalent to dyne-sec/cm^2, and Stokes, Saybolt Universal. In case of Poise, shear stress is in dyne/cm^2 and shear rate in sec^{-1}. Because one poise represents a high viscosity, 1/100 poise, or one centipoise (cp), is common used in petroleum engineering.

In the SI System, the dynamic viscosity units are N-s/m^2, Pa-s or kg/m-s where *N* is Newton and *Pa* is Pascal, and, 1 Pa-s = 1 N-s/m^2 = 1 kg/m-s. In the metric system, the dynamic viscosity is often expressed as g/cm-s, dyne-s/cm^2 or poise (*P*) where,
1 poise = dyne-s/cm^2 = g/cm-s = 1/10 Pa-s.

In petroleum engineering, we are also concerned with the ratio of the viscous force to the inertial force, the latter characterized by the fluid density ρ. This ratio is characterized by the kinematic viscosity, defined as follows:

$$\upsilon = \frac{\mu}{\rho} \tag{1.2}$$

In the SI system, kinematic viscosity uses Stokes or Saybolt Second Universal units. The kinematic viscosity is expressed as m^2/s or Stokes, where 1 Stoke= 10^{-4} m^2/s. Similar to Poise, stokes is a large unit, and it is usually divided by 100 to give the unit called Centistokes.
1 Stoke = 100 Centistokes.
1 Centistokes = 10^{-6} m^2/s

Fluids are divided into two categories according to their flow characteristics: 1) if the viscosity of a liquid remains constant and is independent of the applied shear stress and

time, such a liquid is termed a Newtonian liquid. 2) Otherwise, it belongs to Non-Newtonian fluids. Water and most gases satisfy Newton's criterion and are known as Newtonian fluids. Non-Newtonian fluids exhibit a more complicated relationship between shear stress and velocity gradient than simple linearity (Figure 1-3).

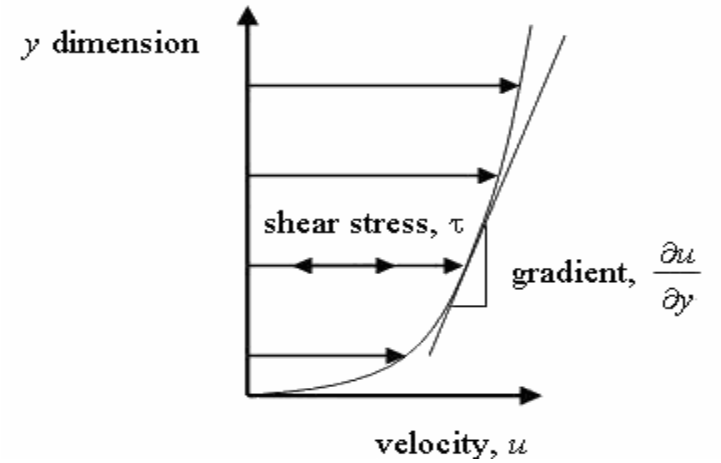

Figure 1-3. Laminar shear of for non-Newtonian fluids flow, after Wikipedia viscosity (2010)

1.2 Role of Gas Viscosity in Petroleum Engineering

The importance of gas viscosity in the oil and gas production and transportation is indicated by its contribution in the resistance to the flow of a fluid both in porous media and pipes. One of the most important things in petroleum engineer routine work is to calculate the pressure at any node in a production and/or transportation system. Since gas viscosity dictates the fluid flow from reservoir into the wellbore according to Darcy's law, and affects the friction pressure drop for fluid flow from bottomhole to the wellhead and in pipeline, we need gas viscosity to optimize the production rate for production system. Gas viscosity is also a key element that controls recovery of hydrocarbon in place or flooding sweep efficiency in gas injection. In drilling fluid design and well control gas viscosity must be known to understand the upward velocity

of gas kick. Gas viscosity is a vital factor for heat transfer in fluid. Right now as most of shallow reservoirs had been produced, increasing demand on oil and gas requires that more deep wells need to be drilled to recover tremendous reserves from deep reservoirs. As we drilled deeper and deeper we meet more high pressure and high temperature (HPHT) reservoirs. Although the hurdle pressure and temperature for HPHT always changes as petroleum exploration and production moves on, at this stage the Society of Petroleum Engineers defines high pressure as a well requiring pressure control equipment with a rated working pressure in excess of 10000 psia or where the maximum anticipated formation pore pressure gradient exceeds 0.8 psi/ft and high temperature as temperature of 150 ^{o}C (or 302 ^{o}F) and up. Most of HPHT reservoirs are lean gas reservoirs containing high methane concentration, some, for instance Puguang gas field in Sichuan, China, with trace to high nonhydrocarbon (Zhang et al., 2010) such as nitrogen, carbon dioxide, and hydrogen sulfide resulting from high temperature. Examples of HPHT reservoirs can be shown by Marsh et al. (2010), which is as follow.

Table 1-1. Examples of HPHT fields

Field	Sector	Operator	Pressure psia	Temperature ^{o}F
Elgin/Franklin	North Sea (UK)	TOTAL	15954.4	374
Shearwater	North Sea (UK)	SHELL	13053.6	356
Devenick	North Sea (UK)	BP	10080.28	305.6
Erskine	North Sea (UK)	TEXACO	13996.36	347
Rhum	North Sea (UK)	BP	12400.92	302
Victoria	North Sea (Norway)	TOTAL	11603.2	392

1.3 Methods to Get Gas Viscosity

In our research, we are interesting in gas viscosity. The mechanisms and molecular theory of gas viscosity have been reasonably well clarified by nonequlibrium statistical mechanics and the kinetic theory of gases. There are two approaches to get gas viscosity. One is direct measurement using gas samples, another is gas viscosity correlations.

Advantage of direct measurement is it gives reliable result so we can use it confidently. But it has the disadvantage of time consuming and cost expensive, and sometimes availability of measuring instrument. Gas viscosity correlations provide a simple and low cost method to predict gas viscosity if correlations are based on accurate lab data. Every precaution should be taken to obtain consistent and accurate data. Data from literatures should be verified before being employed. Inaccuracy and uncertainty in database will jeopardize the reliability of correlation.

CHAPTER II

LITERATURE REVIEW

2.1 Gas Viscosity Measuring Instrument

Instruments used to measure the viscosity of gases can be broadly classified into three categories:

1) Capillary viscometers
2) Falling (or rolling) ball viscometers
3) Vibrating viscometers

Other viscometers might combine features of two or three types of viscometers noted above, In general, during the measurement either the fluid remains stationary and an object moves through it, or the object is stationary and the fluid moves past it. The drag caused by relative motion of the fluid and a surface is a measure of the viscosity. The flow conditions must have a sufficiently small value of Reynolds number for there to be laminar flow.

Before the introduction to the three types of viscometer, knowledge in the derivation of gas viscosity equation (Poiseville's equation) will benefit our understanding of the principle of measurement. We can derive Poiseville's equation starting from the concept of viscosity. The situation we deal with is an incompressible fluid flows through a circular pipe with radius R and length L at a velocity of $u(r)$. It is noted that the velocity is not uniform but varies with the radius, r. Figure 2-1 shows the schematic of fluid flow in a pipe.

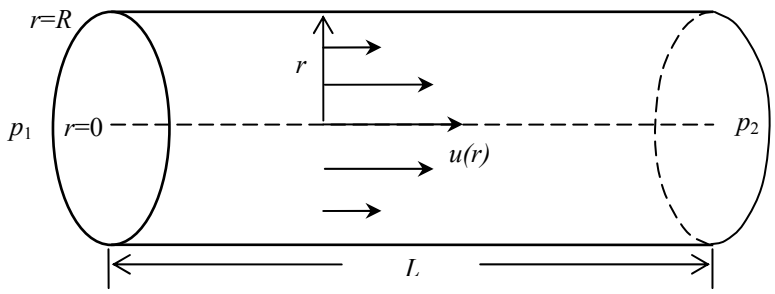

Figure 2-1. Schematic of fluid flow through a pipe

The Poiseville's equation will be valid only if the following assumptions hold:

1) Single phase incompressible fluid flows in the pipe.
2) Laminar flow is the only flow regime inside the pipe.
3) The fluid at the walls of the tube is assumed to be stationary, and the flow rate increases to a maximum at the center of the tube. No slippage happens during the flow (Figure 2-2).
4) The fluid is homogeneous.
5) Pipe is in horizontal position so that the effect of gravitational force on flow can be neglected.
6) Flow is steady-state.
7) Temperature is constant throughout the pipe.
8) Pipe is circular with constant radius, *R*.

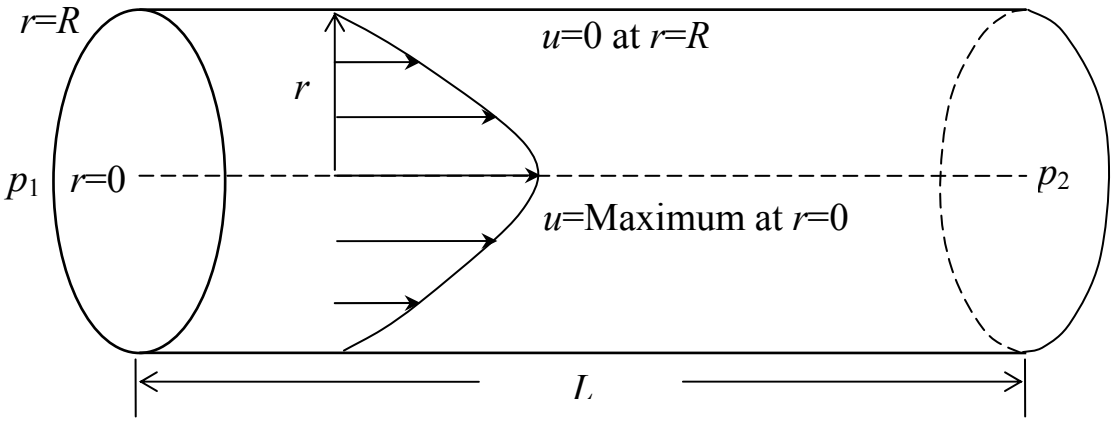

Figure 2-2. Fluid flow profile in a circular pipe

According to the definition of viscosity, $\tau = F / A = \mu(\partial u / \partial y)$, the drag forces (friction force) acting on a fluid layer at radius r as it moves ahead at a velocity of $u(r)$. The drag force F_d acting on a cylinder of fluid at radius r and length L is

$$\frac{F_d}{A} = \mu \frac{du(r)}{dr}$$

where

F_d = The drag force on the surface of layer

r = Radius of the layer, measured from center of pipe

$u(r)$ = Fluid velocity at radius of r

A = Surface area of the layer of fluid, which is equal to $2\pi rL$,

L = Length of the pipe

μ = Fluid viscosity

Substituting surface area into the definition of viscosity we have drag force

$$F_d = \mu 2\pi rL \frac{du(r)}{dr} \tag{2.1}$$

Basing on force balance, forces in the horizontal direction should be summed up to zero for steady-state flow, which can be expressed as

(Force resulting from p_1)= F_d + (Force resulting from p_2)

Expressing in pressure gives

$$p_1 \pi r^2 = F_d + p_2 \pi r^2$$

or

$$F_d = (p_1 - p_2)\pi r^2 \tag{2.2}$$

where

p_1 = Inlet pressure,

p_2 = Outlet pressure,

πr^2 = Cross-section area of the pipe.

Substituting Equation 2.1 into Equation 2.2 yields

$$\mu 2\pi r L \frac{du(r)}{dr} = (p_1 - p_2)\pi r^2 \tag{2.3}$$

Separating variables gives

$$du = -\frac{(p_1 - p_2)\pi r^2}{\mu 2\pi r L} dr = -\frac{(p_1 - p_2) r}{2\mu L} dr \tag{2.4}$$

Integrating from the pipe wall to the center and applying boundary conditions

$$u\,(\mathrm{r}) = u$$

and

$$u(r=R)=0$$

we obtain

$$\int_0^u du = -\frac{(p_1 - p_2)}{2\mu L}\int_R^r r dr = -\frac{(p_1 - p_2)}{2\mu L}\left(\frac{r^2}{2} - \frac{R^2}{2}\right) \tag{2.5}$$

Therefore the velocity of the fluid can be expressed as a function of radius, r.

$$u = \frac{(p_1 - p_2)}{4\mu L}\left(R^2 - r^2\right) \tag{2.6}$$

Using control element concept we can calculate the volumetric flow rate through the pipe q. Integrating the fluid velocity u over each element of cross-sectional area $2\pi r dr$ (Figure 2-3).

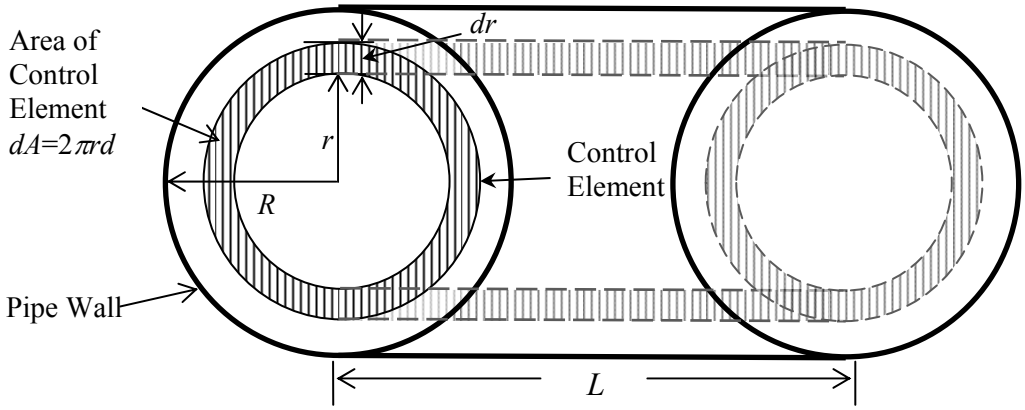

Figure 2-3. Cross section view of a circular pipe

Thus we come up with

$$q = \int_0^R \frac{(p_1 - p_2)}{4\mu L}\left(R^2 - r^2\right)2\pi r dr = \frac{\pi(p_1 - p_2)R^4}{8\mu L} \tag{2.7}$$

where

q = Volumetric flow rate,

Equation 2.7 is the famous Poiseville's equation. It should be kept in mind that Poiseville's equation is applies to incompressible fluids only. For gas, due to its high compressibility the Poiseville's equation cannot be employed directly. To derive similar equation for gas flow in the pipe we will combine real gas law and mass conservation. Now if we know the inlet pressure p_1 and average velocity $\bar{u}_1$, the pressure p and velocity $\bar{u}$ of any point at downstream can be calculated. Mass conservation indicates that mass flow rate is the same for every horizontal location in the pipe

$$\frac{dm_1}{dt} = \frac{dm}{dt} \tag{2.8}$$

where

m = Mass at downstream,

m_1 = Mass at inlet,

t = Time,

Expressing in volume and density gives

$$\frac{d(V_1\rho_1)}{dt} = \frac{d(V\rho)}{dt} \tag{2.9}$$

where

V = Volume at downstream,

V_1 = Volume at inlet,

ρ = Density at downstream,

ρ_1 = Density at inlet,

If we use the average velocity and cross section area to represent the volumetric flow rate, we have

$$\bar{u}_1 A\rho_1 = \bar{u}A\rho \tag{2.10}$$

where

$\bar{u}$ = Average velocity at downstream,

$\bar{u}_1$ = Average velocity at inlet,

A = Cross section area of pipe,

Cancelling out the cross section area yields

$$\bar{u}_1\rho_1 = \bar{u}\rho \tag{2.11}$$

Real gas law gives

$$p_1V_1 = z_1nR_{gas}T_1 \tag{2.12}$$

and

$$pV = znRT \tag{2.13}$$

where

T = Temperature at downstream,

T_1 = Temperature at inlet,

z = Compressibility at downstream,

z_1 = Compressibility at inlet,

n = Mole of gas,

R_{gas} = Gas constant,

for inlet and downstream, respectively.

Multiplying molecular weight to both sides we have

$$p_1 V_1 Mw = z_1 n R_{gas} T_1 Mw \tag{2.14}$$

and

$$pVMw = znR_{gas} TMw \tag{2.15}$$

where

Mw = Molecular weight,

Rearrangement gives

$$p_1 Mw = \frac{z_1 R_{gas} T_1 nMw}{V_1} = z_1 R_{gas} T_1 \rho_1 \tag{2.16}$$

and

$$pMw = \frac{zR_{gas} TnMw}{V} = zR_{gas} T\rho \tag{2.17}$$

Substituting Equations 2.16 and 2.17 into Equation 2.11 we obtain

$$\overline{u}_1 \frac{p_1 Mw}{z_1 R_{gas} T_1} = \overline{u} \frac{pMw}{zR_{gas} T} \tag{2.18}$$

Since temperature is constant, $T_1 = T$, cancelling out Mw, R_{gas}, and temperatures yields

$$\overline{u}_1 \frac{p_1}{z_1} = \overline{u} \frac{p}{z} \tag{2.19}$$

If the pressure drop in the pipe is small comparing with measuring pressure and pressure drop due to kinetic energy change is negligible, which is the case in this study, Equation 2.7 can be expressed in average velocity

$$q = \overline{u} A = \overline{u} \pi R^2 = \frac{\pi (p_1 - p_2) R^4}{8 \mu L}$$

or

$$\overline{u} = \frac{(p_1 - p_2) R^2}{8 \mu L} \tag{2.20}$$

Expressing in derivative is

$$\overline{u} = -\frac{dp}{dl} \frac{R^2}{8 \mu} \tag{2.21}$$

Equation 2.19 can be cast to

$$\overline{u} = \overline{u}_1 \frac{zp_1}{z_1 p} \tag{2.22}$$

Substituting Equation 2.22 into Equation 2.21 we have

$$\overline{u}_1 \frac{zp_1}{z_1 p} = -\frac{dp}{dl}\frac{R^2}{8\mu} \tag{2.23}$$

Separating variables yields

$$-\frac{z_1 p}{zp_1} dp = \frac{8\overline{u}_1 \mu}{R^2} dl \tag{2.24}$$

Integrating from inlet to outlet we have

$$\int_{p1}^{p2} -\frac{z_1 p}{zp_1} dp = \int_0^L \frac{8\overline{u}_1 \mu}{R^2} dl \tag{2.25}$$

Considering the facts that compressibility factor z and viscosity μ are strong functions of pressure and the lack of rigorous expressions for these functions, there is no closed-form expression for integral in Equation 2.25. In case of very low pressure gradient, we employed z_{av} and μ_{av} to denote the average compressibility and viscosity of gas in the pipe. In this study the pressure difference between inlet and outlet is 0-10 psi, which is very small comparing with 3000-25000 psig measuring pressure, thus the variation of viscosity and compressibility with pressure can be neglected. Equation 2.25 is replaced with

$$\int_{p1}^{p2} -\frac{z_1 p}{z_{av} p_1} dp = \int_0^L \frac{8\overline{u}_1 \mu_{av}}{R^2} dl \tag{2.26}$$

or

$$\frac{z_1}{2z_{av} p_1}\left(p_1^2 - p_2^2\right) = \frac{8\overline{u}_1 \mu_{av} L}{R^2} \tag{2.27}$$

Recasting Equation 2.27 gives

$$\frac{z_1}{2z_{av} p_1}\left(p_1 - p_2\right)\left(p_1 + p_2\right) = \frac{8\overline{u}_1 \mu_{av} L}{R^2} \tag{2.28}$$

or

$$\overline{u}_1 = \frac{(p_1 - p_2)R^2}{8\mu_{av}L}\frac{z_1(p_1 + p_2)}{2z_{av}p_1} \tag{2.29}$$

Multiplying by cross section area, $A = \pi R^2$ we have

$$\overline{u}_1 \pi R^2 = \frac{\pi(p_1 - p_2)R^4}{8\mu_{av}L}\frac{z_1(p_1 + p_2)}{2z_{av}p_1} \tag{2.30}$$

Expressing in volumetric flow rate gives

$$q = \frac{\pi(p_1 - p_2)R^4}{8\mu_{av}L}\frac{z_1(p_1 + p_2)}{2z_{av}p_1} \tag{2.31}$$

which has an addition term, $\frac{z_1(p_1 + p_2)}{2z_{av}p_1}$, accounting for compressible fluid flow.

Equation 2.31 is similar to Poiseville's equation. In case of incompressible fluids, $\frac{z_1(p_1 + p_2)}{2z_{av}p_1}$ will collapse to 1, and then Equation 2.31 will end up with Poiseville's equation.

2.1.1 Capillary Viscometers

Transpiration method is the base for capillary viscometer. Capillary viscometer is named after its key part, a cylindrical capillary tube. It also has another often used name, Rankine viscometer. In a capillary viscometer, fluid flows through a cylindrical capillary tube. Figure 2-4 shows a typical capillary viscometer in two positions: (a) is in horizontal position, and (b) is in vertical position. The measurement principle is the combination of Poiseville equation and real gas law. Viscosity is determined by measuring the flow rate of the fluid flowing through the capillary tube and the pressure differential between both ends of the capillary tube. This measurement method is based on the laws of physics; therefore, this is called the absolute measurement of viscosity.

The principle and structure of the capillary viscometer is simple, but accurate measurement is the key for success. The inside of the capillary viscometer must be kept very clean. Also, a thorough drying of the capillary tube is required before each measurement. Temperature control is essential because the capillary tube is susceptible to thermal expansion or contraction under the influence of temperature, especially in lower viscosity ranges. These thermal impacts might introduce errors to the measurement. In addition, capillary tube is hard to withstand high pressure. A constant tube diameter and regular geometric shape at HPHT are necessary to obtain good result. As a result, capillary viscometer is suitable for measurement at low-moderate pressure and temperature.

The measurement of gas viscosity using capillary viscometer is delineated as follow. 1) A drop of clean mercury is introduced into a sufficiently narrow cylindrical glass tube filled with gas, completely fills the cross-section of the tube and forms a practically perfect internal seal as between the spaces on either side of it; 2) changing the viscometer from horizontal to any inclination will cause the mercury pellet start to flow due to the gravity force or the density difference between mercury and gas; 3) mercury pellet quickly come into equilibrium with the proper difference of gas pressure established above and below; 4) actually the descending mercury pellet acts as a piston, forcing the gas through the capillary tube. Any alteration of inclination angle of the viscometer will change the descending velocity of the mercury pellet.

A typical capillary viscometer is a closed glass vessel consisting of two connected tubes as shown in Figure 2-5, one is a fine capillary tube and the other is tube with much larger inner-diameter compared with the former, yet sufficiently narrow for a pellet of mercury to remain intact in it. The governing equation to calculate gas viscosity from capillary viscometer is derived as follow (Rankine, 1910).

Let V be the volume unoccupied by mercury; the volume of the capillary tube is much less than V, therefore it is negligible. Let p denote the steady pressure of the gas in the tube when the viscometer is held horizontally and let Δp be the pressure difference caused by the mercury pellet when the apparatus is vertical. Let p_1 be the pressure and V_1 the volume at any time above the mercury, and p_2, V_2, the corresponding quantities below the mercury. Then

$$V = V_1 + V_2, \text{ and } \Delta p = p_2 - p_1 \tag{2.32}$$

Now if we keep the temperature constant, then real gas law gives

$$pV = p_1V_1 + p_2V_2 \tag{2.33}$$

Substituting Equation 2.32 into Equation 2.33 we obtain

$$pV = p_1V_1 + (p_1 + \Delta p)V_2 = p_1V + \Delta pV_2 \tag{2.34}$$

Since $V_2 = V - V_1$, Equation 2.34 can be rearranged into

$$pV = p_1V + \Delta p(V - V_1)$$

or

$$p_1 = p - \Delta p + \Delta p\left(\frac{V_1}{V}\right) \tag{2.35}$$

From Equation 2.35 we can see that the pressure above the mercury increases linearly with V_1, so does the pressure below the mercury, meanwhile the pressure difference remains constant (caused by the density difference between mercury and gas). Let $dV_{elementary}$ be an elementary volume of gas emerging from the top end of the capillary. This will result in an increase of pressure dp_1, and also an increase dV_1 in V_1. The relation between these quantities is

$$dV_{elementary} = dV_1 + V_1\frac{dp_1}{p_1} \tag{2.36}$$

which can be expressed as

$$dV_{elementary} = \frac{V}{\Delta p}dp_1 + \frac{V}{\Delta p}(p_1 - p + \Delta p)\frac{dp_1}{p_1}$$

$$= \frac{V}{\Delta p} dp_1 \frac{(2p_1 - p + \Delta p)}{p_1} \tag{2.37}$$

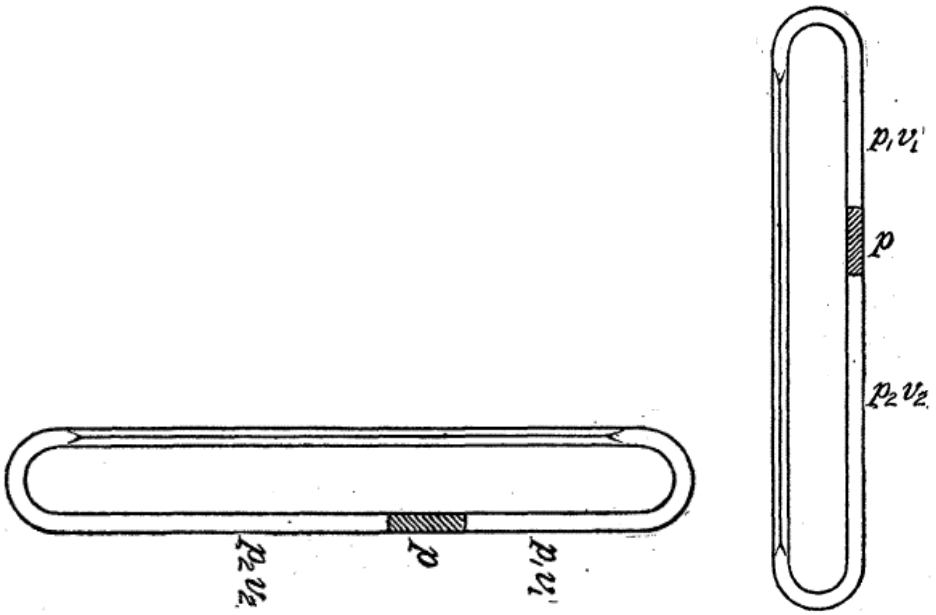

(a) Viscometer in horizontal position (b) Viscometer in vertical position

Figure 2-4. Capillary viscometer in two positions, after Rankine (1910)

Recalling Meyer's (Meyer, 1866) formula for transpiration, and neglecting for the moment the slipping correction, we can write

$$dV_{elementary} = \frac{\pi R^4 (p_2^2 - p_1^2)}{8\mu l 2p_1} dt \tag{2.38}$$

$$\begin{aligned} dV_{elementary} &= \frac{(p_2 + p_1)(p_2 - p_1)\pi R^4}{16\mu p_1 l} dt \\ &= \frac{\Delta p(2p_2 - \Delta p)\pi R^4}{16\mu p_1 l} dt \end{aligned} \tag{2.39}$$

where

$p_2 = p_1 + \Delta p$

Δp = Pressure difference (Reading from gauge) measured in cms. of mercury at 0^oC

μ = Air viscosity

R = Radius of capillary tube

L = Length of the capillary tube

If we assume that p_1 and p_2 change sufficiently slowly for the steady state to be set up without appreciable lag; let $\pi R^4 / 8\mu l = K$, and substituting for p_2 in Equation 2.39, we obtain

$$dV_{elementary} = K\Delta p \frac{\left(2p_2 - \Delta p\right)}{2p_1} dt \tag{2.40}$$

By comparing right hand side of Equations 2.37 and 2.40 we note that they are equal.

$$\frac{V}{\Delta p} dp_1 \frac{\left(2p_1 - p + \Delta p\right)}{p_1} = K\Delta p \frac{\left(2p_2 - \Delta p\right)}{2p_1} dt \tag{2.41}$$

Let $x = 2p_1 + \Delta p$ and $dx = 2dp_1$, Equation 2.41 can be written as

$$\frac{V}{\Delta p}\left(x - p\right)dx = K\Delta p x dt \tag{2.42}$$

Integration of Equation 2.42 gives

$$\frac{V}{\Delta p}\left(x - p\log x\right)\Big|_{x1}^{x2} = K\Delta p dt \tag{2.43}$$

Recalling $p_1 = p - \Delta p + \Delta p\left(\frac{V_1}{V}\right)$ from Equation 2.35, then

$$x = 2\left[p - \Delta p + \Delta p\left(\frac{v_1}{V}\right)\right] + \Delta p = 2p - \Delta p\left(1 - \frac{2v_1}{V}\right) \tag{2.44}$$

Suppose that t is the time taken for the upper volume to increase from V_1 to V_1', the following is the equation giving the air viscosity.

$$\frac{V}{\Delta p}\left\{\frac{2\Delta p\left(V_1^{'} - V_1\right)}{V} - p\log\left[\frac{2p - \Delta p\left(1 - \frac{2V_1^{'}}{V}\right)}{2p - \Delta p\left(1 - \frac{2V_1}{V}\right)}\right]\right\} = K\Delta p t \tag{2.45}$$

By substituting $\pi R^4 / 8\mu l = K$ into Equation 2.45 we have

$$2\left(V_1^{'}-V_1\right)-\frac{pV}{\Delta p}\log\left[\frac{2p-\Delta p\left(1-\frac{2V_1^{'}}{V}\right)}{2p-\Delta p\left(1-\frac{2V_1}{V}\right)}\right]=\frac{\pi R^4\Delta pt}{8\mu l} \qquad (2.46)$$

It should be noted that the capillary attraction in the wider limb makes the value of Δp not proportional to the length of the mercury pellet. If the pellet was undeformed by the downward movement, capillarity would produce no resultant effect, taking account of the symmetry of the ends. Actually, the upper surface is less curved than the lower one during the motion. This results in a diminution of the effective driving pressure.

A classic capillary viscometer used by Rankine (1923) to measure the viscosities of neon, xenon, and krypton is illustrated as Figure 2-5. Detail geometry of the apparatus can be obtained from Rankine (1910).

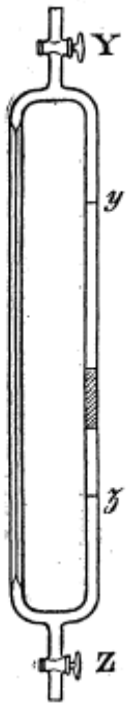

Figure 2-5. A classic capillary viscometer, after Rankine (1910)

2.1.2 Falling (or Rolling) Ball Viscometers

From its name we know that the falling (or rolling) ball viscometer measures viscosity by dropping a column- or sphere-shaped rigid body with known dimensions and density into a sample and measuring the time taken for it to fall a specific distance (Figure 2-6). Another type of device measures traveling time when horizontally transporting a rigid body, such as a piston or a needle, in a sample fluid at a constant speed by the force applied by the electromagnetic field. All falling-body viscometers measure fluid viscosity basing on Stokes' law.

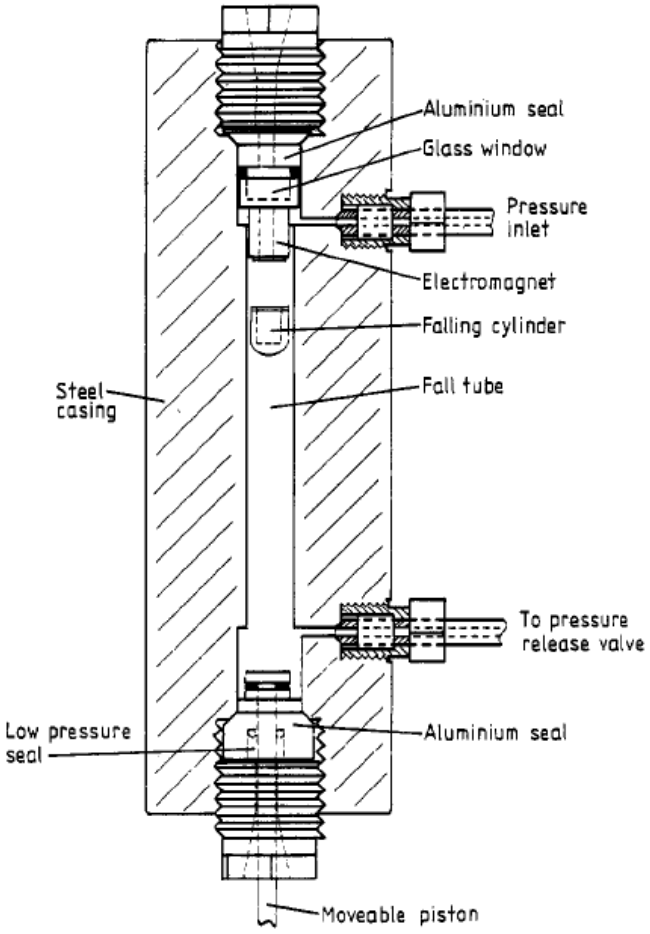

Figure 2-6. Cross section of falling cylinder viscometer body and ancillary components, after Chan and Jckson (1985)

Unlike the vibrating or rotational viscometers, the falling-ball viscometers shown Figure 2-6 cannot continuously measure viscosity. It is also impossible to continuously output digital signals of viscosity coefficient or to control data. In falling ball viscometer the fluid is stationary in a vertical glass tube. A sphere of known size and density is allowed to descend through the fluid. The time for the ball to fall from start point to the end point on the tube can be recorded and the length it travels can be measured. Electronic sensing can be used for timing. At the end of the tube there are two marks, the time for the ball passing these two marks are recorded so that the average velocity of the ball is calculated assuming the distance between these two marks is close enough. Knowing the terminal velocity, the size and density of the sphere, and the density of the liquid, Stokes' Law can be used to calculate the viscosity.

Besides the use of a sphere in falling ball viscometers, both cylinders and needles have been used by various researchers to measure the viscosity. Instruments are also available commercially using these types of geometry. Therefore, commonly used falling ball viscometer includes falling ball, falling cylinder, and falling needle viscometers. Figure 2-7 is the illustration of a falling ball viscometer. Typical falling cylinder viscometer can be referred to Figure 2-6 mentioned above. An example of falling needle viscometer can be seen in Figure 2-8.

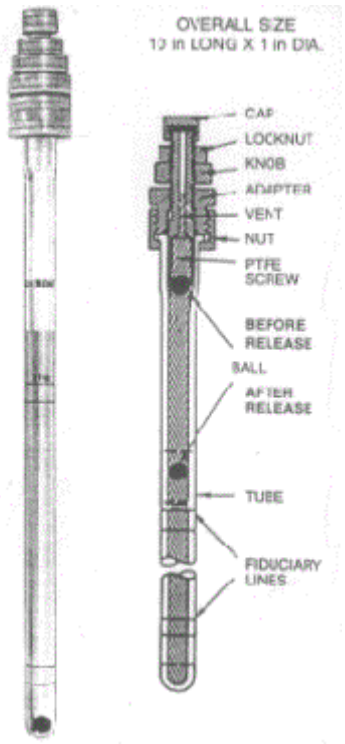

Figure 2-7. Cross section of a falling ball viscometer body, after Florida Atlantic University (2005)

There are some drawbacks when the viscosity is measure by the ball viscometer, these include that the motion of the ball during its descent in the viscometer tube exhibits random slip and spin (Herbert and Stoke, 1886). If we use a cylinder instead of a ball, the problem can be overcome easily. First, a cylinder equipped with stabilizing projections, shows little if any tendency toward dissipating energy in this fashion. Thus the error in measuring experimental fall times is reduced. Second, when ball viscometers are used for measuring low viscosities, the ball diameter must be nearly equal to the tube diameter, making the instrument extremely sensitive to the effects of nonuniform construction, poor reproducibility results. The cylinder however may be easily oriented in a consistent fashion so that any effect of nonuniform construction is constant (Dabir et al., 2007).

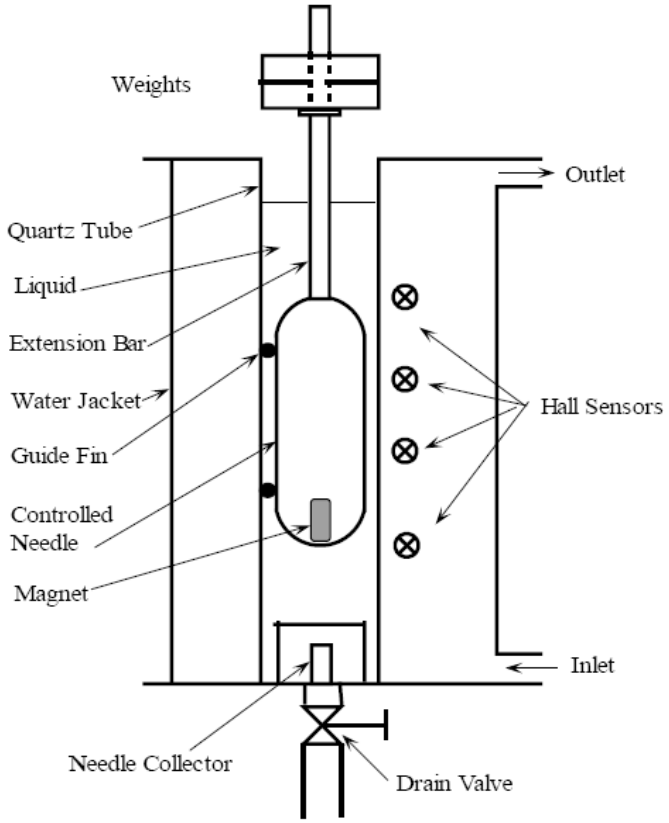

Figure 2-8. Cross section of a falling needle viscometer body, after Park (1994)

Rolling ball viscometers employ the same measuring method as falling ball viscometer except that the falling trajectory is slant instead of vertical. A classic rolling ball viscometer is shown in Figure 2-9.

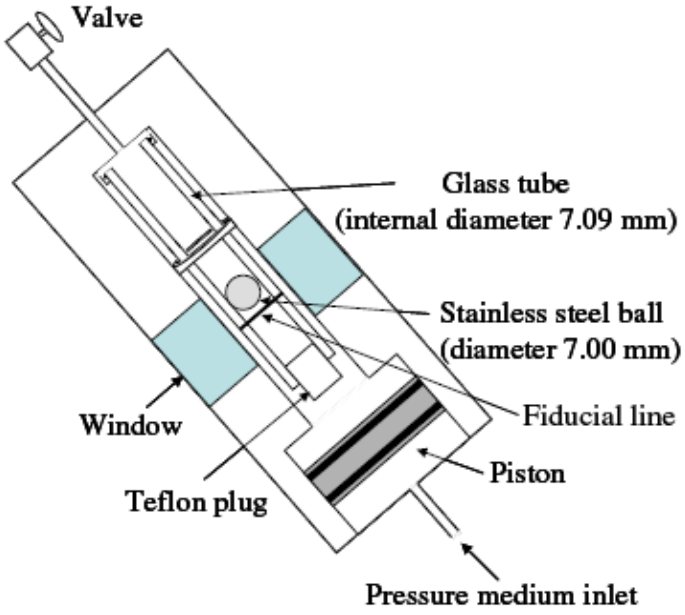

Figure 2-9. Rolling ball viscometer, after Tomida et al. (2005)

2.1.3 Vibrating viscometers

Vibrating viscometers can be dated back to the 1950s Bendix instrument, which is of a class that operates by measuring the damping of an oscillating electromechanical resonator immersed in a fluid whose viscosity is to be determined. The resonator generally oscillates in torsion or transversely as a cantilever beam or tuning fork. They are rugged industrial systems used to measure viscosity in many fields. The principle of vibrating viscometer is that it measures the damping of an oscillating electromechanical resonator immersed in the test liquid. The resonator may be a cantilever beam, oscillating sphere or tuning fork which oscillates in torsion or transversely in the fluid. The resonator's damping is measured by several methods:

1) Measuring the power input necessary to keep the oscillator vibrating at constant amplitude. The higher the viscosity, the more power is needed to maintain the amplitude of oscillation.
2) Measuring the decay time of the oscillation once the excitation is switched off. The higher the viscosity, the faster the signal decays.

3) Measuring the frequency of the resonator as a function of phase angle between excitation and response waveforms. The higher the viscosity, the larger the frequency changes for a given phase change.

The designation of vibrating viscometer usually uses three technologies. There are tuning fork, oscillating sphere, and vibrating rod (or wire) technologies. Each of these technologies is described as follow.

Tuning fork technology-vibrational viscometers designed based on tuning fork technology measure the viscosity by determining the bandwidth and frequency of the vibrating fork resonance; the bandwidth giving the viscosity measurement whilst the frequency giving the fluid density (Figure 2-10). A temperature sensor can be easily accommodated in the instrument for temperature measurement. In addition, other parameters such as viscosity gravity gradients and ignition indices for fuel oils can be calculated.

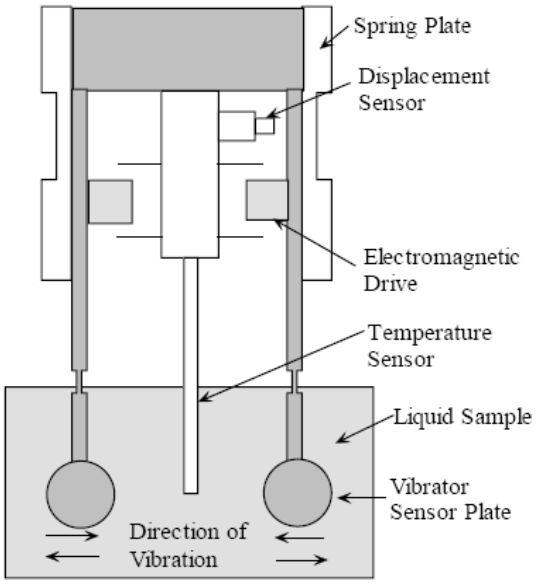

Figure 2-10. Vibrational viscometer employed tuning fork technology, after Paul N. Gardner Co. (2010)

Oscillating sphere technology - in this method a sphere oscillates (Figure 2-11) about its polar axis with precisely controlled amplitude (Steffe, 1992). The viscosity is calculated from the power required to maintain this predetermined amplitude of oscillation. While it is very simple in design, the oscillating sphere viscometer provides viscosity that is density dependent. Therefore, density of the test fluid should be determined independently if kinematic viscosity is required for process control. The principle of oscillating sphere viscometer had been studied by Stokes (1868) many years ago.

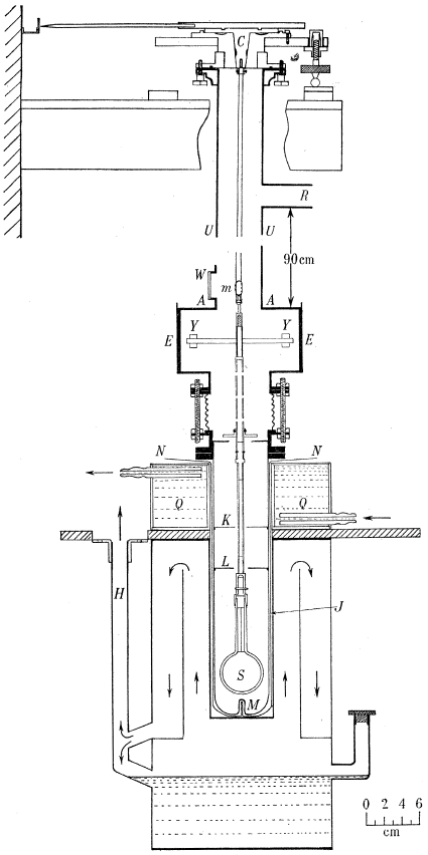

Figure 2-11. An oscillating sphere system for creating controlled amplitude in liquid, after Steffe (1992)

Vibrating rod (or wire) technology - in the viscometer the active part of the sensor is a vibrating rod (or wire). The vibration amplitude varies according to the viscosity of the fluid in which the rod is immersed (Figure 2-12).

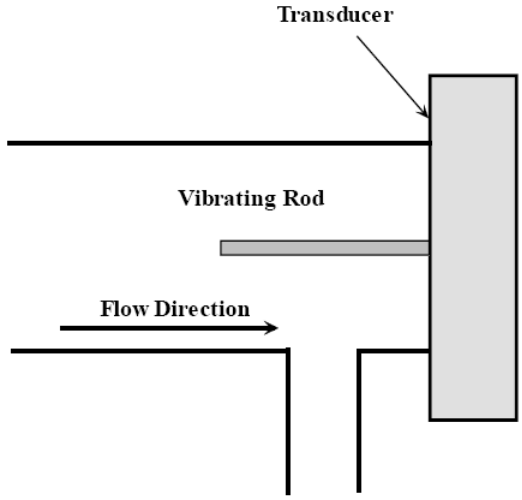

Figure 2-12. Vibrating rod system for measuring dynamic viscosity, after Steffe (1992)

Vibrating viscometers are best suited for many requirements in viscosity measurement. The important features of vibrating viscometers are small sample volume requirement, high sensitivity, ease of operation, continuous readings, wide range, optional internal reference, flow through of the test fluids and consequent easy clean out and prospect of construction with easily available materials. Contrasted to rotational viscometers, which require more maintenance and frequent calibration after intensive use, vibrating viscometers has no moving parts, no weak parts and the sensitive part is very small. Actually even the very basic or acid fluid can be measured by adding a special coating or by changing the material of the sensor. Currently, many industries around the world consider these viscometers as the most efficient system to measure viscosity of any fluid.

2.2 Gas Viscosity Experimental Data

Common approach to estimate gas viscosity comprises direct experimental measurement and gas viscosity correlations. Direct measurement provides reliable and confident result so with the cost of high expense and time consuming and cost expensive. Furthermore, quantity of fluid sample and availability of appropriate measuring instrument that can handle experiment at reservoir condition limit its application. Given the aforementioned disadvantages most PVT lab reports provided gas viscosity estimated from correlations. Although gas viscosity correlation provides a simple and low cost method to predict gas viscosity, accuracy of calculated viscosity is depended on the database it based on. A good gas viscosity correlation needs accurate lab data as its solid base. We cannot evaluate the correlation before we know what kind of lab data is used. One thing for sure is that a correlation cannot guarantee its validity outside of the thermodynamic conditions of lab data. Thus, it is necessary to understand the limitation of available gas viscosities database. In this study a review of available pure nitrogen, methane, and natural gas viscosity is crucial to make our project sense considering high methane concentration in most HPHT gas reservoirs and high nonhydrocarbon concentration such as nitrogen in some HPHT gas reservoirs.

Earhart (1916) determined 10 natural gases viscosities using a capillary viscometer. Yen (1919) measured nitrogen viscosity at temperature of 23 ^{o}C and pressures of 14.7 psia using a capillary viscometer. Boyd (1930) applied the transpiration method, or same principle as capillary viscometer, on measuring nitrogen viscosity at temperatures of 30, 50, and 70 ^{o}C and pressures from 73 to 178.8 atms. Trautz and Zink (1930) measured methane and nitrogen viscosities at temperatures from 23 to 499 ^{o}C. Michels and Gibson (1931) designed an apparatus basing on capillary principle to measure nitrogen viscosity at temperatures of 25, 50, and 75 ^{o}C and pressures from 15.37 to 965.7 atms. Berwald and Johnson (1933) measured 25 natural gases viscosities at temperature of 60 ^{o}F and pressure of 29.4 psia with a capillary viscometer. Rudenko and Schubnikow (1934) measured nitrogen viscosities at temperature from 63 to 77 ^{o}K and pressure less than 8

psia with a capillary viscometer. Adzumi (1937) measured methane, ethane, propane, CH_4-C_2H_2, C_2H_2-C_3H_6, and C_3H_6-C_3H_8 mixtures viscosities at temperature from 0 to 100 ^oC and pressure of 14.7 psia with a capillary viscometer. Sage and Lacey (1938) measured methane and 2 natural gases viscosity at temperatures of 100, 160, and 220 ^oF and pressures up to 2600 psi. Johnston and McCloskey (1940) measured methane and nitrogen viscosity at temperatures from 90 to 200 ^oK and pressures up to 14.7 psia using an oscillating-disk viscometer. Smith and Brown (1943) measured pure ethane and propane viscosities at temperatures from 15 to 200 ^oC and pressures from 100 to 5000 psi utilizing a rolling-ball viscometer. They also developed a viscosity correlation basing on available data. Bicher and Katz (1943) measured pure methane and methane-propane mixture viscosities utilizing a rolling-ball inclined-tube viscometer. They ran experiments at temperatures of 77, 167, 257, 347, and 437 ^oF and pressures from 14.7 to 5000 psia. Comings et al. (Comings and Egly, 1940; Coming et al., 1944) used two Rankine viscometers (capillary viscometer) constructed of Pyrex glass to measure methane and natural gas viscosities at temperatures of 30, 50, 70, and 95 ^oC and pressures from 1 to 171 atms. Similar to Comings's study, Van Itterbeek et al. (1947) measured nitrogen viscosity at temperatures from -312 to 64 ^oF and low to ordinary pressures with an oscillating disc viscometer. Carr (1952) and Stewart (1952) used two Rankine viscometers (capillary viscometer) constructed of Pyrex glass to measure methane and three natural gas viscosities at temperatures from 70 to 200 ^oF and pressures from 14.7 to 10000 psia. Iwasaki (1954) measured pure nitrogen and nitrogen-hydrogen mixture viscosities utilizing an oscillating disc viscometer at temperatures of 25, 100, and 150 ^oC and pressures up to 200 atms. Lambert et al. (1955) measured methane and ethane viscosities an oscillating viscometer at temperatures from 35 to 78 ^oC and low pressures. Ross and Brown (1957) used a capillary tube viscometer to measure pure nitrogen and methane viscosities at temperatures of 25, 0, -25, and -50 ^oC and pressures from 500 to 10000 psig. Ellis and Raw (1958) measured nitrogen viscosity at temperatures from 700 to 1000 ^oC and low pressures through a capillary tube viscometer. Baron et al. (1959) used Rankine viscometer (capillary viscometer) to

measure pure nitrogen and methane viscosities at temperatures of 125, 175, 225, and 275 ^{o}F and pressures from 100 to 8000 psig. To solve the problem of grass capillary viscometer broken at high pressure, he balanced the pressures between inside and outside of tube by charging the annulus around the tube. Kestin and Leidenfrost (1959) constructed an oscillating-disk viscometer to measure pure nitrogen viscosities at temperatures from 19 to 25 ^{o}C and pressures from 0.139 to 62.7 atms. Swift et al. (1959) measured methane viscosity at temperatures from -83 to -150 ^{o}C and pressures from 350 to 710 psia with a falling-body viscometer. Golubev (1959) used the capillary tube viscometer to measure pure nitrogen and methane viscosities at condition of temperatures range from –58.12 to 1292 ºF and pressures range from 14.7 to 14700 psia. Golubev data shows a significant difference compared data from the other available database. Swift et al. (1960) extended his measurement on methane viscosity at temperatures from -82 to -140 ^{o}C and pressures from 85 to 675 psia with a falling-cylinder viscometer. Flynn et al. (1963) developed a capillary viscometer to measure nitrogen viscosity at temperatures of -78, -50, -25, 25, and 100 ^{o}C and pressures from 6.77 to 176 atms. Barua et al. (1964) measured methane viscosity at temperatures from -50 to 150 ^{o}C and pressures up to 200 atms using a capillary viscometer. Carmichael et al. (1965) measured methane viscosity at temperatures of 40, 100, 220, 340, and 400 ^{o}F and pressures from 14.7 to 5000 psia using a rotating-cylinder type viscometer. Lee (1965) presented viscosity values of pure methane basing on work done by Mario Gonzalez. Data were acquired at temperature from 100 to 340 ^{o}F and pressure from 200 to 8000 psia. Recommended methane viscosity values are presented in Table 2-1. Lee claimed that viscosity values corresponding to the region of this investigation are accurate within ±5% percent. Lee also collected pure hydrocarbons such as ethane, propane, n-butane, n-pentane, and n-decane and gas mixtures (methane-propane, methane-butane, and methane-decane) viscosities in order to derive gas viscosity correlation. He considered the following mole percentage: 10, 20, 30, 40, 50, 60, 70, 80, and 90 percent in binary mixtures. Giddings et al. (1965) developed a versatile absolute capillary-tube viscometer to measure methane viscosity at temperatures from 40 to 280 ^{o}F and pressures from 100

to 8000 psia. Wilson (1965) constructed a rolling ball viscometer to measure 10 natural gases viscosity at temperatures from 77 to 400 ^{o}F and pressures from 1000 to 10000 psia. Dipippo et al. (1966) constructed an oscillating disc viscometer to measure nitrogen viscosity at temperatures from 75 to 410 ^{o}F and pressures from 5.7 to 25 psia. Lee and Gonzalez et al. (Gonzalez et al., 1966; Gonzalez et al.,1970) measured the viscosities of eight natural gases using a capillary-tube viscometer to honor the true reservoirs, for all of the samples, the range of temperature is 100 to 340 ºF and the range of pressure is from 14.7 to 8000 psia. Gonzalez et al. (1966) published his methane viscosity data covered temperatures from 100 to 340 ºF and pressures from 200 to 8000 psia. Huang et al. (1966) measured methane viscosities at temperatures from -170 to 0 ºC and pressure up to 5000 psia with a falling cylinder type viscometer. Van Itterbeek et al. (1966) provided nitrogen viscosities measured by a oscillating disk viscometer at temperatures of 70, 77.3, 83.9 and 90.1 ºK and pressures from 0.5 to 98 atms. Boon et al. (1967) provided methane and nitrogen viscosities measured by a capillary viscometer at temperatures from 91 to 114 ºK and the corresponding saturated vapor pressures. Kestin and Yata (1968) measured pure methane, nitrogen, and H_2-N_2, CH_4-CO_2, CH_4-C_4H_{10} binary mixtures viscosities using an oscillating-disk viscometer at temperatures 20 and 30 ºC and pressures from 1 to 25 atms. Grevendonk et al. (1970) measured liquid nitrogen viscosity using a torsionally vibrating piezoelectric crystal viscometer at temperatures from 66 to 124 ºK and pressures from vapor pressure to 196 x 10^5 N/m^2. Helleman et al. (Helleman et al., 1970; Helleman et, al. 1973) measured methane viscosities at temperatures from 96 to 187 ºK and pressures up to 100 atms and nitrogen viscosities at temperatures from 77 to 203 ºF and pressures of 14.7 psia using an oscillating-disk viscometer. Diehl et al. (1970) used Geopal viscometer (capillary tube viscometer) to determine the pure hydrocarbon and nitrogen gas viscosities. For all of the samples, the range of temperature is 32 to 302 ºF and the range of pressure is from 14.7 to 7350 psia. Latto and Saunders (1972) measured nitrogen viscosity at temperatures from 90 to 400 ºK and pressures from 1 to 150 atms using a capillary viscometer. Stephan and Lucas (1979) collected a large database of gas viscosities from

several investigators with different methods including torsional crystal, oscillating disk, rolling ball, rotating cylinder, capillary tube, and falling ball. The data includes gases such as pure hydrocarbons (methane to n-decane), nitrogen, and carbon dioxide. The range of temperatures and pressures differs from one component to another. In general the temperatures range is from 212 to 1832 ºF and the pressures range is from 14.7 to 10290 psia. Diller (1980) measured the viscosity of compressed gases and liquid methane at temperatures between 100 and 300 ºK and pressures up to 4350 psia with a torsionally oscillating quartz crystal viscometer. As a extension of his work in 1980, Diller (1983) used same viscometer to measure the viscosity of compressed gases and liquid nitrogen at temperatures between 90 and 300 ºK and pressures up to 4350 psia. Hongo et al. (1988) used Maxwell type oscillating-disc viscometer to measure the viscosity of methane and methane-chlorodifluoromethane mixtures in the temperature range from 298.15 to 373.15 ^{o}K and at pressures up to 5MP. Van Der Gulik et al. (1988) used vibrating wire viscometer to measure the viscosity of methane at 25 ºC and pressures from 1 to 10,000 bar. Vogel et al. (1999) used a vibrating wire viscometer to measure the viscosity of methane at temperature of 260, 280, 300, 320, 340, and 360 ºK and pressures up to 20 MPa. Assael et al. (2001) employed a vibrating wire viscometer to measure the viscosity of methane at the temperature range from 313 to 455 ^{o}K at a pressure close to atmospheric and in the temperature range from 240 to 353 ^{o}K at pressures up to 15 MPa. Schley et al. (2004) used a vibrating-wire viscometer to measure methane viscosity at temperatures of 260, 280, 300, 320, 340, and 360 K and at pressures up to 29 MPa. Seibt et al. (2006) measured nitrogen viscosity with a vibrating-wire viscometer. The measurements were performed along the six isotherms of 298.15, 323.15, 348.15, 373.15, 398.15, and 423.15 ^{o}K and at pressures up to a maximum of 35 MPa. Tables 2-1 to 2-4 show experimental data of methane viscosity from some investigators. Table 2-5 depicts experimental data of nitrogen viscosity from some investigators.

Table 2-1. Methane viscosity collected by Lee (1965)

Pressure (psia)	Temperature (^{o}F)						
	100	160	220	280	340	400	460
14.70	0.01140	0.01250	0.01340	0.01440	0.01530	0.01660	0.01750
100.00	0.01190	0.01300	0.01400	0.01500	0.01600	0.01700	0.01790
200.00	0.01200	0.01300	0.01410	0.01510	0.01610	0.01710	0.01800
300.00	0.01210	0.01310	0.01410	0.01510	0.01620	0.01720	0.01800
400.00	0.01220	0.01320	0.01420	0.01520	0.01620	0.01730	0.01810
500.00	0.01240	0.01330	0.01430	0.01530	0.01630	0.01730	0.01820
600.00	0.01250	0.01350	0.01440	0.01540	0.01640	0.01740	0.01830
800.00	0.01280	0.01370	0.01460	0.01550	0.01650	0.01760	0.01840
1000.00	0.01320	0.01400	0.01480	0.01570	0.01670	0.01780	0.01860
1250.00	0.01370	0.01450	0.01520	0.01600	0.01700	0.01800	0.01880
1500.00	0.01440	0.01490	0.01560	0.01630	0.01720	0.01830	0.01910
1750.00	0.01520	0.01540	0.01600	0.01680	0.01750	0.01850	0.01930
2000.00	0.01600	0.01600	0.01640	0.01700	0.01780	0.01860	0.01950
2500.00	0.01770	0.01720	0.01740	0.01780	0.01850	0.01940	0.02010
3000.00	0.01950	0.01860	0.01860	0.01870	0.01930	0.02010	0.02070
3500.00	0.02120	0.02020	0.01970	0.01970	0.02010	0.02070	0.02130
4000.00	0.02310	0.02170	0.02090	0.02060	0.02090	0.02140	0.02190
4500.00	0.02490	0.02320	0.02200	0.02170	0.02180	0.02220	0.02250
5000.00	0.02660	0.02460	0.02330	0.02280	0.02260	0.02300	0.02320
6000.00	0.02990	0.02740	0.02570	0.02500	0.02440	0.02450	0.02460
7000.00	0.03280	0.02990	0.02810	0.02710	0.02620	0.02610	0.02600
8000.00	0.03550	0.03230	0.03000	0.02910	0.02810	0.02750	0.02730
9000.00	0.03800	0.03450	0.03220	0.03100	0.03000	0.02910	0.02860
10000.00	0.04060	0.03660	0.03420	0.03300	0.03180	0.03050	0.03000
Note: viscosity in cp							

Table 2-2. Methane viscosity by Diehl et al. (1970)

Pressure (psia)	Temperature (^{o}F)						
	86	104	122	140	158	176	194
14.70	0.01116	0.01150	0.01183	0.01216	0.01248	0.01279	0.01310
220.50	0.01140	0.01170	0.01205	0.01235	0.01270	0.01300	0.01330
367.50	0.01155	0.01190	0.01220	0.01255	0.01285	0.01320	0.01350
735.00	0.01210	0.01240	0.01270	0.01300	0.01335	0.01365	0.01400
1102.50	0.01290	0.01315	0.01340	0.01365	0.01395	0.01425	0.01455
1470.00	0.01390	0.01410	0.01430	0.01450	0.01470	0.01490	0.01515
1837.50	0.01510	0.01520	0.01530	0.01545	0.01560	0.01575	0.01590
2205.00	0.01640	0.01640	0.01645	0.01650	0.01655	0.01665	0.01675
2940.00	0.01905	0.01895	0.01885	0.01875	0.01870	0.01865	0.01860
3675.00	0.02175	0.02150	0.02125	0.02105	0.02085	0.02070	0.02055
4410.00	0.02410	0.02380	0.02350	0.02320	0.02290	0.02265	0.02240
5145.00	0.02650	0.02610	0.02570	0.02530	0.02490	0.02455	0.02425
5880.00	0.02880	0.02830	0.02780	0.02730	0.02685	0.02640	0.02600
6615.00	0.03105	0.03045	0.02990	0.02930	0.02875	0.02825	0.02775
7350.00	0.03320	0.03250	0.03190	0.03125	0.03060	0.03000	0.02945
Note: viscosity in cp							

Table 2-2. Continued

Pressure (psia)	Temperature (^{o}F)					
	212	230	248	266	280	302
14.70	0.01341	0.01371	0.01400	0.01430	0.01459	0.01488
220.50	0.01360	0.01395	0.01425	0.01455	0.01485	0.01515
367.50	0.01380	0.01410	0.01440	0.01470	0.01500	0.01530
735.00	0.01430	0.01460	0.01490	0.01515	0.01545	0.01575
1102.50	0.01480	0.01505	0.01535	0.01560	0.01585	0.01610
1470.00	0.01540	0.01565	0.01590	0.01615	0.01635	0.01655
1837.50	0.01610	0.01630	0.01650	0.01670	0.01690	0.01710
2205.00	0.01685	0.01700	0.01715	0.01730	0.01750	0.01770
2940.00	0.01860	0.01865	0.01870	0.01880	0.01890	0.01900
3675.00	0.02045	0.02040	0.02035	0.02030	0.02025	0.02025
4410.00	0.02220	0.02205	0.02190	0.02180	0.02170	0.02160
5145.00	0.02395	0.02370	0.02350	0.02330	0.02315	0.02300
5880.00	0.02565	0.02535	0.02505	0.02475	0.02450	0.02430
6615.00	0.02730	0.02690	0.02655	0.02620	0.02590	0.02565
7350.00	0.02890	0.02845	0.02805	0.02765	0.02730	0.02700
Note: viscosity in cp						

Table 2-3. Methane viscosity by Stephan and Lucas (1979)

Pressure (psia)	Temperature (^{o}F)					
	80.33	116.3	152.3	188.3	224.3	260.3
14.70	0.01100	0.01170	0.01230	0.01300	0.01350	0.01420
294.00	0.01150	0.01210	0.01270	0.01340	0.01400	0.01460
441.00	0.01170	0.01230	0.01190	0.01360	0.01420	0.01480
588.00	0.01200	0.01260	0.01320	0.01380	0.01440	0.01500
677.67	0.01210	0.01270	0.01330	0.01390	0.01450	0.01510
808.50	0.01240	0.01300	0.01350	0.01410	0.01470	0.01530
882.00	0.01250	0.01310	0.01360	0.01420	0.01480	0.01540
1029.00	0.01290	0.01340	0.01390	0.01440	0.01500	0.01550
1176.00	0.01320	0.01370	0.01410	0.01460	0.01510	0.01570
1323.00	0.01360	0.01400	0.01440	0.01480	0.01530	0.01580
1470.00	0.01390	0.01430	0.01460	0.01500	0.01550	0.01600
1764.00	0.01490	0.01510	0.01530	0.01560	0.01600	0.01640
2058.00	0.01600	0.01590	0.01600	0.01620	0.01650	0.01690
2205.00	0.01650	0.01630	0.01640	0.01650	0.01680	0.01710
2940.00	0.01920	0.01870	0.01840	0.01830	0.01830	0.01850
4410.00	0.02450	0.02330	0.02250	0.02200	0.02160	0.02150
5880.00	0.03030	0.02850	0.02710	0.02610	0.02530	0.02470
7350.00	0.03490	0.03260	0.03090	0.02960	0.02860	0.02780
8820.00	0.03880	0.03620	0.03430	0.03290	0.03170	0.03070
10290.00	0.04260	0.03950	0.03730	0.03570	0.03450	0.03350
Note: viscosity in cp						

Table 2-3. Continued

Pressure (psia)	Temperature (^{o}F)					
	296.3	332.3	368.3	404.3	440.3	476.3
14.70	0.01470	0.01540	0.01600	0.01660	0.01720	0.01770
294.00	0.01530	0.01600	0.01660	0.01720	0.01780	0.01840
441.00	0.01540	0.01610	0.01670	0.01730	0.01790	0.01850
588.00	0.01560	0.01620	0.01680	0.01740	0.01800	0.01860
677.67	0.01570	0.01630	0.01690	0.01750	0.01810	0.01870
808.50	0.01580	0.01640	0.01700	0.01760	0.01820	0.01880
882.00	0.01590	0.01640	0.01700	0.01760	0.01820	0.01880
1029.00	0.01600	0.01660	0.01720	0.01780	0.01830	0.01890
1176.00	0.01620	0.01670	0.01730	0.01790	0.01850	0.01910
1323.00	0.01630	0.01690	0.01750	0.01810	0.01860	0.01920
1470.00	0.01650	0.01700	0.01760	0.01820	0.01870	0.01930
1764.00	0.01690	0.01740	0.01800	0.01850	0.01900	0.01960
2058.00	0.01730	0.01780	0.01830	0.01880	0.01930	0.01990
2205.00	0.01750	0.01800	0.01850	0.01900	0.01950	0.02010
2940.00	0.01870	0.01900	0.01950	0.01990	0.02040	0.02090
4410.00	0.02140	0.02150	0.02170	0.02190	0.02220	0.02250
5880.00	0.02440	0.02410	0.02410	0.02410	0.02430	0.02450
7350.00	0.02730	0.02680	0.02660	0.02640	0.02630	0.02630
8820.00	0.03000	0.02940	0.02890	0.02860	0.02830	0.02820
10290.00	0.03260	0.03180	0.03130	0.03070	0.03030	0.03000
Note: viscosity in cp						

Table 2-4. Methane viscosity by Golubev (1959)

Pressure (psia)	Temperature (^{o}F)						
	77	122	167	212	302	392	482
14.70	0.01108	0.01182	0.01260	0.01331	0.01471	0.01603	0.01725
146.96	0.01120	0.01193	0.01270	0.01340	0.01477	0.01611	0.01728
293.92	0.01137	0.01210	0.01280	0.01350	0.01483	0.01617	0.01733
587.84	0.01180	0.01247	0.01312	0.01377	0.01512	0.01634	0.01745
881.76	0.01237	0.01295	0.01350	0.01416	0.01530	0.01653	0.01765
1175.68	0.01310	0.01352	0.01392	0.01452	0.01556	0.01675	0.01785
1469.59	0.01395	0.01417	0.01445	0.01497	0.01580	0.01700	0.01809
2204.39	0.01652	0.01610	0.01600	0.01627	0.01685	0.01775	0.01872
2939.19	0.01930	0.01830	0.01787	0.01787	0.01807	0.01867	0.01947
3673.99	0.02187	0.02062	0.02002	0.01965	0.01942	0.01975	0.02030
4408.78	0.02455	0.02300	0.02205	0.02142	0.02085	0.02075	0.02120
5143.58	0.02705	0.02530	0.02401	0.02320	0.02230	0.02182	0.02205
5878.38	0.02942	0.02745	0.02593	0.02486	0.02370	0.02290	0.02295
7347.97	0.03365	0.03145	0.02955	0.02815	0.02635	0.02500	0.02470
8817.57	0.03740	0.03485	0.03277	0.03120	0.02887	0.02705	0.02645
10287.16	0.04087	0.03820	0.03545	0.03395	0.03130	0.02910	0.02820
11756.76	0.04410	0.04095	0.03855	0.03655	0.03367	0.03107	0.02995
Note: viscosity in cp							

Table 2-5. Nitrogen viscosity collected by Stephan and Lucas (1979)

Temperature	Pressure (psi)					
^{o}F	14.504	145	290	435	580	725
-343	0.2633	0.2677	0.2728	0.2777	0.2826	0.2876
-334	0.2113	0.2154	0.2197	0.2244	0.229	0.2336
-325	0.1677	0.1713	0.1753	0.1793	0.1832	0.1875
-316	0.00552	0.1366	0.14	0.1433	0.1467	0.1501
-307	0.00586	0.1111	0.1136	0.1164	0.1192	0.1219
-298	0.0062	0.09326	0.09528	0.09737	0.09951	0.1018
-289	0.00654	0.08093	0.08266	0.08429	0.08602	0.08777
-280	0.00688	0.0713	0.07297	0.07459	0.07616	0.07772
-271	0.00722	0.00783	0.06397	0.06584	0.0676	0.06929
-262	0.00756	0.00811	0.05517	0.05728	0.05925	0.06112
-253	0.00789	0.0084	0.04626	0.04902	0.0514	0.05354
-244	0.00821	0.00868	0.00953	0.03974	0.04335	0.04612
-235	0.00852	0.00896	0.00968	0.01155	0.03369	0.0381
-226	0.00883	0.00925	0.00988	0.01107	0.01805	0.02945
-217	0.00914	0.00954	0.0101	0.01103	0.01314	0.01998
-208	0.00945	0.00983	0.01028	0.01112	0.0125	0.01551
-190	0.01006	0.01041	0.01085	0.01145	0.01232	0.01365
-172	0.01066	0.01098	0.01138	0.01186	0.01252	0.0134
-154	0.01124	0.01154	0.01189	0.01232	0.01286	0.01353
-136	0.01181	0.01209	0.01241	0.01279	0.01325	0.0138
-118	0.01237	0.01263	0.01293	0.01327	0.01367	0.01415
-100	0.01292	0.01316	0.01344	0.01376	0.01411	0.01452
-82	0.01346	0.01369	0.01395	0.01424	0.01456	0.01493
-64	0.01399	0.01421	0.01445	0.01472	0.01502	0.01535
-46	0.0145	0.01471	0.01494	0.01519	0.01546	0.01577
-28	0.015	0.0152	0.01542	0.01566	0.01591	0.01619
-10	0.01549	0.01568	0.01589	0.01612	0.01635	0.01661
Note: viscosity in cp						

Table 2-5. Continued

Temperature	Pressure (psi)					
^{o}F	14.504	145	290	435	580	725
8	0.01597	0.01615	0.01635	0.01657	0.01679	0.01703
26	0.01644	0.01662	0.0168	0.01701	0.01722	0.01745
44	0.01691	0.01708	0.01726	0.01745	0.01765	0.01787
62	0.01737	0.01753	0.01771	0.01789	0.01808	0.01829
80	0.01782	0.01797	0.01815	0.01832	0.0185	0.0187
98	0.01826	0.01841	0.01858	0.01874	0.01892	0.0191
116	0.0187	0.01885	0.019	0.01916	0.01934	0.01951
134	0.01913	0.01928	0.01942	0.01958	0.01975	0.01991
152	0.01956	0.01971	0.01985	0.02	0.02015	0.02032
170	0.02	0.02014	0.02028	0.02042	0.02056	0.02073
260	0.02204	0.02216	0.02228	0.0224	0.02253	0.02267
350	0.02396	0.02406	0.02417	0.02428	0.02439	0.02451
440	0.02577	0.02586	0.02596	0.02606	0.02615	0.02626
530	0.02747	0.02756	0.02764	0.02774	0.02782	0.02791
620	0.02908	0.02916	0.02924	0.02932	0.0294	0.02948
710	0.03062	0.03069	0.03077	0.03084	0.03091	0.03099
800	0.0321	0.03217	0.03224	0.0323	0.03237	0.03244
980	0.03491	0.03497	0.03503	0.03509	0.03514	0.03521
1160	0.03753	0.03758	0.03763	0.03769	0.03774	0.03779
1340	0.03999	0.04004	0.04008	0.04013	0.04018	0.04023
1520	0.04232	0.04236	0.0424	0.04245	0.04249	0.04253
1700	0.04453	0.04457	0.04461	0.04465	0.04469	0.04473
1880	0.04662	0.04666	0.04669	0.04673	0.04677	0.0468
Note: viscosity in cp						

Table 2-5. Continued

Temperature ^{o}F	Pressure (psi)					
	870	1015	1160	1305	1450	1813
-343	0.2927	0.2978	0.3027	-	-	-
-334	0.2383	0.2429	0.2475	0.2523	0.2568	0.2687
-325	0.1914	0.1957	0.1998	0.2041	0.2084	0.2191
-316	0.1537	0.1573	0.1609	0.1645	0.1682	0.1777
-307	0.1248	0.1278	0.1308	0.1338	0.1369	0.1448
-298	0.104	0.1063	0.1087	0.1111	0.1136	0.12
-289	0.08951	0.09135	0.09319	0.09507	0.097	0.102
-280	0.07922	0.08076	0.08229	0.08386	0.08542	0.08949
-271	0.07089	0.07242	0.07392	0.07539	0.07681	0.08034
-262	0.06294	0.06469	0.06636	0.06794	0.06948	0.07308
-253	0.05553	0.05737	0.0591	0.06078	0.06243	0.06636
-244	0.04849	0.05041	0.05255	0.05437	0.05608	0.06005
-235	0.04135	0.04407	0.04633	0.04836	0.05023	0.05445
-226	0.03424	0.03763	0.04033	0.0427	0.04479	0.04931
-217	0.02686	0.03131	0.03462	0.0373	0.0397	0.04427
-208	0.02068	0.02544	0.02923	0.03229	0.03487	0.04012
-190	0.0157	0.01847	0.02147	0.02434	0.02696	0.03248
-172	0.0146	0.01614	0.018	0.02004	0.02211	0.02698
-154	0.01437	0.01542	0.01666	0.01805	0.01958	0.02347
-136	0.01446	0.01525	0.01616	0.01719	0.01832	0.02139
-118	0.01469	0.01532	0.01604	0.01685	0.01774	0.0202
-100	0.01499	0.01553	0.01612	0.01678	0.0175	0.01951
-82	0.01534	0.0158	0.01632	0.01688	0.01748	0.01918
-64	0.01572	0.01613	0.01657	0.01758	0.01799	0.01912
-46	0.01611	0.01647	0.01687	0.0173	0.01776	0.01903
-28	0.0165	0.01683	0.01719	0.01758	0.01799	0.01912
-10	0.01689	0.0172	0.01753	0.01788	0.01825	0.01927
Note: viscosity in cp						

Table 2-5. Continued

Temperature	Pressure (psi)					
^{o}F	870	1015	1160	1305	1450	1813
8	0.01729	0.01758	0.01788	0.01819	0.01854	0.01946
26	0.0177	0.01796	0.01824	0.01852	0.01884	0.01969
44	0.0181	0.01835	0.01861	0.01887	0.01917	0.01995
62	0.0185	0.01874	0.01898	0.01923	0.0195	0.02023
80	0.0189	0.01912	0.01935	0.01959	0.01984	0.02052
98	0.0193	0.0195	0.01972	0.01995	0.02018	0.02082
116	0.0197	0.01989	0.0201	0.02032	0.02053	0.02113
134	0.02009	0.02028	0.02047	0.02068	0.02089	0.02145
152	0.02048	0.02067	0.02085	0.02105	0.02126	0.02178
170	0.02087	0.02106	0.02124	0.02142	0.02162	0.02212
260	0.0228	0.02294	0.02308	0.02324	0.02339	0.0238
350	0.02463	0.02474	0.02487	0.02499	0.02513	0.02546
440	0.02636	0.02647	0.02658	0.02669	0.0268	0.02709
530	0.028	0.0281	0.02819	0.02829	0.02839	0.02864
620	0.02957	0.02965	0.02974	0.02982	0.02991	0.03014
710	0.03107	0.03114	0.03122	0.0313	0.03138	0.03159
800	0.03251	0.03258	0.03266	0.03273	0.03281	0.03299
980	0.03527	0.03533	0.03539	0.03546	0.03552	0.03568
1160	0.03785	0.0379	0.03795	0.03801	0.03807	0.03821
1340	0.04027	0.04032	0.04037	0.04042	0.04047	0.0406
1520	0.04258	0.04262	0.04267	0.04271	0.04276	0.04287
1700	0.04476	0.04481	0.04485	0.04489	0.04493	0.04503
1880	0.04684	0.04687	0.04691	0.04695	0.04699	0.04708
Note: viscosity in cp						

Table 2-5. Continued

Temperature	Pressure (psi)					
^{o}F	2176	2538	2901	3626	4351	5802
-343	-	-	-	-	-	-
-334	0.2808	0.2927	0.3047	0.3288	0.3533	-
-325	0.2301	0.2411	0.2523	0.2747	0.2979	0.3445
-316	0.1872	0.1971	0.2071	0.2279	0.2491	0.2928
-307	0.153	0.1614	0.1702	0.1884	0.2075	0.2475
-298	0.1267	0.1338	0.1412	0.1568	0.1733	0.2092
-289	0.1075	0.1131	0.1191	0.1321	0.1462	0.1774
-280	0.09376	0.09825	0.103	0.1135	0.1253	0.152
-271	0.08395	0.08763	0.0915	0.09992	0.1094	0.1317
-262	0.07644	0.07972	0.08305	0.09002	0.0977	0.1161
-253	0.06993	0.07325	0.0764	0.08255	0.08902	0.1041
-244	0.06376	0.0673	0.07056	0.07655	0.08232	0.09503
-235	0.05821	0.06167	0.06507	0.07127	0.07686	0.088
-226	0.05323	0.05677	0.06007	0.06631	0.07204	0.08241
-217	0.04863	0.05229	0.05563	0.06172	0.06748	0.0775
-208	0.04438	0.04811	0.05154	0.05765	0.06325	0.07311
-190	0.03694	0.04082	0.04425	0.05032	0.05576	0.06544
-172	0.03126	0.03503	0.03836	0.04427	0.04959	0.05895
-154	0.02719	0.03066	0.03382	0.03946	0.0445	0.05354
-136	0.02454	0.02755	0.03045	0.03573	0.04049	0.04903
-118	0.02281	0.02543	0.02797	0.0328	0.03757	0.03529
-100	0.02173	0.02397	0.02624	0.0306	0.0347	0.04227
-82	0.02105	0.02301	0.025	0.02391	0.03268	0.03975
-64	0.02038	0.02173	0.02413	0.02767	0.03114	0.03773
-46	0.02045	0.02198	0.02354	0.02673	0.0299	0.03602
-28	0.02038	0.02173	0.02314	0.02604	0.02895	0.03464
-10	0.0204	0.02161	0.02288	0.02552	0.0282	0.03353
Note: viscosity in cp						

Table 2-5. Continued

Temperature	Pressure (psi)					
^{o}F	2176	2538	2901	3626	4351	5802
8	0.02048	0.02159	0.02274	0.02517	0.02764	0.03259
26	0.02062	0.02163	0.02269	0.02492	0.02722	0.03182
44	0.02081	0.02174	0.02271	0.02477	0.02691	0.03121
62	0.02103	0.02188	0.02279	0.02372	0.02669	0.03073
80	0.02126	0.02206	0.02289	0.02466	0.02654	0.03035
98	0.02151	0.02226	0.02304	0.0247	0.02644	0.03004
116	0.02178	0.02248	0.02321	0.02477	0.02641	0.0298
134	0.02206	0.02271	0.02341	0.02487	0.02642	0.02963
152	0.02236	0.02297	0.02363	0.02501	0.02647	0.02952
170	0.02268	0.02326	0.02387	0.02518	0.02656	0.02947
260	0.02423	0.0247	0.02518	0.02616	0.0273	0.02961
350	0.02583	0.02621	0.02661	0.02744	0.02834	0.03025
440	0.0274	0.02773	0.02806	0.02877	0.02953	0.03115
530	0.02892	0.0292	0.02949	0.03011	0.03076	0.03216
620	0.03038	0.03064	0.03089	0.03144	0.03201	0.03323
710	0.0318	0.03203	0.03226	0.03274	0.03326	0.03435
800	0.03318	0.03339	0.0336	0.03404	0.0345	0.03548
980	0.03585	0.03602	0.03619	0.03656	0.03695	0.03776
1160	0.03835	0.0385	0.03965	0.03897	0.0393	0.03999
1340	0.04073	0.04085	0.04099	0.04127	0.04156	0.04216
1520	0.04299	0.0431	0.04322	0.04346	0.04372	0.04426
1700	0.04514	0.04524	0.04535	0.04557	0.0458	0.04628
1880	0.04718	0.04728	0.04737	0.04758	0.04778	0.04819
Note: viscosity in cp						

Table 2-5. Continued

Temperature	Pressure (psi)						
^{o}F	6527	7252	8702	10153	11603	13053	14504
-325	0.3678	0.3914	-	-	-	-	-
-316	0.3151	0.3376	-	-	-	-	-
-307	0.2685	0.2896	-	-	-	-	-
-298	0.2283	0.2478	-	-	-	-	-
-289	0.1945	0.2121	-	-	-	-	-
-280	0.1668	0.1826	-	-	-	-	-
-271	0.1445	0.1581	-	-	-	-	-
-262	0.1268	0.1386	-	-	-	-	-
-253	0.1131	0.123	-	-	-	-	-
-244	0.1025	0.1108	-	-	-	-	-
-235	0.09427	0.1012	-	-	-	-	-
-226	0.08782	0.0937	-	-	-	-	-
-217	0.08264	0.08774	-	-	-	-	-
-208	0.07794	0.08267	-	-	-	-	-
-190	0.07	0.0743	0.08271	-	-	-	-
-172	0.06331	0.06749	0.0755	0.08316	-	-	-
-154	0.05761	0.06167	0.06936	0.07671	0.08374	-	-
-136	0.05292	0.05675	0.06401	0.07111	0.07789	0.08443	-
-118	0.04906	0.05263	0.05963	0.06227	0.07275	0.07905	0.08545
-100	0.04584	0.04926	0.05584	0.0665	0.06832	0.07435	0.0805
-82	0.04313	0.04638	0.0526	0.05867	0.06451	0.07026	0.07606
-64	0.04085	0.04396	0.04987	0.05562	0.06118	0.06671	0.07211
-46	0.03901	0.04188	0.0475	0.05295	0.05827	0.06356	0.06871
-28	0.03743	0.04015	0.04547	0.05064	0.0557	0.06074	0.06573
-10	0.0361	0.03869	0.04371	0.04865	0.05344	0.05823	0.06306
Note: viscosity in cp							

Table 2-5. Continued

Temperature	Pressure (psi)						
^{o}F	6527	7252	8702	10153	11603	13053	14504
8	0.03501	0.03745	0.0422	0.04691	0.05148	0.05605	0.06067
26	0.03412	0.03641	0.04091	0.04539	0.04976	0.05414	0.05853
44	0.03337	0.03554	0.03982	0.04406	0.04825	0.05245	0.05661
62	0.03276	0.03481	0.03387	0.04291	0.0469	0.05093	0.05489
80	0.03226	0.0342	0.03805	0.0419	0.0457	0.04956	0.05336
98	0.03186	0.0337	0.03734	0.04101	0.04465	0.04834	0.052
116	0.03153	0.03328	0.03675	0.04024	0.04374	0.04725	0.05078
134	0.03127	0.03293	0.03625	0.03958	0.04295	0.04629	0.04969
152	0.03108	0.03266	0.03583	0.03901	0.04225	0.04546	0.04872
170	0.03095	0.03247	0.0355	0.03855	0.04163	0.04476	0.04785
260	0.03086	0.03209	0.0345	0.03701	0.03954	0.04212	0.04471
350	0.03125	0.03226	0.03433	0.03645	0.0386	0.04076	0.04301
440	0.03199	0.03286	0.03465	0.03645	0.03831	0.04019	0.04209
530	0.03289	0.03364	0.0352	0.03679	0.03842	0.04008	0.04176
620	0.03388	0.03455	0.0359	0.03733	0.03877	0.04026	0.0418
710	0.03493	0.03552	0.03674	0.03801	0.03931	0.04064	0.04208
800	0.036	0.03654	0.03762	0.03878	0.03997	0.04118	0.04241
980	0.03819	0.03863	0.03955	0.0405	0.04149	0.04252	0.04357
1160	0.04036	0.04073	0.04152	0.04233	0.04318	0.04405	0.04495
1340	0.04247	0.04281	0.04349	0.04419	0.04494	0.04569	0.04647
1520	0.04453	0.04482	0.04542	0.04605	0.0467	0.04737	0.04807
1700	0.04653	0.04679	0.04732	0.04788	0.04845	0.04906	0.04968
1880	0.04844	0.04867	0.04916	0.04966	0.05018	0.05072	0.05128
Note: viscosity in cp							

Literature review shows that although numerous researches on gas viscosity were undertaken, no data for the gas viscosities are available above the 14700 psia that the HPHT region beings, therefore the validities of correlations that based experimental data are doubted.

2.3 Available Gas Viscosity Correlations

Since good gas viscosity correlation provides a simple and low cost method to predict gas viscosity, we reviewed several well known correlations used to determine gas viscosity in industry. Here we discuss the most useful correlations such as Comings-Mayland-Egly (Comings and Egly, 1940; Comings et al., 1944) correlation, Smith-Brown (1943) correlation, Bicher-Katz (1943) correlation, Carr-Kobayashi-Burrrow (1954) correlation, Jossi-Stiel-Thodos (1962) correlation, and Lee-Gonzalez-Eakin (Gonzalez et al., 1970) correlation. In addition, the National Institute of Standard and Technology (NIST) (2000) has developed a computer program that predicts thermodynamic and transport properties of hydrocarbon fluids. Londono (2001) optimized existing gas viscosity and density correlations (or gas z-factor, then calculate gas density using EOS) and developed new gas viscosity and density correlations all basing on his collected database. Sutton (2005) optimized existing gas viscosity to developed new gas viscosity basing on a database containing thousands data points. Viswanathan (2007) modified Lee-Gonzalez-Eakin correlation using the NIST methane values. Discussing on these correlations and their databases gives an insight of current understanding of gas viscosity.

2.3.1 Comings-Mayland-Egly Correlation (1940, 1944)

Inspired by analogy to the approximate equality of the compressibility factors for a wide variety of compounds at equal reduced temperatures and pressures, Comings-Mayland-Egly correlation (Comings and Egly, 1940) proposed graphical correlation to estimate gas viscosity using Viscosity Ratio versus Reduced Pressure Charts (Figure 2-13). Viscosity ratio was defined as the ratio of viscosity at interested pressure temperature to

the viscosity at same temperature, but at pressure of one atmosphere. Essentially, the principle behind this analogy is the theory of corresponding states. Therefore it is not valid for most polar molecules. Data used in this correlation consists of viscosity of carbon dioxide, nitrogen, ammonia, water, methane, propane, and butane available from literatures.

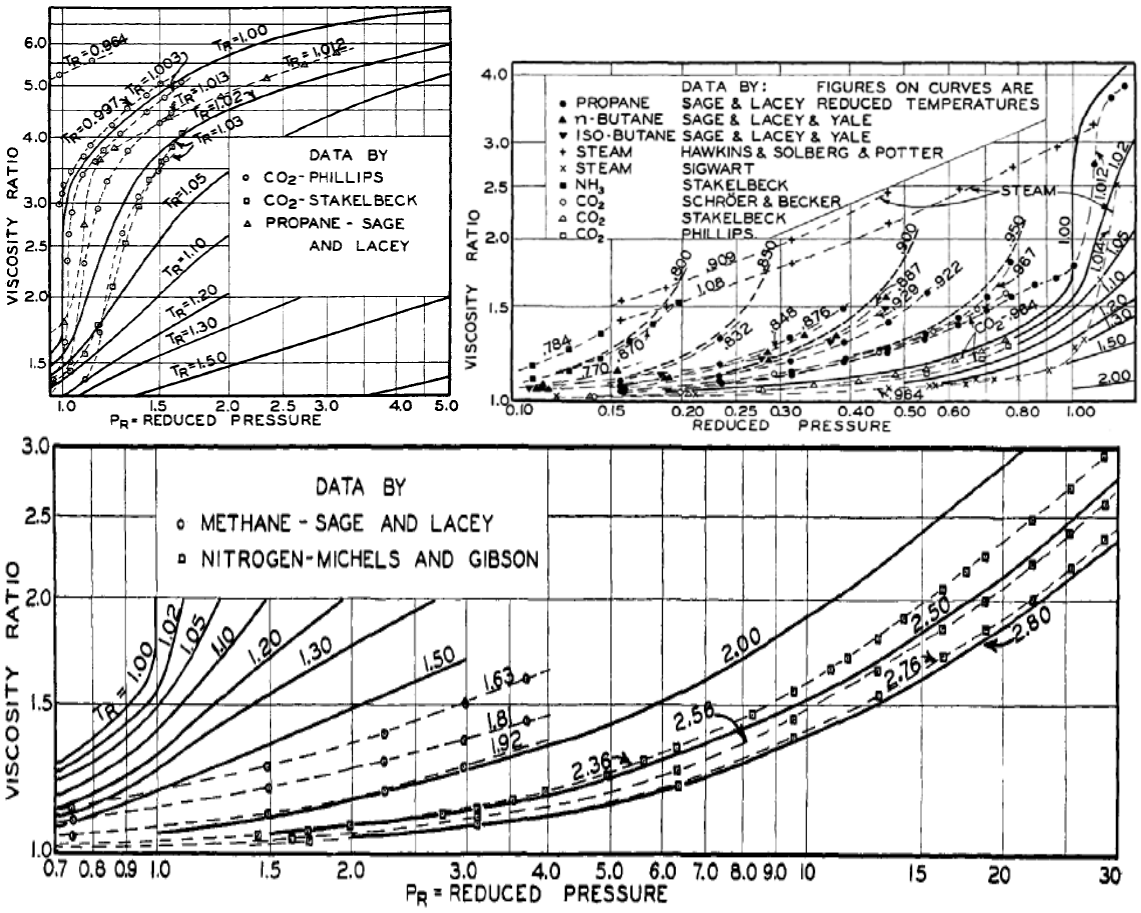

Figure 2-13. Viscosity ratio versus reduced pressure charts used to estimate gas viscosity, after Comings and Egly (1940)

In 1944 Comings et al. (1944) measured viscosity of N_2, CO_2, CH_4, C_2H_6, and C_3H_8 at pressure from 14.7 to 14196 psia and temperature from 14 to 374 ^oF. With these lab data and the data collected in 1940 (Table 3-6). Comings et al. (1944) improved this correlation by exploiting the analogy between viscosity and kinetic pressure. Both the

kinetic pressure and viscosity are the results of the transfer of momentum in that the kinetic pressure is normal to the wall and viscosity is parallel to the wall. Therefore viscosity should be proportional to kinetic pressure. In brief, this correlation bases on corresponding states theory. This approach applies four steps to get natural gas viscosity. Firstly we need to get the gas viscosity at interested temperature and pressure of one atmosphere, μ_1, which can be obtained from the International Critical Table. Secondly the reduced pressure and reduced temperature are calculated. Thirdly go to Figures 2-14 or 2-15 to read the logarithm of the viscosity ratio, $log(\mu/\mu_{1)}$, or viscosity ratio, μ/μ_1. Finally with the viscosity ratio and viscosity at interested temperature and pressure of one atmosphere obtained in first step gas viscosity at interested condition can be calculated.

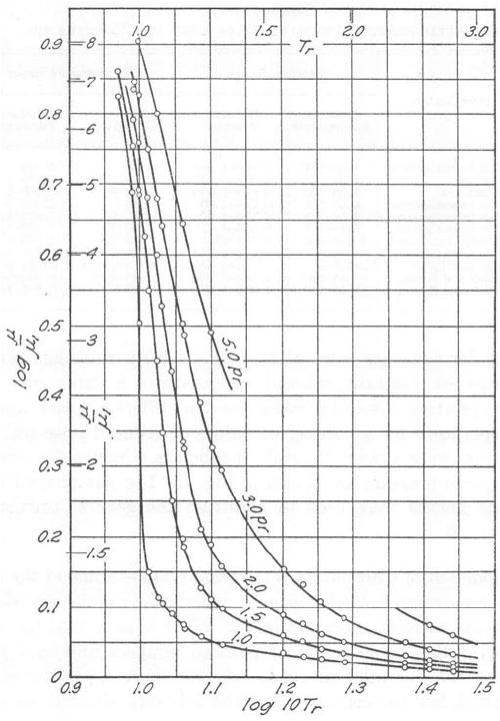

Figure 2-14. Viscosity ratio versus reduced temperature, after Comings et al. (1944)

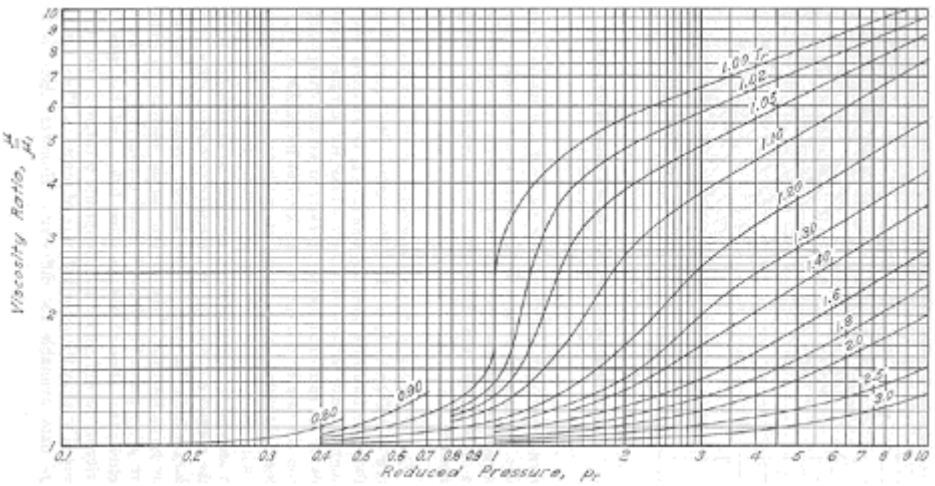

Figure 2-15. Viscosity ratio versus reduced pressure, after Comings et al. (1944)

Inevitably, Comings-Mayland-Egly correlation is good for pure gas. Its validity for natural gas is still questionable because there is no natural gas or gas mixtures viscosity in the database. The highest pressure and temperature for methane viscosity are 2514 psia 203 ^{o}F, respectively. As a result, no data at high pressure and temperature is available to support its validity for gas viscosity in HPHT reservoir. Comings also indicated that the correlation gives 10-12% error for ethane viscosity at reduced pressure higher than 2.0.

Table 2-6. Viscosity-temperature-pressure data used for Comings-Mayland-Egly (1940, 1944) correlation

Composition	Investigators	Pressure psia	Temperature ^{o}F
CO_2	Comings, Mayland, and Egly	65-2013	104
CO_2	Phillips	14.7-1646	68-104
CO_2	Schroer and Becker	14.7-860	86.5
CO_2	Stakelbeck	73-1763.5	14-104
C_2H_4	Comings, Mayland, and Egly	64.6-2013	104
C_2H_4	Comings, Mayland, and Egly	74.6-2513	86-203
CH_4	Comings, Mayland, and Egly	64.6-2513	86-203
N_2	Michels and Gilbson	161-14196	77-167
C_3H_8	Comings, Mayland, and Egly	64.6-614.3	86-220
C_3H_8	Sage and Lacey	701-999	160-220
C_3H_8	Smith and Brown	999-4996.6	203-374
C_2H_6	Smith and Brown	749.5-4996.6	59-167
n-butane	Sage and Lacey	Vapor pressure-2000	100-220
i-butane	Sage and Lacey	Vapor pressure-2000	100-220
NH_3	Stakelbeck	14.7-323	-4-176
Steam	Hawkins and Solberg	14.7-4000	640-761
Steam	Sigwart	14.74	714

2.3.2 Smith-Brown Correlation (1943)

Smith and Brown (1943) estimated fluid viscosity using theorem of corresponding states. The theory of corresponding states is based on the concept that the physics properties of different substances exhibit a similar behavior at the same values of reduced temperature and pressure. The theory is not rigorous, but it usually gives a good approximation with a minimum of effort. Smith and Brown believed theorem of corresponding states can provide a relationship between $\eta/\sqrt{M}$ and reduced pressure

for paraffins, where η is viscosity and M is molecular weight. Since few experimental data is available, Smith and Brown built a rolling ball viscometer to determine the viscosities of ethane and propane in the range 100 to 5000 psia and 150 to 200 ^{o}C. Basing on viscosity of methane, ethane, propane, butane, pentane, hexane, octane, decane and bicomponent mixtures (Table 2-7), a graphical correlation as shown in Figure 2-16 was constructed.

Table 2-7. Viscosity-temperature-pressure data used for Smith-Brown (1943) correlation

Composition	Investigators	Pressure psia	Temperature ^{o}F
CH_4	Sage and Lacey	701-999	160-220
C_2H_6	Smith and Brown	749.5-4996.6	59-167
C_3H_8	Smith and Brown	999-4996.6	203-374
C_3H_8	Sage and Lacey	<2000	100-220
n-Butane	Sage and Lacey	Vapor pressure-2000	100-220
i-Butane	Sage and Lacey	Vapor pressure-2000	100-220
n-Pentane	Hubbard and Brown	1000	77-482
n-Pentane	Bridgman	<171000	86-167
i-Butane	Bridgman	<171000	86-167
n-Hexane	Bridgman	<171000	86-167
n-Octane	Bridgman	<142000	86-167
n-Decane	Dow	<85000	86-167
n-Hexane-n-Decane mixtures	Dow	<57000	86-167
C_2H_6-$C_{12}H_{26}$	Evans	unknown	32-212

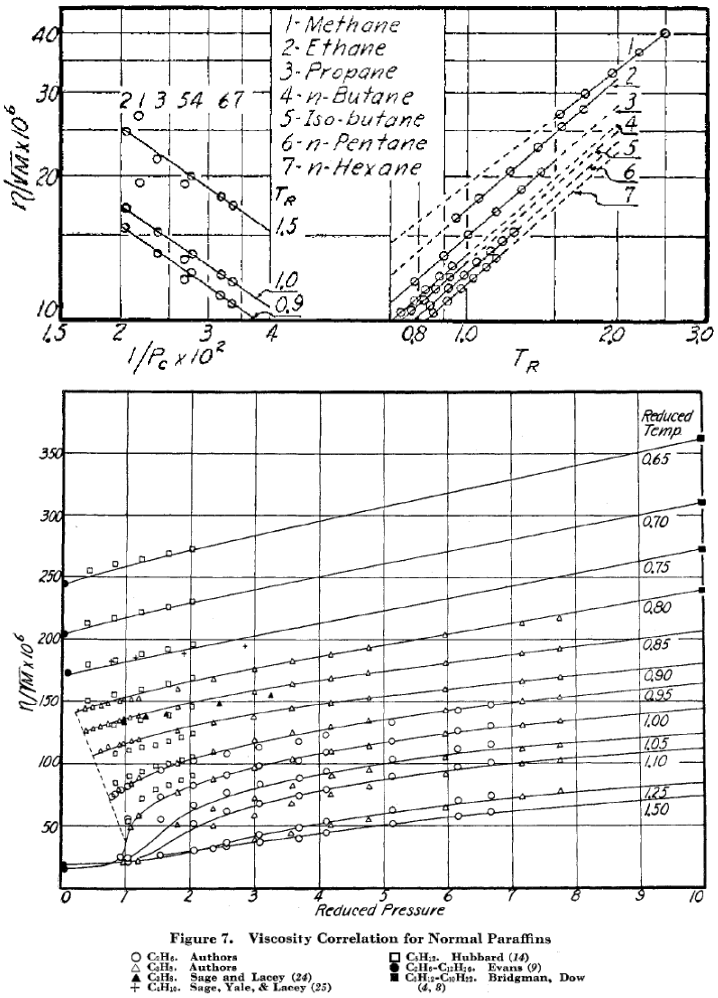

Figure 2-16. Viscosity correlation for normal paraffins, after Smith and Brown (1943)

Smith-Brown correlation is not applicable for methane as shown in Figure 2-16 (*top*). Smith verified that it is a very good approximation for ethane and higher paraffins viscosity. This correlation gives better estimation on liquids than gases.

2.3.3 Bicher-Katz Correlation (1943)

With a rolling ball viscometer Bicher-Katz (1943) correlation expanded Smith-Brown database through measuring methane, propane, and methane-propane mixture viscosity at pressure from 400-5000 psia and temperature from 77 to 437 ^{o}F, which covered a

larger temperature range comparing with Smith and Brown data**.** In their database they also included the viscosity of natural gas from Berwald and Johnson (1933) and Sage and Lacey (1938) (Table 2-8). For gas viscosity at high temperature Bicher and Katz inserted a coefficient K into $\eta/\sqrt{M}$ to adjusted deviation from ideal gas behavior (Figure 2-17).

Table 2-8. Viscosity-temperature-pressure data used for Bicher-Katz (1943) correlation

Composition	Investigators	Pressure psia	Temperature ^{o}F
CH_4	Sage and Lacey	701-999	160-220
C_2H_6	Smith and Brown	749.5-4996.6	59-167
C_3H_8	Smith and Brown	999-4996.6	203-374
C_3H_8	Sage and Lacey	<2000	100-220
n-Butane	Sage and Lacey	Vapor pressure-2000	100-220
i-Butane	Sage and Lacey	Vapor pressure-2000	100-220
n-Pentane	Hubbard and Brown	1000	77-482
n-Pentane	Bridgman	<171000	86-167
i-Butane	Bridgman	<171000	86-167
n-Hexane	Bridgman	<171000	86-167
n-Octane	Bridgman	<142000	86-167
n-Decane	Dow	<85000	86-167
n-Hexane-n-Decane mixture	Dow	<57000	86-167
2 natural gases	Sage and Lacey	<2600	100-220
25 Natural gases	Berwald and Johnson	<500	60
CH_4	Bicher and Katz	400-5000	77-437
C_3H_8	Bicher and Katz	400-5000	77-437
Methane-Propane mixtures	Bicher and Katz	400-5000	77-437

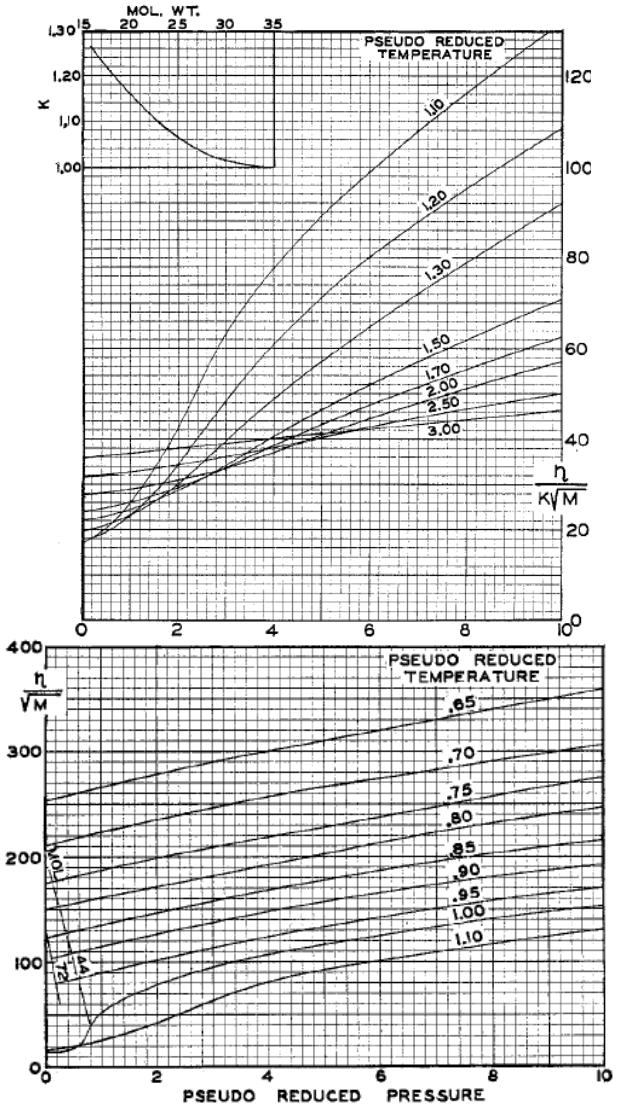

Figure 2-17. Viscosity of paraffin hydrocarbons at high-reduced temperatures (*top*) and at low-reduced temperatures (*bottom*), after Bicher and Katz (1943)

2.3.4 Carr-Kobayashi-Burrrow Correlation (1954)

Carr-Kobayashi-Burrrow (1954) correlation inherited the spirit of Comings-Mayland-Egly correlation. It is an upgraded version of Comings-Mayland-Egly correlation. It includes two steps to estimate natural gas viscosity. First we need to get the gas viscosity at atmospheric conditions. Equations 2.47 through 2.51 are used to calculate gas

viscosity at this condition. Once viscosity at atmospheric conditions is available, it is calibrated to reservoir conditions, or reservoir pressure and temperature conditions, by applying charts or correlation. Figures 2-18 and 2-19 are used to calibrate viscosity at atmospheric conditions to reservoir conditions. In the calibration, the concepts of pseudoreduced pressure and pseudoreduced temperature are applied. Gas viscosity ratio, μ_g/μ_{1atm}, is estimated from these curves. Using gas viscosity ratio and gas viscosity at atmospheric conditions, gas viscosity at reservoir conditions can be calculated.

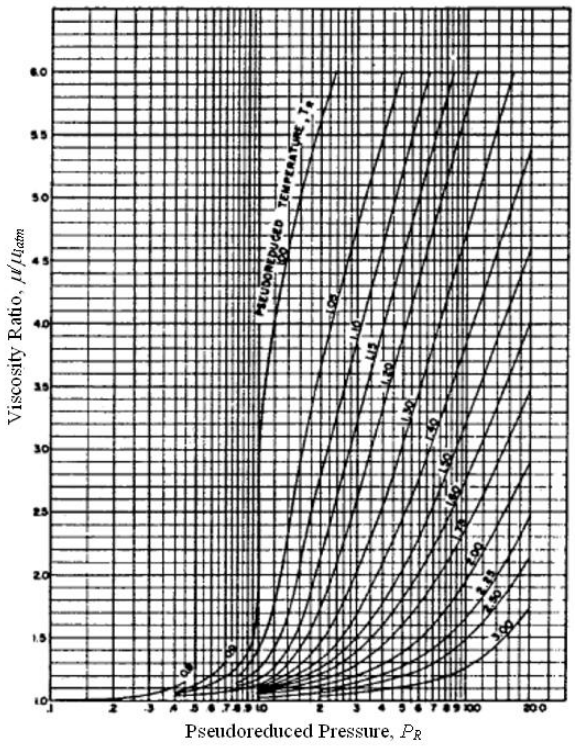

Figure 2-18. Viscosity ratio versus pseudo-reduced pressure, after Carr et al. (1954)

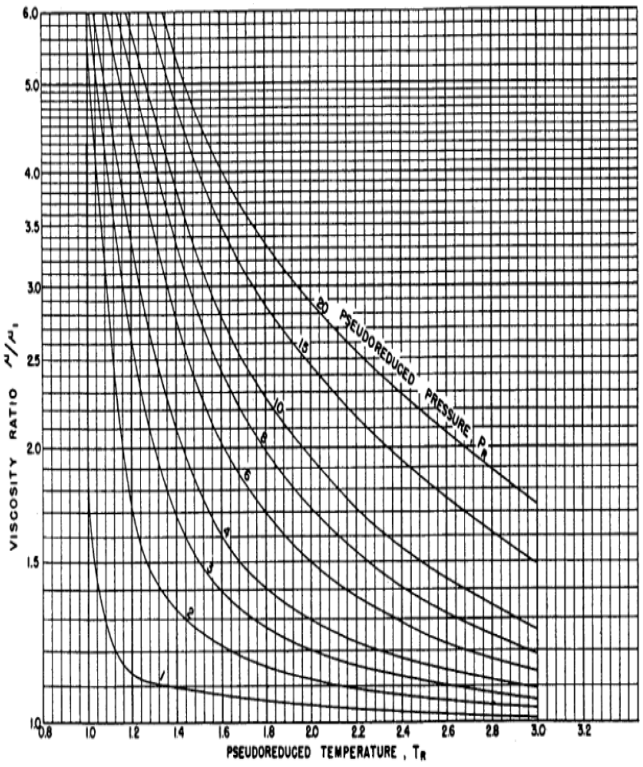

Figure 2-19. Viscosity ratio versus pseudo-reduced temperature, after Carr et al. (1954)

$$\mu_{1atm} = (\mu_{1atm} \text{ uncorrected}) + (N_2 \text{ correction}) + (CO_2 \text{ correction}) + (H_2S \text{ correction}) \tag{2.47}$$

$$\mu_{1atm} \text{ uncorrected} = (1.709 \times 10^{-5} - 2.062 \times 10^{-6} \gamma_g)T + 8.188 \times 10^{-3} - 6.15 \times 10^{-3} \log \gamma_g \tag{2.48}$$

$$N_2 \text{ correction} = y_{N_2}\left[(8.48 \times 10^{-3}) \log \gamma_g + 9.59 \times 10^{-3}\right] \tag{2.49}$$

$$CO_2 \text{ correction} = y_{CO_2}\left[(9.08 \times 10^{-3}) \log \gamma_g + 6.24 \times 10^{-3}\right] \tag{2.50}$$

$$H_2S \text{ correction} = y_{H_2S}\left[(8.49 \times 10^{-3}) \log \gamma_g + 3.73 \times 10^{-3}\right]. \tag{2.51}$$

where

μ_{1atm} = Gas viscosity at 1 atm, cp

γ_g = Gas specific gravity (air=1)

y_{N_2,CO_2,H_2S} = Mole fraction of the non-hydrocarbon component

T = Temperature, ^oF

The advantage of Carr-Kobayashi-Burrrow correlation is that it could correct the effect of non-hydrocarbons, which affect the natural gas viscosity significantly. It also gives 1.50 percent absolute error for the gas viscosity according to Carr's report.

Carr-Kobayashi-Burrrow correlation based on the measurement of pure components such as nitrogen, carbon dioxide, methane, ethylene, propane, simulated mixture samples, and natural gas. Table 2-9 lists the fluid sample and measuring pressure temperature range of the experimental data used to develop this correlation. It is observed that this correlation based on limited pressure and temperature range. Therefore its application in HPHT is not yet to be proved by more extensive lab data at HPHT.

Table 2-9. Viscosity-temperature-pressure data used for Carr-Kobayashi-Burrrow (1954) correlation

Composition	Investigators	Pressure psia	Temperature ^{o}F	Memo
CH_4	Comings, Mayland, and Egly	64.6-2513	86-203	
CH_4	Bicher and Katz	14.7-500	77-437	
CH_4	Carr, Kobayashi, and Burrrow	14.7-8030	71-200	
N_2	Michels and Gilbson	161-14196	77-167	
N_2-0.6, CH_4-73.4, C_2H_6-25.6, C_3H_6-0.2, C_3H_8-0.2	Carr, Kobayashi, and Burrrow	14.7-10030	77.7-150.2	Simulated high ethane content gas
He-0.8, N_2-15.8, CH_4-73.1, C_2H_6-6.1, C_3H_8-3.4, i-C_4H_{10}-0.2, n-C_4H_{10}-0.6	Carr, Kobayashi, and Burrrow	14.7-9580	79.7-150.4	High nitrogen content natural gas
N_2-0.3, CH_4-95.6, C_2H_6-3.6, C_3H_8-0.5	Carr, Kobayashi, and Burrrow	14.7-8465	85.1-220	Simulated low ethane content gas
C_2H_4	Comings, Mayland, and Egly	74.6-2513	86-203	
C_2H_4	Gonikberg	<2500	75-158	
CO_2	Golubev	<2500	122-212	
CO_2	Comings, Mayland, and Egly	65-2013	104	
CO_2	Phillips	14.7-1764	68-104	
C_3H_8	Comings, Mayland, and Egly	64.6-614.3	86-220	
Note: Composition is in mole percent				

Another inconvenience of Carr et al. correlation comes from the use of chart to get gas viscosity at interested point. As the advance of computer and more accurate calculations can be achieved by computer program, correlations are more desirable since computer program will calculate the viscosity through correlation but not charts or figures. Dempsey (1965) developed following correlation to replace Figures 2-18 and 2-19.

$$\ln\left[T_{pr}\left(\frac{\mu_g}{\mu_{1atm}}\right)\right] = a_0 + a_1 p_{pr} + a_2 p_{pr}^2 + a_3 p_{pr}^3 + T_{pr}\left(a_4 + a_5 p_{pr} + a_6 p_{pr}^2 + a_7 p_{pr}^3\right) + T_{pr}^2\left(a_8 + a_9 p_{pr} + a_{10} p_{pr}^2 + a_{11} p_{pr}^3\right) + T_{pr}^3\left(a_{12} + a_{13} p_{pr} + a_{14} p_{pr}^2 + a_{15} p_{pr}^3\right) \quad (2.52)$$

where

T_{pr} = Pseudo-reduced temperature,

p_{pr} = Pseudo-reduced pressure,

a_0-a_{15} = Coefficients of the equation, which are

a_0 = -2.46211820
a_1 = 2.97054714
a_2 = -0.28626405
a_3 = 0.008054205
a_4 = 2.80860949
a_5 = -3.49803305
a_6 = 0.360373020
a_7 = -0.01044324
a_8 = -0.793385684
a_9 = 1.39643306
a_{10} = -0.149144925
a_{11} = 0.00441015512
a_{12} = 0.0839387178
a_{13} = -0.186408848
a_{14} = 0.0203367881
a_{15} = -0.000609579263

2.3.5 Jossi-Stiel-Thodos Correlation (1962)

Basing upon the experimental data of pure components including argon, nitrogen, oxygen, carbon dioxide, sulfur dioxide, methane, ethane, propane, *i*-butane, *n*-butane, and *n*-pentane (Table 2-10), Jossi et al. (1962) developed a correlation for the viscosity of gas mixtures. The relationship between the residual viscosity modulus $\left(\mu_g - \mu^*\right)\xi$ and reduced density ρ_r is the cornerstone for Jossi-Stiel-Thodos correlation. The critical properties of the gas such as critical pressure, temperature, and density, interested pressure temperature, and the molecular weight are as inputs. Jossi-Stiel-Thodos correlation for normally behaving substances is expressed as follow:

$$\left[\left(\mu_g - \mu^*\right)\xi + 10^{-4}\right]^{\frac{1}{4}} = 0.1023 + 0.023364\rho_r + 0.058533\rho_r^2 - 0.0400758\rho_r^3 + 0.009332\rho_r^4 \quad (2.53)$$

where

$$\rho_r = \frac{\rho_g}{\rho_c} \quad (2.54)$$

$$\xi = \frac{T_c^{\frac{1}{6}}}{M_w^{\frac{1}{2}} p_c^{\frac{2}{3}}} \quad (2.55)$$

$$\mu^* = \frac{3.40 \times 10^{-4} T_r^{0.94}}{\xi} \text{ for } T_r \le 1.50 \quad (2.56)$$

$$\mu^* = \frac{1.778 \times 10^{-4}\left(4.58T_r - 1.67\right)^{5/8}}{\xi} \text{ for } T_r > 1.50 \quad (2.57)$$

where

ρ_c = Critical density, g/cc

ρ_g = Gas density, g/cc

ρ_r = Reduced density

T_c = Critical temperature, ^{o}K

T_r = Reduced temperature, ^{o}K

p_c = Critical pressure, atm

M_w = Molecular weight

μ_g = Gas viscosity, cp

μ^* = Gas viscosity at low pressures (1.47-73.5 psia), cp

Figures 2-20 and 2-21 compared the correlation with the experimental data for both normal behaving substances and substances investigated by Jossi.

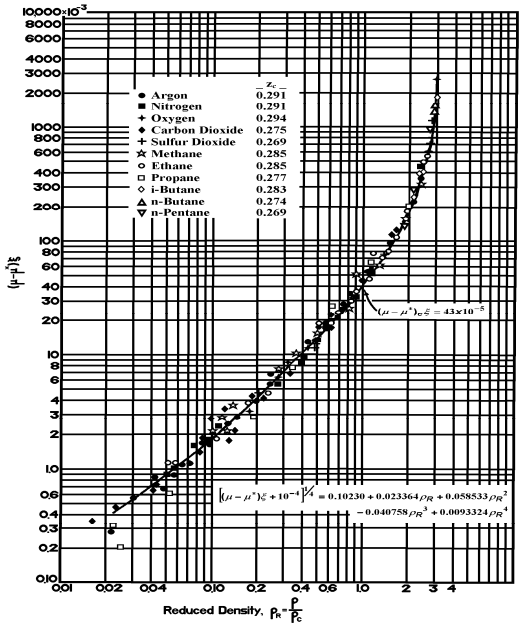

Figure 2-20. Relationship between the residual viscosity modulus $\left(\mu_g - \mu^*\right)\xi$ and reduced density ρ_r for normally behaving substances, after Jossi et al. (1962)

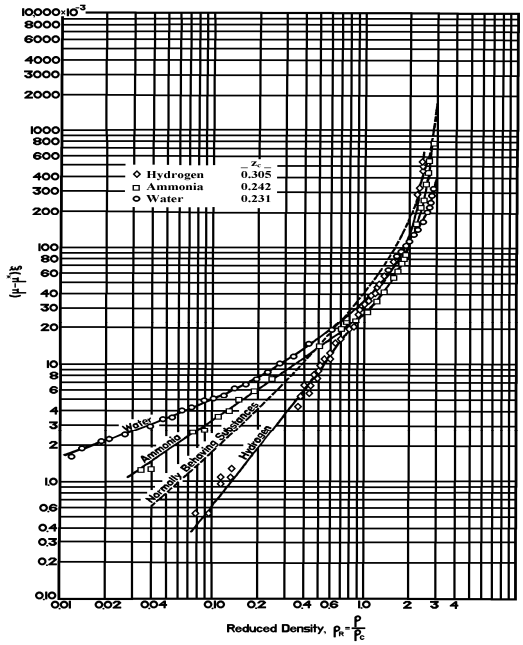

Figure 2-21. Relationship between the residual viscosity modulus $\left(\mu_g - \mu^*\right)\xi$ and reduced density ρ_r for the substances investigated, after Jossi et al. (1962)

Jossi-Stiel-Thodos correlation relied on pure substances. It may not be suitable for gas mixture. Its database covered methane viscosity data from Comings et al. (1940 and 1944), Baron et al. (1959), Swift et al. (1959), and Kuss (1952), which are in low to moderate pressure and temperature. Jossi reported approximately 4 percent average absolute error and also stated that this correlation should only be applied for values of reduced density below 2.0. We cannot endorse this correlation for HPHT condition before we have data to proof it.

Table 2-10. Viscosity-temperature-pressure data used for Jossi-Stiel-Thodos (1962) correlation

Composition	Investigators	Pressure psia	Temperature ^{o}F
Hydrogen	Gibson	323-1822	-330-(-321)
Hydrogen	Golubev	14.7-11760	-432-482
Hydrogen	Johns	14.7-1458	116-260
Hydrogen	Michels	294-44100	32-302
Hydrogen	Schaefer	<184875	-434-932
Hydrogen	van Itterbeek	220-12348	-343-(-298)
Argon	Iwasaki	14.7-735	68-86
Argon	Kiyama	14.7-1470	122-572
Argon	Michels	<29392	32-167
Argon	Rudenko	14.7	freezing point-boiling point
Nitrogen	Iwasaki	291-2770	76-301
Nitrogen	Michels	161-14196	77-167
Nitrogen	Rudenko	14.2-356	-333-(-297)
Nitrogen	Shubnikov	14.2-356	-333-(-297)
Oxygen	Galkov	17.7-356	-290-(-260)
Oxygen	Gibson	323-1822	-330-(-321)
Oxygen	Rudenko	14.2-356	-321-(-297)
Oxygen	van Itterbeek	4.2-356	-321-(-297)
Carbon Dioxide	Michels	<29392	32-167
Carbon Dioxide	Kiyama	14.7-1470	122-572
Carbon Dioxide	Michels	14.7-29400	32-167
Carbon Dioxide	Stakelbeck	14.7-294	-20-80

Table 2-10. Continued

Composition	Investigators	Pressure psia	Temperature ^{o}F
Sulfur dioxide	Awberry	< vapor pressure	5-86
Sulfur dioxide	Stakelbeck	14.7-294	<104
Ammonia	Carmichael	17-5915	100-400
Ammonia	Kiyama	14.7-1470	122-572
Ammonia	Shimotake	250-5000	212-392
Ammonia	Stakelbeck	14.7-294	-20-80
Water	Hawkins	14.7-2800	550-850
Water	Richter	normal pressure	<572
Water	Schille	normal pressure	282-1000
Water	Shugayev	normal pressure	282-1410
Water	Sigwart	normal pressure	282-1000
Water	Timroth	14.2-2845	482-842
Methane	Baron	114.7-8014.7	125-275
Methane	Comings, Mayland, and Egly	64.6-2513	86-203
Methane	Kuss	<8820	68-176
Methane	Swift	85-675	-220-(-115.6)
Ethane	Baron	114.7-8014.7	125-275
Ethane	Smith and Brown	749.5-4996.6	59-167
Ethane	Swift	25-716	-112-89.6
Propane	Baron	114.7-8014.7	125-275
Propane	Comings, Mayland, and Egly	64.6-614.3	86-220
Propane	Lipkin	<140	-100-100
Propane	Sage and Lacey	<2000	100-220
Propane	Smith and Brown	999-4996.6	203-374
Propane	Swift	50-620	-22-206
i-Butane	Lipkin	<140	-100-100
i-Butane	Sage and Lacey	<2000	100-220
n-Butane	Lipkin	<140	-100-100
n-Butane	Sage and Lacey	<2000	100-220
n-Butane	Swift	45-250	68-212
n-Pentane	Lohrenz	10000	253-286
n-Pentane	Reamer and Sage	15.7-5000	100-280

2.3.6 Lee-Gonzalez-Eakin Correlation (1970)

To honor natural gas in petroleum engineering and develop a gas viscosity correlation, Gonzalez et al. (1970) measured viscosities of eight natural gases for temperature from 100 to 340 oF and pressure from 14.7 to 8000 psia. Combining with some pure components such as methane, ethane, and propane (Table 2-11), Gonzalez et al. (1970) derived a correlation that is simpler than Carr-Kobayashi-Burrrow correlation to predict gas viscosity at reservoir conditions. The inputs required in Lee-Gonzalez-Eakin correlation are gas density, molecular weight of gas, and temperature. Equations 2.58 through 2.61 are used to get gas viscosity provided molecular and density at interested condition known.

$$\mu_g = 10^{-4} K \exp\left(X \rho_g{}^{Y}\right). \tag{2.58}$$

$$K = \frac{(9.379 + 0.01607 M_w) T^{1.5}}{209.2 + 19.26 M_w + T}. \tag{2.59}$$

where

$$X = 3.448 + \left[\frac{986.4}{T}\right] + 0.01009 M_w. \tag{2.60}$$

$$Y = 2.447 - 0.2224 X. \tag{2.61}$$

where

μ_g = Gas viscosity, cp

ρ_g = Gas density, g/cc

M_W = Molecular weight

T = Temperature, ^{o}R

Table 2-11. Viscosity-temperature-pressure data used for Lee-Gonzalez-Eakin (1970) correlation

Composition	Investigators	Pressure psia	Temperature ^{o}F	Memo
Methane	Gonzalez, Bukacek and Lee	200-8000	100-340	
Methane	Carr, Kobayashi, and Burrrow	14.7-8030	71-200	
Ethane	Eakin, Starling and Dolan	200-8000	77-340	
Propane	Starling, Eakin and Ellington	100-8000	77-280	
n-Butane	Dolan, Starling and Lee	1000-8000	100-340	
i-Butane	Gonzalez and Lee	100-8000	100-340	
n-Pentane	Lee and Ellington	2000-3000	100-340	
n-Decane	Lee and Ellington	200-8000	100-340	
2,2-Dimethylpropane	Gonzalez and Lee	100-8000	100-340	
Methane-propane mixtures	Gidding	14.7-8000	100-280	
Methane-*n*-Butane mixtures	Dolan, Ellington and Lee	200-8000	100-340	
Methane-*n*-Decane mixtures	Lee, Gonzalez and Eakin	Bubble point-7000	100-340	
N_2-0.6, CH_4-73.4, C_2H_6-25.6, C_3H_6-0.2, C_3H_8-0.2	Carr, Kobayashi, and Burrrow	14.7-10030	77.7-150.2	Simulated high ethane content gas
He-0.8, N_2-15.8, CH_4-73.1, C_2H_6-6.1, C_3H_8-3.4, i-C_4H_{10}-0.2, n-C_4H_{10}-0.6	Carr, Kobayashi, and Burrrow	14.7-9580	79.7-150.4	High nitrogen content natural gas
N_2-0.3, CH_4-95.6, C_2H_6-3.6, C_3H_8-0.5	Carr, Kobayashi, and Burrrow	14.7-8465	85.1-220	Simulated low ethane content gas
Eight natural gases	Lee, Gonzalez and Eakin	14.7-8000	100-340	Compositions are in Table 2-12

Table 2-12. Composition of eight natural gas samples (Gonzalez et al., 1970)

Sample No.	1	2	3	4	5	6	7	8
N2	0.21	5.2	0.55	0.04	-	0.67	4.8	1.4
CO2	0.23	0.19	1.7	2.04	3.2	0.64	0.9	1.4
He	-	-	-	-	-	0.05	0.03	0.03
C1	97.8	92.9	91.5	88.22	86.3	80.9	80.7	71.7
C2	0.95	0.94	3.1	5.08	6.8	9.9	8.7	14
C3	0.42	0.48	1.4	2.48	2.4	4.6	2.9	8.3
nC4	0.23	0.18	0.5	0.58	0.48	1.35	1.7	1.9
iC4	-	0.01	0.67	0.87	0.43	0.76	-	0.77
C5	0.09	0.06	0.28	0.41	0.22	0.6	0.13	0.39
C6	0.06	0.06	0.26	0.15	0.1	0.39	0.06	0.09
C7+	0.03	-	0.08	0.13	0.04	0.11	0.03	0.01
Total	100.0	100.0	100.0	100.0	100.0	100.0	100.0	100.0
Note: Composition is in mole percent								

In deriving this correlation, recommended viscosity values are based on smoothed plots of viscosity versus temperature, viscosity versus pressure. Lee-Gonzalez-Eakin correlation gives 2.0 percent average absolute error at low pressure and 4 percent at high pressure. It provides better result if gas specific gravity is less than 1.0. The correlation can be used to forecast gas viscosity at temperature from 100 to 340 ^{o}F and pressure from 100 to 8000 psi, according to Lee.

One of disadvantages of Lee-Gonzalez-Eakin correlation is that it uses density, molecular weight, and temperature as input variables to calculate natural gas viscosity. Petroleum engineers prefer pressure to density when they estimate gas viscosity in routine work because most of time pressure is easy to get instead of density.

Another disadvantage is this correlation does not consider natural gas that contains high percentage of non-hydrocarbon. We used nitrogen to test the validity of Lee-Gonzalez-Eakin correlation in predicting non-hydrocarbons viscosity. As our expected, it ended up with the conclusion that this correlation is unable to forecast non-hydrocarbons viscosity. Lab experiment in nitrogen viscosity illustrates that this correlation is

inappropriate for nitrogen. This will be shown in our result. In reality, non-hydrocarbons such as nitrogen, carbon dioxide, and hydrogen sulfide are often found in natural gas. As wells become deeper and deeper, more and more non-hydrocarbons are found in the gas reservoir, some reservoirs even have up to 50-60 percent of non-hydrocarbons. Gas reservoirs in South China Sea contain 55-60 volume percent of carbon dioxide and hydrogen sulfide. Sour gas reservoirs in East China Sea are discovered with 20-30 volume percent carbon dioxide. Development and production of sour gas require a correlation that can remove the effect of these non-hydrocarbons.

Lee-Gonzalez-Eakin correlation covers a relatively short pressure range. Its application in high pressure, i.e. greater than 10000 psi is still uncertain. Now more and more reservoirs discovered are deep and under high pressure and high temperature, and the major component of the reservoir fluids is methane. Therefore, a model that predicts methane viscosity at high pressure and temperature is desirable.

2.3.7 NIST Program

The National Institute of Standard and Technology (NIST) (2000) provides a program, NIST reference fluid thermodynamic and transport properties-REFPROP (Lemmon, 2007), version 8.0, through which thermodynamic and transport properties of hydrocarbon can be estimated. Not only pure components, but also mixtures containing up to 20 components can be input into the program to get their thermodynamic properties. The range of the pressure and temperature are up to 44100 psi and 1340 ^{o}F, respectively. In REFPROP, viscosity and is modeled with either an extended corresponding states method, or in some cases the friction theory method. Gas viscosity can be obtained from this program, but one thing needed to be aware is that the program predicts the fluid properties using correlation developed at low-moderate pressure and temperature. The correlations were based on the lab data collected from literatures. Comparing densities of methane and nitrogen from NIST program with lab data from

literatures (Boyd, 1930; Bicher and Katz, 1943; Carr, 1952; Iwasaki, 1954; Ellis and Raw, 1959; Golubev, 1959; Swift et al., 1959; Barua et al., 1964; Wilson, 1965; Dipippo et al., 1966; Lee et al., 1966; Gonzalez et al., 1966; Van Itterbeek et al., 1966; Helleman et al., 1970; Latto and Saunders, 1972; Stephan and Lucas, 1979; Diller, 1980; Diller, 1983; Straty and Diller, 1980; Setzmann and Wagner, 1991; Nowak et al., 1997a; Nowak et al., 1997b; Klimeck et al., 1998) indicates that differences are so small thus can be neglected (Figures 2-22 and 2-23). It is also noted that density data covers low to high pressure and temperature. Pressure range for methane and nitrogen densities are 3.6 to 72518 and 14.7 to 7350 psia, respectively. Temperature range for methane and nitrogen densities are 8.3 to 656.3 and 32 to 476.3 ^{o}F, respectively. As a result, these available density data can be used to derive our new gas viscosity correlation at low to high pressure and temperature. Comparing viscosities of methane and nitrogen from NIST program with lab data from literatures (Earhart, 1916; Boyd, 1930; Bicher and Katz, 1943; Comings et al., 1944; Van Itterbeek et al., 1947; Carr, 1952; Iwasaki, 1954; Ross and Brown, 1957; Ellis and Raw, 1959; Kestin and Leidenfrost, 1959; Swift et al., 1959; Golubev, 1959; Swift et al., 1959; Flynn et al., 1963; Barua et al., 1964; Wilson, 1965; Dipippo et al., 1966; Lee et al., 1966; Gonzalez et al., 1966; Van Itterbeek et al., 1966; Helleman et al., 1970; Diehl et al., 1970; Latto and Saunders, 1972; Stephan and Lucas, 1979; Diller, 1980; Diller, 1983) indicates differences are so small thus can be neglected (Figures 2-22 and 2-23). Pressure range for methane and nitrogen viscosities are 14.7 to 11757 and 14.5 to 14504 psia, respectively. Temperature range for methane and nitrogen viscosities are 77 to 482 and -342.7 to 1880 ^{o}F, respectively. As a result, these available density and viscosity data can be used to derive our new gas viscosity correlation. As more and more studies are conducted on gas viscosity at high pressure and high temperature, the validity of extrapolating correlations that are derived from low-moderate pressure and temperature condition to predict gas viscosity at high pressure and high temperature is doubted. NIST indicates that they will update their database as more data available.

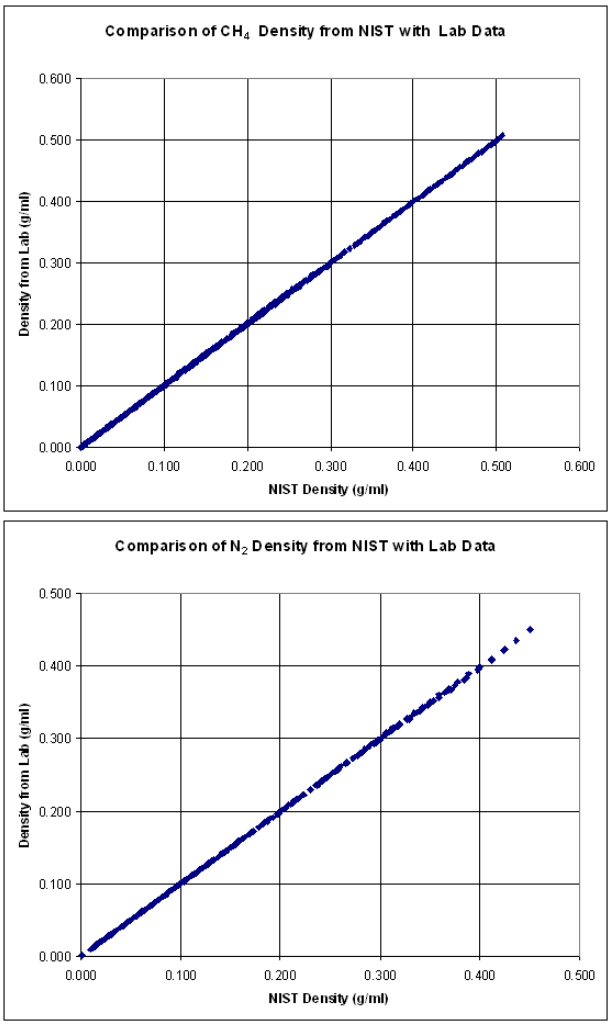

Figure 2-22. Comparisons of CH4 *(top)* and N2 *(bottom)* densities between NIST values and lab data

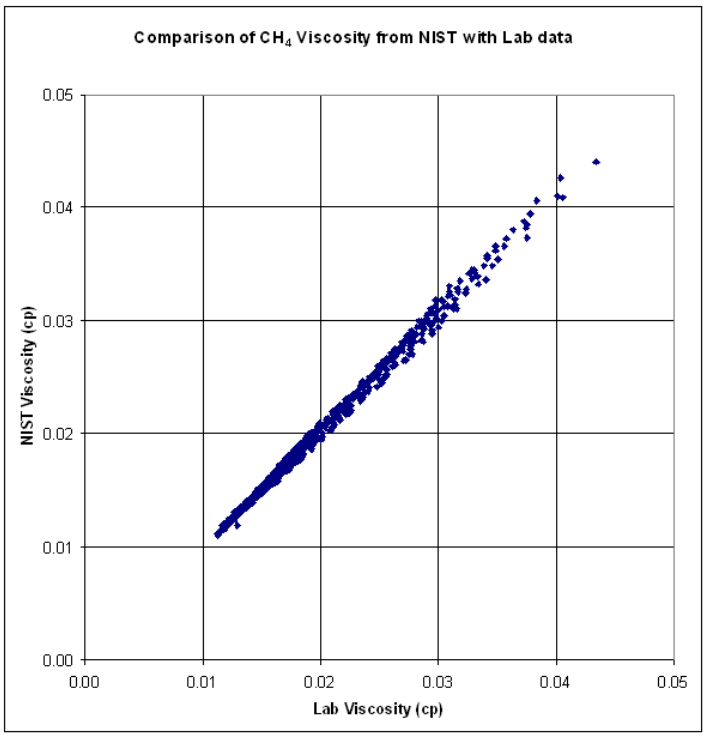

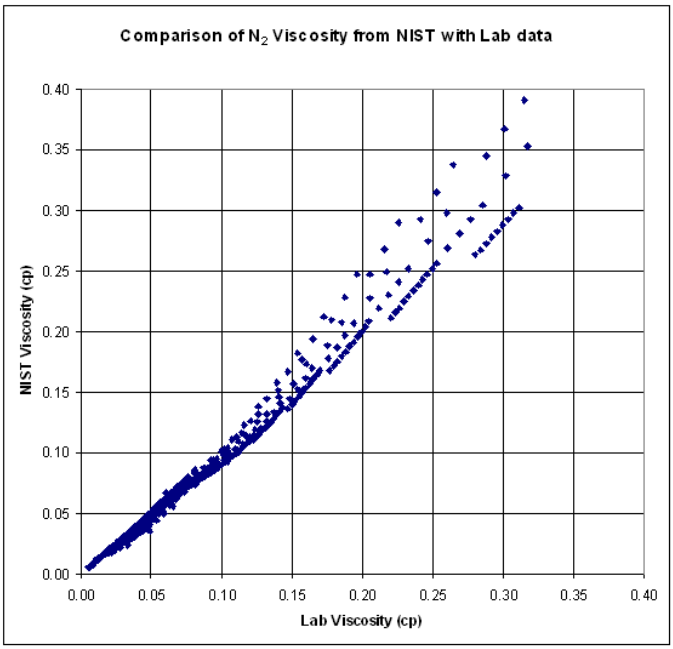

Figure 2-23. Comparisons of CH4 *(top)* and N2 *(bottom)* viscosities between NIST value and lab data

2.3.8 Londono Correlations (2001)

Londono (2001) collected a total of 13656 data points from former investigators to optimize Jossi-Stiel-Thodos and Lee-Gonzalez-Eakin gas viscosity correlations and Dranchuk-Abou-Kassem and Nishimi-Saito gas density correlations. Londono indicated that these data points have properties such as composition, viscosity, density, temperature, pressure, pseudoreduced properties, and gas compressibility factor from hydrocarbon and non-hydrocarbon. He used this database to evaluate the applicability of the existing models to determine hydrocarbon gas viscosity and density (or gas z-factor, then calculate gas density using EOS). In addition, he developed new models/calculation approaches to determine hydrocarbon viscosity and provided an optimization of the existing equations-of-state (EOS) for the calculation of the gas z-factor. In brief, Londono modified existing correlations' coefficients or constants basing on his database with nonlinear least-square statistical method, while kept the original forms unchanged. The optimized Jossi-Stiel-Thodos correlation is

$$\left[\left(\mu_g - \mu^*\right)\xi + 10^{-4}\right]^{\frac{1}{4}} = 0.170018 + 0.990675\rho_r - 0.407490\rho_r^2 - 0.066959\rho_r^3 + 0.007359\rho_r^4 \tag{2.62}$$

where

$$\rho_r = \frac{\rho_g}{\rho_c} \tag{2.63}$$

$$\xi = \frac{T_c^{4.76271}}{M_w^{3.83480} p_c^{2.72582}} \tag{2.64}$$

where

ρ_c = Critical density, g/cc

ρ_g = Gas density, g/cc

ρ_r = Reduced density

T_c = Critical temperature, ^{o}K

p_c = Critical pressure, atm

M_w = Molecular weight

μ_g = Gas viscosity, cp

μ^* = Gas viscosity at low pressures (1.47-73.5 psia), cp

ξ = Viscosity parameter

The optimized Lee-Gonzalez-Eakin correlation is

$$\mu_g = 10^{-4} K \exp\left(X \rho_g{}^{Y}\right). \tag{2.65}$$

$$K = \frac{(19.9216 + 0.0326212 M_w) T^{1.38392}}{210.076 + 18.5762 M_w + T}. \tag{2.66}$$

where

$$X = 3.84699 + \left[\frac{991.303}{T}\right] + 0.00924455 M_w. \tag{2.67}$$

$$Y = 2.11068 - 0.136279 X. \tag{2.68}$$

where

μ_g = Gas viscosity, cp

ρ_g = Gas density, g/cc

M_W = Molecular weight

T = Temperature, ^{o}R

It is obvious that Londono optimized existing gas viscosity and density correlations (or gas z-factor, then calculate gas density using EOS) and developed new gas viscosity and density correlations all basing on his collected database. He did not perform experiment by himself, thus no new data were added to the database. A review of his database showed that the highest pressures for hydrocarbons/natural gas and nonhydrocarbons (N_2, CO_2) viscosity data are 11760 and 14708 psia, respectively. It should be noted that correlation is only as good as experimental data it based on. Therefore, we can conclude that the uncertainty of Londono correlations at HPHT still exists.

2.3.9 Sutton Correlation (2005)

Sutton (2005) collected 5881 data points of gas viscosity data done by Gonzalez et al. (1970), Knapstad et al. (1990), Canet et al. (2002), Audonnet and Padua (2004), and Elsharkawy (2004) to developed a correlation. His database consists of viscosity data for methane, propane, methane-propane, methane-butane, methane-n-decane and natural gas viscosity. The methane-decane binary mixtures also used to estimate the behavior of a gas condensate that has a large heptanes-plus component. The database in which the correlation is based upon does not include the pure methane viscosities data above 10,000 psi, therefore Sutton correlation is not proved to be suitable for HPHT gas reservoirs. Sutton correlation is as follow:

$$\mu_{gsc}\xi = 10^{-4}[0.807T_{pr}^{0.618} - 0.357\exp(-0.449T_{pr}) + 0.340\exp(-4.058T_{pr}) + 0.018]. \quad (2.69)$$

$$\mu_g = \mu_{gsc}\exp\left(X\rho_g{}^{Y}\right). \quad (2.70)$$

where

$$\xi = 0.949\left(\frac{T_{pc}}{Mw^3 p_{pc}^4}\right)^{\frac{1}{6}}. \quad (2.71)$$

$$X = 3.47 + \left[\frac{1.588}{T}\right] + 0.0009Mw. \quad (2.72)$$

$$Y = 1.66378 - 0.04679X. \quad (2.73)$$

where

M_w = Molecular weight

p_{pc} = Pseudocritical pressure, psia

T = Temperature, ^{o}R

T_{pc} = Pseudocritical temperature, $^{\circ}$R

T_{pr} = Pseudoreduced temperature

μ_g = Gas viscosity, cp

μ_{gsc} = Low pressure gas viscosity, cp

ρ_g = Gas density, g/cc

ξ = Viscosity normalizing parameter

2.3.10 Viswanathan Correlation (2007)

Viswanathan (2007) used a Cambridge Viscosity SPL440 viscometer to measure the viscosity of pure methane. He measured methane viscosity at temperature of 116, 152, 188, 224, and 260 ^{o}F and pressure from 4500 to 20000 psia. Using NIST values at temperatures of 100, 150, 200, 250, 300, 350, and 400 ^{o}F and pressure from 5000 to 30000 psia with interval of 1000 psia, Viswanathan modified Lee-Gonzalez-Eakin correlation as follows:

$$\mu_g = K \exp\left(X\rho_g{}^{Y}\right). \tag{2.74}$$

$$K = \frac{0.0001*(5.0512 - 0.2888M_w)T^{1.832}}{-443.8 + 12.9M_w + T}. \tag{2.75}$$

where

$$X = -6.1166 + \left[\frac{3084.9437}{T}\right] + 0.3938M_w. \tag{2.76}$$

$$Y = 0.5893 - 0.1563X. \tag{2.77}$$

where

μ_g = Gas viscosity, cp

ρ_g = Gas density, g/cc

M_W = Molecular weight

T = Temperature, ^{o}R

Summary, no measured gas viscosity at high pressure and high temperature is available so far. Thus correlations derived from data obtaining at low-moderate pressure and temperature cannot be simply extrapolated to high pressure and high temperature

conditions. Experiments that measure gas viscosity at high pressure and high temperature must be conducted before we derived correlation that can predict gas viscosity accurately. As a result, a correlation covered both low and high pressure and temperature is highly recommended. But it needs measured data as its solid base.

CHAPTER III

OBJECTIVE

Because a good correlation needs a wide range viscosity data as its cornerstone, the lack of methane and nitrogen viscosity at HPHT required we put enormous effort towards the viscosity of pure methane and nitrogen at HPHT. By adding methane and natural gas viscosity at high pressures and high temperatures, a new correlation can be derived to predict gas viscosity at HPHT.

Another fact needed to be addressed is that more nitrogen is found as we move to high pressure and high temperature reservoirs. High concentration nitrogen in natural gas affects not only the heat value of natural gas but also gas viscosity, which is critical to petroleum engineering. The importance of gas viscosity is seen in its contribution in the resistance to the flow of a fluid both in porous media and pipes during gas production and transportation. Nitrogen is also one of common inject gases in gas injection projects, thus an accurate estimation of its viscosity is vital to analyze reservoir performance. Due to lack of correlation for nitrogen viscosity and the fact that hydrocarbon viscosity correlation is inappropriate for nitrogen viscosity, a new correlation that is tailored for nitrogen viscosity will be derived based on our experimental data. It provides a good approach to get nitrogen viscosity at HPHT.

CHAPTER IV

METHODOLOGY

4.1 Experiment Facility

As mention before we need viscosity at HPHT to develop a new correlation through which accurate viscosity can be guaranteed. To fill the viscosity data we will put our effort in measuring gas viscosity at HPHT through appropriate facility. Falling-body principle is employed in setup our experimental facility. Dr. Teodoriu, Dr. McCain, Mr. Anup Viswanathan, and Mr. Frank Platt (Viswanathan, 2007; Viswanathan and McCain, 2005; Viswanathan et al., 2006) prepared and installed this delicate apparatus. The facility consists of gas source, gas booster system, temperature control system, measuring system, and data acquisition system. Figure 4-1 shows the setup of apparatus. Figure 4-2 illustrates the layout of facility. Following is a detail description of the facility.

Figure 4-1. The setup of apparatus for this study

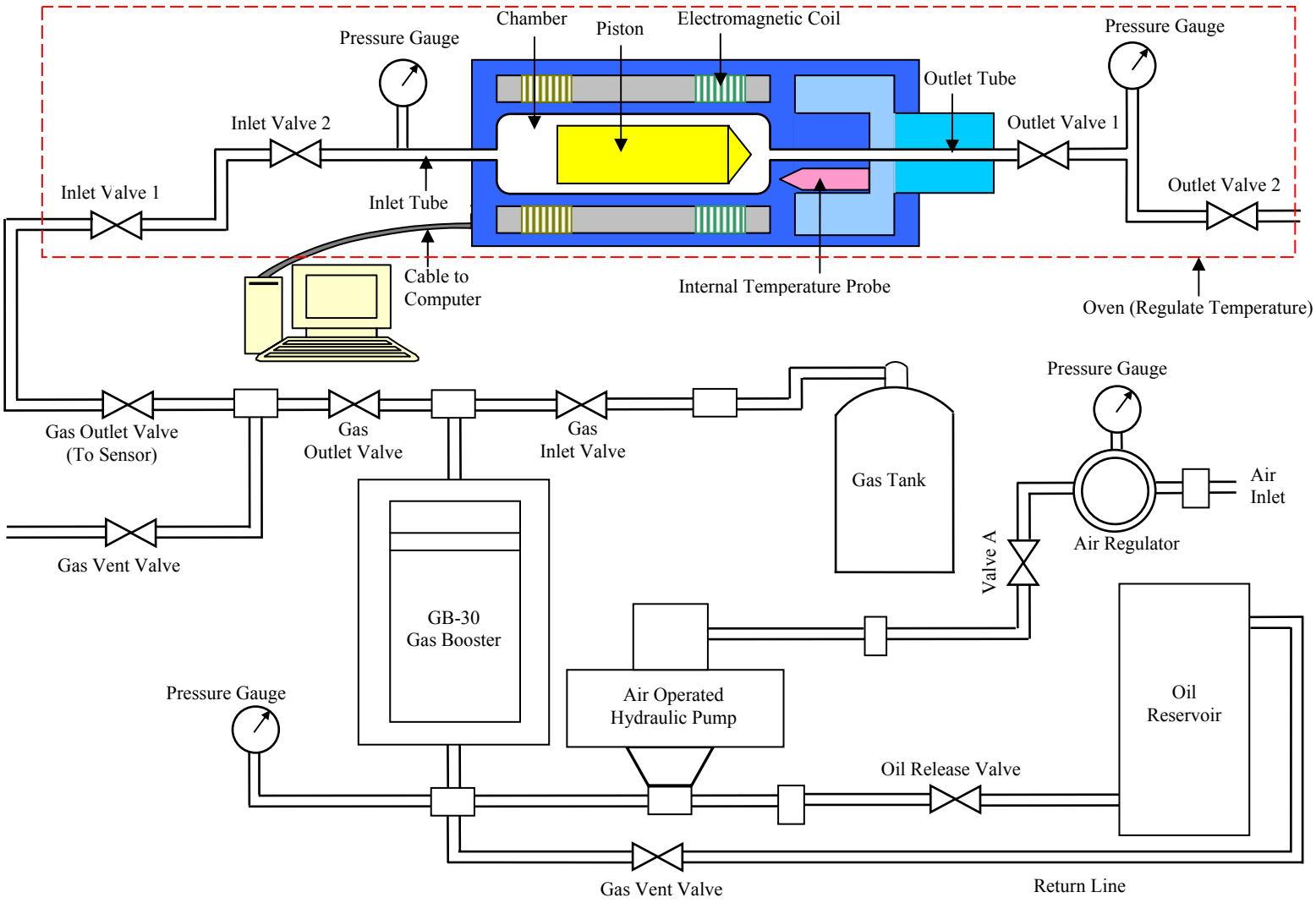

Figure 4-2. Schematic of experimental facility

4.1.1 Gas Source

The gas we used for viscosity measurement is nitrogen, methane, and air. A gas tank that supplies low pressure gas is used as original source. Gas tank is connected to the inlet of gas booster system where gas is compressed to high pressure for measurement. Through gas booster system we can compress gas from 1000 psi to 25000 psi.

4.1.2 Gas Booster System

Since the gas tank cannot provide pressure required by experiment, a gas booster system was used to compress the gases to high pressures that match the requirement. The gas booster system is consisting of a hydraulic pump coupled with the gas booster cylinder to increase the pressure of a given gas sample. The gas booster system as used in this project was manufactured by High Pressure Equipment Company. It belongs to Model GBS-30 (Figure 4-3) which means it is rated for use up to 30,000 psi and has a one-to-one ratio. Displacement per stroke is 112 cubic inches (1835 ml). Model GBS-30 is complete and ready to operate. All that is required is an air supply for the pump and a commercially available container of compressed gas.

Figure 4-3. Gas booster system used to compress gas in this study

The gas booster system includes manual valves, air regulator, filter and lubricator, air gauge, high pressure gauge, reservoir, oil filter, pump, gas booster and related high pressure tubing and fittings. The two major parts are air operated hydraulic pump which uses house air at a pressure of 70 psia to pump hydraulic oil out of the oil reservoir and the gas booster cylinder which contains a piston to separate the oil and the gas.

Operation is by means of an air operated hydraulic pump which pressurizes one end of the gas booster which then compresses the gas in the opposite end of the booster. To accomplish this, the gas inlet valve is opened to permit gas to fill the gas end of the booster. Check valves are provided to permit gas flow in one direction only. With the gas outlet valve open, the hydraulic pump is operated in order to pressurize the hydraulic end of the booster. Thus, the gas is compressed in the booster. If required pressure is not reached by the end of the stroke, the gas booster can easily be recycled for additional strokes. Note the gauge on these systems is connected to the hydraulic side of the booster. On the Model GBS-30 which has a 1 to 1 ratio, there is a direct reading of the pressure in the gas end of the booster.

There are some drawbacks with the proto gas booster system. One of them is that the rate of release of high pressure gas from the system is hard to be regulated, whereas the gas outlet valve supplied is inadequate for this measure of control. Another difficulty is the rate of release of oil from the gas booster cylinder cannot be controlled accurately. An excessively rapid drop in pressure can cause the o-rings in the gas booster cylinder to disintegrate and this can have dangerous implications. In order to improve the system to be more efficient and safe, some changes were made to the gas booster system in the laboratory. An extra pressure transducer was attached to the gas line since the main pressure gauge on the gas booster system was connected to the oil line and this only approximately described the true gas pressure. A couple of micro-tip controlled valves were installed to help in carefully regulating the high pressure gas, and the vented oil.

Followings are the steps to operate the gas booster system:

1) All the valves are initially closed. The cylinder which contains the gas sample is connected to the inlet of the gas booster system and cranked open. The inlet valve in the gas booster system is also opened. All other valves are in the close position. Gas starts to fill in the gas booster cylinder pushing the piston down.
2) The oil vent valve is now opened to allow for any remaining hydraulic oil in the gas booster cylinder to trickle into the oil reservoir. This ensures that the cylinder is now completely filled with the gas sample alone. The gas inlet valve is now closed.
3) Valve A, the master valve for supplying air to the pump is opened and then the air regulator is slowly opened to the desired level. This sets the pump in motion and oil starts coming in from the bottom of the gas booster cylinder. The oil vent valve should now be closed to allow the oil to accumulate in the cylinder.
4) On opening the air regulator further, more and more oil passes into the gas booster cylinder from the oil reservoir. This causes a reduction of volume of the gas sample thus increasing the pressure.
5) When the desired pressure has been reached, both Valve *A* and the air regulator should be closed so that the pressure does not keep increasing.
6) The gas outlet valve can now be opened to supply high pressure gas as required.
7) When the experiments have ceased, the oil vent valve is now carefully opened to release the oil back into the reservoir. This causes an increase in volume of the gas and causes the pressure to go down.
8) The gas vent valve can now be opened to purge any remaining gas from the system.

The high pressure gas from the gas booster system is now available to be connected to the measurement sensor for the measurement of gas viscosity.

4.1.3 Temperature Control System - Oven

The temperature of the measuring system is controlled by a mechanical convection oven, which was manufactured by Yamato Scientific America Inc. The measuring system was placed inside the oven. The oven mode is DKN400 (Figure 4-4) with electric capacity of 115V AC, 12A and temperature setting range from 0 to 320 ^{o}C . The overheat protection function incorporated into the oven prevents the damage to oven and measuring system in case of human error. With this oven we can manipulate the measuring temperature as we want. One drawback of this setup is that it usually takes 5 to 6 hours for temperature reaching constant when we change to a new temperature own to the fact that the convection medium used to transfer heat to measuring system is air.

Figure 4-4. The temperature control system in this study

4.1.4 Measurement System - Cambridge Viscometer

Every type of viscometer has its advantages and disadvantages. In this research a modified falling body viscometer is used to measure gases viscosity at HPHT. The

viscometer we used is Cambridge Viscosity SPL440 viscometer. It is a piston-style viscometer designed by Cambridge Viscosity, Inc. exclusively for measuring viscosities of petroleum fluids, oils and gases. The measurable range of the gas viscosity is from 0.02 to 0.2 cp. The accuracy of the VISCOpvt is reported to be around 1% of full scale of range. Its operating pressure is up to 25000 psi, respectively. The viscometer schematic is shown in Figure 4-5. The Cambridge VISCOpvt works on the principle of a known piston traversing back and forth in a measuring chamber containing the fluid sample. The piston is driven magnetically by two coils located at opposite ends. The time taken by the piston to complete one motion is correlated to the viscosity of the fluid in the measuring chamber by a proprietary equation.

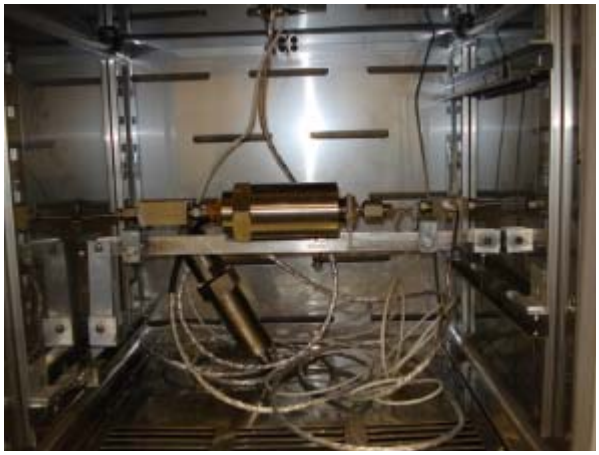

Figure 4-5. Schematic of the measurement system in this study

There are some disadvantages with the original SPL440 viscometer to measure gas viscosity. First, the viscometer was initially supplied in the oil measurement mode, where the measurement chamber is inclined at an angle of 45° from the horizontal. The time of travel becomes very short if the medium is gas. Thereby the accuracy of the travel time cannot be guaranteed. This problem is overcome by making the whole arrangement horizontal or nearly horizontal. Keeping it horizontal gives the added advantage of nullifying any gravity effects. Another disadvantage is that the prototype cannot work efficiently with only two valves used to control the flow of fluid with one at

the inlet tube and another at the outlet tube. These two valves are installed far away from the cell. Therefore it requires large volume of test sample. This installation also increases the time for gas to reach equilibrium considering the pressure difference between two ends of the cell caused by the movement of piston. Dr. Teodoriu modified the configuration of the original design by one pressure gauge at the inlet (very close to the cell), one more valve at the inlet, and one more valve at the outlet. This modification drastically reduces the time to reach equilibrium and cut down the required volume of test sample to 30-40 %. Pressure gauge close to the cell provides more accurate data than before.

The general procedures to operate the viscometer are:

1) After the installation of the whole experiment facility and gas in gas booster system had been compressed and ready to be used, connect the inlet end of the viscometer to the outlet line of the gas booster system.
2) Adjust the sensor's temperature to the desired temperature by regulating the oven temperature.
3) Open outlet valve of viscometer; open inlet valve of viscometer; open the outlet valves at the gas booster system. Let the gas from gas booster system purge the existing gas in the chamber and flow line for about one minute.
4) Now close the outlet valve of viscometer; keep inlet valve of viscometer open to fill the chamber with measured gas until the pressure reaches the desired value.
5) Close inlet valve of viscometer; wait for the temperature in the chamber becomes constant.
6) Adjust the pressure to the measured pressure; close the outlet valve of viscometer; close the inlet valve of viscometer.
7) Start to measure gas viscosity at certain pressure and temperature.
8) After finish one measurement, keep temperature constant and change pressure to other value to continue another measurement.

9) When the experiment finishes, close the outlet valves at the gas booster system; close the inlet valve of viscometer; open outlet valves to vent gas.

4.1.5 Data Acquisition System

The Cambridge viscometer was also supplied with RS-232 serial communication support, allowing the data measured by the viscometer to be synchronized with a desktop computer. We setup a new recording control panel through which the measurement is controlled (Figure 4-6). This gives the provision to save the data for later analysis. The software used to record the measured data is ViscoLab. Through data acquisition system we can output measured pressure, average temperature, average gas viscosity, current temperature, and current gas viscosity. The measured interval can be adjusted as requirement. With this system, manual recording of the experiment is not necessary and large storage of measurement data becomes feasible.

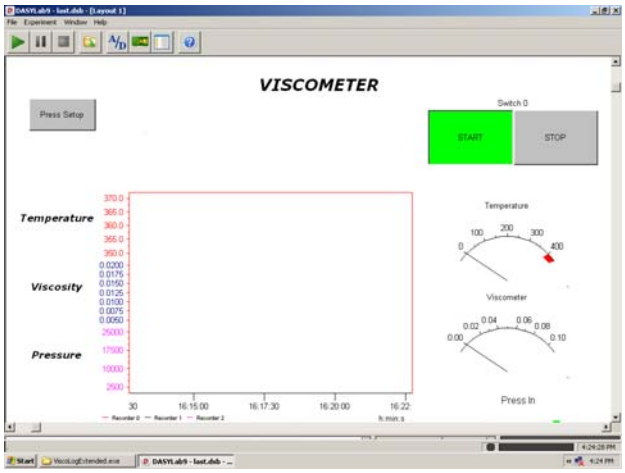

Figure 4-6. Recording control panel to control the experiment

4.2 Experiment Procedure

The measurement in this stage is limited to nitrogen and methane. We started experiment with measuring nitrogen viscosity considering safety and easy calibration. Constrained

by the viscometer measurement capacity of 0.02-0.2 cp and the viscometer rated pressure of 25000 psig, we selected 3000 psi as the minimum pressure and 25000 psig as the maximum for nitrogen. After finishing some experiments or particular time interval, the facility was disassembled and all components were cleaned. These were done because after particular period there are some contaminants trapped inside the chamber and piston (Figure 4-7) will introduce system error to the measurement. After the cleaning, all parts were assembled and ready to be used immediately. As we finished the experiment on nitrogen viscosity, we switched to methane viscosity. We selected 4000 psi as the minimum pressure and 25000 psig as the maximum for methane because the viscometer cannot provide accurate data at pressure less than 4000 psig.

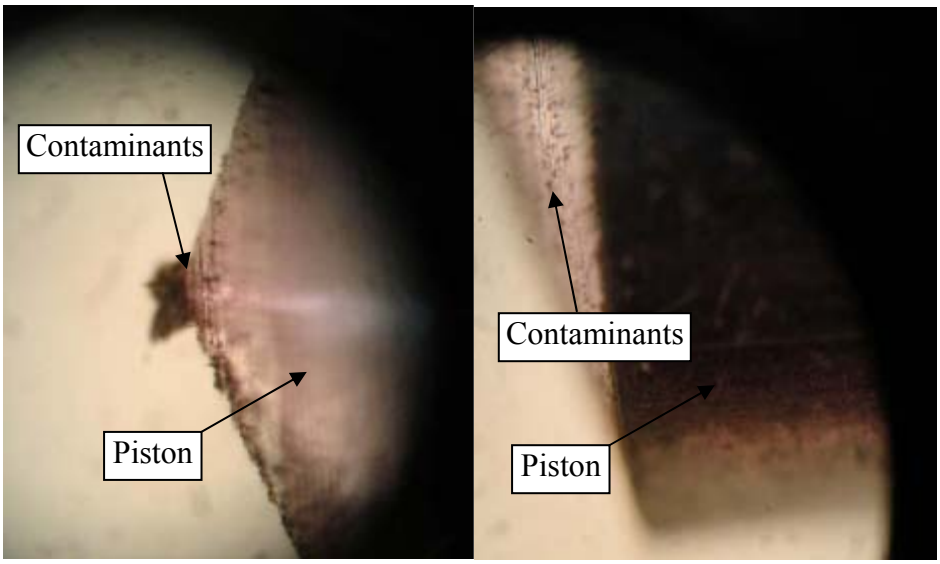

Figure 4-7. Contaminants trapped on the piston

We decide the measurement procedure according to 1) the time required reaching temperature equilibrium in measurement system is much longer than the time to reach pressure equilibrium in the system, while the time for pressure reaching equilibrium takes less than 10 seconds, 2) safety and data calibration requirements, 3) the viscometer rated pressure and temperature, and 4) enough measuring data point to develop viscosity

correlation. Therefore temperature will be the same and only the pressure is changed in an experiment. After completing one experiment, we change to another temperature.

The following steps are used to implement our experiments:

1) We start experiment on measuring nitrogen viscosity. The first experiment is at lowest temperature.
2) Set the temperature at the desired value and wait until temperature in the measuring system becomes constant. This may take 5-7 hours.
3) In an experiment, we begin the measurement from lowest pressure of 3000 psi and keep temperature constant. The measurement of viscosity at particular pressure and temperature usually lasts 15-30 minutes.
4) Increase the pressure by 500 psi while keep temperature stable, measure viscosity at this pressure and temperature for 15-30 minutes.
5) Continue the measurement by increasing the pressure until we reach the highest pressure, which is $\leq$ 25000 psig, and always keep temperature constant during this step, then measure viscosity at this pressure and temperature for 15-30 minutes.
6) Decrease the pressure by 500 psi and keep temperature constant at the same time, and then measure viscosity at this pressure and temperature for 15-30 minutes.
7) Keep reducing pressure until touching the lowest pressure and keep temperature constant at the same time, again measuring time for each pressure and temperature is 15-30 minutes. So far we finish one experiment.
8) Steps 3-7 are repeated several times to understand the repeatability of the measurement, i.e., we measure viscosity at same pressure and temperature several times.
9) Through Steps 3-8 we finish the measurement for one temperature. We change the temperature and wait 5-7 hours until it becomes constant, then repeat Steps 3-8 to get viscosity for this new temperature.

10) Continue to more temperatures until we finish measurement of nitrogen viscosity.
11) Upon completing nitrogen viscosity measurement we transfer to methane and repeat the same step we measure nitrogen viscosity.

The cleaning of the viscometer is dependent on the number of experiments or the viscometer running time. Repeated measurement provides abundant data for calibration in the data analysis.

4.3 Measurement Principle of Viscometer in This Study

The knowledge of geometry of measuring cell is important to understand the principle behind the measurement. The cell is a cylinder-shaped chamber with a piston inside (Figures 4-1 and 4-8). Table 4-1 lists the dimension of chamber and piston.

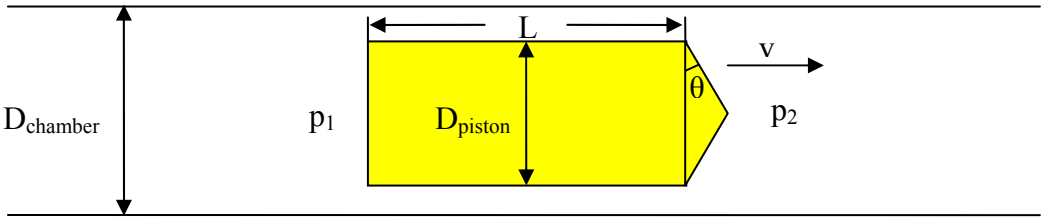

Figure 4-8. Piston moves inside of chamber of viscometer using in this study

Table 4-1. The dimension of chamber and piston (Malaguti and Suitter, 2010)

Piston		
Overall Length of Piston (Include the cone)	0.9412	inches
Length of piston flank(rectangle part, exclude height of cone)	0.87658	inches
Outer diameter of Piston	0.312	inches
Base angle of the cone (θ)	22.5	degree
Height of the cone	0.06462	inches
Surface area of the cone(exclude base area)	0.07808	in^2
Surface area of the piston flank (exclude the base and cone)	5.50773	in^2
Weight of piston	4.807	g
Chamber		
Inner diameter of chamber	0.314	inches
Length of chamber	1.4	inches

In our study, the viscometer is placed horizontally. Therefore the chamber and piston are in horizontal position. Figure 4-8 shows the cut away view of chamber inside which a piston is moving from left to right. The piston is driven by an electromagnetic force. For simplification, the following assumptions are made:

1) The time to accelerate is negligible or very short time for piston from static to reach constant speed. This is because the acceleration time is very small compared to the 2-way piston travel time. The flow in annulus is steady-state flow.
2) A known, constant electromagnetic force applied during one way travel.
3) Piston is moving in the center of chamber and does not touch the chamber wall.
4) Fourth assumption is that both piston and chamber built from same material and have same roughness.
5) The test fluid is Newtonian.
6) Gas viscosity is uniform throughout the chamber. Actually the pressure difference between two ends of piston is 0-10 psi, which is very small comparing with 3000-25000 psig measuring pressure, thus the variation of viscosity with pressure can be neglected. So does the density.

7) Pressure drop along the annulus between piston and chamber is mainly friction pressure drop, and the contribution from kinetic energy change is so small that it is negligible.
8) For the laminar flow there is no slip on the surfaces of chamber and piston.

Assumption 7) can be proved by the first law of thermodynamics or the principle of conservation of energy based on the uniform constructions of chamber and piston and the pressure difference in assumption 6).

Forces on piston can be analyzed in two dimensions, horizontal and vertical directions. For the purpose of this study, vertical forces are not considered. In horizontal direction, when the piston moves with a constant velocity, v, the pressure in front of the piston is higher than that behind the piston. In addition, the fluid flowing from the front of piston through the annulus between piston and chamber wall to back of piston results in the drag forces on the cone and flank of piston. Because the chamber and piston are in horizontal position, the potential energy change is zero. As a result the piston is subjected to five forces, the electromagnetic force, the drag force on the cone surface, the drag force on the flank of the piston, the fluid forces in front of and behind the piston. According to the force equilibrium, we have the following form.

$$F_{em} + F_{behind} = DF_{piston\ cone} + DF_{piston\ flank} + F_{front} \tag{4.1}$$

where

F_{em} = Electromagnetic force,

$DF_{piston\ cone}$ = Drag force on the cone surface,

$DF_{piston\ flank}$ = Drag force on the flank of the piston,

F_{front} = Fluid force in front of the piston,

F_{behind} = Fluid force behind the piston.

The fluid force behind the piston is

$$F_{behind} = p_1 A_{piston\ base} = \pi \frac{D_{piston}^2}{4} p_1 \tag{4.2}$$

where

p_1 = Pressure behind the piston,

$A_{piston\ base}$ = Area of base of piston.

The fluid force in front of the piston is

$$F_{front} = p_2 A_{cone\ base} = p_2 A_{piston\ base} = \pi \frac{D_{piston}^2}{4} p_2 \tag{4.3}$$

where

p_2 = Pressure in front of the piston,

$A_{cone\ base}$ = Area of base of cone.

The drag force on the flank of the piston can be derived according to the flow regime of fluid flowing around the piston. The drag force will be analyzed in two cases. One is laminar flow and another is turbulent flow. When piston moves at a constant velocity the volume of the fluid displaced by the piston is equal to the volume flows through the annulus during a specific time interval, Δt. we have

$$V_{displacing} = V_{displaced} \tag{4.4}$$

where

$V_{displacing}$ = Displacing volume when piston moves ahead,

$V_{displaced}$ = Displaced fluid volume that flows through annulus and back to the behind of piston.

The displacing and displaced volumes can be expressed by

$$L_{displacing} A_{piston\ base} = L_{fluid\ \ flow} A_{annulus} \tag{4.5}$$

in terms of travel distance and cross section area.

where

$L_{displacing}$ = Travel distance of piston during a specific time interval,

$L_{fluid\ \ flow}$ = Travel distance of fluid flow in annulus during a specific time interval,

$A_{annulus}$ = Cross section area of annulus.

Replacing travel distance with velocity and time interval and knowing that annulus area is the difference between chamber cross section area and piston base area, we obtain

$$v_{piston}\Delta t A_{piston\ base} = \bar{v}_{fluid}\Delta t\left(A_{chamber} - A_{piston\ base}\right) \tag{4.6}$$

where

v_{piston} = Piston velocity,

$\bar{v}_{fluid}$ = Mean fluid flow velocity,

Cancelling out the same term on both hand sides and expressing area in diameter results in

$$v_{piston}\frac{\pi}{4}D_{piston}^2 = \bar{v}_{fluid}\left(\frac{\pi}{4}D_{chamber}^2 - \frac{\pi}{4}D_{piston}^2\right) \tag{4.7}$$

where

D_{piston} = Piston diameter,

$D_{chamber}$ = Chamber diameter,

After several rearrangement of Equation 4.7 we come up with

$$\bar{v}_{fluid} = v_{piston}\frac{D_{piston}^2}{\left(D_{chamber}^2 - D_{piston}^2\right)} \tag{4.8}$$

It should be noted that fluid velocity in Equation 4.8 is average velocity in the annulus. In our case, the diameter of piston and chamber are 0.312 and 0.314 inches, respectively. Therefore the average fluid velocity is 77.75 times of piston velocity. For the case of laminar flow, we assume fluid velocities on piston and chamber walls are zero and reach maximum in the center of annulus. Bourgoyne et al. (1986) provide an analytical solution for the pressure drop along the annulus. Now we consider a control fluid volume in the annulus, which can be represented by rectangular slot flow as far as the ratio of piston diameter to chamber diameter exceeds 0.3. In our case the ratio is 0.312/0.314, which is much higher than 0.3. Now consider a rectangular slot with an area of *A* and height of *h* used to represent the annular flow in our apparatus (Figure 4-9). The area and height can be expressed in diameters, which are

$$A = Wh = \frac{\pi}{4}\left(D_{chamber}^{2} - D_{piston}^{2}\right) \tag{4.9}$$

where

$$W = \frac{\pi}{2}\left(D_{chamber} + D_{piston}\right) \tag{4.10}$$

and

$$h = \frac{1}{2}\left(D_{chamber} - D_{piston}\right) \tag{4.11}$$

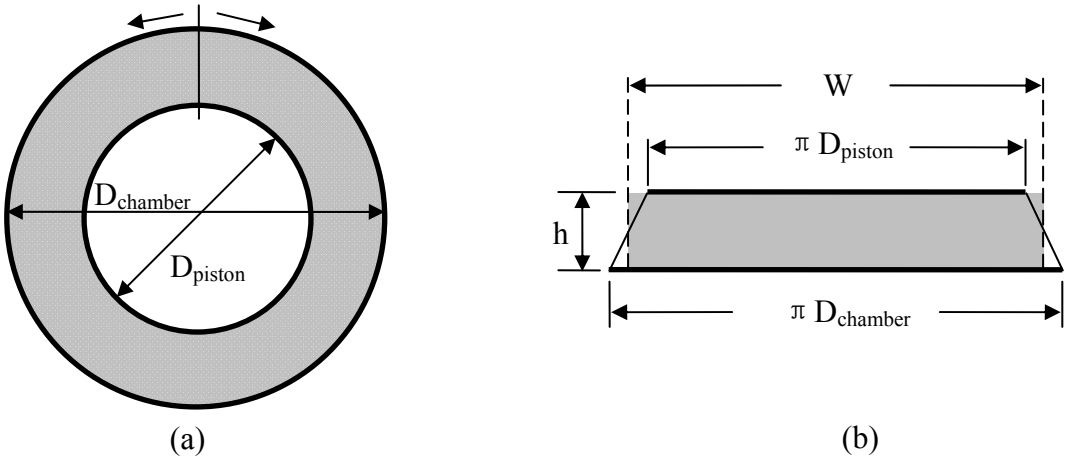

Figure 4-9. Representing the annulus as a slot: (a) annulus and (b) equivalent slot, after Bourgoyne et al. (1986)

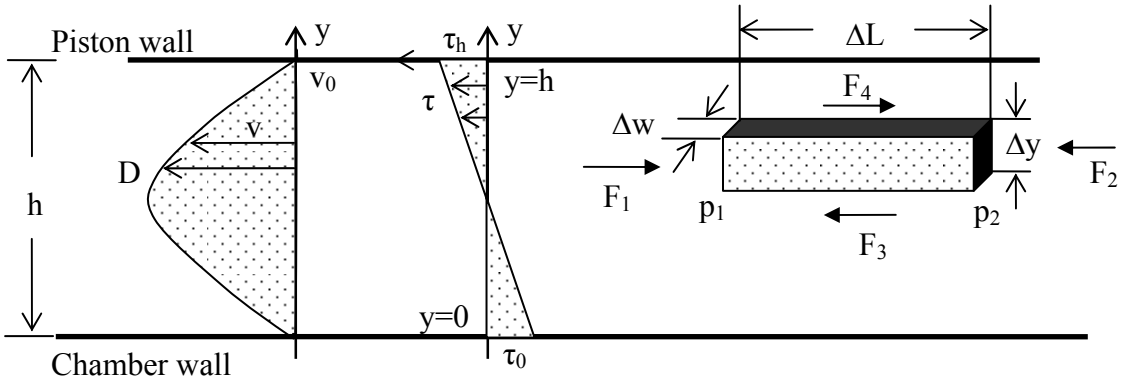

Figure 4-10. Free body diagram for controlled fluid volume in a slot, after Bourgoyne et al. (1986)

We deal with a controlled fluid volume (Figure 4-10) with width Δw and thickness Δy. According to Bourgoyne et al. (1986), Force equilibrium in horizontal direction gives

$$F_1 + F_4 = F_2 + F_3 \tag{4.12}$$

where

$$F_1 = p_1 \Delta w \Delta y \tag{4.13}$$

$$F_2 = p_2 \Delta w \Delta y = \left(p_1 + \frac{dp_f}{dL} \Delta L \right) \Delta w \Delta y \tag{4.14}$$

$$F_3 = \tau_y \Delta w \Delta L \tag{4.15}$$

and

$$F_4 = \tau_{y+\Delta y} \Delta w \Delta L = \left(\tau_y + \frac{d\tau}{dy} \Delta y \right) \Delta w \Delta L \tag{4.16}$$

where

ΔL = Length of controlled fluid volume,

τ = Shear stress,

$\frac{dp_f}{dL}$ = Frictional pressure gradient in annulus,

$\frac{d\tau}{dy}$ = Shear stress gradient in y direction,

Substituting Equations 4.13 through 4.16 into Equations 4.12 yields

$$p_1 \Delta w \Delta y + \left(\tau_y + \frac{d\tau}{dy} \Delta y \right) \Delta w \Delta L = \left(p_1 + \frac{dp_f}{dL} \Delta L \right) \Delta w \Delta y + \tau_y \Delta w \Delta L \tag{4.17}$$

Expanding and cancelling out the same terms on both sides gives

$$\frac{d\tau}{dy} \Delta y \Delta w \Delta L = \frac{dp_f}{dL} \Delta L \Delta w \Delta y \tag{4.18}$$

Dividing Equations 4.18 by $\Delta y \Delta w \Delta L$, we have

$$\frac{d\tau}{dy} = \frac{dp_f}{dL} \tag{4.19}$$

Because dp_f/dL is not a function of y, Equation 4.19 can be integrated with respect to y. Separating variables and integrating gives

$$\tau = y \frac{dp_f}{dL} + \tau_0 \tag{4.20}$$

where τ_0 is the constant of integration that corresponds to the shear stress at y=0. From the definition of shear rate, $\dot{\gamma}$, we obtain

$$\dot{\gamma} = -\frac{dv}{dy} \tag{4.21}$$

Combining Equations 4.21 with the definition of viscosity for Newtonian fluid gives

$$\tau = \mu\dot{\gamma} = -\mu\frac{dv}{dy} = y\frac{dp_f}{dL} + \tau_0 \tag{4.22}$$

where

μ = Newtonian fluid viscosity,

v = Newtonian fluid velocity,

Again, separating variable and integrating yields

$$v = -\frac{y^2}{2\mu}\frac{dp_f}{dL} - \frac{\tau_0 y}{\mu} + v_0 \tag{4.23}$$

where v_0 is the second constant of integration that corresponds to the fluid velocity at y=0. Applying the boundary condition

$$v_0 = 0 \text{ at } y=0, \tag{4.24}$$

we have

$$0 = -\frac{0^2}{2\mu}\frac{dp_f}{dL} - \frac{\tau_0 0}{\mu} + v_0 \tag{4.25}$$

Similarly applying the boundary condition

$$v_0 = 0 \text{ at } y=\text{h}, \tag{4.26}$$

we have

$$0 = -\frac{h^2}{2\mu}\frac{dp_f}{dL} - \frac{\tau_0 h}{\mu} + v_0 \tag{4.27}$$

Therefore, the constants of integration v_0 and τ_0 are

$$v_0 = 0 \tag{4.28}$$

and

$$\tau_0 = -\frac{h}{2}\frac{dp_f}{dL}. \tag{4.29}$$

Substituting Equations 4.28 and 4.29 into 4.23 gives

$$v = \frac{1}{2\mu}\frac{dp_f}{dL}\left(hy - y^2\right) \tag{4.30}$$

The flow rate q is the product of velocity v and area A. Integrating the controlled volume flow rate throughout the interval 0 to h and recalling Equation 4.30 we obtain total flow rate

$$q = \int_0^h v dA = \int_0^h v W dy = \frac{W}{2\mu}\frac{dp_f}{dL}\int_0^h \left(hy - y^2\right) dy \tag{4.31}$$

Integrating Equations 4.31 yields

$$q = \frac{Wh^3}{12\mu}\frac{dp_f}{dL} \tag{4.32}$$

Substituting Equations 4.10 and 4.11 into 4.32, we obtain

$$q = \frac{\pi}{192\mu}\frac{dp_f}{dL}\left(D_{chamber}^2 - D_{piston}^2\right)\left(D_{chamber} - D_{piston}\right)^2 \tag{4.33}$$

Expressing the flow rate in terms of the mean flow velocity and solving for the frictional pressure gradient gives

$$\bar{v}_{fluid} = \frac{q}{A} = \frac{\frac{\pi}{192\mu}\frac{dp_f}{dL}\left(D_{chamber}^2 - D_{piston}^2\right)\left(D_{chamber} - D_{piston}\right)^2}{\frac{\pi}{4}\left(D_{chamber}^2 - D_{piston}^2\right)}$$

or

$$\frac{dp_f}{dL} = \frac{q}{A} = \frac{48\mu\bar{v}_{fluid}}{\left(D_{chamber} - D_{piston}\right)^2}. \tag{4.34}$$

Integrating Equation 4.34 and recalling $\bar{v}_{fluid} = v_{piston}\frac{D_{piston}^2}{\left(D_{chamber}^2 - D_{piston}^2\right)}$ we have friction pressure drop along the annulus

$$\begin{aligned} p_2 - p_1 &= \int_0^{L_{piston\ flank}} \frac{dp_f}{dL} dL = \frac{48\mu\bar{v}_{fluid} L_{piston\ flank}}{\left(D_{chamber} - D_{piston}\right)^2} \\ &= \frac{48\mu\left[v_{piston}\frac{D_{piston}^2}{\left(D_{chamber}^2 - D_{piston}^2\right)}\right] L_{piston\ flank}}{\left(D_{chamber} - D_{piston}\right)^2} \\ &= \frac{48\mu v_{piston} D_{piston}^2 L_{piston\ flank}}{\left(D_{chamber} - D_{piston}\right)^3 \left(D_{chamber} + D_{piston}\right)} \end{aligned} \tag{4.35}$$

Substituting Equations 4.11 and 4.34 into 4.29 we have shear stress on piston wall, which is opposite to the shear stress on fluid.

$$\begin{aligned} -\tau_0 &= -\left(-\frac{h}{2}\frac{dp_f}{dL}\right) = \frac{D_{chamber} - D_{piston}}{4}\frac{48\mu\bar{v}_{fluid}}{\left(D_{chamber} - D_{piston}\right)^2} \\ &= \frac{12\mu\bar{v}_{fluid}}{D_{chamber} - D_{piston}} \end{aligned} \tag{4.36}$$

Thus the drag force on the flank of the piston, $DF_{piston\ flank}$, is

$$DF_{piston\ flank} = A_{piston\ flank}\left(-\tau_0\right) = \frac{12\pi D_{piston} L_{piston\ flank}\mu\bar{v}_{fluid}}{D_{chamber} - D_{piston}} \tag{4.37}$$

for laminar flow.

where

$L_{piston\ flank}$ = Length of piston flank.

If flow in the annulus is turbulence, the drag force on the flank of the piston can be analyzed by employing Reynolds number and friction factor.

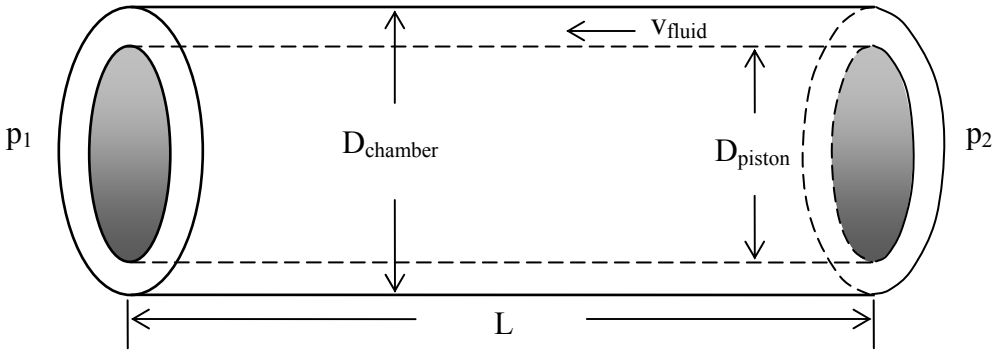

Figure 4-11. Schematic of fluid flow through an annulus between piston and chamber

For Figure 4-11, force balance requires that

$$\begin{aligned}(p_2 - p_1)A_{annulus} &= DF_{chamber} + DF_{piston\ flank} \\ &= \tau_{piston}\pi D_{piston}L_{piston\ flank} + \tau_{chamber}\pi D_{chamber}L_{piston\ flank}\end{aligned} \tag{4.38}$$

Since piston diameter is very close to chamber diameter and basing on symmetrical geometry, we have following observations

$$\tau_{chamber} = \tau_{piston}, \tag{4.39}$$

and

$$D_{chamber} \cong D_{piston}. \tag{4.40}$$

Therefore, we obtain

$$DF_{chamber} \cong DF_{piston\ flank} \tag{4.41}$$

and

$$(p_2 - p_1)\frac{\pi}{4}\left(D_{chamber}^2 - D_{piston}^2\right) = \pi\tau_{piston}L_{piston\ flank}\left(D_{piston} + D_{chamber}\right) \tag{4.42}$$

or

$$\frac{(p_2 - p_1)}{L_{piston\ flank}} = \frac{4\tau_{piston}}{\left(D_{chamber} - D_{piston}\right)} \tag{4.43}$$

Introducing the definition of the Fanning friction factor (Wikipedia, 2009), *f*, which is the ratio of the shear stress on the tubular wall applied by unit volume of fluid to its kinetic energy.

$$f = \frac{shear\ stress\ on\ the\ wall / volume\ fluid}{kinetic\ energy / volume\ fluid} \tag{4.44}$$

or

$$f = \frac{\tau_{piston} + \tau_{chamber}}{\frac{1}{2}\rho_f \bar{v}_{fluid}^2}. \tag{4.45}$$

where

ρ_f = Fluid density.

Recalling $\tau_{piston} = \tau_{chamber}$, we have

$$\tau_{piston} = \frac{1}{4} f \rho_f \bar{v}_{fluid}^2 \tag{4.46}$$

The fanning friction factor for smooth pipe, which is as in our case, and a Reynolds number range of 2,100 to 100,000, can be approximated by the following form (Blasius, 1913):

$$f = \frac{0.0791}{N_{\mathrm{Re}}^{0.25}} \tag{4.47}$$

where N_{Re} is the Reynolds number, which is expressed as:

$$N_{\mathrm{Re}} = \frac{D_e \bar{v}_{fluid} \rho_f}{\mu} \tag{4.48}$$

where

D_e = Equivalent circular diameter,

The equivalent circular diameter D_e is equal to four times the hydraulic radius r_H.

$$D_e = 4 r_H \tag{4.49}$$

and the hydraulic radius is defined as the ratio of the cross-sectional area to the wetted perimeter of the flow channel. In our case it is

$$r_H = \frac{\frac{\pi}{4}\left(D_{chamber}^2 - D_{piston}^2\right)}{\pi\left(D_{piston} + D_{chamber}\right)} = \frac{D_{chamber} - D_{piston}}{4} \tag{4.50}$$

Substituting Equation 4.50 into 4.49, we have

$$D_e = 4\frac{\left(D_{chamber} - D_{piston}\right)}{4} = D_{chamber} - D_{piston} \quad (4.51)$$

Substituting Equation 4.51 into 4.48, we have

$$N_{\mathrm{Re}} = \frac{\left(D_{chamber} - D_{piston}\right)\overline{v}_{fluid}\rho_f}{\mu} \quad (4.52)$$

Substituting Equation 4.52 into 4.47, we have

$$f = \frac{0.0791}{\left[\frac{\left(D_{chamber} - D_{piston}\right)\overline{v}_{fluid}\rho_f}{\mu}\right]^{0.25}} \quad (4.53)$$

Substituting Equation 4.53 into 4.46, we have

$$\tau_{piston} = \frac{1}{4}\left\{\frac{0.0791}{\left[\frac{\left(D_{chamber} - D_{piston}\right)\overline{v}_{fluid}\rho_f}{\mu}\right]^{0.25}}\right\}\rho_f \overline{v}_{fluid}^2 \quad (4.54)$$

Simplifying Equation 4.54 yields

$$\tau_{piston} = \frac{0.0198\rho_f^{0.75}\mu^{0.25}\overline{v}_{fluid}^{1.75}}{\left(D_{chamber} - D_{piston}\right)^{0.25}} \quad (4.55)$$

Thus the drag force on the flank of the piston, $DF_{piston\ flank}$, is expressed as

$$DF_{piston\ flank} = \tau_{piston} A_{piston\ flank} = \frac{0.0198\pi D_{piston} L_{piston\ flank}\rho_f^{0.75}\mu^{0.25}\overline{v}_{fluid}^{1.75}}{\left(D_{chamber} - D_{piston}\right)^{0.25}} \quad (4.56)$$

for turbulent flow in annulus.

The drag force on the cone surface, $DF_{piston\ cone}$, can be estimated by applying Stokes' law (Castleman, 1926). Figure 4-8 illustrates a piston traveling through a homogeneous fluid. If the motion of the sphere is sufficiently slow, the inertia terms become negligible. Under this condition the cone of the piston experience a drag force resulting from the viscous fluid flow around the cone surface. The magnitude of drag force is dependent on the flow regime, laminar or turbulent flow.

For laminar flow, the drag force is calculated from Stokes law. Stokes law has shown that for creeping flow (Castleman, 1926) (i.e., the streamlines of fluid movement pass smoothly about the particle and there is no eddying downstream of it) the drag force is related to the piston velocity through the fluid by:

$$DF_{piston\ cone} = 3\pi D_{piston} \mu v_{piston}. \tag{4.57}$$

This equation is found to give acceptable accuracy for Reynolds numbers below 0.1. For Reynolds numbers greater than 0.1, empirically determined friction factors must be used.

In case of turbulent flow, the concept of friction factor is introduced to estimate drag force. It is defined by:

$$f = \frac{DF_{piston\ cone}}{AE_k}. \tag{4.58}$$

Then the drag force can be expressed as:

$$DF_{piston\ cone} = f\ AE_k \tag{4.59}$$

where

A = Characteristic area of the cone,

E_k = Kinetic energy per unit volume.

The characteristic area of the cone in our case is given by:

$$A = \frac{1}{4}\pi D_{piston}^2. \tag{4.60}$$

The kinetic energy per unit volume is given by:

$$E_k = \frac{\rho_f v_{piston}^2}{2}. \tag{4.61}$$

The friction factor f is a function of the Reynolds number and, in the case of non-spherical shapes, a term called the sphericity. Sphericity, ψ, is defined as the surface area of a sphere containing the same volume as the particle divided by the surface area of the particle. In our case the particle is a cone with following geometry:

Base diameter =D_{piston},

Angle between base and flank = 22.5 degree, thus height of the cone is

$$\text{Height of the cone} = \frac{D_{piston}}{2}\tan\left(22.5^{o}\right). \tag{4.62}$$

Therefore the volume and surface area of the cone are

$$A_{cone} = \pi\left(\frac{D_{piston}}{2}\right)\left\{\left(\frac{D_{piston}}{2}\right)^{2} + \left(\frac{D_{piston}}{2}\tan\left(22.5^{o}\right)\right)^{2}\right\}^{0.5} + \pi\left(\frac{D_{piston}}{2}\right)^{2} \tag{4.63}$$

$$V_{cone} = \frac{1}{3}\pi\left(\frac{D_{piston}}{2}\right)^{2}\left(\frac{D_{piston}}{2}\tan\left(22.5^{o}\right)\right) = \frac{1}{3}\pi\left(0.051777D_{piston}^{3}\right) \tag{4.64}$$

The ball that has equivalent volume to the cone will have an equivalent diameter of

$$\frac{4}{3}\pi\left(\frac{D_{equivalent}}{2}\right)^{3} = \frac{1}{3}\pi\left(0.051777D_{piston}^{3}\right)$$

or

$$D_{equivalent} = \sqrt[3]{0.103554}D_{piston} \tag{4.65}$$

where

$D_{equivalent}$ = Equivalent ball diameter,

Then the surface area of the equivalent ball is

$$A_{equivalent} = 4\pi\left(\frac{\sqrt[3]{0.103554}D_{piston}}{2}\right)^{2} = \pi\left(0.220517D_{piston}^{2}\right) \tag{4.66}$$

Sphericity of the cone according to the definition is

$$\psi = \frac{A_{equivalent}}{A_{cone}} = \frac{\pi\left(0.220517D_{piston}^{2}\right)}{\pi\left(\frac{D_{piston}}{2}\right)\left\{\left(\frac{D_{piston}}{2}\right)^{2} + \left(\frac{D_{piston}}{2}\tan\left(22.5^{o}\right)\right)^{2}\right\}^{0.5} + \pi\left(\frac{D_{piston}}{2}\right)^{2}} \tag{4.67}$$

$$= 0.424$$

Bourgoyne et al. (1986) developed a graphical correlation to estimate the friction-factor from given Reynolds-number and sphericity. A directed read of friction factor can be accomplished using Figure 4-12.

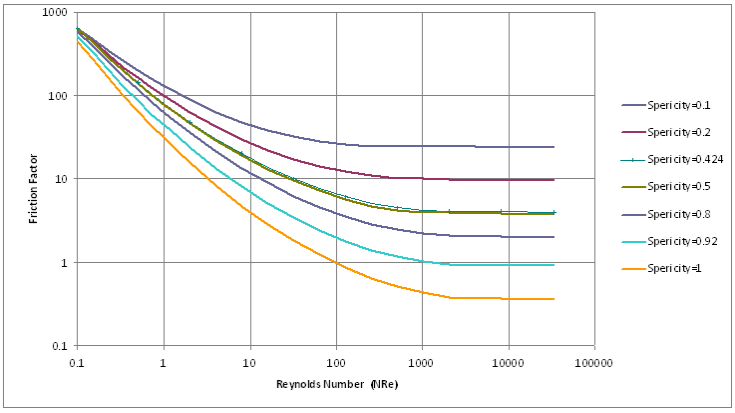

Figure 4-12. Friction factor vs. particle Reynolds number for particles of different sphericities, after Bourgoyne et al. (1986)

Reynolds number is expressed as

$$N_{\mathrm{Re}} = \frac{\rho_f v_{piston} D_{piston}}{\mu}. \tag{4.68}$$

For the piston in our study, whose sphericity is 0.424, the relationship between friction factor and Reynolds number can be expressed as

$$\begin{aligned} f &= 10^{1.9068-0.78036\log(N_{\mathrm{Re}})+0.117434[\log(N_{\mathrm{Re}})]^2} \\ &= 10^{1.9068-0.78036\log\left(\frac{\rho_f v_{piston} D_{piston}}{\mu}\right)+0.117434\left[\log\left(\frac{\rho_f v_{piston} D_{piston}}{\mu}\right)\right]^2} \end{aligned} \tag{4.69}$$

Therefore the drag force on the cone surface is

$$DF_{piston\ cone} = \left(\frac{\pi\rho_f v_{piston}^2 D_{piston}^2}{8}\right) 10^{1.9068-0.78036\log\left(\frac{\rho_f v_{piston} D_{piston}}{\mu}\right)+0.117434\left[\log\left(\frac{\rho_f v_{piston} D_{piston}}{\mu}\right)\right]^2} \tag{4.70}$$

Including these forces into force balance Equation 4.1, we have

$$F_{em} + \pi\frac{D_{piston}^2}{4} p_1 = 3\pi D_{piston}\mu v_{piston} + \frac{12\pi D_{piston} L_{piston\ flank}\mu\bar{v}_{fluid}}{D_{chamber} - D_{piston}} + \pi\frac{D_{piston}^2}{4} p_2$$

or

$$F_{em} = 3\pi D_{piston}\mu v_{piston} + \frac{12\pi D_{piston} L_{piston\ flank}\mu\bar{v}_{fluid}}{D_{chamber} - D_{piston}} + \pi\frac{D_{piston}^2}{4}(p_2 - p_1) \tag{4.71}$$

for laminar flow, and

$$F_{em} + \pi \frac{D_{piston}^2}{4} p_1 = \left(\frac{\pi \rho_f v_{piston}^2 D_{piston}^2}{8} \right) 10^{1.9068 - 0.78036 \log\left(\frac{\rho_f v_{piston} D_{piston}}{\mu} \right) + 0.117434 \left[\log\left(\frac{\rho_f v_{piston} D_{piston}}{\mu} \right) \right]^2} + \frac{0.0198 \pi D_{piston} L_{piston\ flank} \rho_f^{0.75} \mu^{0.25} \bar{v}_{fluid}^{1.75}}{\left(D_{chamber} - D_{piston} \right)^{0.25}} + \pi \frac{D_{piston}^2}{4} p_2$$

or

$$F_{em} = \left(\frac{\pi \rho_f v_{piston}^2 D_{piston}^2}{8} \right) 10^{1.9068 - 0.78036 \log\left(\frac{\rho_f v_{piston} D_{piston}}{\mu} \right) + 0.117434 \left[\log\left(\frac{\rho_f v_{piston} D_{piston}}{\mu} \right) \right]^2} + \frac{0.0198 \pi D_{piston} L_{piston\ flank} \rho_f^{0.75} \mu^{0.25} \bar{v}_{fluid}^{1.75}}{\left(D_{chamber} - D_{piston} \right)^{0.25}} + \pi \frac{D_{piston}^2}{4} \left(p_2 - p_1 \right) \tag{4.72}$$

for turbulent flow.

Substituting Equation 4.8 into Equations 4.71 and 4.72 we obtain

$$F_{em} = 3 \pi D_{piston} \mu v_{piston} + \frac{12 \pi D_{piston} L_{piston\ flank} \mu v_{piston} \dfrac{D_{piston}^2}{\left(D_{chamber}^2 - D_{piston}^2 \right)}}{D_{chamber} - D_{piston}} + \pi \frac{D_{piston}^2}{4} \left(p_2 - p_1 \right) \tag{4.73}$$

for laminar flow, and

$$F_{em} = \left(\frac{\pi \rho_f v_{piston}^2 D_{piston}^2}{8} \right) 10^{1.9068 - 0.78036 \log\left(\frac{\rho_f v_{piston} D_{piston}}{\mu} \right) + 0.117434 \left[\log\left(\frac{\rho_f v_{piston} D_{piston}}{\mu} \right) \right]^2} + \frac{0.0198 \pi D_{piston} L_{piston\ flank} \rho_f^{0.75} \mu^{0.25} \left[v_{piston} \dfrac{D_{piston}^2}{\left(D_{chamber}^2 - D_{piston}^2 \right)} \right]^{1.75}}{\left(D_{chamber} - D_{piston} \right)^{0.25}} + \pi \frac{D_{piston}^2}{4} \left(p_2 - p_1 \right) \tag{4.74}$$

for turbulent flow.

Again substituting Equation 4.35 into Equation 4.73 we obtain

$$F_{em} = 3\pi D_{piston}\mu v_{piston} + \frac{12\pi D_{piston} L_{piston\ flank}\mu v_{piston} D_{piston}^2}{\left(D_{chamber} - D_{piston}\right)^2\left(D_{chamber} + D_{piston}\right)}$$
$$+ \pi\frac{D_{piston}^2}{4}\frac{48\mu v_{piston} D_{piston}^2 L_{piston\ flank}}{\left(D_{chamber} - D_{piston}\right)^3\left(D_{chamber} + D_{piston}\right)}$$

or

$$F_{em} = 3\pi D_{piston}\mu v_{piston} + \frac{12\pi L_{piston\ flank}\mu v_{piston} D_{piston}^3 D_{chamber}}{\left(D_{chamber} - D_{piston}\right)^3\left(D_{chamber} + D_{piston}\right)} \quad (4.75)$$

for laminar flow.

Recalling $\frac{\left(p_2 - p_1\right)}{L_{piston\ flank}} = \frac{4\tau_{piston}}{\left(D_{chamber} - D_{piston}\right)}$ and $\tau_{piston} = \frac{1}{4} f\rho_f \bar{v}_{fluid}^2$, we have

$$\frac{\left(p_2 - p_1\right)}{L_{piston\ flank}} = \frac{4\left(\frac{1}{4} f\rho_f \bar{v}_{fluid}^2\right)}{\left(D_{chamber} - D_{piston}\right)}$$
$$= \frac{10^{1.9068 - 0.78036\log\left(\frac{\rho_f v_{piston} D_{piston}}{\mu}\right) + 0.117434\left[\log\left(\frac{\rho_f v_{piston} D_{piston}}{\mu}\right)\right]^2}\rho_f\left[v_{piston}\frac{D_{piston}^2}{\left(D_{chamber}^2 - D_{piston}^2\right)}\right]^2}{\left(D_{chamber} - D_{piston}\right)}$$

or

$$p_2 - p_1 = \frac{10^{1.9068 - 0.78036\log\left(\frac{\rho_f v_{piston} D_{piston}}{\mu}\right) + 0.117434\left[\log\left(\frac{\rho_f v_{piston} D_{piston}}{\mu}\right)\right]^2}\rho_f v_{piston}^2 D_{piston}^4 L_{piston\ flank}}{\left(D_{chamber} - D_{piston}\right)^3\left(D_{chamber} + D_{piston}\right)^2} \quad (4.76)$$

Again substituting Equation 4.76 into Equation 4.74 we obtain

$$F_{em} = \left(\frac{\pi\rho_f v_{piston}^2 D_{piston}^2}{8}\right) 10^{1.9068-0.78036\log\left(\frac{\rho_f v_{piston} D_{piston}}{\mu}\right)+0.117434\left[\log\left(\frac{\rho_f v_{piston} D_{piston}}{\mu}\right)\right]^2}$$
$$+\frac{0.0198\pi D_{piston} L_{piston\ flank} \rho_f^{0.75} \mu^{0.25}\left[v_{piston}\frac{D_{piston}^2}{\left(D_{chamber}^2 - D_{piston}^2\right)}\right]^{1.75}}{\left(D_{chamber} - D_{piston}\right)^{0.25}} \quad (4.77)$$
$$+\pi\frac{D_{piston}^2}{4}\left(\frac{10^{1.9068-0.78036\log\left(\frac{\rho_f v_{piston} D_{piston}}{\mu}\right)+0.117434\left[\log\left(\frac{\rho_f v_{piston} D_{piston}}{\mu}\right)\right]^2}\rho_f v_{piston}^2 D_{piston}^4 L_{piston\ flank}}{\left(D_{chamber} - D_{piston}\right)^3\left(D_{chamber} + D_{piston}\right)^2}\right)$$

for turbulent flow.

Equations 4.75 and 4.77 are the governing equations for viscosity measurement in laminar and turbulent flow. Now we consider the laminar flow case. Extracting μv_{piston} from terms on the right-hand side of Equation 4.75 yields

$$F_{em} = \mu v_{piston}\left[3\pi D_{piston} + \frac{12\pi L_{piston\ flank} D_{piston}^3 D_{chamber}}{\left(D_{chamber} - D_{piston}\right)^3\left(D_{chamber} + D_{piston}\right)}\right] \quad (4.78)$$

Piston velocity can be expressed as

$$v_{piston} = \frac{L_{chamber}}{t} \quad (4.79)$$

where

$L_{chamber}$ = Chamber length,

t = Piston travel time from one end of chamber length to the other,

Substituting Equation 4.79 into Equation 4.78 and recasting gives

$$\mu = \frac{F_{em} t}{L_{chamber}\left[3\pi D_{piston} + \frac{12\pi L_{piston\ flank} D_{piston}^3 D_{chamber}}{\left(D_{chamber} - D_{piston}\right)^3\left(D_{chamber} + D_{piston}\right)}\right]} \quad (4.80)$$

Equation 4.80 indicates that under laminar flow condition fluid viscosity can be estimated by recording the travel time, assuming the geometry of piston and chamber, and electromagnetic force are given. After a thorough review of "viscous drag" paper (Cambridge Viscosity Inc., 2010) provided by the manufacturer-Cambridge we found that Cambridge derived an equation that is similar to Equation 4.80 for laminar flow. It should be noted that the derivation in the "viscous drag" paper is not completely shown. Therefore we cannot check its validity.

For turbulent flow, substituting Equation 4.79 into Equation 4.77 we have

$$F_{em} = \left(\frac{\pi\rho_f L_{chamber}^2 D_{piston}^2}{8t^2}\right) 10^{1.9068-0.78036\log\left(\frac{\rho_f L_{chamber} D_{piston}}{\mu t}\right)+0.117434\left[\log\left(\frac{\rho_f L_{chamber} D_{piston}}{\mu t}\right)\right]^2}$$

$$+\frac{0.0198\pi D_{piston} L_{piston\ flank} \rho_f^{0.75} \mu^{0.25} \left[\frac{D_{piston}^2 L_{chamber}}{t\left(D_{chamber}^2 - D_{piston}^2\right)}\right]^{1.75}}{\left(D_{chamber} - D_{piston}\right)^{0.25}}$$

$$+\pi\frac{D_{piston}^2}{4}\left(\frac{10^{1.9068-0.78036\log\left(\frac{\rho_f L_{chamber} D_{piston}}{\mu t}\right)+0.117434\left[\log\left(\frac{\rho_f L_{chamber} D_{piston}}{\mu t}\right)\right]^2} \rho_f L_{chamber}^2 D_{piston}^4 L_{piston\ flank}}{\left(D_{chamber} - D_{piston}\right)^3 \left(D_{chamber} + D_{piston}\right)^2 t^2}\right)$$

or

$$\begin{aligned} F_{em} &= \left(\frac{\pi\rho_f L_{chamber}^2 D_{piston}^2}{8t^2}\right) 10^{1.9068-0.78036\log\left(\frac{\rho_f L_{chamber} D_{piston}}{\mu t}\right)+0.117434\left[\log\left(\frac{\rho_f L_{chamber} D_{piston}}{\mu t}\right)\right]^2} \\ &+\frac{0.0198\pi\rho_f^{0.75}\mu^{0.25} D_{piston}^{4.5} L_{chamber}^{1.75} L_{piston\ flank}}{\left(D_{chamber} - D_{piston}\right)^2 \left(D_{chamber} + D_{piston}\right)^{1.75} t^{1.75}} \\ &+\frac{\pi 10^{1.9068-0.78036\log\left(\frac{\rho_f L_{chamber} D_{piston}}{\mu t}\right)+0.117434\left[\log\left(\frac{\rho_f L_{chamber} D_{piston}}{\mu t}\right)\right]^2} \rho_f D_{piston}^6 L_{chamber}^2 L_{piston\ flank}}{4\left(D_{chamber} - D_{piston}\right)^3 \left(D_{chamber} + D_{piston}\right)^2 t^2} \end{aligned} \tag{4.81}$$

Since the viscosity, μ, cannot be separated from time, t, in Equation 4.81, the estimation of viscosity can only be done by solving Equation 4.81 implicitly. A trial and error method would be used to build a relationship between viscosity and travel time. After the relationship is constructed viscosity can be measured by recording the one-way travel time. Another difficulty for turbulent flow is that fluid density at interested condition must be known. Therefore the measurement of fluid density need to be run simultaneously, otherwise density will be calculated through an equation-of-states, which requires the composition of fluid. To eliminate the complexity turbulent flow should be avoided during the experiment. The manufacturer did not provided information about the application of viscometer under the turbulent flow condition.

4.4 Calibration of Experimental Data

4.4.1 Raw data and the Manufacturer's Converted Equation

Apparently the raw data from experiment is not true gas viscosity if we note the big difference between raw viscosity data and NIST values in both methane and nitrogen viscosity at different pressures and temperatures in Figures 4-13 through 4-16. The manufacturer did not provide the proprietary equation that leads to the raw data. Therefore we do not know the relationship between piston traveling time and raw viscosity data in this black box. Since the raw measured viscosity reading directly from the viscometer is not the true gas viscosity, the manufacturer of Cambridge viscometer provided an equation to convert the raw data to what they believe is true gas viscosity. The equation to correct the pressure effect is

$$\eta_{c,p} = \eta_M * ((A + 4.61\text{E-}05 * P) / A)^{2.875}. \tag{4.82}$$

where

p = Pressure, psia

η_M = Measured viscosity, cp

$\eta_{c,p}$ =P-corrected viscosity, cp

A = Annulus (measurement chamber diameter-piston diameter) in thousandths of an inch.

For the viscometer we used, the measurement chamber diameter is 0.314 inches, piston diameter is 0.312 inches. Therefore, A is

$$A = (0.314 - 0.312) * 1000 = 2. \tag{4.83}$$

As a result, the equation used to convert measured viscosity to corrected viscosity becomes

$$\eta_{c,p} = \eta_M * ((2 + 4.61\text{E-}05 * P)/2)^{2.875}. \tag{4.84}$$

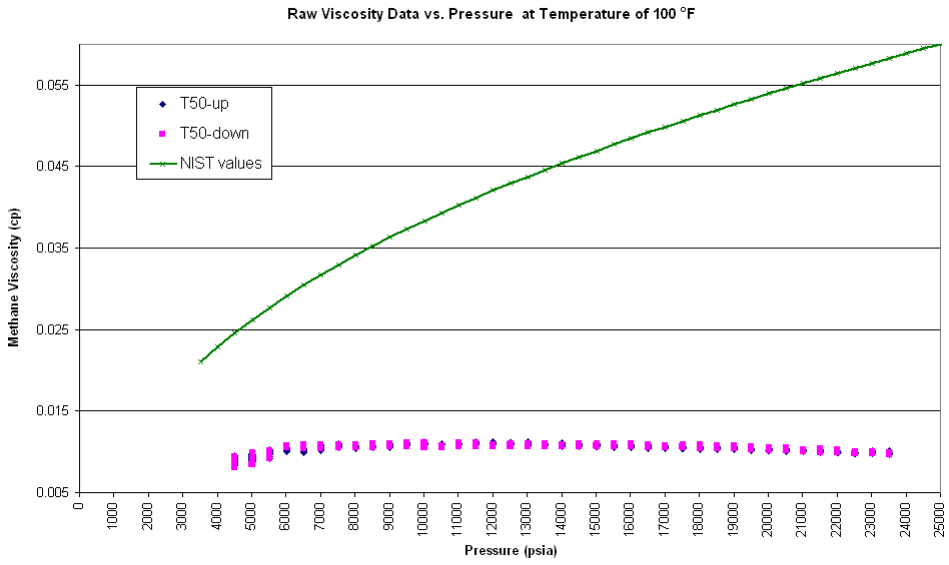

Figure 4-13. Comparison of raw viscosity data with NIST values for methane at temperature of 100 ^{o}F

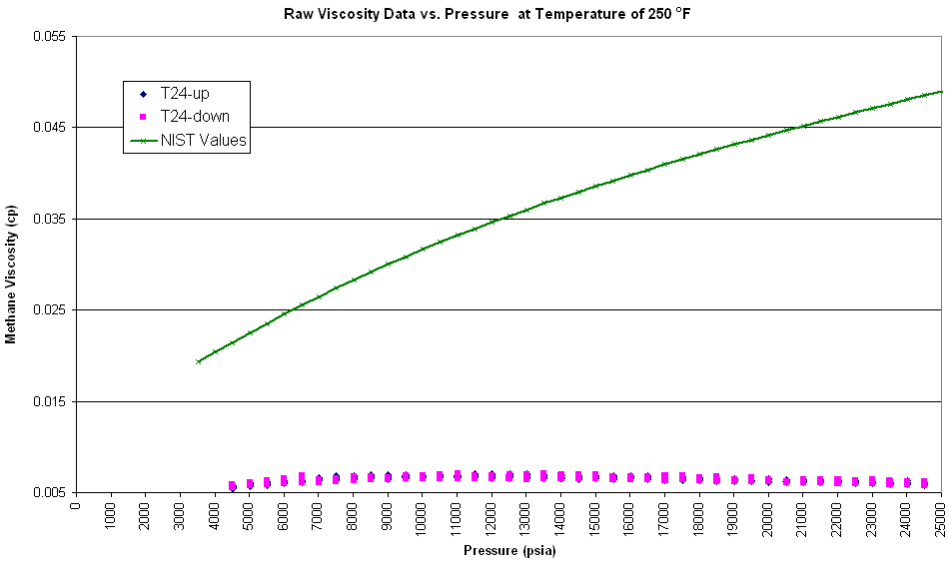

Figure 4-14. Comparison of raw viscosity data with NIST values for methane at temperature of 250 ^{o}F

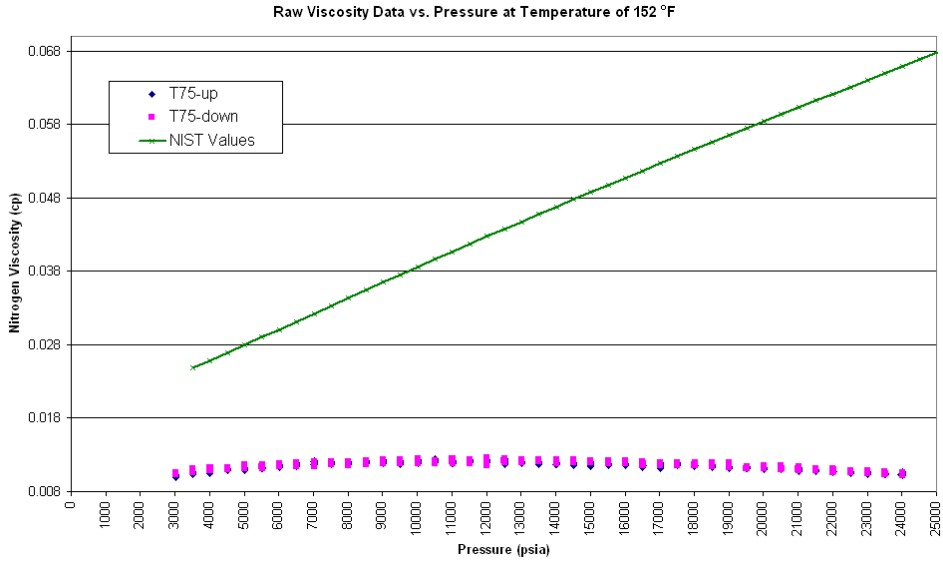

Figure 4-15. Comparison of raw viscosity data with NIST values for nitrogen at temperature of 152 ^{o}F

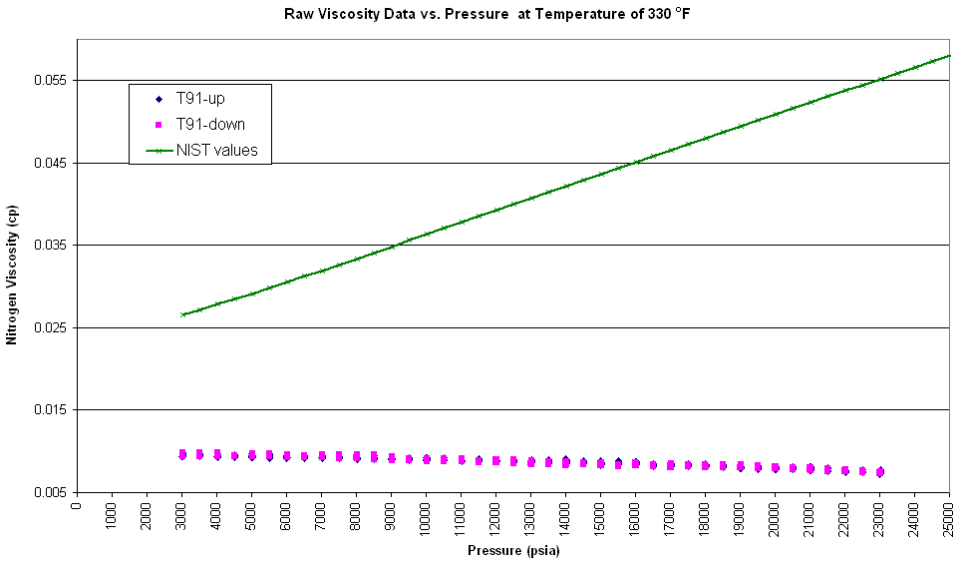

Figure 4-16. Comparison of raw viscosity data with NIST values for nitrogen at temperature of 330 ^{o}F

4.4.2 New Converted Equation to Convert Raw Data to True Viscosity

A close look at this equation indicates that it only considers the effect of pressure, and omits temperature. Thus the validity of this equation is needed to be checked with the available viscosity data. Comparing these converted data with NIST values for methane viscosity at temperatures of 100 and 250 ^{o}F and nitrogen viscosity at temperatures of 152 and 330 ^{o}F indicated that these converted data are not true gas viscosities (Figures 4-17 through 4-20). It is noted that the converted viscosities deviate from NIST values for both methane and nitrogen.

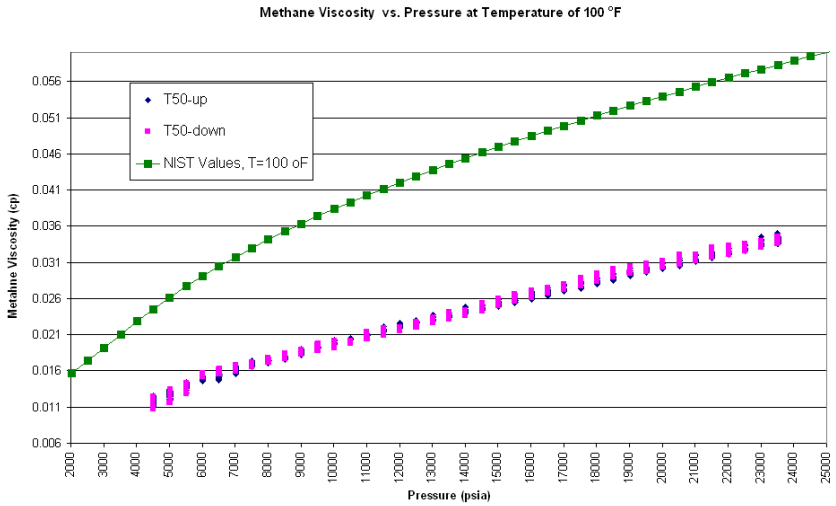

Figure 4-17. Comparison of pressure-converted methane viscosity with NIST values at temperature of 100 ^{o}F

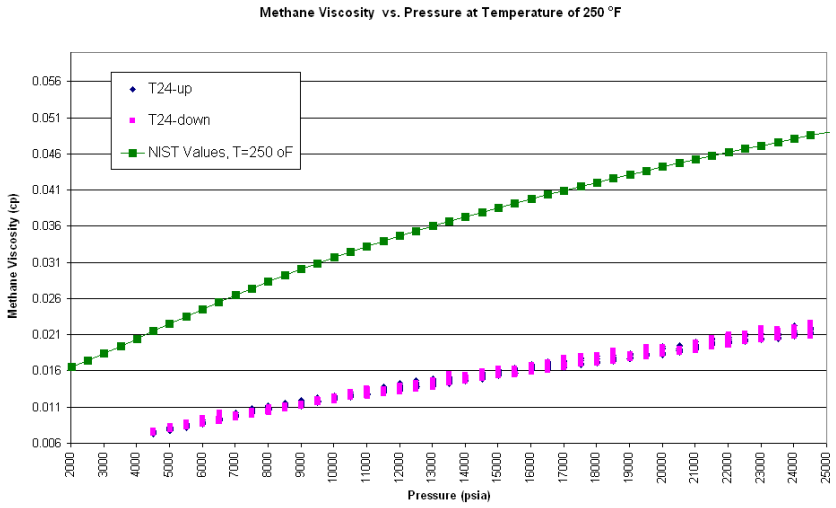

Figure 4-18. Comparison of pressure-converted methane viscosity with NIST values at temperature of 250 ^{o}F

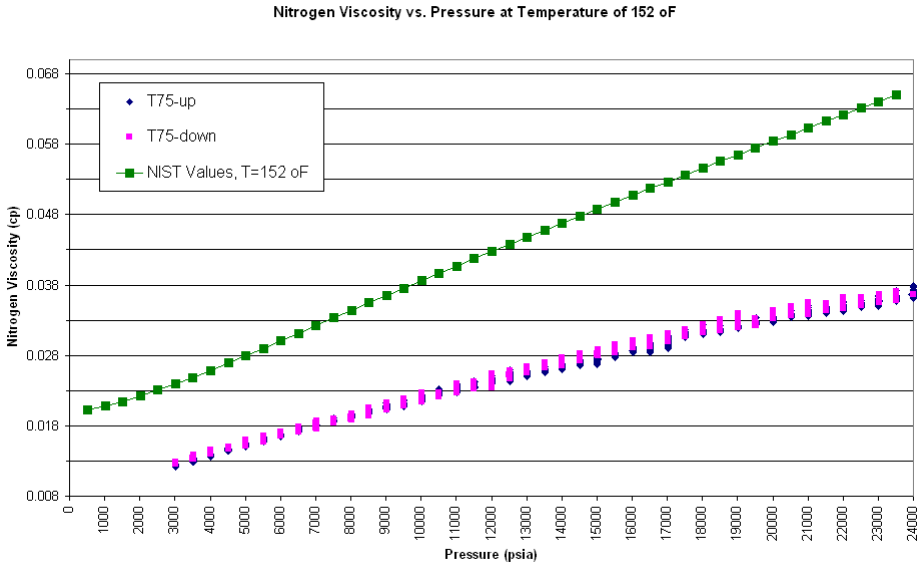

Figure 4-19. Comparison of pressure-converted nitrogen viscosity with NIST values at temperature of 152 ^{o}F

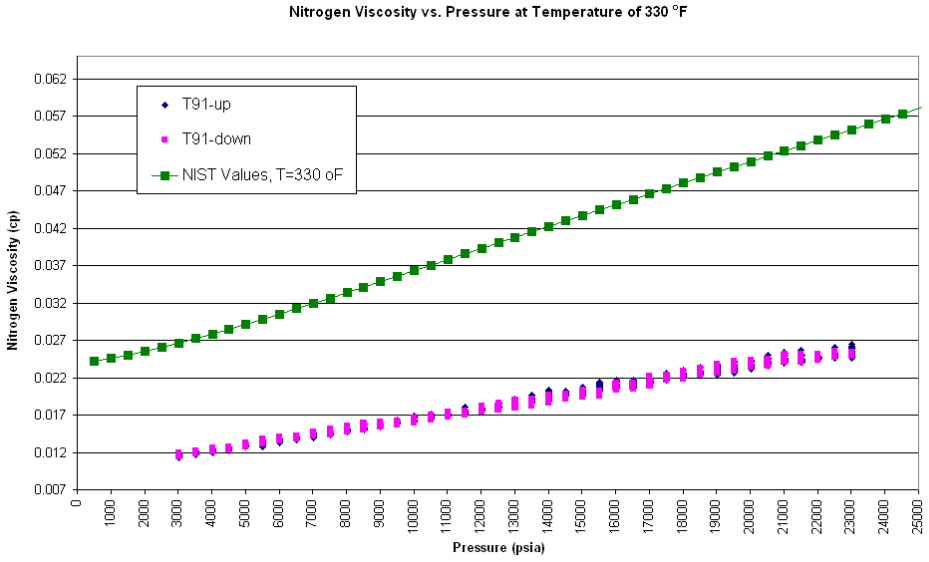

Figure 4-20. Comparison of pressure-converted nitrogen viscosity with NIST values at temperature of 330 ^{o}F

Since the equation provided by manufacturer cannot convert raw data into true viscosity, a new calibration equation is necessary and vital. To be convenient, we denoted the viscosity calculated from manufacturer's equation as pressure-converted viscosity since it only consists pressure correction. The viscosity calculated from the new calibration equation we are going to develop is denoted as pressure-temperature-converted viscosity because both pressure and temperature corrections are incorporated. To develop the new equation we respect two facts: 1) obviously temperature plays a vital role. Its effect on gas viscosity cannot be neglected. So it must be included into the converted equation as pressure. 2) To honor gas viscosity at low-moderate pressure provided by former investigators, we used their data as our calibration goal since these data are agree with each other thus are accepted by most researchers. Since nitrogen and methane viscosity at moderate pressure range, 3000 to 8000 psig, had been studied thoroughly and accepted by people, we calibrated our data to the existing viscosity data at the range of 3000 to 8000 psig using pressure and temperature as variables in the calibrating equation.

The development of new equation is shown in the following steps:

1) Candidate database for constructing new calibration equation

   As mentioned above, nitrogen and methane viscosity at moderate pressure range, 3000 to 8000 psig, had been studied thoroughly and accepted by people, we calibrated raw data to the existing viscosity data at those conditions using pressure and temperature as variables in the calibrating equation.

2) Raw data pre-process

   For the sake of high quality data acquisition, same temperature pressure experiments are repeated. Two to seven experiments were run to check the repeatability of the viscometer. Experiments with high repeatability are chosen as the database to develop new calibration equation. Data recorded at unstable pressure and temperature are removed. Outliers are excluded. After this pre-

process, only data with good quality are input into the database for generating the new calibration equation.

3) Converting raw data using manufacturer's equation

Although how manufacturer came up with Equation 4.82 is a black box to us. In this work we kept Equation 4.82 to honor that manufacturer had corrected the pressure effect on viscosity. But since they omitted the temperature effect, we will implement what had left behind. Comparing pressure-converted viscosity with NIST values at pressure range of 3000 to 8000 psi as shown in Figures 4-17 through 4-20 we found that there is a gap between pressure-converted viscosity and true viscosity. So we need to find out a correlation that can convert the pressure-converted viscosity to true viscosity. This can be done by rotating the pressure-converted viscosity to the position that is parallel to true viscosity, and then apply a vertical shift to make it overlap with the true viscosity at pressure range of 3000 to 8000 psi.

4) Converting the pressure-converted viscosity to true viscosity

As said in step 3), the conversion requires a rotation and a vertical shift. Mathematically a non-linear regression method is applied to get the correlation due to two facts. a) the relation between slope of pressure-converted viscosity and slope of NIST values is not a simple linear-relationship, and b) The vertical shift is a function of temperature. The pressure-converted viscosities at different pressure temperature are collected (Tables 4-2 and 4-4). NIST viscosity at corresponding pressure temperature is also collected (Tables 4-3 and 4-5). A statistical analysis gave that the following term

$$\left[\frac{C_1 * \mathrm{Ln}(T)}{T} + C_2 * \mathrm{Ln}(T) + C_3\right] * (p - 3014.7)$$

where

p = Pressure, psia

T = Temperature, ^{o}F

C_1, C_2, and C_3 = Coefficients

can rotate the pressure-converted viscosity to the position that is parallel to NIST viscosity. But the rotation still cannot match the converted viscosity with true viscosity, as a result, a vertical shift term

$$C_4 * T + C_5$$

where

C_4 and C_5 = Coefficients

is required so that two viscosity can overlap.

5) Determination of coefficients

The coefficients are determined by obtaining minimum variance from converted viscosity and NIST viscosity, which are

C_1= 1.35379E-05 C_2= 2.26139E-07 C_3= -6.1948E-07

C_4= 9.363238E-06 C_5= 1.023E-03

6) Summing up all terms to get new calibration equation

Summing up pressure-corrected viscosity, rotation term, and vertical shift term we come up with the pressure-temperature-corrected viscosity, or true viscosity, which is expressed as

$$\eta_t = \eta_{c,p} + Rotation\ term + Vertical\ shift\ term$$

or

$$\begin{aligned}\eta_t &= \eta_M * ((2 + 4.61E-05 * P)/2)^{2.875} \\ &+ \left[\frac{1.35379E-05 * \mathrm{Ln}(T)}{T} + 2.26139E-07 * \mathrm{Ln}(T) - 6.1948E-07\right] \\ &* (p - 3014.7) + 9.363238E-06 * T + 0.01023\end{aligned} \quad (4.85)$$

where

p = Pressure, psia

T = Temperature, ^{o}F

η_M = Raw data or measured viscosity, cp

η_t = True viscosity, cp

Table 4-2. Pressure-corrected nitrogen viscosity

Pressure	Temperature (^{o}F)					
(psia)	116	134	152	170	200	250
3014.7	0.01336	0.01324	0.01292	0.01271	0.01247	0.01212
3514.7	0.01425	0.01384	0.01368	0.01312	0.01299	0.01252
4014.7	0.01520	0.01443	0.01433	0.01410	0.01355	0.01312
4514.7	0.01597	0.01527	0.01516	0.01465	0.01400	0.01359
5014.7	0.01659	0.01581	0.01572	0.01540	0.01455	0.01409
5514.7	0.01749	0.01659	0.01655	0.01618	0.01514	0.01460
6014.7	0.01817	0.01722	0.01720	0.01683	0.01586	0.01507
6514.7	0.01888	0.01790	0.01804	0.01743	0.01639	0.01537
7014.7	0.01959	0.01861	0.01867	0.01792	0.01707	0.01576
7514.7	0.02038	0.01936	0.01923	0.01854	0.01764	0.01635
8014.7	0.02118	0.02015	0.01984	0.01912	0.01825	0.01694

Table 4-2. Continued

Pressure	Temperature (^{o}F)				
(psia)	260	280	300	330	350
3014.7	0.012035	0.011923	0.011835	0.01129	0.010814
3514.7	0.012456	0.012348	0.012175	0.011813	0.01123
4014.7	0.012892	0.012733	0.012485	0.011997	0.011939
4514.7	0.013247	0.012951	0.012718	0.012282	0.01228
5014.7	0.013565	0.013411	0.013201	0.012656	0.012453
5514.7	0.013873	0.013844	0.013507	0.013007	0.012727
6014.7	0.014261	0.014277	0.013856	0.013354	0.012908
6514.7	0.01466	0.014692	0.014293	0.013703	0.013301
7014.7	0.015177	0.01512	0.01471	0.013952	0.013624
7514.7	0.01569	0.01553	0.015247	0.01438	0.014048
8014.7	0.016218	0.015946	0.015544	0.014636	0.014334

Table 4-3. Nitrogen viscosity from NIST

Pressure	Temperature (^{o}F)					
(psia)	116	134	152	170	200	250
3014.7	0.02353	0.023724	0.023938	0.024169	0.024583	0.025333
3514.7	0.024604	0.024731	0.024886	0.025065	0.025403	0.02605
4014.7	0.025723	0.025783	0.025878	0.026002	0.02626	0.026799
4514.7	0.026874	0.026867	0.026901	0.02697	0.027147	0.027576
5014.7	0.028047	0.027974	0.027948	0.027961	0.028058	0.028375
5514.7	0.029231	0.029094	0.029009	0.02897	0.028986	0.029191
6014.7	0.030421	0.030222	0.030081	0.029989	0.029927	0.030021
6514.7	0.031611	0.031353	0.031157	0.031014	0.030875	0.030862
7014.7	0.032798	0.032483	0.032234	0.032042	0.031829	0.031709
7514.7	0.033978	0.03361	0.03331	0.033071	0.032786	0.032562
8014.7	0.035152	0.034731	0.034383	0.034098	0.033743	0.033418

Table 4-3. Continued

Pressure	Temperature (^{o}F)				
(psia)	260	280	300	330	350
3014.7	0.025489	0.025806	0.026129	0.02662	0.026952
3514.7	0.026188	0.026473	0.026765	0.027216	0.027523
4014.7	0.026919	0.027169	0.02743	0.027838	0.02812
4514.7	0.027677	0.027891	0.028119	0.028483	0.028738
5014.7	0.028456	0.028634	0.028828	0.029147	0.029375
5514.7	0.029253	0.029394	0.029555	0.029828	0.030028
6014.7	0.030064	0.030168	0.030295	0.030522	0.030694
6514.7	0.030885	0.030953	0.031047	0.031228	0.031372
7014.7	0.031714	0.031746	0.031806	0.031942	0.032058
7514.7	0.032548	0.032545	0.032573	0.032663	0.032752
8014.7	0.033386	0.033348	0.033344	0.03339	0.033451

Table 4-4. Pressure-corrected methane viscosity

Pressure	Temperature (°F)						
(psia)	100	120	140	160	180	188	200
4514.7	0.01180	0.01091	0.01008	0.00949	0.00892	0.00872	0.00844
5014.7	0.01304	0.01195	0.01098	0.01034	0.00995	0.00950	0.00894
5514.7	0.01394	0.01289	0.01149	0.01104	0.01062	0.01026	0.00959
6014.7	0.01547	0.01354	0.01231	0.01168	0.01124	0.01107	0.01046
6514.7	0.01591	0.01400	0.01341	0.01238	0.01184	0.01156	0.01102
7014.7	0.01622	0.01459	0.01415	0.01298	0.01236	0.01201	0.01163
7514.7	0.01711	0.01521	0.01500	0.01364	0.01283	0.01254	0.01218
8014.7	0.01774	0.01587	0.01558	0.01375	0.01354	0.01301	0.01269

Table 4-4. Continued

Pressure	Temperature (°F)					
(psia)	220	225	230	250	260	280
4514.7	0.00802	0.007977	0.007837	0.007502	0.007343	0.007072
5014.7	0.008687	0.008627	0.0085	0.007961	0.007856	0.007505
5514.7	0.009226	0.009111	0.008954	0.008435	0.008353	0.00798
6014.7	0.009758	0.009669	0.009475	0.008902	0.008819	0.008413
6514.7	0.010405	0.010208	0.009997	0.009339	0.009286	0.008892
7014.7	0.010717	0.010633	0.010504	0.00983	0.009647	0.009296
7514.7	0.011451	0.011093	0.010897	0.010291	0.010079	0.009679
8014.7	0.011816	0.011747	0.011352	0.010727	0.010605	0.010097

Table 4-4. Continued

Pressure	Temperature (°F)					
(psia)	300	320	340	360	380	415
4514.7	0.006833	0.006619	0.00615	0.006281	0.006134	0.005942
5014.7	0.007186	0.006821	0.006531	0.006593	0.00639	0.006176
5514.7	0.007579	0.007169	0.00709	0.006909	0.006657	0.006376
6014.7	0.00794	0.007546	0.007484	0.00726	0.007018	0.006591
6514.7	0.008369	0.007955	0.007757	0.007485	0.007176	0.006885
7014.7	0.008705	0.008299	0.007987	0.007671	0.007413	0.007084
7514.7	0.009026	0.008634	0.008245	0.007983	0.007652	0.007294
8014.7	0.009376	0.008916	0.008583	0.008143	0.0079	0.007536

Table 4-5. Methane viscosity from NIST

Pressure	Temperature (^{o}F)						
(psia)	100	120	140	160	180	188	200
4514.7	0.02454	0.02377	0.02315	0.02265	0.02226	0.02212	0.02195
5014.7	0.02615	0.02529	0.02459	0.02401	0.02353	0.02337	0.02315
5514.7	0.02766	0.02674	0.02596	0.02531	0.02477	0.02458	0.02433
6014.7	0.02909	0.02811	0.02728	0.02657	0.02597	0.02576	0.02546
6514.7	0.03045	0.02941	0.02853	0.02777	0.02712	0.02688	0.02656
7014.7	0.03173	0.03065	0.02972	0.02892	0.02822	0.02797	0.02763
7514.7	0.03296	0.03184	0.03086	0.03002	0.02928	0.02902	0.02865
8014.7	0.03412	0.03297	0.03196	0.03108	0.03031	0.03003	0.02963

Table 4-5. Continued

Pressure	Temperature (^{o}F)					
(psia)	220	225	230	250	260	280
4514.7	0.021708	0.021658	0.021612	0.02146	0.021401	0.021315
5014.7	0.022844	0.022778	0.022716	0.022503	0.022416	0.022277
5514.7	0.023958	0.023877	0.0238	0.023533	0.02342	0.023231
6014.7	0.025042	0.024949	0.024859	0.024541	0.024405	0.02417
6514.7	0.026095	0.025989	0.025888	0.025526	0.025367	0.025091
7014.7	0.027113	0.026997	0.026886	0.026483	0.026305	0.025991
7514.7	0.028098	0.027972	0.027852	0.027412	0.027217	0.026868
8014.7	0.029049	0.028916	0.028786	0.028314	0.028102	0.027722

Table 4-5. Continued

Pressure	Temperature (^{o}F)					
(psia)	300	320	340	360	380	415
4514.7	0.021266	0.021246	0.021253	0.021282	0.021331	0.021456
5014.7	0.022178	0.022113	0.022078	0.022069	0.022082	0.022151
5514.7	0.023085	0.022978	0.022904	0.022858	0.022837	0.022851
6014.7	0.023983	0.023835	0.023724	0.023643	0.023589	0.023551
6514.7	0.024864	0.02468	0.024534	0.02442	0.024336	0.024248
7014.7	0.025728	0.02551	0.025331	0.025187	0.025073	0.024939
7514.7	0.026572	0.026322	0.026113	0.02594	0.0258	0.025622
8014.7	0.027395	0.027116	0.026879	0.02668	0.026514	0.026294

The new calibration equation is applied to converted measured viscosity (or raw data) to pressure-temperature-corrected viscosity for the measurement at condition of pressure from 3000 to 25000 psig and temperature from 98 to 415 ^{o}F. Figures 4-21 through 4-24 illustrate the comparisons of converted gas viscosity using the new correlation with NIST values for methane viscosity at temperatures of 100 and 250 ^{o}F and nitrogen at temperatures of 152 and 330 ^{o}F. These comparisons indicate that converted viscosities are close to NIST values at pressure range of 3000 to 8000 psig for both methane and nitrogen as expected. Thus raw data are converted to gas viscosity using the new converted equation obtained from our analysis. It should be borne in mind that Equation 4.85 can only be valid for this specific viscometer used in this investigation.

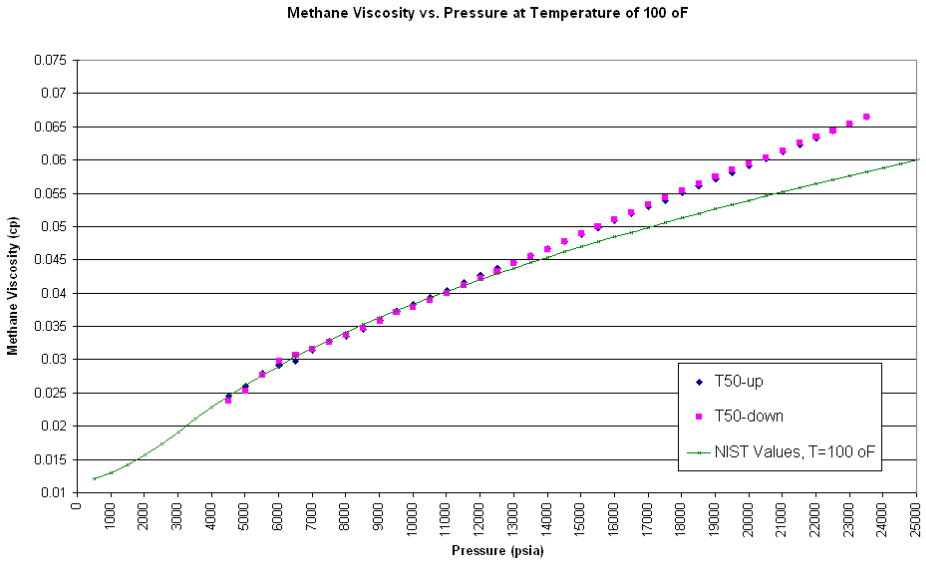

Figure 4-21. Comparison of pressure-temperature-converted methane viscosity with NIST values at temperature of 100 ^{o}F

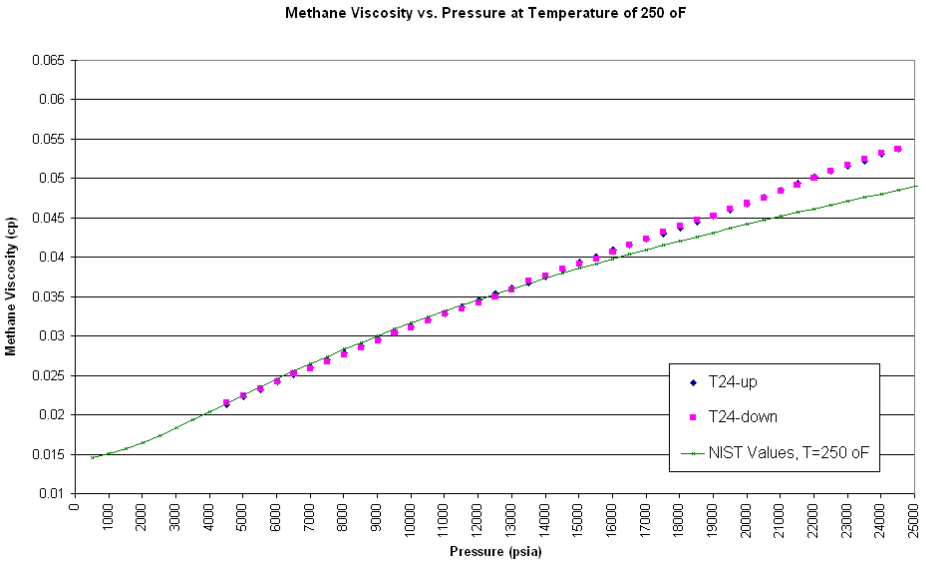

Figure 4-22. Comparison of pressure-temperature-converted methane viscosity with NIST values at temperature of 250 ^{o}F

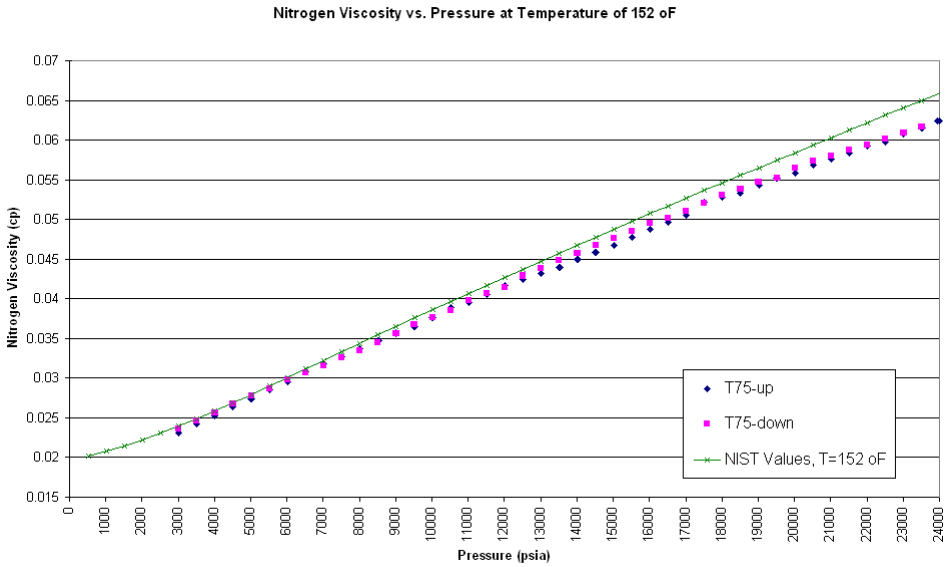

Figure 4-23. Comparison of pressure-temperature-converted nitrogen viscosity with NIST values at temperature of 152 ^{o}F

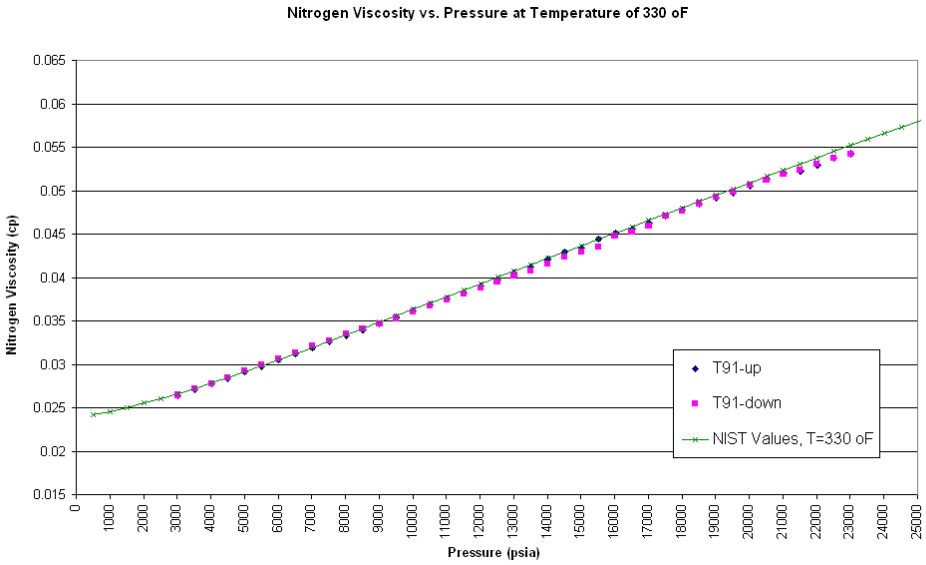

Figure 4-24. Comparison of pressure-temperature-converted nitrogen viscosity with NIST values at temperature of 330 ^{o}F

CHAPTER V

EXPERIMENTAL RESULTS

5.1 Nitrogen Viscosity Measurement

The nitrogen is prepared by ACETYLENE OXYGEN Co.. The mole fraction of nitrogen is 99.95%. Initial pressure in the gas tank is 1500 psig. Lots of efforts were investigated on nitrogen viscosity. There are totally 91 tests on nitrogen viscosity. Measuring condition is at pressures range from 3000 to 24500 psig with interval of 500 psi and at temperatures of 99, 105, 109, 111, 116, 134, 152, 165, 170, 174, 187, 200, 250, 260, 280, 300, 330, and 350 ^{o}F. Table 5-1 lists the experiments we had done on measuring nitrogen viscosity. Experiment data are used to develop the new converted equation. The more experiments we did on nitrogen, the more confident we are on the new converted equation. These experimental data are also used to develop a new gas viscosity correlation that is specified for nitrogen viscosity.

Table 5-1. Statistic of nitrogen viscosity experiment in this study

Composition	Temperature ^{o}F	Pressure psia	No. of Experiment
N_2	99	3014.7-13514.7	4
N_2	105	3014.7-14014.7	3
N_2	109	3014.7-13514.7	3
N_2	111	3014.7-14014.7	3
N_2	116	3014.7-23014.7	7
N_2	134	3014.7-22014.7	14
N_2	151	3014.7-13514.7	3
N_2	152	3014.7-24014.7	10
N_2	165	3014.7-15514.7	3
N_2	170	3014.7-23514.7	11
N_2	174	3014.7-15014.7	4
N_2	187	3014.7-17014.7	2
N_2	200	3014.7-24514.7	6
N_2	250	3014.7-22514.7	4
N_2	260	3014.7-24514.7	6
N_2	280	3014.7-24514.7	2
N_2	300	3014.7-24514.7	2
N_2	330	3014.7-23514.7	2
N_2	350	3014.7-24514.7	2

5.2 Nitrogen Viscosity Analysis

Comparing lab data from this study with NIST values and data from other investigators illuminated that extrapolating correlation based on low-moderate pressure/temperature to HPHT yields unacceptable result. For all experiments on nitrogen viscosity, lab data deviated from NIST value at high pressure at temperature of 116 ^{o}F (Figures 5-1 to 5-4). Similar result can be observed for temperature of 134, 152, 170, 200, 250, 260, 280, 300, 330, and 350 ^{o}F as show in Figures A-1 to A-27 in Appendix *A*. The deviation of NIST values from experimental data can be as high as 4.91% at pressure higher than 25014.7 psia. At high pressure nitrogen viscosities from lab are lower than NIST values. The difference between lab data and NIST values increases as pressure increases. This

difference at high pressure indicates that existing correlation cannot provide accurate viscosity to optimize the production of gas reservoirs with moderate-high nitrogen concentration at HPHT.

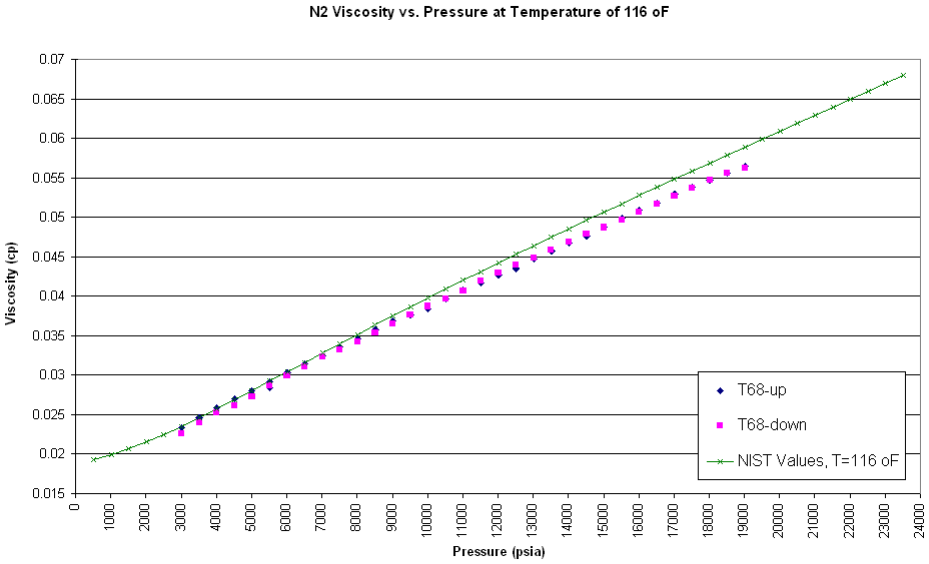

Figure 5-1. Nitrogen viscosity vs. pressure at 116 ^{o}F (Test 68)

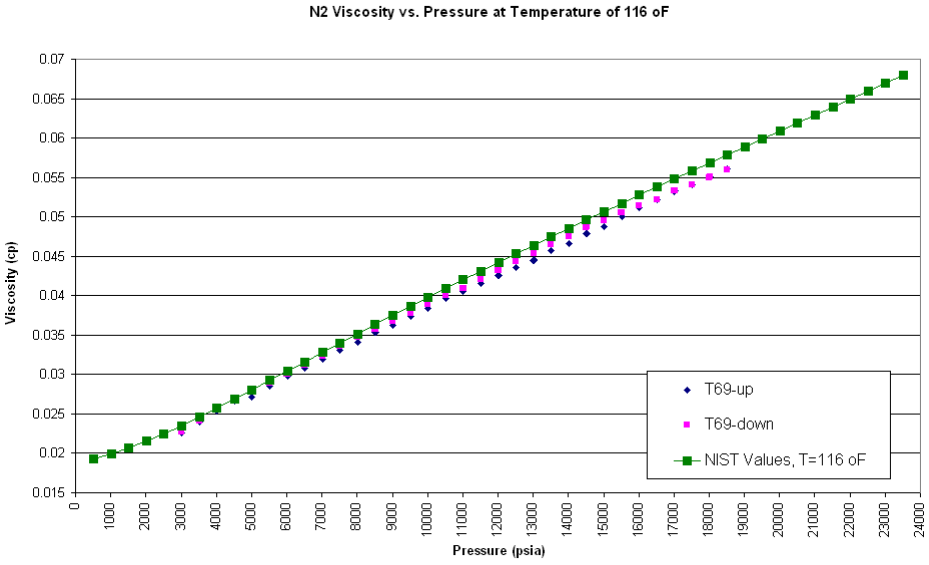

Figure 5-2. Nitrogen viscosity vs. pressure at 116 ^{o}F (Test 69)

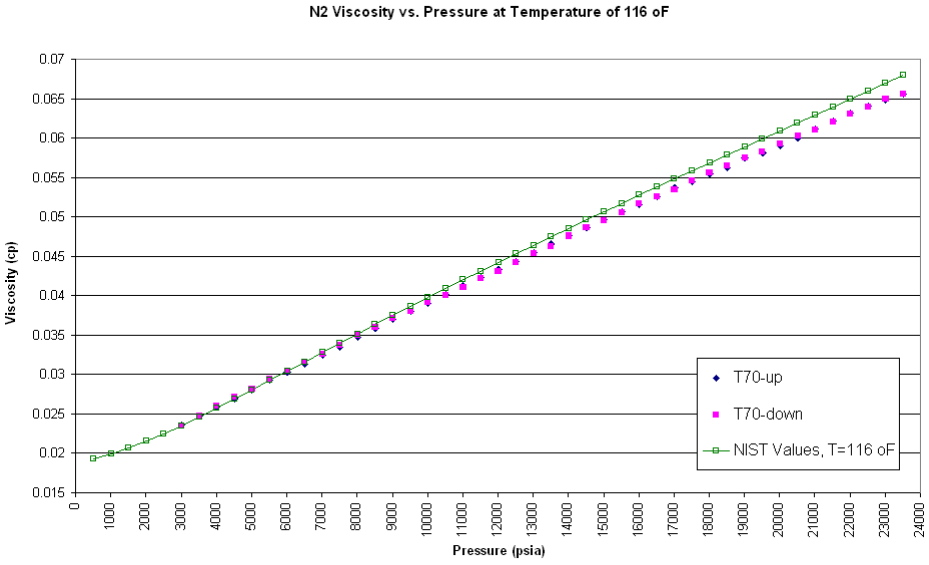

Figure 5-3. Nitrogen viscosity vs. pressure at 116 ^{o}F (Test 70)

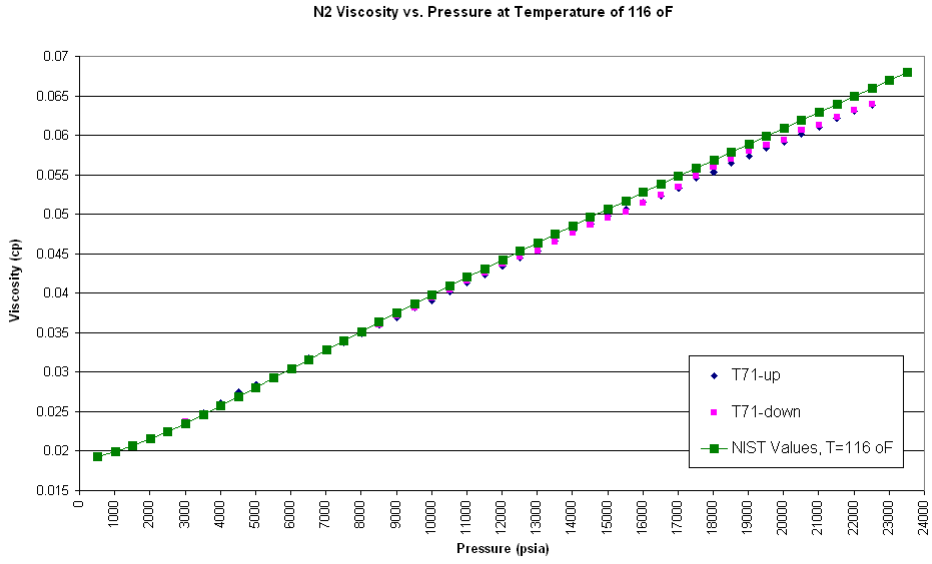

Figure 5-4. Nitrogen viscosity vs. pressure at 116 ^{o}F (Test 71)

Nitrogen, as a non-hydrocarbon, shows different thermodynamics properties from normal paraffins. Its viscosity varying with pressure and temperature does not follow the theorem of corresponding state as we see in hydrocarbon. So far no correlation is available to estimate nitrogen viscosity. A correlation that is particular for nitrogen viscosity is highly desirable and urgent as we encounter more and more high nitrogen HPHT gas reservoir. To develop this correlation we consider the both convenience and popularity. Since Lee-Gonzalez-Eakin correlation is one of the most common used viscosity correlations in petroleum engineering and easy to be coded into a program, we employed the same form as Lee-Gonzalez-Eakin correlation and changed the coefficients so that the new correlation can be used for nitrogen viscosity only. Database used to develop correlation consists of both literature experimental data and our lab data. A non-linear regression method was applied in preparing the correlation. Therefore, the nitrogen viscosity correlation gives a very convenient way to determine nitrogen viscosity at a large range of pressure temperature condition.

To illustrate the importance of our lab data and correlation, Nitrogen viscosities from new correlation are compared with Lee-Gonzalez-Eakin correlation and NIST values. In the comparison, viscosity at temperatures of 116, 200, 300, and 350 ^{o}F and pressure from 3514.7 to 25014.7 psia are selected to investigate the effect of pressure and temperature. Considering the observation that Lee-Gonzalez-Eakin correlation shows exponential increase of nitrogen viscosity as pressure increases, which deviates radically from both lab data and NIST value (Figures 5-5 through 5-8), we concluded that Lee-Gonzalez-Eakin correlation is inappropriate for nitrogen viscosity. As a result we switched to the comparison between our data with NIST values. Two observations were made basing on the comparison:

1) Our nitrogen viscosity is lower than NIST values at high pressure region
2) For same temperature, the nitrogen viscosity difference becomes larger as pressure increases

Error analysis in Table 5-2 indicates that even the absolute error is low, the relative error can be as high as 4.91% at temperature of 200 ^{o}F and pressure of 23514.7 psia. It should be noted that data in this study are used as base for both absolute error and relative error. Figures 5-9 through 5-12 show the comparisons between new correlation and NIST values.

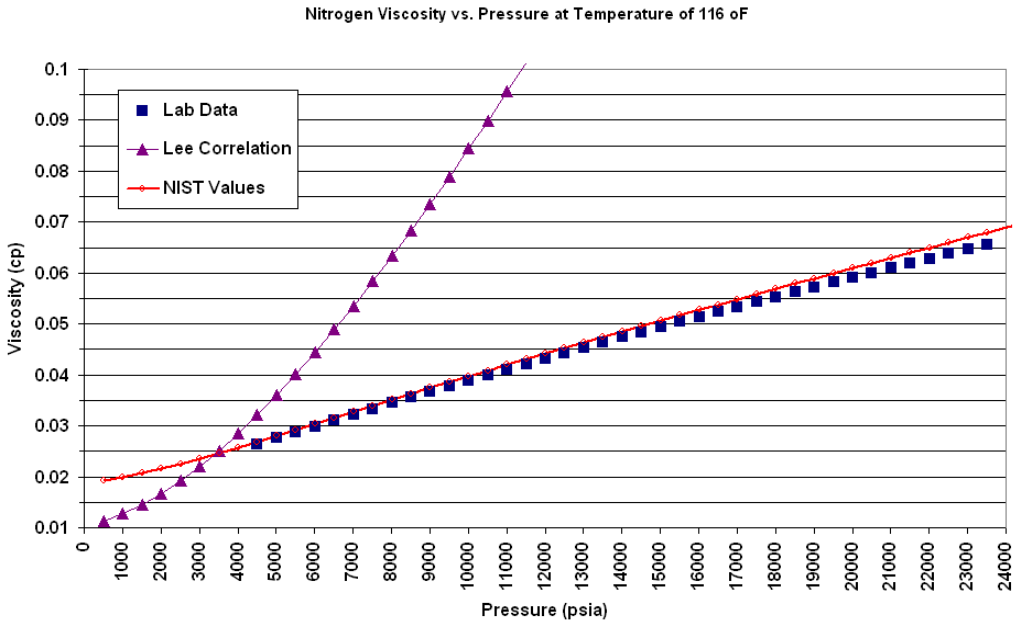

Figure 5-5. Lee-Gonzalez-Eakin correlation is inappropriate for nitrogen viscosity at temperature of 116 ^{o}F

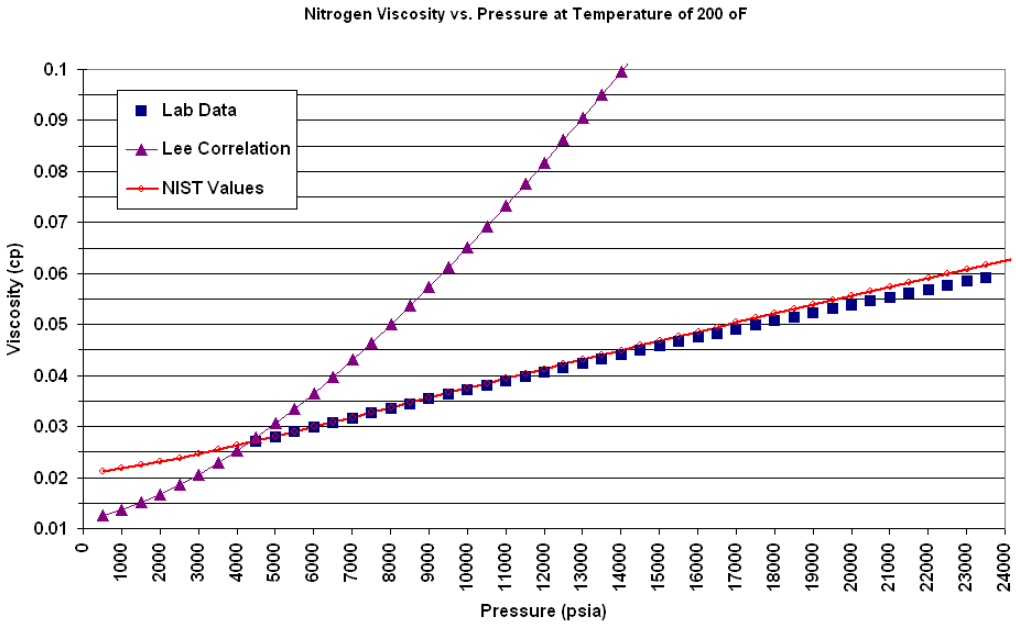

Figure 5-6. Lee-Gonzalez-Eakin correlation is inappropriate for nitrogen viscosity at temperature of 220 ^{o}F

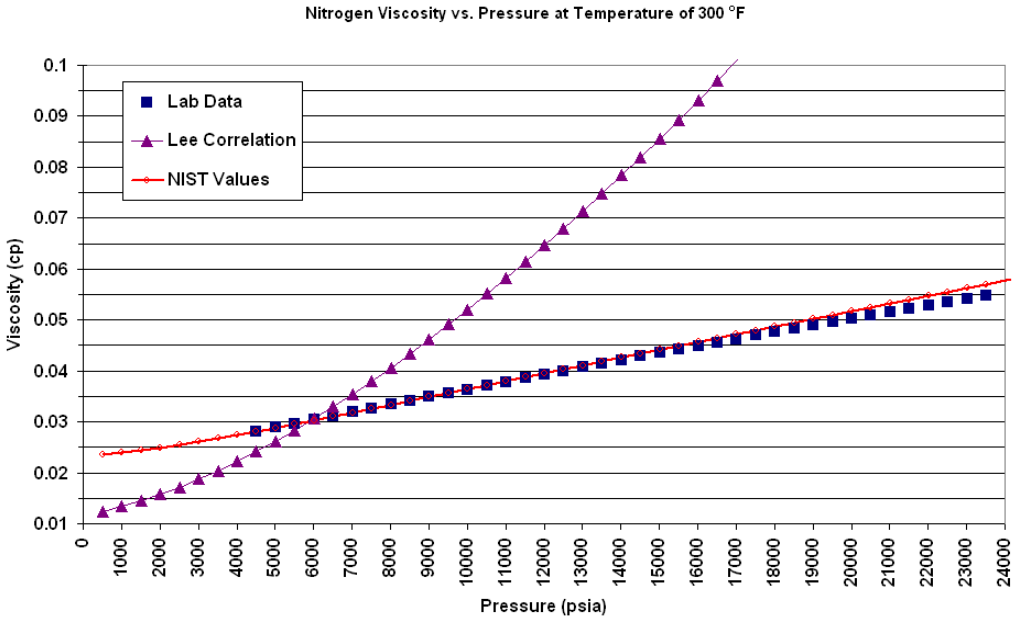

Figure 5-7. Lee-Gonzalez-Eakin correlation is inappropriate for nitrogen viscosity at temperature of 300 ^{o}F

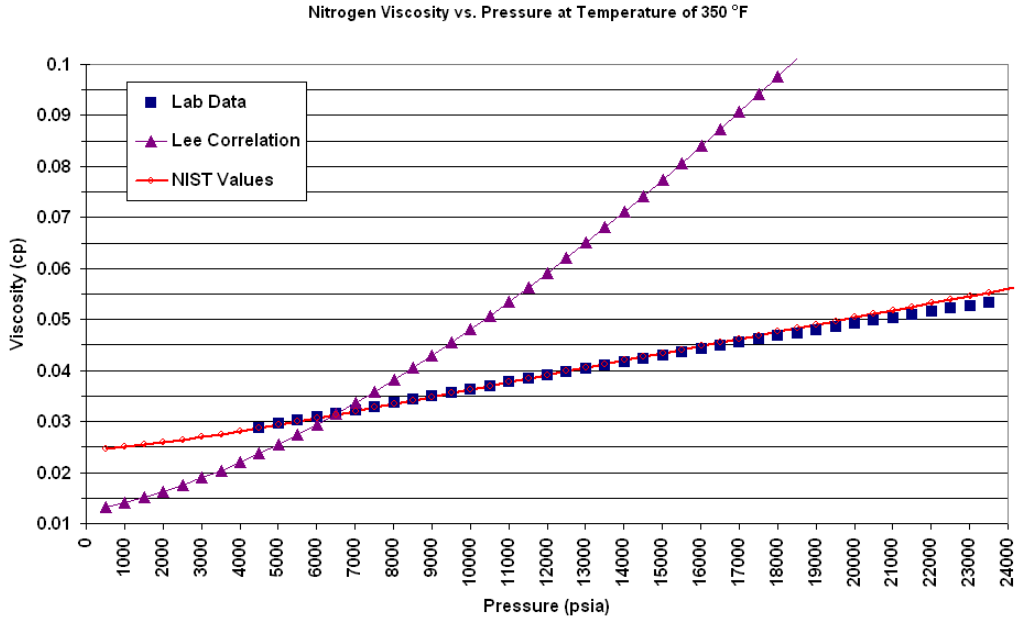

Figure 5-8. Lee-Gonzalez-Eakin correlation is inappropriate for nitrogen viscosity at temperature of 350 ^{o}F

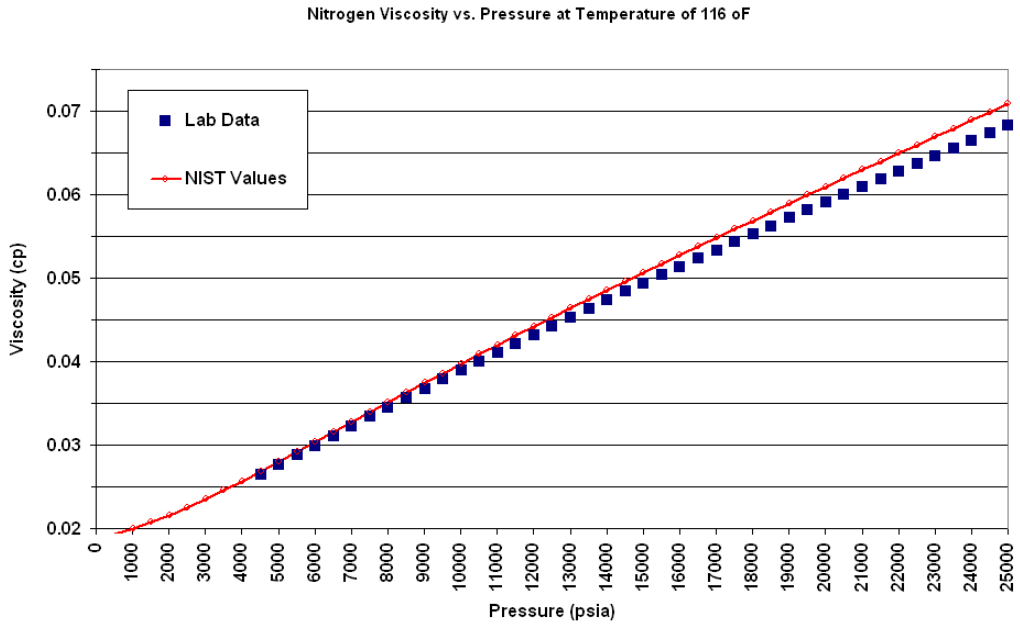

Figure 5-9. Comparison between new correlation and NIST values at temperature of 116 ^{o}F

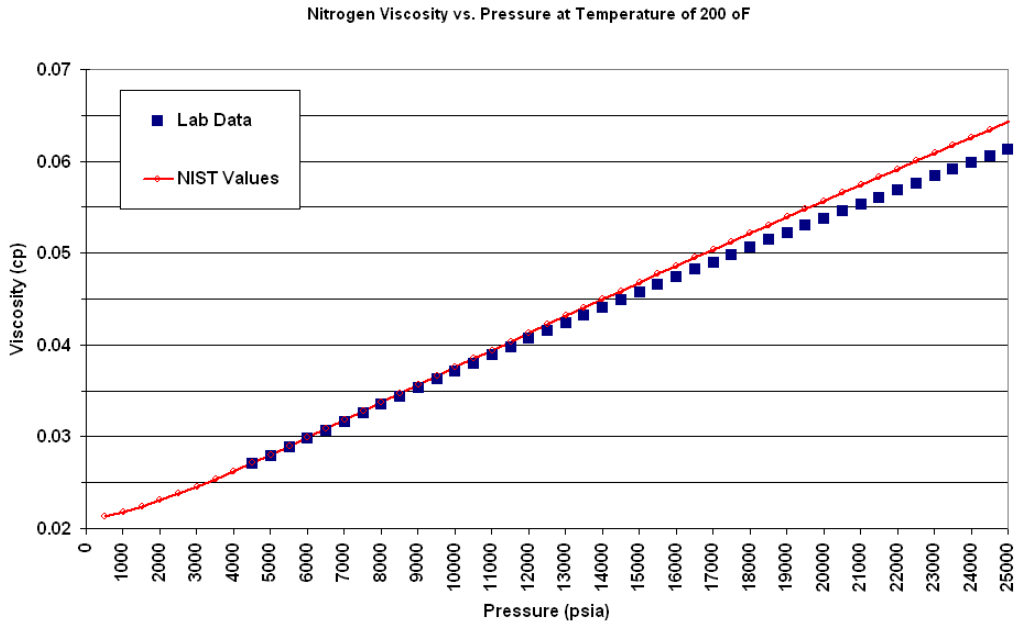

Figure 5-10. Comparison between new correlation and NIST values at temperature of 200 ^{o}F

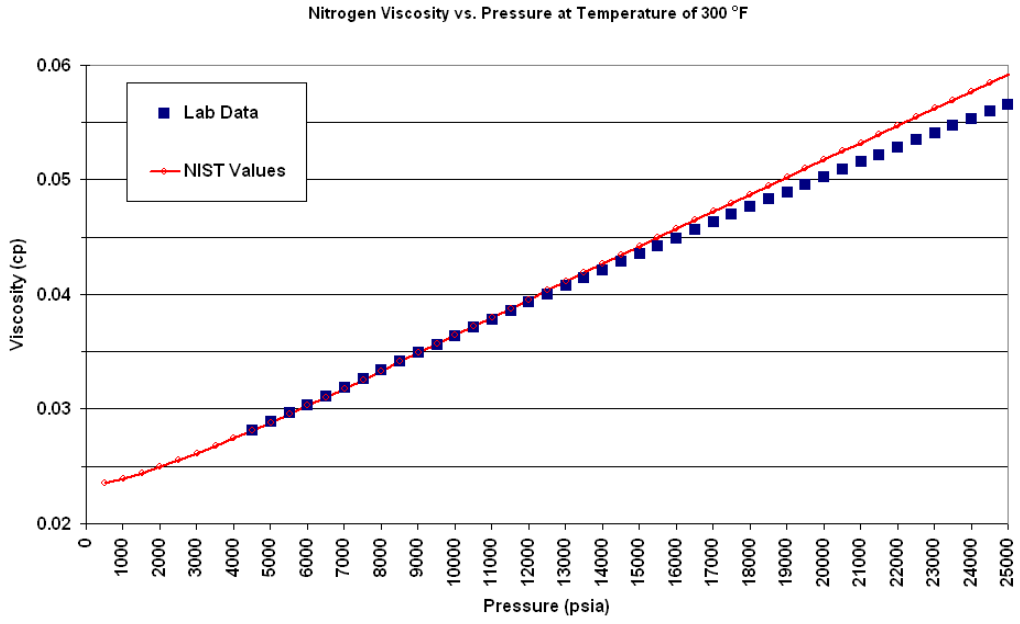

Figure 5-11. Comparison between new correlation and NIST values at temperature of 300 ^{o}F

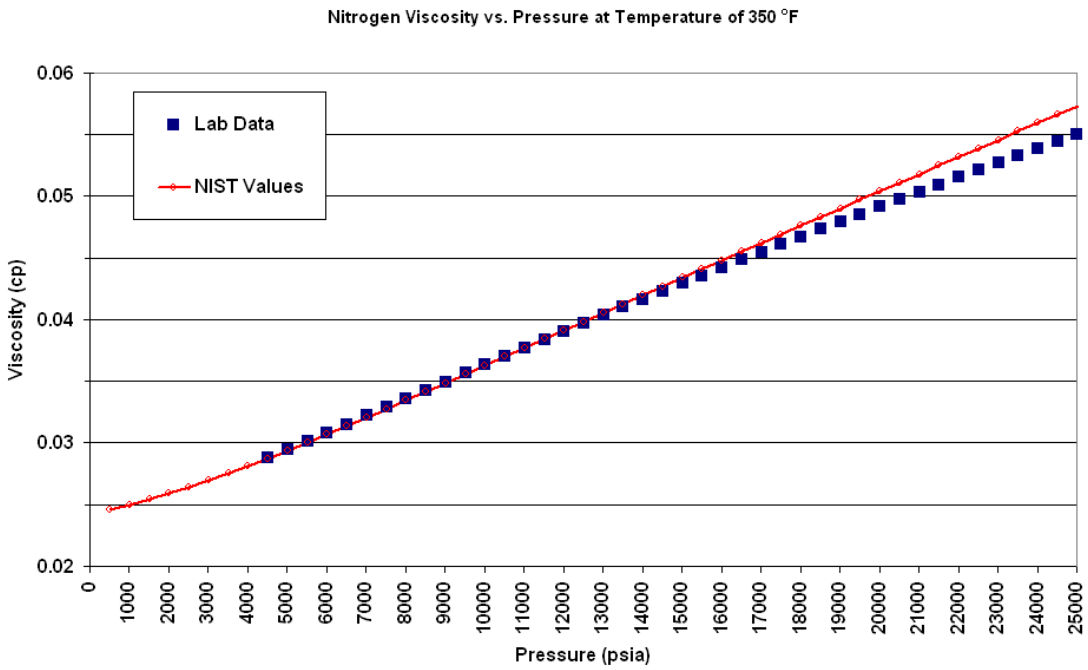

Figure 5-12. Comparison between new correlation and NIST values at temperature of 350 ^{o}F

Table 5-2. Error analysis for nitrogen viscosity from NIST program

Temperature (^{o}F)	Absolute Error (cp) Pressure (psia)			Relative Error (%) Pressure (psia)		
	10015	20015	23515	10015	20015	23515
	NIST					
116	0.00082	0.00188	0.00263	2.0962	3.1841	3.8554
200	0.00044	0.00193	0.00301	1.1927	3.5843	4.9099
300	0.00008	0.00150	0.00262	0.2158	2.9869	4.6299
350	-0.00005	0.00126	0.00234	-0.1332	2.5626	4.2463

5.3 Methane Viscosity Measurement

Methane used in the experiment is provided by MATHESON TRIGAS Inc.. The mole fraction of methane is 99.98%. Initial pressure in the gas tank is 1500 psig. Measurement had been done at pressure range from 4500 to 25000 psig and temperature of 100, 120,

140, 160, 180, 188, 200, 220, 225, 230, 250, 260, 280, 300, 320, 340, 360, 380, and 415 ^{o}F. Again, Table 5-3 lists the experiments we had done on measuring methane viscosity. Totally 50 experiments had been run in order to prepare an abundant dataset for our gas viscosity correlation.

Table 5-3. Statistic of methane viscosity experiment in this study

Composition	Temperature ^{o}F	Pressure psia	No. of Experiment
CH_4	100	4514.7-25014.7	2
CH_4	111	4014.7-24014.7	2
CH_4	120	4514.7-24514.7	2
CH_4	131	4514.7-23514.7	2
CH_4	140	4514.7-25014.7	2
CH_4	151	4514.7-24514.7	4
CH_4	160	4514.7-25014.7	2
CH_4	171	4514.7-24514.7	3
CH_4	180	4514.7-25014.7	2
CH_4	188	4514.7-24514.7	3
CH_4	200	4014.7-24514.7	3
CH_4	220	5014.7-25014.7	3
CH_4	225	4514.7-25014.7	1
CH_4	230	4514.7-24514.7	1
CH_4	250	4514.7-24514.7	2
CH_4	260	4514.7-25014.7	2
CH_4	280	4514.7-25014.7	2
CH_4	300	4514.7-24514.7	2
CH_4	320	4514.7-25014.7	2
CH_4	340	4514.7-25014.7	2
CH_4	360	4514.7-24514.7	2
CH_4	380	4514.7-25014.7	2
CH_4	415	4514.7-24514.7	2

5.4 Methane Viscosity Analysis

Same as the procedure to analyze nitrogen, lab data are compared with NIST values and data (low-moderate pressure/temperature) from other investigators. Through the comparison, we found that lab data match with NIST values at low-moderate pressure, but at high pressure methane viscosities from lab are higher than NIST values for the experiments at temperature of 100 ^{o}F (Figures 5-13 to 5-14). Similar result can be observed for temperature of 120, 140, 160, 180, 188, 200, 220, 225, 230, 250, 260, 280, 300, 320, 340, 360, 380, and 415 ^{o}F as show in Figures B-1 to B-37 in Appendix B. The difference between lab data and NIST values decreases as temperature increases; this difference increases as pressure increases.

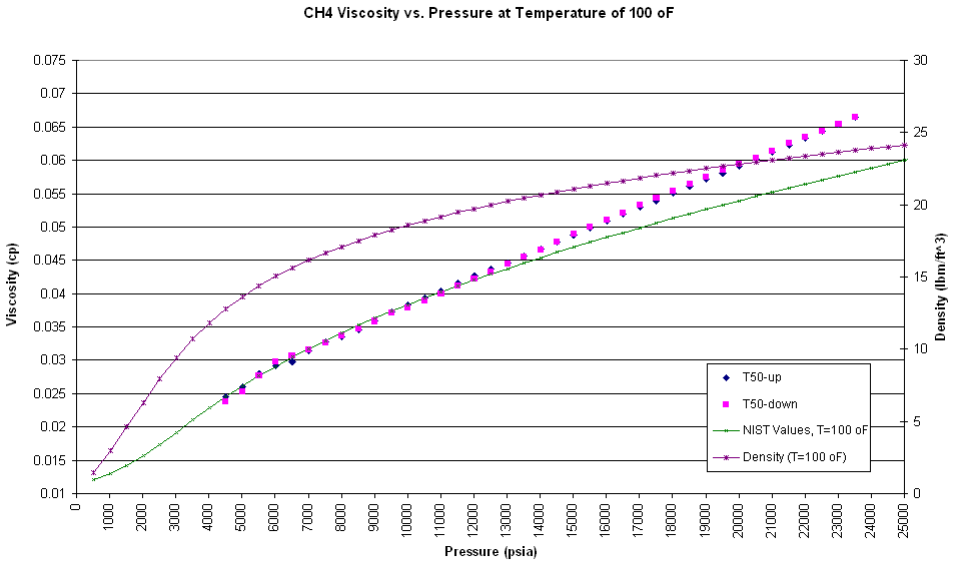

Figure 5-13. Methane viscosity vs. pressure at 100 ^{o}F (Test 50)

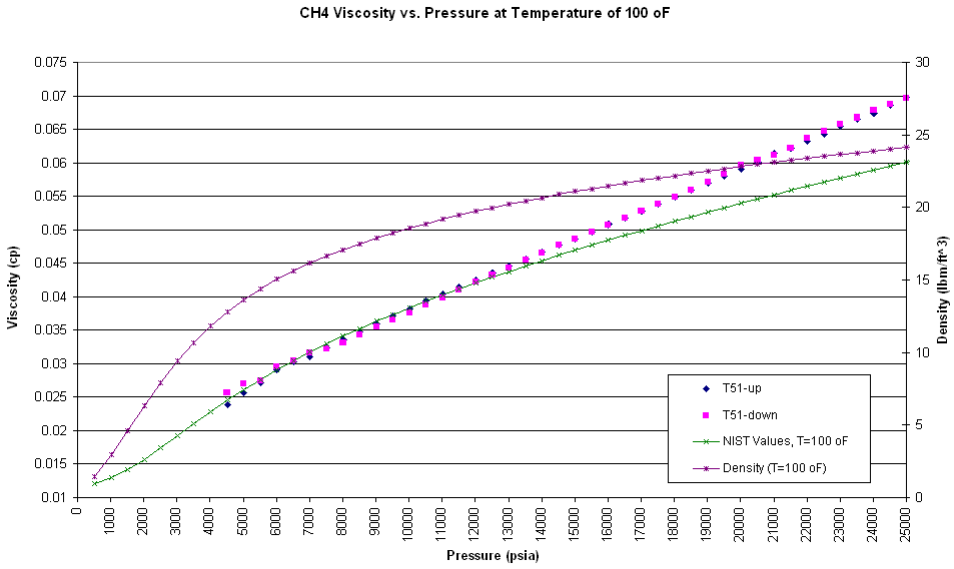

Figure 5-14. Methane viscosity vs. pressure at 100 ^{o}F (Test 51)

As we mentioned before, we developed our new correlation in the same form as Lee-Gonzalez-Eakin correlation. Lee-Gonzalez-Eakin correlation is based on low-moderate pressure experimental data and proved to be not accurate enough at HPHT by our experiment results. Again, easy to be used and coded into computer program are our top priority in constructing new correlation. Basing on our experiment result and existing viscosity data at low pressure, a modified Lee-Gonzalez-Eakin gas viscosity correlation was constructed using non-linear regression method. This correlation covers larger pressure and temperature range than available correlations. Therefore, it gives more confidence on estimating gas viscosity.

The significance of this correlation is testified by the comparison our viscosity with Lee-Gonzalez-Eakin correlation, NIST values, and Viswanathan correlation. In the comparison, viscosity at temperatures of 100, 200, 300, and 415 ^{o}F are selected to investigate the effect of pressure and temperature. These comparisons indicate that at high pressure, new correlation gives higher methane viscosity than Lee-Gonzalez-Eakin correlation, NIST values, and Viswanathan correlation. The difference becomes smaller

as temperature increases, while as pressure increases, the difference increases. The relative error at low temperature such as 100 ^{o}F can be up to -10.12%, -11.03%, and -16.13% for Lee-Gonzalez-Eakin correlation, NIST, and Viswanathan, respectively. At high temperature such as 415 ^{o}F the relative error can be as high as -2.47%, -9.12%, and -11.01% for Lee-Gonzalez-Eakin correlation, NIST, and Viswanathan, respectively. Table 5-4 shows the results of error analysis. It should be noted that data in this study are used as base for both absolute error and relative error. Figures 5-15 through 5-18 show the comparisons methane viscosity in this study with existing correlations.

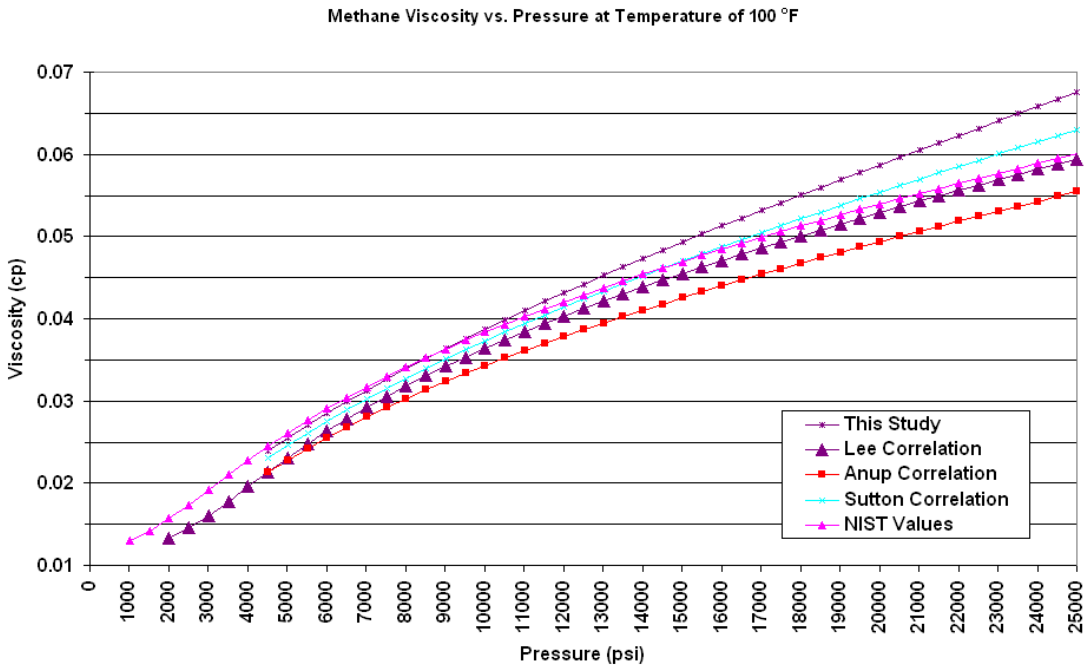

Figure 5-15. Comparison this study with existing correlations at temperature of 100 ^{o}F

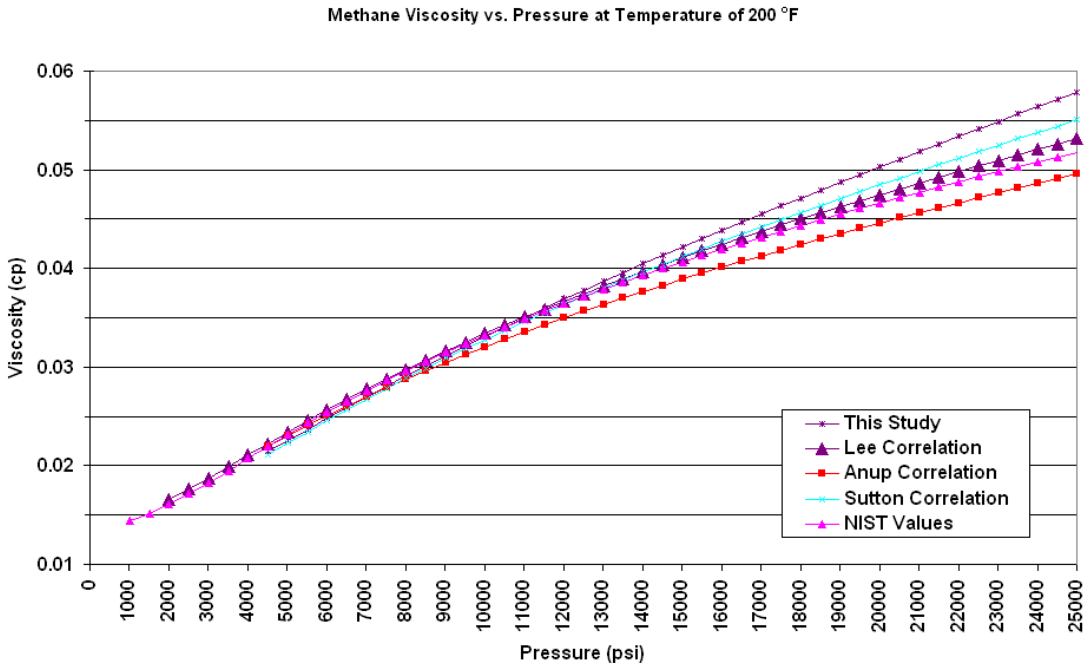

Figure 5-16. Comparison this study with existing correlations at temperature of 200 ^{o}F

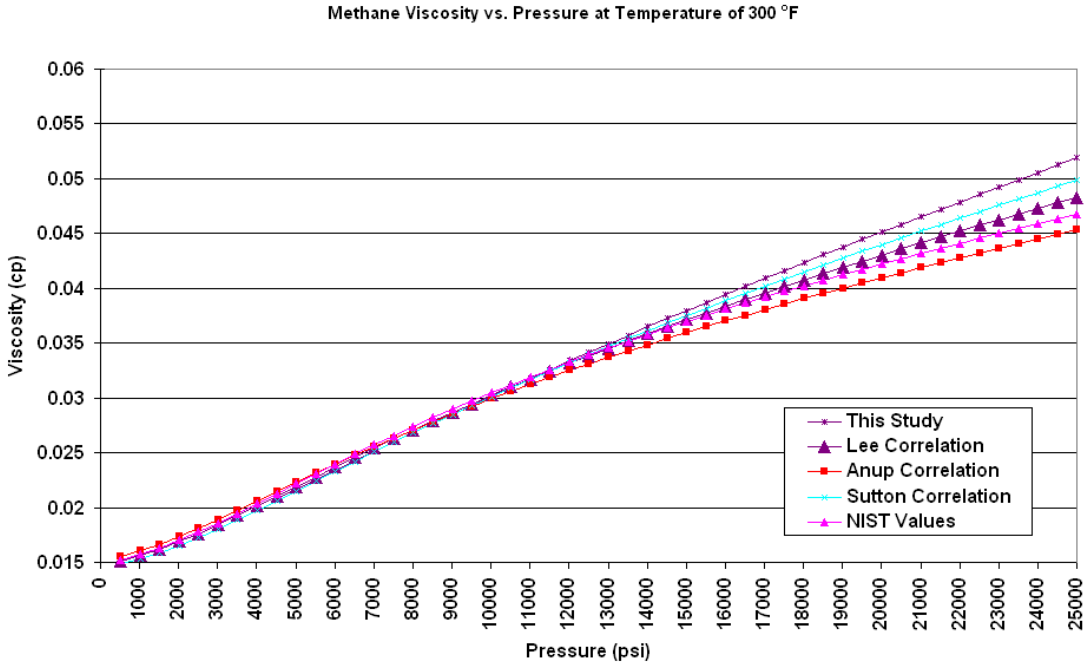

Figure 5-17. Comparison this study with existing correlations at temperature of 300 ^{o}F

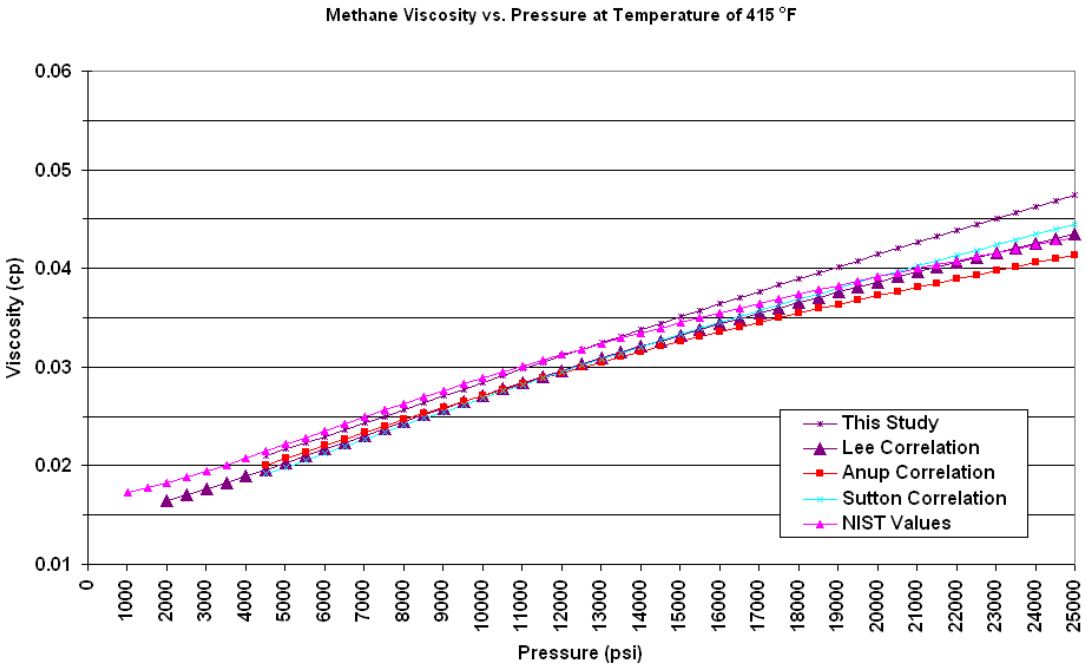

Figure 5-18. Comparison this study with existing correlations at temperature of 415 ^{o}F

Table 5-4. Error analysis for methane viscosity from different correlations

Temperature (^{o}F)	Absolute Error (cp) Pressure (psia)			Relative Error (%) Pressure (psia)		
	10015	20015	25015	10015	20015	25015
	Lee-Gonzalez-Eakin Correlation					
100	-0.00032	-0.00444	-0.00683	-0.82	-7.56	-10.12
200	0.00028	-0.00281	-0.00472	0.85	-5.59	-8.16
300	0.00095	-0.00131	-0.00282	3.16	-2.89	-5.44
415	0.00161	0.00002	-0.00118	4.63	0.04	-2.47
	NIST Program					
100	-0.00038	-0.00479	-0.00744	-0.98	-8.15	-11.03
200	0.00013	-0.00366	-0.00611	0.38	-7.27	-10.55
300	0.00031	-0.00291	-0.00514	1.04	-6.45	-9.91
415	0.00042	-0.00234	-0.00437	1.46	-5.60	-9.12
	Viswanathan Correlation					
100	-0.00261	-0.00810	-0.01089	-6.74	-13.79	-16.13
200	-0.00107	-0.00572	-0.00829	-3.23	-11.36	-14.31
300	-0.00024	-0.00418	-0.00655	-0.78	-9.26	-12.63
415	0.00027	-0.00307	-0.00527	0.94	-7.36	-11.01

CHAPTER VI

NEW GAS VISCOSITY CORRELATIONS

6.1 Nitrogen Viscosity Correlation

The aforementioned differences for both nitrogen and methane at high pressure indicate that available correlations give unacceptable result at HPHT. Two gas viscosity correlations were developed upon the completed experiments on methane and nitrogen viscosity. One is specified for methane viscosity to honor the importance of methane in HPHT gas reservoirs; another is tailored for nitrogen considering the fact that some HPHT reservoirs contain significant amount of nitrogen.

Due to the lack of nitrogen viscosity data at HPHT and correlation that is suitable for nitrogen viscosity, a correlation that provides accurate nitrogen viscosity is preferred. Since Lee-Gonzalez-Eakin correlation is one of the most common used viscosity correlations in petroleum engineering and can be coded into computer program easily, we developed a correlation that has the same form as Lee-Gonzalez-Eakin correlation. The coefficients in the correlation were updated using NIST values and lab data from our experiment. Due to the fact that we do not have viscosity data at pressure from 500 to 2999 psi in our experiment, NIST values at this pressure range were used. As we already showed in Chapter II, NIST values match with lab data very well at pressure from 500 to 2999 psi. Combining NIST values at pressure from 514.7 to 2514.7 psia with our lab data at pressure from 3014.7 to 24514.7 psia the coefficients were determined, and then the final form of correlation was developed. This correlation is tailored for nitrogen viscosity. It is expressed as:

$$\mu_g = K \exp\left(X \rho_g{}^{Y}\right). \tag{6.1}$$

$$K = \frac{0.0001 * (9.206483 + 3.550036 M_w) T^{1.217156}}{208.9852 + 18.70586 M_w + T}. \tag{6.2}$$

where

$$X = -3.41179 + \left[\frac{999.9949}{T}\right] + 0.14457226 M_w . \quad (6.3)$$

$$Y = 1.293365 + 0.11245 X . \quad (6.4)$$

where

μ_g = Gas viscosity, cp

ρ_g = Gas density, g/cc

M_W = Molecular weight

T = Temperature, R

New correlation that based on lab data and NIST values (Table 6-1) covers larger pressure and temperature. It eliminated the embarrassment fact of lacking correlation to calculate nitrogen viscosity. Thus it provided an easy but reliable approach to determine nitrogen viscosity when petroleum engineers deal with high nitrogen HPHT reservoir.

Table 6-1. Data used to develop nitrogen viscosity correlation

Pressure	Temperature (oF)					
(psia)	116	134	152	170	200	250
514.7	0.019345	0.019771	0.020193	0.02061	0.021296	0.022414
1014.7	0.01999	0.020387	0.020783	0.021177	0.021828	0.022897
1514.7	0.020736	0.021096	0.021457	0.02182	0.022426	0.023433
2014.7	0.021582	0.021894	0.022213	0.022537	0.023088	0.02402
2514.7	0.022518	0.022773	0.023043	0.023323	0.023809	0.024654
3014.7	0.023344	0.02364	0.023728	0.023941	0.024386	0.025195
3514.7	0.024604	0.024595	0.024851	0.024699	0.025257	0.025939
4014.7	0.025919	0.025547	0.025853	0.026036	0.026169	0.026888
4514.7	0.027063	0.02675	0.027038	0.026937	0.026972	0.027711
5014.7	0.028055	0.027653	0.027954	0.028042	0.027872	0.028558
5514.7	0.029326	0.0288	0.029148	0.029168	0.028804	0.029416
6014.7	0.030382	0.029793	0.030153	0.030173	0.02988	0.030239
6514.7	0.031464	0.030834	0.031353	0.031124	0.030758	0.030883
7014.7	0.032543	0.031905	0.032339	0.031971	0.031789	0.03162
7514.7	0.033704	0.033018	0.033251	0.032947	0.032705	0.032555
8014.7	0.034875	0.034169	0.034219	0.033878	0.033667	0.033494
8514.7	0.035969	0.035258	0.035219	0.034711	0.034534	0.034212
9014.7	0.037071	0.036345	0.036191	0.035596	0.035564	0.035015
9514.7	0.038043	0.037568	0.037012	0.036507	0.036531	0.035661
10014.7	0.039160	0.037993	0.038116	0.037269	0.037403	0.0364
10514.7	0.040056	0.039071	0.039339	0.038284	0.038248	0.037461
11014.7	0.041098	0.040124	0.039978	0.039276	0.039071	0.038295
11514.7	0.042163	0.041445	0.041031	0.040181	0.039937	0.039196
12014.7	0.043098	0.042464	0.042063	0.041123	0.04076	0.040078
12514.7	0.044248	0.043453	0.042871	0.041906	0.04162	0.040866
13014.7	0.045402	0.044475	0.043651	0.042836	0.042424	0.041651
13514.7	0.046322	0.045475	0.044413	0.043746	0.043342	0.042484
14014.7	0.047623	0.0464	0.045371	0.04461	0.044206	0.043
14514.7	0.048683	0.047166	0.046265	0.045549	0.044919	0.043715
15014.7	0.049568	0.048247	0.047084	0.046079	0.045791	0.044493
Note: viscosity in cp						

Table 6-1. Continued.

Pressure	Temperature (^{o}F)					
(psia)	116	134	152	170	200	250
15514.7	0.050592	0.049266	0.048075	0.047023	0.046517	0.045475
16014.7	0.051764	0.050264	0.049088	0.047862	0.047192	0.046351
16514.7	0.052672	0.051207	0.049954	0.048649	0.048031	0.047241
17014.7	0.053605	0.05222	0.050862	0.049491	0.048815	0.048091
17514.7	0.054731	0.053216	0.052445	0.050268	0.049518	0.048763
18014.7	0.055697	0.054021	0.053098	0.051093	0.050487	0.049704
18514.7	0.056688	0.054946	0.053637	0.051915	0.051173	0.050559
19014.7	0.057709	0.055809	0.054551	0.052777	0.051948	0.05102
19514.7	0.058486	0.056899	0.055435	0.053651	0.053018	0.051942
20014.7	0.059449	0.057801	0.056138	0.054433	0.053677	0.052681
20514.7	0.060453	0.058634	0.057104	0.055233	0.054713	0.053849
21014.7	0.061207	0.059407	0.057874	0.05592	0.055375	0.054375
21514.7	0.062227	0.060503	0.058565	0.056644	0.05594	0.055036
22014.7	0.063335	0.061437	0.059415	0.057361	0.056725	0.05572
22514.7	0.064221	-	0.060009	0.057992	0.057472	0.056405
23014.7	0.065187	-	0.060928	0.058939	0.058197	0.057207
23514.7	0.065890	-	0.061715	0.059527	0.058906	0.057812
24014.7	-	-	0.062615	0.060454	0.059759	-
24514.7	-	-	-	-	0.060374	-
Note: viscosity in cp						

Table 6-1. Continued

Pressure	Temperature (^{o}F)				
(psia)	260	280	300	330	350
514.7	0.022634	0.023071	0.023502	0.024142	0.024562
1014.7	0.023108	0.023528	0.023945	0.024563	0.024971
1514.7	0.023633	0.024033	0.024431	0.025023	0.025416
2014.7	0.024207	0.024583	0.024958	0.025521	0.025895
2514.7	0.024827	0.025175	0.025525	0.026054	0.026408
3014.7	0.025341	0.025691	0.0260644	0.026213	0.026199
3514.7	0.02611	0.026465	0.0267543	0.027087	0.026968
4014.7	0.026895	0.027199	0.0274147	0.027623	0.02803
4514.7	0.027598	0.027766	0.0279982	0.028261	0.028724
5014.7	0.028265	0.028575	0.0288316	0.028986	0.029251
5514.7	0.028922	0.029357	0.0294874	0.029689	0.029879
6014.7	0.029657	0.03014	0.0301861	0.030388	0.030412
6514.7	0.030405	0.030904	0.0309738	0.031089	0.031159
7014.7	0.03127	0.031681	0.0317405	0.03169	0.031836
7514.7	0.032132	0.03244	0.0326275	0.032471	0.032612
8014.7	0.033008	0.033206	0.0332753	0.033078	0.033252
8514.7	0.033814	0.034034	0.0340652	0.033856	0.033951
9014.7	0.034548	0.034817	0.0348356	0.034723	0.034644
9514.7	0.035435	0.03552	0.0355664	0.035516	0.035391
10014.7	0.036164	0.036352	0.0362704	0.036222	0.03619
10514.7	0.036966	0.037109	0.037045	0.03689	0.036907
11014.7	0.03794	0.037968	0.0377955	0.037683	0.037543
11514.7	0.038501	0.038726	0.0385455	0.038204	0.038125
12014.7	0.039358	0.03951	0.0392036	0.039061	0.038825
12514.7	0.040237	0.040282	0.0399718	0.039725	0.039535
13014.7	0.041008	0.041068	0.0406165	0.040374	0.040161
13514.7	0.041758	0.041772	0.0412419	0.041066	0.040862
14014.7	0.04249	0.042391	0.0420897	0.041731	0.041482
14514.7	0.043394	0.04311	0.0427644	0.042345	0.042209
15014.7	0.044105	0.043879	0.0434234	0.043255	0.042845
Note: viscosity in cp					

Table 6-1. Continued

Pressure	Temperature (^{o}F)				
(psia)	260	280	300	330	350
15514.7	0.04482	0.044519	0.0440919	0.043831	0.043588
16014.7	0.04556	0.045284	0.0447748	0.044429	0.044109
16514.7	0.046467	0.046077	0.0455216	0.045059	0.044793
17014.7	0.047162	0.046819	0.0460829	0.04561	0.045602
17514.7	0.047831	0.047445	0.0468567	0.046205	0.046173
18014.7	0.048523	0.048267	0.0473977	0.047103	0.046742
18514.7	0.049305	0.048955	0.0483329	0.047899	0.047433
19014.7	0.050202	0.049607	0.0489835	0.048599	0.047751
19514.7	0.051041	0.050233	0.0495366	0.049106	0.048567
20014.7	0.051797	0.050873	0.0505066	0.049923	0.048764
20514.7	0.05261	0.051545	0.0508617	0.050343	0.049353
21014.7	0.053359	0.052255	0.0515341	0.050965	0.049894
21514.7	0.05414	0.053122	0.0520189	0.051458	0.050773
22014.7	0.054842	0.05386	0.0529056	0.052154	0.051344
22514.7	0.055556	0.054358	0.0536604	0.052833	0.052074
23014.7	0.056203	0.054914	0.0539155	0.053437	0.052615
23514.7	0.056774	0.055518	0.0545946	0.053902	0.053167
24014.7	0.057433	0.055971	0.0550585	-	0.053758
24514.7	0.058238	0.056712	0.055598	-	0.054709
Note: viscosity in cp					

To a certain level, the differences between lab data and values from correlation reflect the quality of the experiment. We also want to know the accuracy of new nitrogen viscosity correlation. The evaluation can be accomplished by comparing the calculated viscosity from correlation with lab data. Therefore error analysis gives us a confident interval of the new correlation. It should be noted that lab data are used as base for both absolute error and relative error. Tables 6-2 and 6-3 show the absolute error and relative error. Average absolute error is -4.31E-06 cp. Average relative error is -0.0247%.

Table 6-2. Absolute error by comparing nitrogen viscosity data with values from correlation

Pressure	Temperature (^{o}F)					
(psia)	116	134	152	170	200	250
	Absolute Error (cp)					
514.7	-6.65E-05	-4.27E-05	-2.21E-05	-3.39E-06	2.17E-05	4.86E-05
1014.7	-2.02E-04	-1.69E-04	-1.41E-04	-1.17E-04	-8.29E-05	-4.39E-05
1514.7	-2.70E-04	-2.32E-04	-1.98E-04	-1.69E-04	-1.28E-04	-8.03E-05
2014.7	-3.06E-04	-2.62E-04	-2.23E-04	-1.88E-04	-1.41E-04	-8.57E-05
2514.7	-3.29E-04	-2.77E-04	-2.33E-04	-1.93E-04	-1.39E-04	-7.40E-05
3014.7	-1.61E-04	-2.05E-04	-2.76E-05	3.47E-05	6.72E-05	8.03E-05
3514.7	-3.68E-04	-1.65E-04	-2.08E-04	1.73E-04	2.29E-05	7.20E-05
4014.7	-5.87E-04	-8.15E-05	-2.29E-04	-2.31E-04	-2.73E-05	-1.12E-04
4514.7	-6.06E-04	-2.22E-04	-4.06E-04	-1.74E-04	5.62E-05	-1.47E-04
5014.7	-4.55E-04	-4.28E-05	-2.94E-04	-3.02E-04	6.07E-05	-1.90E-04
5514.7	-5.74E-04	-9.76E-05	-4.51E-04	-4.40E-04	4.39E-05	-2.32E-04
6014.7	-4.75E-04	5.81E-06	-4.12E-04	-4.49E-04	-1.08E-04	-2.31E-04
6514.7	-4.02E-04	6.23E-05	-5.67E-04	-4.03E-04	-6.04E-05	-4.57E-05
7014.7	-3.31E-04	8.53E-05	-5.11E-04	-2.53E-04	-1.64E-04	4.67E-05
7514.7	-3.48E-04	6.17E-05	-3.83E-04	-2.36E-04	-1.55E-04	-5.76E-05
8014.7	-3.84E-04	-7.65E-06	-3.18E-04	-1.79E-04	-1.95E-04	-1.67E-04
8514.7	-3.51E-04	-2.33E-05	-2.91E-04	-2.91E-05	-1.44E-04	-6.06E-05
9014.7	-3.37E-04	-4.30E-05	-2.44E-04	6.24E-05	-2.62E-04	-4.08E-05
9514.7	-2.02E-04	-2.09E-04	-5.37E-05	1.20E-04	-3.22E-04	1.32E-04
10014.7	-2.23E-04	4.13E-04	-1.56E-04	3.20E-04	-2.94E-04	2.05E-04
10514.7	-3.32E-05	3.73E-04	-3.85E-04	2.58E-04	-2.46E-04	-4.71E-05
11014.7	8.42E-07	3.48E-04	-3.83E-05	2.13E-04	-1.82E-04	-7.88E-05
11514.7	3.33E-06	4.61E-05	-1.15E-04	2.45E-04	-1.69E-04	-1.83E-04
12014.7	1.25E-04	3.90E-05	-1.78E-04	2.33E-04	-1.20E-04	-2.73E-04
12514.7	2.10E-05	5.10E-05	-2.48E-05	3.73E-04	-1.14E-04	-2.76E-04
13014.7	-9.31E-05	2.19E-05	1.47E-04	3.58E-04	-6.04E-05	-2.82E-04
13514.7	1.60E-05	7.20E-06	3.30E-04	3.56E-04	-1.25E-04	-3.40E-04
14014.7	-2.64E-04	6.10E-05	3.08E-04	3.90E-04	-1.44E-04	-8.77E-05

Table 6-2. Continued

Pressure	Temperature (^{o}F)					
(psia)	116	134	152	170	200	250
	Absolute Error (cp)					
14514.7	-3.11E-04	2.64E-04	3.45E-04	3.46E-04	-1.79E-05	-4.10E-05
15014.7	-1.91E-04	1.46E-04	4.48E-04	7.03E-04	-5.72E-05	-6.18E-05
15514.7	-2.17E-04	8.17E-05	3.73E-04	6.39E-04	4.28E-05	-2.91E-04
16014.7	-3.96E-04	3.08E-05	2.68E-04	6.73E-04	1.89E-04	-4.21E-04
16514.7	-3.20E-04	2.95E-05	3.06E-04	7.53E-04	1.65E-04	-5.69E-04
17014.7	-2.75E-04	-4.91E-05	2.95E-04	7.73E-04	1.89E-04	-6.83E-04
17514.7	-4.30E-04	-1.14E-04	-3.97E-04	8.52E-04	2.91E-04	-6.24E-04
18014.7	-4.30E-04	4.33E-06	-1.65E-04	8.77E-04	1.20E-04	-8.39E-04
18514.7	-4.63E-04	-3.54E-06	1.75E-04	9.00E-04	2.28E-04	-9.71E-04
19014.7	-5.29E-04	4.60E-05	1.37E-04	8.79E-04	2.42E-04	-7.14E-04
19514.7	-3.58E-04	-1.37E-04	1.20E-04	8.40E-04	-4.37E-05	-9.24E-04
20014.7	-3.77E-04	-1.37E-04	2.81E-04	8.88E-04	7.57E-05	-9.53E-04
20514.7	-4.41E-04	-7.32E-05	1.76E-04	9.13E-04	-1.85E-04	-1.42E-03
21014.7	-2.61E-04	4.73E-05	2.61E-04	1.05E-03	-7.74E-05	-1.24E-03
21514.7	-3.50E-04	-1.61E-04	4.21E-04	1.14E-03	1.24E-04	-1.21E-03
22014.7	-5.32E-04	-2.10E-04	4.20E-04	1.23E-03	1.01E-04	-1.20E-03
22514.7	-4.98E-04	-	6.68E-04	1.41E-03	1.15E-04	-1.19E-03
23014.7	-5.44E-04	-	5.85E-04	1.27E-03	1.45E-04	-1.31E-03
23514.7	-3.35E-04	-	6.34E-04	1.48E-03	1.86E-04	-1.23E-03
24014.7	-	-	5.66E-04	1.35E-03	8.08E-05	-
24514.7	-	-	-	-	2.10E-04	-

Table 6-2. Continued

Pressure	Temperature (^{o}F)				
(psia)	260	280	300	330	350
	Absolute Error (cp)				
514.7	5.18E-05	5.56E-05	5.81E-05	5.50E-05	5.10E-05
1014.7	-3.84E-05	-3.01E-05	-2.54E-05	-2.27E-05	-2.47E-05
1514.7	-7.32E-05	-6.26E-05	-5.53E-05	-4.92E-05	-5.00E-05
2014.7	-7.72E-05	-6.46E-05	-5.44E-05	-4.68E-05	-4.54E-05
2514.7	-6.50E-05	-4.97E-05	-3.78E-05	-2.78E-05	-2.54E-05
3014.7	1.02E-04	8.78E-05	5.03E-05	4.06E-04	7.56E-04
3514.7	5.22E-05	2.48E-06	2.25E-05	1.57E-04	5.89E-04
4014.7	1.53E-05	-1.40E-05	5.08E-05	2.71E-04	1.53E-04
4514.7	8.31E-05	1.58E-04	1.77E-04	3.03E-04	1.05E-04
5014.7	2.03E-04	1.03E-04	6.78E-05	2.62E-04	2.38E-04
5514.7	3.45E-04	8.72E-05	1.48E-04	2.55E-04	2.82E-04
6014.7	4.17E-04	7.86E-05	1.94E-04	2.58E-04	4.26E-04
6514.7	4.79E-04	9.38E-05	1.55E-04	2.66E-04	3.63E-04
7014.7	4.28E-04	9.69E-05	1.40E-04	3.77E-04	3.74E-04
7514.7	3.79E-04	1.21E-04	6.04E-06	3.09E-04	2.86E-04
8014.7	3.15E-04	1.37E-04	1.11E-04	4.15E-04	3.36E-04
8514.7	3.20E-04	8.76E-05	7.18E-05	3.50E-04	3.25E-04
9014.7	3.93E-04	8.07E-05	5.01E-05	1.93E-04	3.20E-04
9514.7	3.08E-04	1.51E-04	6.48E-05	1.08E-04	2.58E-04
10014.7	3.77E-04	8.77E-05	1.03E-04	1.08E-04	1.41E-04
10514.7	3.68E-04	9.53E-05	6.62E-05	1.41E-04	1.04E-04
11014.7	1.82E-04	-4.29E-06	4.96E-05	4.61E-05	1.43E-04
11514.7	4.02E-04	-7.61E-06	2.85E-05	2.18E-04	2.34E-04
12014.7	3.23E-04	-4.13E-05	9.47E-05	5.03E-05	2.02E-04
12514.7	2.15E-04	-6.93E-05	4.66E-05	7.18E-05	1.57E-04
13014.7	2.10E-04	-1.16E-04	1.16E-04	1.03E-04	1.90E-04
13514.7	2.20E-04	-8.61E-05	2.01E-04	8.80E-05	1.45E-04
14014.7	2.42E-04	2.45E-05	5.78E-05	9.47E-05	1.76E-04

Table 6-2. Continued

Pressure	Temperature (^{o}F)				
(psia)	260	280	300	330	350
	Absolute Error (cp)				
14514.7	8.73E-05	2.80E-05	8.25E-05	1.49E-04	9.62E-05
15014.7	1.20E-04	-2.18E-05	1.19E-04	-9.90E-05	1.04E-04
15514.7	1.44E-04	5.20E-05	1.40E-04	-1.60E-05	9.00E-07
16014.7	1.37E-04	-5.29E-06	1.43E-04	4.03E-05	1.15E-04
16514.7	-4.12E-05	-9.39E-05	7.78E-05	5.94E-05	6.04E-05
17014.7	-1.30E-05	-1.36E-04	1.94E-04	1.55E-04	-1.22E-04
17514.7	3.67E-05	-6.81E-05	9.16E-05	2.01E-04	-7.03E-05
18014.7	5.84E-05	-2.01E-04	2.18E-04	-5.90E-05	-1.86E-05
18514.7	-1.44E-05	-2.02E-04	-5.40E-05	-2.22E-04	-9.57E-05
19014.7	-2.06E-04	-1.74E-04	-4.42E-05	-2.93E-04	1.97E-04
19514.7	-3.45E-04	-1.21E-04	5.75E-05	-1.74E-04	-1.12E-05
20014.7	-4.04E-04	-8.78E-05	-2.60E-04	-3.68E-04	3.98E-04
20514.7	-5.25E-04	-9.14E-05	3.31E-05	-1.70E-04	4.08E-04
21014.7	-5.84E-04	-1.35E-04	5.23E-06	-1.76E-04	4.65E-04
21514.7	-6.80E-04	-3.40E-04	1.60E-04	-5.86E-05	1.79E-04
22014.7	-7.02E-04	-4.20E-04	-9.02E-05	-1.45E-04	1.98E-04
22514.7	-7.39E-04	-2.64E-04	-2.11E-04	-2.21E-04	5.59E-05
23014.7	-7.12E-04	-1.69E-04	1.65E-04	-2.22E-04	9.97E-05
23514.7	-6.13E-04	-1.26E-04	1.13E-04	-8.95E-05	1.30E-04
24014.7	-6.05E-04	6.56E-05	2.71E-04	-	1.17E-04
24514.7	-7.44E-04	-3.27E-05	3.54E-04	-	-2.60E-04

Table 6-3. Relative error by comparing nitrogen viscosity data with values from correlation

Pressure	Temperature (^{o}F)					
(psia)	116	134	152	170	200	250
	Relative Error (%)					
514.7	-0.344	-0.216	-0.109	-0.016	0.102	0.217
1014.7	-1.008	-0.830	-0.681	-0.553	-0.380	-0.192
1514.7	-1.301	-1.101	-0.923	-0.773	-0.571	-0.343
2014.7	-1.419	-1.198	-1.004	-0.834	-0.612	-0.357
2514.7	-1.459	-1.216	-1.009	-0.828	-0.582	-0.300
3014.7	-0.689	-0.867	-0.116	0.145	0.276	0.319
3514.7	-1.495	-0.672	-0.837	0.701	0.091	0.278
4014.7	-2.263	-0.319	-0.887	-0.888	-0.104	-0.415
4514.7	-2.238	-0.829	-1.500	-0.646	0.208	-0.530
5014.7	-1.623	-0.155	-1.053	-1.077	0.218	-0.666
5514.7	-1.959	-0.339	-1.548	-1.507	0.153	-0.789
6014.7	-1.563	0.020	-1.367	-1.489	-0.362	-0.762
6514.7	-1.278	0.202	-1.810	-1.294	-0.196	-0.148
7014.7	-1.017	0.268	-1.581	-0.793	-0.516	0.148
7514.7	-1.032	0.187	-1.152	-0.717	-0.475	-0.177
8014.7	-1.102	-0.022	-0.930	-0.527	-0.580	-0.500
8514.7	-0.975	-0.066	-0.827	-0.084	-0.417	-0.177
9014.7	-0.910	-0.118	-0.675	0.175	-0.737	-0.116
9514.7	-0.532	-0.557	-0.145	0.329	-0.882	0.369
10014.7	-0.568	1.087	-0.409	0.859	-0.787	0.564
10514.7	-0.083	0.955	-0.977	0.674	-0.643	-0.126
11014.7	0.002	0.867	-0.096	0.543	-0.466	-0.206
11514.7	0.008	0.111	-0.279	0.610	-0.424	-0.466
12014.7	0.290	0.092	-0.424	0.566	-0.294	-0.681
12514.7	0.047	0.117	-0.058	0.890	-0.274	-0.677
13014.7	-0.205	0.049	0.337	0.836	-0.142	-0.677
13514.7	0.035	0.016	0.742	0.814	-0.289	-0.800
14014.7	-0.554	0.131	0.680	0.875	-0.325	-0.204

Table 6-3. Continued

Pressure	Temperature (^{o}F)					
(psia)	116	134	152	170	200	250
	Relative Error (%)					
14514.7	-0.640	0.561	0.746	0.759	-0.040	-0.094
15014.7	-0.385	0.303	0.951	1.525	-0.125	-0.139
15514.7	-0.428	0.166	0.776	1.358	0.092	-0.640
16014.7	-0.766	0.061	0.546	1.406	0.401	-0.909
16514.7	-0.607	0.058	0.612	1.549	0.344	-1.205
17014.7	-0.513	-0.094	0.580	1.563	0.387	-1.421
17514.7	-0.785	-0.214	-0.757	1.695	0.588	-1.280
18014.7	-0.772	0.008	-0.311	1.717	0.238	-1.687
18514.7	-0.816	-0.006	0.326	1.734	0.446	-1.921
19014.7	-0.916	0.082	0.251	1.666	0.465	-1.399
19514.7	-0.612	-0.242	0.217	1.566	-0.082	-1.779
20014.7	-0.634	-0.236	0.501	1.631	0.141	-1.809
20514.7	-0.730	-0.125	0.308	1.653	-0.338	-2.631
21014.7	-0.427	0.080	0.450	1.874	-0.140	-2.283
21514.7	-0.563	-0.266	0.720	2.010	0.221	-2.190
22014.7	-0.840	-0.341	0.706	2.152	0.178	-2.146
22514.7	-0.775	-	1.113	2.436	0.200	-2.113
23014.7	-0.834	-	0.961	2.156	0.249	-2.287
23514.7	-0.509	-	1.027	2.489	0.316	-2.129
24014.7	-	-	0.904	2.238	0.135	-
24514.7	-	-	-	-	0.347	-

Table 6-3. Continued

Pressure	Temperature (^{o}F)				
(psia)	260	280	300	330	350
	Relative Error (%)				
514.7	0.229	0.241	0.247	0.228	0.208
1014.7	-0.166	-0.128	-0.106	-0.092	-0.099
1514.7	-0.310	-0.261	-0.226	-0.196	-0.197
2014.7	-0.319	-0.263	-0.218	-0.184	-0.175
2514.7	-0.262	-0.197	-0.148	-0.107	-0.096
3014.7	0.404	0.342	0.193	1.551	2.886
3514.7	0.200	0.009	0.084	0.578	2.185
4014.7	0.057	-0.051	0.185	0.981	0.547
4514.7	0.301	0.568	0.631	1.073	0.367
5014.7	0.719	0.361	0.235	0.902	0.813
5514.7	1.194	0.297	0.503	0.857	0.942
6014.7	1.404	0.261	0.642	0.850	1.400
6514.7	1.577	0.304	0.501	0.857	1.165
7014.7	1.367	0.306	0.441	1.191	1.174
7514.7	1.180	0.373	0.019	0.952	0.878
8014.7	0.955	0.412	0.333	1.255	1.009
8514.7	0.948	0.257	0.211	1.033	0.958
9014.7	1.136	0.232	0.144	0.556	0.923
9514.7	0.869	0.425	0.182	0.304	0.730
10014.7	1.042	0.241	0.284	0.297	0.391
10514.7	0.995	0.257	0.179	0.382	0.281
11014.7	0.479	-0.011	0.131	0.122	0.381
11514.7	1.045	-0.020	0.074	0.571	0.615
12014.7	0.822	-0.104	0.242	0.129	0.519
12514.7	0.535	-0.172	0.117	0.181	0.396
13014.7	0.512	-0.282	0.285	0.256	0.474
13514.7	0.526	-0.206	0.487	0.214	0.356
14014.7	0.570	0.058	0.137	0.227	0.424

Table 6-3. Continued

Pressure	Temperature (^{o}F)				
(psia)	260	280	300	330	350
	Relative Error (%)				
14514.7	0.201	0.065	0.193	0.352	0.228
15014.7	0.272	-0.050	0.273	-0.229	0.242
15514.7	0.321	0.117	0.317	-0.037	0.002
16014.7	0.301	-0.012	0.320	0.091	0.260
16514.7	-0.089	-0.204	0.171	0.132	0.135
17014.7	-0.028	-0.291	0.420	0.340	-0.266
17514.7	0.077	-0.144	0.196	0.435	-0.152
18014.7	0.120	-0.416	0.460	-0.125	-0.040
18514.7	-0.029	-0.413	-0.112	-0.464	-0.202
19014.7	-0.410	-0.350	-0.090	-0.603	0.412
19514.7	-0.676	-0.241	0.116	-0.353	-0.023
20014.7	-0.780	-0.173	-0.515	-0.737	0.815
20514.7	-0.997	-0.177	0.065	-0.338	0.827
21014.7	-1.095	-0.259	0.010	-0.346	0.933
21514.7	-1.256	-0.641	0.308	-0.114	0.352
22014.7	-1.280	-0.781	-0.170	-0.279	0.385
22514.7	-1.329	-0.485	-0.393	-0.417	0.107
23014.7	-1.267	-0.307	0.307	-0.416	0.190
23514.7	-1.079	-0.227	0.206	-0.166	0.244
24014.7	-1.053	0.117	0.493	-	0.218
24514.7	-1.278	-0.058	0.637	-	-0.476

6.2 Methane Viscosity Correlation

Since Lee-Gonzalez-Eakin correlation is one of the most common used viscosity correlations in petroleum engineering and can be coded into computer program easily, we developed a correlation that has the same form as Lee-Gonzalez-Eakin correlation. The coefficients in the correlation were updated using NIST values and lab data from our experiment. Due to the fact that we do not have viscosity data at pressure from 500 to 4500 psi in our experiment, NIST values at this pressure range were used. As we already showed in Chapter II, NIST values match with lab data very well at pressure from 500 to 4500 psi. Combining NIST values at pressure from 514.7 to 4014.7 psia with our lab data at pressure from 4514.7 to 24514.7 psia the coefficients were determined. A non-linear

regression approach is applied in determining the coefficients. As a result, the final form of correlation was developed. New gas viscosity correlation is as follows:

$$\mu_g = K \exp\left(X\rho_g{}^{Y}\right). \tag{6.5}$$

where

$$K = \frac{0.0001 * (9.18999 + 3.0893 M_w) T^{1.2288}}{208.99 + 18.83933 M_w + T}. \tag{6.6}$$

$$X = 3.56014 + \left[\frac{1000.01}{T}\right] + 0.124465 M_w. \tag{6.7}$$

$$Y = 2.47862 - 0.12294 X. \tag{6.8}$$

where

μ_g = Gas viscosity, cp

ρ_g = Gas density, g/cc

M_W = Molecular weight

T = Temperature, R

New correlation that based on lab data and NIST values (Table 6-3) covers larger pressure and temperature range than original Lee-Gonzalez-Eakin correlation. It covers both low and high pressure and temperature and gives more confidence on gas viscosity estimation when petroleum engineers deal with HPHT reservoir.

Table 6-4. Data used to develop new methane viscosity correlation

Pressure	Temperature (oF)				
(psia)	100	120	140	160	180
514.7	0.01216	0.01248	0.01280	0.01312	0.01343
1014.7	0.01303	0.01328	0.01355	0.01382	0.01409
1514.7	0.01420	0.01436	0.01453	0.01473	0.01494
2014.7	0.01568	0.01568	0.01573	0.01583	0.01595
2514.7	0.01739	0.01720	0.01711	0.01708	0.01709
3014.7	0.01921	0.01884	0.01859	0.01843	0.01834
3514.7	0.02105	0.02052	0.02013	0.01984	0.01964
4014.7	0.02284	0.02218	0.02166	0.02126	0.02095
4514.7	0.02454	0.02377	0.02309	0.02265	0.02226
5014.7	0.02630	0.02531	0.02447	0.02399	0.02376
5514.7	0.02772	0.02675	0.02547	0.02517	0.02490
6014.7	0.02977	0.02790	0.02678	0.02628	0.02599
6514.7	0.03082	0.02886	0.02836	0.02746	0.02707
7014.7	0.03156	0.02995	0.02959	0.02854	0.02806
7514.7	0.03298	0.03108	0.03093	0.02968	0.02900
8014.7	0.03413	0.03224	0.03200	0.03027	0.03018
8514.7	0.03529	0.03344	0.03314	0.03124	0.03110
9014.7	0.03656	0.03470	0.03421	0.03232	0.03195
9514.7	0.03772	0.03585	0.03523	0.03349	0.03279
10014.7	0.03879	0.03700	0.03620	0.03446	0.03376
10514.7	0.03989	0.03807	0.03726	0.03548	0.03484
11014.7	0.04101	0.03915	0.03813	0.03647	0.03552
11514.7	0.04205	0.04020	0.03896	0.03739	0.03643
12014.7	0.04305	0.04118	0.03986	0.03837	0.03732
12514.7	0.04401	0.04218	0.04079	0.03931	0.03825
13014.7	0.04505	0.04311	0.04182	0.04022	0.03916
13514.7	0.04609	0.04412	0.04270	0.04113	0.04005
14014.7	0.04714	0.04512	0.04369	0.04210	0.04088
14514.7	0.04822	0.04614	0.04461	0.04304	0.04179
15014.7	0.04915	0.04709	0.04558	0.04388	0.04272
15514.7	0.05020	0.04812	0.04654	0.04467	0.04361
16014.7	0.05126	0.04901	0.04743	0.04586	0.04443
16514.7	0.05220	0.05004	0.04834	0.04690	0.04530
17014.7	0.05323	0.05106	0.04926	0.04776	0.04612
17514.7	0.05428	0.05204	0.05015	0.04856	0.04708
18014.7	0.05533	0.05303	0.05112	0.04955	0.04799

Table 6-4. Continued

Pressure	Temperature (oF)				
(psia)	100	120	140	160	180
18514.7	0.05636	0.05393	0.05204	0.05047	0.04881
19014.7	0.05743	0.05490	0.05284	0.05123	0.04966
19514.7	0.05836	0.05588	0.05378	0.05217	0.05056
20014.7	0.05937	0.05693	0.05474	0.05302	0.05138
20514.7	0.06041	0.05789	0.05556	0.05391	0.05220
21014.7	0.06187	0.05888	0.05657	0.05479	0.05306
21514.7	0.06257	0.05993	0.05744	0.05567	0.05391
22014.7	0.06355	0.06096	0.05839	0.05656	0.05481
22514.7	0.06461	0.06220	0.05931	0.05753	0.05566
23014.7	0.06575	0.06277	0.06017	0.05837	0.05650
23514.7	0.06683	0.06402	0.06116	0.05914	0.05719
24014.7	0.06777	0.06505	0.06209	0.05975	0.05819
24514.7	0.06893	0.06603	0.06301	0.06064	0.05915
25014.7	0.07002	-	0.06389	0.06173	0.06007

Table 6-4. Continued

Pressure	Temperature (^{o}F)				
(psia)	188	200	220	225	230
514.7	0.01355	0.01374	0.01405	0.01413	0.01420
1014.7	0.01420	0.01437	0.01464	0.01471	0.01478
1514.7	0.01502	0.01516	0.01538	0.01544	0.01550
2014.7	0.01600	0.01609	0.01626	0.01630	0.01634
2514.7	0.01711	0.01715	0.01724	0.01726	0.01729
3014.7	0.01832	0.01830	0.01830	0.01831	0.01832
3514.7	0.01957	0.01950	0.01942	0.01940	0.01939
4014.7	0.02085	0.02072	0.02056	0.02053	0.02050
4514.7	0.02212	0.02195	0.02171	0.02171	0.02162
5014.7	0.02337	0.02292	0.02284	0.02283	0.02275
5514.7	0.02460	0.02403	0.02385	0.02378	0.02366
6014.7	0.02589	0.02538	0.02484	0.02480	0.02465
6514.7	0.02684	0.02640	0.02596	0.02580	0.02564
7014.7	0.02776	0.02748	0.02674	0.02670	0.02661
7514.7	0.02877	0.02850	0.02794	0.02762	0.02747
8014.7	0.02971	0.02948	0.02877	0.02874	0.02839
8514.7	0.03064	0.03050	0.02954	0.02968	0.02934
9014.7	0.03149	0.03146	0.03031	0.03051	0.03023
9514.7	0.03242	0.03238	0.03115	0.03133	0.03108
10014.7	0.03334	0.03332	0.03201	0.03216	0.03189
10514.7	0.03410	0.03425	0.03291	0.03287	0.03263
11014.7	0.03504	0.03514	0.03371	0.03372	0.03348
11514.7	0.03594	0.03596	0.03453	0.03445	0.03419
12014.7	0.03677	0.03680	0.03535	0.03526	0.03501
12514.7	0.03759	0.03770	0.03620	0.03607	0.03589
13014.7	0.03848	0.03840	0.03689	0.03690	0.03658
13514.7	0.03932	0.03912	0.03776	0.03753	0.03733
14014.7	0.04026	0.04003	0.03856	0.03862	0.03804
14514.7	0.04117	0.04092	0.03947	0.03943	0.03892
15014.7	0.04216	0.04172	0.04031	0.04041	0.03989
15514.7	0.04307	0.04246	0.04113	0.04106	0.04068
16014.7	0.04396	0.04323	0.04193	0.04184	0.04139
16514.7	0.04486	0.04398	0.04270	0.04250	0.04211
17014.7	0.04570	0.04480	0.04363	0.04331	0.04306
17514.7	0.04647	0.04568	0.04432	0.04406	0.04382
18014.7	0.04734	0.04667	0.04517	0.04471	0.04463

Table 6-4. Continued

Pressure	Temperature (^{o}F)				
(psia)	188	200	220	225	230
18514.7	0.04821	0.04773	0.04586	0.04561	0.04537
19014.7	0.04907	0.04840	0.04661	0.04642	0.04619
19514.7	0.04995	0.04919	0.04725	0.04724	0.04691
20014.7	0.05088	0.05013	0.04789	0.04804	0.04773
20514.7	0.05136	0.05092	0.04872	0.04879	0.04858
21014.7	0.05210	0.05188	0.04949	0.04951	0.04935
21514.7	0.05296	0.05270	0.05039	0.05036	0.05010
22014.7	0.05377	0.05347	0.05116	0.05115	0.05086
22514.7	0.05460	0.05418	0.05199	0.05191	0.05166
23014.7	0.05550	0.05503	0.05282	0.05280	0.05243
23514.7	0.05637	0.05584	0.05369	0.05365	0.05321
24014.7	0.05726	0.05650	0.05416	0.05442	0.05394
24514.7	0.05795	0.05731	0.05494	0.05522	0.05454
25014.7	-	-	0.05587	0.05608	-

Table 6-4. Continued

Pressure	Temperature (^{o}F)				
(psia)	250	260	280	300	320
514.7	0.01451	0.01466	0.01496	0.01526	0.01555
1014.7	0.01506	0.01519	0.01547	0.01574	0.01602
1514.7	0.01573	0.01585	0.01609	0.01634	0.01658
2014.7	0.01652	0.01662	0.01682	0.01702	0.01723
2514.7	0.01741	0.01748	0.01762	0.01778	0.01795
3014.7	0.01837	0.01840	0.01849	0.01860	0.01872
3514.7	0.01938	0.01938	0.01941	0.01947	0.01954
4014.7	0.02041	0.02039	0.02036	0.02036	0.02039
4514.7	0.02147	0.02140	0.02132	0.02126	0.02124
5014.7	0.02239	0.02238	0.02221	0.02208	0.02191
5514.7	0.02333	0.02334	0.02315	0.02294	0.02272
6014.7	0.02426	0.02427	0.02405	0.02376	0.02356
6514.7	0.02516	0.02520	0.02499	0.02466	0.02443
7014.7	0.02611	0.02602	0.02586	0.02546	0.02524
7514.7	0.02704	0.02692	0.02670	0.02624	0.02604
8014.7	0.02794	0.02791	0.02758	0.02705	0.02679
8514.7	0.02882	0.02873	0.02844	0.02776	0.02754
9014.7	0.02959	0.02961	0.02928	0.02866	0.02834
9514.7	0.03046	0.03041	0.03002	0.02943	0.02908
10014.7	0.03126	0.03118	0.03083	0.03022	0.02982
10514.7	0.03205	0.03194	0.03157	0.03094	0.03065
11014.7	0.03287	0.03269	0.03237	0.03165	0.03141
11514.7	0.03375	0.03338	0.03320	0.03241	0.03212
12014.7	0.03455	0.03429	0.03399	0.03353	0.03283
12514.7	0.03537	0.03504	0.03479	0.03438	0.03354
13014.7	0.03614	0.03586	0.03556	0.03508	0.03425
13514.7	0.03676	0.03666	0.03632	0.03584	0.03501
14014.7	0.03752	0.03739	0.03714	0.03659	0.03575
14514.7	0.03835	0.03827	0.03792	0.03725	0.03651
15014.7	0.03932	0.03906	0.03885	0.03805	0.03727
15514.7	0.03998	0.03988	0.03949	0.03882	0.03810
16014.7	0.04084	0.04051	0.04035	0.03961	0.03885
16514.7	0.04148	0.04127	0.04105	0.04048	0.03964
17014.7	0.04222	0.04194	0.04193	0.04115	0.04048
17514.7	0.04294	0.04281	0.04259	0.04196	0.04115
18014.7	0.04365	0.04357	0.04336	0.04275	0.04189

Table 6-4. Continued

Pressure	Temperature (^{o}F)				
(psia)	250	260	280	300	320
18514.7	0.04437	0.04445	0.04407	0.04336	0.04282
19014.7	0.04514	0.04521	0.04480	0.04414	0.04350
19514.7	0.04593	0.04609	0.04559	0.04491	0.04408
20014.7	0.04665	0.04681	0.04622	0.04564	0.04476
20514.7	0.04757	0.04759	0.04702	0.04646	0.04544
21014.7	0.04842	0.04847	0.04786	0.04708	0.04606
21514.7	0.04932	0.04915	0.04849	0.04791	0.04686
22014.7	0.05008	0.04996	0.04915	0.04868	0.04759
22514.7	0.05083	0.05080	0.04987	0.04928	0.04836
23014.7	0.05141	0.05165	0.05060	0.05005	0.04894
23514.7	0.05204	0.05226	0.05132	0.05071	0.04976
24014.7	0.05294	0.05263	0.05195	0.05156	0.05083
24514.7	0.05357	0.05335	0.05263	0.05200	0.05155
25014.7	-	0.05407	0.05337	-	0.05228

Table 6-4. Continued

Pressure	Temperature (^{o}F)			
(psia)	340	360	380	415
514.7	0.01584	0.01613	0.01642	0.01691
1014.7	0.01629	0.01656	0.01683	0.01730
1514.7	0.01683	0.01708	0.01732	0.01776
2014.7	0.01745	0.01766	0.01789	0.01828
2514.7	0.01813	0.01831	0.01850	0.01885
3014.7	0.01886	0.01901	0.01917	0.01946
3514.7	0.01964	0.01974	0.01987	0.02010
4014.7	0.02044	0.02050	0.02059	0.02077
4514.7	0.02096	0.02128	0.02133	0.02147
5014.7	0.02181	0.02206	0.02205	0.02217
5514.7	0.02283	0.02284	0.02278	0.02284
6014.7	0.02369	0.02366	0.02361	0.02353
6514.7	0.02443	0.02435	0.02424	0.02429
7014.7	0.02512	0.02500	0.02494	0.02496
7514.7	0.02585	0.02578	0.02565	0.02564
8014.7	0.02665	0.02641	0.02637	0.02635
8514.7	0.02748	0.02740	0.02714	0.02697
9014.7	0.02841	0.02817	0.02786	0.02764
9514.7	0.02908	0.02886	0.02859	0.02827
10014.7	0.02980	0.02954	0.02922	0.02892
10514.7	0.03058	0.03032	0.02995	0.02957
11014.7	0.03133	0.03110	0.03054	0.03028
11514.7	0.03202	0.03178	0.03123	0.03083
12014.7	0.03279	0.03243	0.03194	0.03145
12514.7	0.03356	0.03306	0.03261	0.03214
13014.7	0.03432	0.03378	0.03333	0.03280
13514.7	0.03501	0.03437	0.03400	0.03346
14014.7	0.03577	0.03503	0.03467	0.03411
14514.7	0.03650	0.03568	0.03530	0.03472
15014.7	0.03720	0.03639	0.03599	0.03531
15514.7	0.03804	0.03708	0.03661	0.03577
16014.7	0.03912	0.03780	0.03730	0.03642
16514.7	0.03971	0.03849	0.03797	0.03698
17014.7	0.04039	0.03918	0.03866	0.03767
17514.7	0.04099	0.03986	0.03934	0.03830
18014.7	0.04203	0.04057	0.04000	0.03915

Table 6-4. Continued

Pressure	Temperature (^{o}F)			
(psia)	340	360	380	415
18514.7	0.04272	0.04138	0.04068	0.03965
19014.7	0.04339	0.04184	0.04132	0.04041
19514.7	0.04404	0.04255	0.04194	0.04088
20014.7	0.04458	0.04325	0.04254	0.04145
20514.7	0.04526	0.04391	0.04323	0.04214
21014.7	0.04588	0.04420	0.04380	0.04257
21514.7	0.04658	0.04486	0.04431	0.04303
22014.7	0.04711	0.04544	0.04502	0.04380
22514.7	0.04788	0.04599	0.04570	0.04420
23014.7	0.04836	0.04653	0.04628	0.04465
23514.7	0.04891	0.04717	0.04677	0.04531
24014.7	0.04939	0.04778	0.04740	0.04559
24514.7	0.05011	0.04895	0.04796	0.04620
25014.7	0.05071	-	0.04866	-

The accuracy of the new methane correlation is vital for future viscosity estimation. As well as error analysis for nitrogen viscosity we compared the calculated viscosity from correlation with lab data. In analysis lab data are used as base for both absolute error and relative error. Tables 6-5 and 6-6 show the absolute error and relative error. Average absolute error is 7.06E-06 cp. Average relative error is 0.1068%.

Table 6-5. Absolute error by comparing methane viscosity data with values from correlation

Pressure	Temperature (^{o}F)						
(psia)	100	120	140	160	180	188	200
	Absolute Error (cp)						
514.7	1.17E-03	1.15E-03	1.13E-03	1.11E-03	1.09E-03	1.08E-03	1.06E-03
1014.7	8.66E-04	8.62E-04	8.55E-04	8.46E-04	8.32E-04	8.26E-04	8.16E-04
1514.7	5.58E-04	5.70E-04	5.78E-04	5.81E-04	5.79E-04	5.78E-04	5.74E-04
2014.7	2.54E-04	2.82E-04	3.05E-04	3.21E-04	3.33E-04	3.36E-04	3.39E-04
2514.7	-2.69E-05	1.34E-05	4.80E-05	7.67E-05	1.00E-04	1.07E-04	1.17E-04
3014.7	-2.62E-04	-2.19E-04	-1.79E-04	-1.42E-04	-1.11E-04	-9.95E-05	-8.44E-05
3514.7	-4.42E-04	-4.03E-04	-3.65E-04	-3.26E-04	-2.91E-04	-2.78E-04	-2.60E-04
4014.7	-5.62E-04	-5.39E-04	-5.05E-04	-4.71E-04	-4.35E-04	-4.23E-04	-4.03E-04
4514.7	-6.27E-04	-6.24E-04	-5.40E-04	-5.75E-04	-5.44E-04	-5.34E-04	-5.14E-04
5014.7	-8.10E-04	-6.85E-04	-5.44E-04	-6.22E-04	-8.46E-04	-6.09E-04	-3.66E-04
5514.7	-6.97E-04	-6.82E-04	-1.87E-04	-5.27E-04	-7.87E-04	-6.72E-04	-3.54E-04
6014.7	-1.28E-03	-4.42E-04	-1.78E-04	-3.95E-04	-7.00E-04	-8.03E-04	-5.77E-04
6514.7	-9.14E-04	-4.59E-05	-4.71E-04	-3.49E-04	-6.15E-04	-6.20E-04	-4.99E-04
7014.7	-2.79E-04	1.76E-04	-4.49E-04	-2.31E-04	-4.63E-04	-4.23E-04	-4.92E-04
7514.7	-3.70E-04	3.26E-04	-5.63E-04	-2.04E-04	-2.91E-04	-3.35E-04	-4.43E-04
8014.7	-2.28E-04	4.04E-04	-4.48E-04	3.48E-04	-3.77E-04	-1.90E-04	-3.68E-04
8514.7	-1.34E-04	4.14E-04	-4.22E-04	4.93E-04	-2.20E-04	-6.91E-05	-3.61E-04
9014.7	-1.78E-04	3.28E-04	-3.58E-04	5.09E-04	-1.32E-05	1.19E-04	-3.10E-04
9514.7	-1.48E-04	3.30E-04	-2.67E-04	4.11E-04	1.78E-04	2.06E-04	-2.34E-04
10014.7	-5.87E-05	2.98E-04	-1.54E-04	4.83E-04	2.18E-04	2.90E-04	-1.90E-04
10514.7	-2.04E-05	3.29E-04	-1.42E-04	4.98E-04	1.38E-04	5.06E-04	-1.56E-04
11014.7	-1.16E-05	3.36E-04	3.36E-05	5.17E-04	4.33E-04	5.40E-04	-9.99E-05
11514.7	4.35E-05	3.46E-04	2.23E-04	5.99E-04	4.85E-04	5.93E-04	1.73E-05
12014.7	1.15E-04	4.12E-04	3.33E-04	5.99E-04	5.54E-04	6.94E-04	1.00E-04
12514.7	2.21E-04	4.37E-04	4.01E-04	6.18E-04	5.57E-04	8.02E-04	1.06E-04
13014.7	2.26E-04	5.25E-04	3.57E-04	6.57E-04	5.69E-04	8.24E-04	3.03E-04
13514.7	2.24E-04	5.15E-04	4.44E-04	6.86E-04	5.96E-04	8.80E-04	4.64E-04
14014.7	1.83E-04	4.96E-04	4.14E-04	6.47E-04	6.55E-04	8.35E-04	4.31E-04

Table 6-5. Continued

Pressure	Temperature (^{o}F)						
(psia)	100	120	140	160	180	188	200
	Absolute Error (cp)						
14514.7	1.16E-04	4.51E-04	4.30E-04	6.19E-04	6.36E-04	7.99E-04	4.09E-04
15014.7	1.70E-04	4.57E-04	3.99E-04	6.85E-04	5.85E-04	6.77E-04	4.61E-04
15514.7	1.10E-04	3.83E-04	3.58E-04	7.98E-04	5.66E-04	6.33E-04	5.67E-04
16014.7	1.95E-05	4.29E-04	3.82E-04	4.90E-04	6.13E-04	5.96E-04	6.29E-04
16514.7	4.19E-05	3.26E-04	3.70E-04	3.26E-04	5.90E-04	5.40E-04	7.09E-04
17014.7	-4.41E-05	2.39E-04	3.49E-04	3.31E-04	6.11E-04	5.29E-04	7.09E-04
17514.7	-1.49E-04	1.60E-04	3.42E-04	3.88E-04	4.88E-04	5.94E-04	6.47E-04
18014.7	-2.71E-04	8.15E-05	2.50E-04	2.58E-04	4.12E-04	5.41E-04	4.62E-04
18514.7	-3.76E-04	8.14E-05	2.02E-04	1.82E-04	4.14E-04	4.86E-04	2.02E-04
19014.7	-5.18E-04	3.78E-06	2.68E-04	2.66E-04	3.84E-04	4.39E-04	3.28E-04
19514.7	-5.39E-04	-9.61E-05	1.83E-04	1.58E-04	2.92E-04	3.52E-04	3.30E-04
20014.7	-6.42E-04	-2.67E-04	7.26E-05	1.37E-04	2.75E-04	2.20E-04	1.74E-04
20514.7	-7.86E-04	-3.61E-04	1.05E-04	6.20E-05	2.60E-04	5.35E-04	1.65E-04
21014.7	-1.34E-03	-4.86E-04	-7.12E-05	1.78E-06	1.87E-04	5.76E-04	-2.98E-05
21514.7	-1.16E-03	-6.64E-04	-9.99E-05	-7.26E-05	1.31E-04	5.06E-04	-7.47E-05
22014.7	-1.26E-03	-8.45E-04	-2.25E-04	-1.48E-04	1.26E-05	4.63E-04	-7.71E-05
22514.7	-1.44E-03	-1.23E-03	-3.19E-04	-3.18E-04	-5.20E-05	4.07E-04	-3.23E-05
23014.7	-1.71E-03	-9.58E-04	-3.64E-04	-3.60E-04	-1.14E-04	2.76E-04	-1.22E-04
23514.7	-1.92E-03	-1.37E-03	-5.35E-04	-3.36E-04	-3.81E-05	1.63E-04	-1.78E-04
24014.7	-1.99E-03	-1.56E-03	-6.48E-04	-1.53E-04	-2.66E-04	3.45E-05	-1.00E-04
24514.7	-2.29E-03	-1.70E-03	-7.66E-04	-2.64E-04	-4.68E-04	9.71E-05	-1.63E-04
25014.7	-2.53E-03	-	-8.40E-04	-5.70E-04	-6.23E-04	-	-

Table 6-5. Continued

Pressure	Temperature (^{o}F)					
(psia)	220	225	230	250	260	280
	Absolute Error (cp)					
514.7	1.04E-03	1.03E-03	1.02E-03	9.91E-04	9.74E-04	9.40E-04
1014.7	7.97E-04	7.92E-04	7.87E-04	7.64E-04	7.51E-04	7.25E-04
1514.7	5.65E-04	5.63E-04	5.60E-04	5.45E-04	5.37E-04	5.18E-04
2014.7	3.41E-04	3.41E-04	3.40E-04	3.37E-04	3.32E-04	3.22E-04
2514.7	1.29E-04	1.32E-04	1.34E-04	1.39E-04	1.40E-04	1.39E-04
3014.7	-6.32E-05	-5.93E-05	-5.57E-05	-4.20E-05	-3.72E-05	-3.14E-05
3514.7	-2.33E-04	-2.27E-04	-2.22E-04	-2.02E-04	-1.95E-04	-1.83E-04
4014.7	-3.74E-04	-3.68E-04	-3.62E-04	-3.39E-04	-3.29E-04	-3.13E-04
4514.7	-4.87E-04	-5.33E-04	-4.78E-04	-4.55E-04	-4.37E-04	-4.20E-04
5014.7	-5.66E-04	-6.11E-04	-5.87E-04	-4.21E-04	-4.84E-04	-4.40E-04
5514.7	-5.13E-04	-5.19E-04	-4.77E-04	-3.88E-04	-5.02E-04	-4.87E-04
6014.7	-4.54E-04	-4.99E-04	-4.36E-04	-3.45E-04	-4.83E-04	-4.84E-04
6514.7	-5.19E-04	-4.69E-04	-4.01E-04	-2.75E-04	-4.67E-04	-5.24E-04
7014.7	-2.61E-04	-3.35E-04	-3.62E-04	-2.64E-04	-3.48E-04	-4.91E-04
7514.7	-4.38E-04	-2.50E-04	-2.18E-04	-2.33E-04	-3.08E-04	-4.42E-04
8014.7	-2.61E-04	-3.72E-04	-1.53E-04	-1.87E-04	-3.71E-04	-4.33E-04
8514.7	-4.19E-05	-3.28E-04	-1.31E-04	-1.36E-04	-2.73E-04	-4.09E-04
9014.7	1.61E-04	-1.98E-04	-6.06E-05	2.32E-05	-2.46E-04	-3.76E-04
9514.7	2.80E-04	-5.63E-05	3.43E-05	5.85E-05	-1.53E-04	-2.46E-04
10014.7	3.69E-04	4.99E-05	1.45E-04	1.61E-04	-4.19E-05	-2.07E-04
10514.7	4.00E-04	2.66E-04	3.27E-04	2.56E-04	6.40E-05	-9.99E-05
11014.7	5.16E-04	3.19E-04	3.83E-04	3.09E-04	1.79E-04	-6.89E-05
11514.7	6.09E-04	4.87E-04	5.63E-04	2.99E-04	3.43E-04	-7.75E-05
12014.7	6.81E-04	5.65E-04	6.26E-04	3.49E-04	2.70E-04	-5.01E-05
12514.7	7.06E-04	6.35E-04	6.08E-04	3.66E-04	3.49E-04	-4.29E-05
13014.7	8.88E-04	6.64E-04	7.76E-04	4.31E-04	3.53E-04	-1.16E-05
13514.7	8.84E-04	8.88E-04	8.74E-04	6.39E-04	3.65E-04	1.52E-05
14014.7	9.26E-04	6.35E-04	1.01E-03	6.94E-04	4.39E-04	-1.95E-05

Table 6-5. Continued

Pressure	Temperature (^{o}F)					
(psia)	220	225	230	250	260	280
	Absolute Error (cp)					
14514.7	8.59E-04	6.62E-04	9.50E-04	6.68E-04	3.60E-04	-2.23E-05
15014.7	8.51E-04	5.13E-04	8.02E-04	5.01E-04	3.51E-04	-1.89E-04
15514.7	8.50E-04	6.79E-04	8.21E-04	6.34E-04	3.16E-04	-6.35E-05
16014.7	8.63E-04	7.10E-04	9.18E-04	5.46E-04	4.54E-04	-1.73E-04
16514.7	9.07E-04	8.54E-04	9.91E-04	6.88E-04	4.65E-04	-1.27E-04
17014.7	7.78E-04	8.41E-04	8.34E-04	7.22E-04	5.51E-04	-2.62E-04
17514.7	8.85E-04	8.75E-04	8.58E-04	7.61E-04	4.36E-04	-1.87E-04
18014.7	8.15E-04	1.00E-03	8.26E-04	8.11E-04	4.23E-04	-2.30E-04
18514.7	9.02E-04	8.84E-04	8.54E-04	8.43E-04	2.93E-04	-2.11E-04
19014.7	9.27E-04	8.45E-04	7.97E-04	8.21E-04	2.67E-04	-2.19E-04
19514.7	1.06E-03	7.93E-04	8.32E-04	7.69E-04	1.25E-04	-2.98E-04
20014.7	1.19E-03	7.49E-04	7.75E-04	7.87E-04	1.29E-04	-2.17E-04
20514.7	1.12E-03	7.57E-04	6.78E-04	5.98E-04	7.28E-05	-3.11E-04
21014.7	1.10E-03	7.81E-04	6.50E-04	4.77E-04	-9.07E-05	-4.48E-04
21514.7	9.46E-04	6.72E-04	6.34E-04	2.94E-04	-6.26E-05	-3.77E-04
22014.7	9.25E-04	6.25E-04	6.16E-04	2.52E-04	-1.62E-04	-3.48E-04
22514.7	8.33E-04	6.03E-04	5.48E-04	2.19E-04	-2.84E-04	-3.77E-04
23014.7	7.37E-04	4.44E-04	5.11E-04	3.50E-04	-4.36E-04	-4.12E-04
23514.7	6.04E-04	3.28E-04	4.47E-04	4.26E-04	-3.50E-04	-4.52E-04
24014.7	8.64E-04	2.81E-04	4.35E-04	2.37E-04	-2.48E-05	-3.99E-04
24514.7	8.12E-04	1.96E-04	5.57E-04	3.07E-04	-5.45E-05	-4.13E-04
25014.7	6.06E-04	5.50E-05	-	-	-7.62E-05	-4.74E-04

Table 6-5. Continued

Pressure	Temperature (^{o}F)					
(psia)	300	320	340	360	380	415
	Absolute Error (cp)					
514.7	9.05E-04	8.67E-04	8.27E-04	7.87E-04	7.45E-04	6.67E-04
1014.7	6.95E-04	6.65E-04	6.32E-04	5.97E-04	5.59E-04	4.90E-04
1514.7	4.97E-04	4.74E-04	4.46E-04	4.18E-04	3.86E-04	3.27E-04
2014.7	3.09E-04	2.92E-04	2.73E-04	2.51E-04	2.25E-04	1.75E-04
2514.7	1.32E-04	1.23E-04	1.10E-04	9.36E-05	7.49E-05	3.42E-05
3014.7	-3.01E-05	-3.22E-05	-3.92E-05	-4.97E-05	-6.35E-05	-9.42E-05
3514.7	-1.75E-04	-1.73E-04	-1.74E-04	-1.78E-04	-1.88E-04	-2.10E-04
4014.7	-3.02E-04	-2.94E-04	-2.91E-04	-2.92E-04	-2.96E-04	-3.14E-04
4514.7	-4.05E-04	-3.90E-04	-9.76E-05	-3.88E-04	-3.84E-04	-4.14E-04
5014.7	-3.94E-04	-2.72E-04	-1.99E-04	-4.58E-04	-4.33E-04	-4.96E-04
5514.7	-4.05E-04	-2.82E-04	-4.60E-04	-5.14E-04	-4.74E-04	-5.25E-04
6014.7	-3.76E-04	-3.09E-04	-5.44E-04	-5.90E-04	-5.95E-04	-5.52E-04
6514.7	-4.07E-04	-3.61E-04	-4.98E-04	-5.32E-04	-5.02E-04	-6.47E-04
7014.7	-3.46E-04	-3.48E-04	-4.04E-04	-4.27E-04	-4.81E-04	-6.40E-04
7514.7	-2.72E-04	-3.23E-04	-3.38E-04	-4.47E-04	-4.59E-04	-6.38E-04
8014.7	-2.33E-04	-2.48E-04	-3.52E-04	-3.13E-04	-4.43E-04	-6.64E-04
8514.7	-9.35E-05	-1.86E-04	-3.90E-04	-5.51E-04	-4.81E-04	-5.95E-04
9014.7	-1.52E-04	-1.73E-04	-5.41E-04	-5.58E-04	-4.72E-04	-5.75E-04
9514.7	-8.49E-05	-1.10E-04	-4.34E-04	-4.96E-04	-4.79E-04	-5.17E-04
10014.7	-5.39E-05	-5.03E-05	-3.86E-04	-4.31E-04	-3.82E-04	-4.79E-04
10514.7	4.16E-05	-8.72E-05	-3.92E-04	-4.65E-04	-3.95E-04	-4.49E-04
11014.7	1.43E-04	-6.43E-05	-3.86E-04	-5.12E-04	-2.71E-04	-4.76E-04
11514.7	1.87E-04	-2.73E-06	-3.24E-04	-4.60E-04	-2.49E-04	-3.49E-04
12014.7	-1.47E-04	6.27E-05	-3.50E-04	-3.88E-04	-2.54E-04	-3.03E-04
12514.7	-2.06E-04	1.16E-04	-3.76E-04	-2.91E-04	-2.19E-04	-3.21E-04
13014.7	-1.26E-04	1.60E-04	-3.95E-04	-2.94E-04	-2.39E-04	-3.13E-04
13514.7	-1.23E-04	1.48E-04	-3.58E-04	-1.79E-04	-2.21E-04	-3.14E-04
14014.7	-1.09E-04	1.50E-04	-3.97E-04	-1.28E-04	-2.02E-04	-3.10E-04

Table 6-5. Continued

Pressure	Temperature (^{o}F)					
(psia)	300	320	340	360	380	415
	Absolute Error (cp)					
14514.7	-1.35E-05	1.27E-04	-4.05E-04	-8.63E-05	-1.48E-04	-2.60E-04
15014.7	-6.55E-05	8.91E-05	-4.02E-04	-1.03E-04	-1.67E-04	-2.06E-04
15514.7	-9.48E-05	-1.09E-05	-5.28E-04	-9.83E-05	-1.18E-04	-1.22E-05
16014.7	-1.52E-04	-4.39E-05	-9.12E-04	-1.32E-04	-1.31E-04	-2.88E-05
16514.7	-2.85E-04	-1.24E-04	-8.11E-04	-1.43E-04	-1.40E-04	4.87E-05
17014.7	-2.40E-04	-2.52E-04	-7.97E-04	-1.68E-04	-1.69E-04	-1.56E-06
17514.7	-3.28E-04	-2.25E-04	-7.11E-04	-1.75E-04	-1.97E-04	-5.35E-06
18014.7	-4.07E-04	-2.67E-04	-1.07E-03	-2.19E-04	-2.03E-04	-2.22E-04
18514.7	-3.06E-04	-5.10E-04	-1.09E-03	-3.61E-04	-2.40E-04	-9.72E-05
19014.7	-3.79E-04	-5.01E-04	-1.08E-03	-1.63E-04	-2.35E-04	-2.37E-04
19514.7	-4.51E-04	-3.95E-04	-1.06E-03	-2.27E-04	-2.09E-04	-9.44E-05
20014.7	-4.90E-04	-3.95E-04	-9.32E-04	-2.76E-04	-1.75E-04	-4.77E-05
20514.7	-6.20E-04	-3.98E-04	-9.59E-04	-2.82E-04	-2.28E-04	-1.27E-04
21014.7	-5.59E-04	-3.44E-04	-9.16E-04	6.45E-05	-1.72E-04	5.55E-05
21514.7	-6.98E-04	-4.86E-04	-9.61E-04	4.53E-05	-5.01E-05	1.96E-04
22014.7	-7.93E-04	-5.44E-04	-8.45E-04	1.02E-04	-1.42E-04	2.49E-05
22514.7	-7.20E-04	-6.55E-04	-9.70E-04	1.90E-04	-2.03E-04	2.26E-04
23014.7	-8.15E-04	-5.77E-04	-8.05E-04	2.74E-04	-1.65E-04	3.75E-04
23514.7	-8.11E-04	-7.48E-04	-7.15E-04	2.73E-04	-3.66E-05	3.07E-04
24014.7	-9.96E-04	-1.17E-03	-5.63E-04	2.77E-04	-4.78E-05	6.22E-04
24514.7	-4.16E-04	-1.23E-03	-6.38E-04	-2.66E-04	-1.02E-05	6.06E-04
25014.7	-	-1.32E-03	-6.12E-04	-	-9.98E-05	-

Table 6-6. Relative error analysis by comparing methane viscosity data with values from correlation

Pressure	Temperature (^{o}F)						
(psia)	100	120	140	160	180	188	200
	Relative Error (%)						
514.7	9.584	9.217	8.847	8.482	8.112	7.964	7.746
1014.7	6.645	6.492	6.311	6.121	5.906	5.815	5.677
1514.7	3.932	3.971	3.975	3.943	3.877	3.848	3.787
2014.7	1.623	1.801	1.937	2.028	2.085	2.102	2.107
2514.7	-0.155	0.078	0.280	0.449	0.585	0.626	0.683
3014.7	-1.365	-1.162	-0.963	-0.769	-0.605	-0.543	-0.461
3514.7	-2.098	-1.966	-1.812	-1.641	-1.481	-1.418	-1.332
4014.7	-2.462	-2.429	-2.333	-2.214	-2.078	-2.026	-1.945
4514.7	-2.557	-2.626	-2.340	-2.537	-2.446	-2.413	-2.343
5014.7	-3.079	-2.707	-2.225	-2.595	-3.563	-2.604	-1.597
5514.7	-2.514	-2.549	-0.733	-2.094	-3.160	-2.730	-1.471
6014.7	-4.303	-1.584	-0.665	-1.501	-2.692	-3.102	-2.274
6514.7	-2.965	-0.159	-1.662	-1.272	-2.270	-2.310	-1.890
7014.7	-0.885	0.588	-1.516	-0.810	-1.650	-1.523	-1.791
7514.7	-1.121	1.049	-1.821	-0.687	-1.003	-1.163	-1.554
8014.7	-0.667	1.252	-1.399	1.150	-1.250	-0.641	-1.247
8514.7	-0.379	1.237	-1.273	1.577	-0.708	-0.226	-1.183
9014.7	-0.486	0.944	-1.048	1.574	-0.041	0.377	-0.985
9514.7	-0.391	0.920	-0.758	1.228	0.542	0.636	-0.723
10014.7	-0.151	0.804	-0.426	1.402	0.647	0.871	-0.569
10514.7	-0.051	0.865	-0.382	1.404	0.397	1.484	-0.455
11014.7	-0.028	0.858	0.088	1.418	1.220	1.542	-0.284
11514.7	0.104	0.860	0.573	1.603	1.331	1.652	0.048
12014.7	0.267	1.001	0.836	1.562	1.486	1.888	0.272
12514.7	0.501	1.035	0.984	1.571	1.457	2.133	0.280
13014.7	0.501	1.219	0.854	1.632	1.452	2.142	0.790
13514.7	0.487	1.169	1.040	1.668	1.489	2.238	1.185
14014.7	0.388	1.100	0.948	1.536	1.603	2.074	1.076

Table 6-6. Continued

Pressure	Temperature (^{o}F)						
(psia)	100	120	140	160	180	188	200
	Relative Error (%)						
14514.7	0.240	0.977	0.963	1.439	1.523	1.939	0.999
15014.7	0.347	0.970	0.875	1.562	1.370	1.605	1.105
15514.7	0.219	0.796	0.769	1.787	1.299	1.471	1.337
16014.7	0.038	0.875	0.805	1.068	1.380	1.356	1.456
16514.7	0.080	0.652	0.766	0.695	1.303	1.204	1.611
17014.7	-0.083	0.469	0.708	0.693	1.325	1.158	1.583
17514.7	-0.275	0.307	0.682	0.800	1.036	1.278	1.417
18014.7	-0.490	0.154	0.488	0.522	0.858	1.143	0.990
18514.7	-0.667	0.151	0.387	0.361	0.847	1.009	0.424
19014.7	-0.902	0.007	0.507	0.520	0.773	0.895	0.677
19514.7	-0.923	-0.172	0.340	0.302	0.578	0.704	0.671
20014.7	-1.082	-0.470	0.133	0.259	0.535	0.433	0.347
20514.7	-1.302	-0.623	0.190	0.115	0.498	1.043	0.325
21014.7	-2.167	-0.826	-0.126	0.003	0.353	1.106	-0.057
21514.7	-1.847	-1.108	-0.174	-0.130	0.243	0.956	-0.142
22014.7	-1.979	-1.386	-0.385	-0.262	0.023	0.862	-0.144
22514.7	-2.228	-1.977	-0.537	-0.552	-0.094	0.746	-0.060
23014.7	-2.601	-1.526	-0.605	-0.616	-0.201	0.497	-0.222
23514.7	-2.869	-2.139	-0.876	-0.569	-0.067	0.289	-0.318
24014.7	-2.941	-2.405	-1.044	-0.257	-0.458	0.060	-0.177
24514.7	-3.322	-2.579	-1.216	-0.436	-0.792	0.168	-0.284
25014.7	-3.607	-	-1.315	-0.923	-1.037	-	-

Table 6-6. Continued

Pressure	Temperature (^{o}F)					
(psia)	220	225	230	250	260	280
	Relative Error (%)					
514.7	7.376	7.282	7.194	6.833	6.645	6.285
1014.7	5.444	5.384	5.322	5.071	4.943	4.685
1514.7	3.672	3.645	3.612	3.465	3.389	3.221
2014.7	2.097	2.091	2.081	2.037	2.000	1.917
2514.7	0.749	0.765	0.775	0.797	0.799	0.786
3014.7	-0.346	-0.324	-0.304	-0.229	-0.202	-0.170
3514.7	-1.198	-1.169	-1.143	-1.044	-1.004	-0.942
4014.7	-1.820	-1.791	-1.767	-1.662	-1.616	-1.540
4514.7	-2.243	-2.455	-2.210	-2.122	-2.041	-1.972
5014.7	-2.480	-2.678	-2.580	-1.879	-2.161	-1.983
5514.7	-2.151	-2.182	-2.015	-1.664	-2.149	-2.102
6014.7	-1.827	-2.011	-1.771	-1.421	-1.990	-2.013
6514.7	-2.001	-1.819	-1.566	-1.093	-1.854	-2.098
7014.7	-0.975	-1.254	-1.360	-1.010	-1.337	-1.899
7514.7	-1.566	-0.906	-0.794	-0.861	-1.143	-1.654
8014.7	-0.908	-1.296	-0.537	-0.669	-1.330	-1.569
8514.7	-0.142	-1.105	-0.445	-0.472	-0.951	-1.437
9014.7	0.530	-0.648	-0.201	0.079	-0.832	-1.285
9514.7	0.899	-0.180	0.110	0.192	-0.504	-0.819
10014.7	1.154	0.155	0.455	0.515	-0.134	-0.671
10514.7	1.214	0.808	1.001	0.798	0.200	-0.317
11014.7	1.531	0.945	1.143	0.940	0.546	-0.213
11514.7	1.765	1.414	1.647	0.886	1.028	-0.233
12014.7	1.927	1.602	1.788	1.011	0.787	-0.147
12514.7	1.950	1.762	1.695	1.034	0.995	-0.123
13014.7	2.407	1.800	2.120	1.191	0.984	-0.032
13514.7	2.342	2.366	2.340	1.739	0.995	0.042
14014.7	2.400	1.645	2.644	1.849	1.173	-0.052

Table 6-6. Continued

Pressure	Temperature (^{o}F)					
(psia)	220	225	230	250	260	280
	Relative Error (%)					
14514.7	2.177	1.678	2.441	1.742	0.940	-0.059
15014.7	2.112	1.270	2.010	1.274	0.899	-0.487
15514.7	2.068	1.654	2.018	1.585	0.793	-0.161
16014.7	2.059	1.697	2.218	1.338	1.121	-0.428
16514.7	2.125	2.009	2.352	1.658	1.128	-0.309
17014.7	1.784	1.942	1.938	1.711	1.313	-0.626
17514.7	1.996	1.986	1.959	1.773	1.020	-0.438
18014.7	1.803	2.244	1.851	1.857	0.971	-0.530
18514.7	1.967	1.937	1.883	1.900	0.658	-0.478
19014.7	1.989	1.820	1.724	1.820	0.590	-0.490
19514.7	2.252	1.679	1.774	1.675	0.271	-0.654
20014.7	2.480	1.560	1.624	1.687	0.276	-0.469
20514.7	2.290	1.551	1.396	1.258	0.153	-0.662
21014.7	2.224	1.576	1.317	0.986	-0.187	-0.936
21514.7	1.878	1.335	1.266	0.596	-0.127	-0.778
22014.7	1.808	1.221	1.210	0.504	-0.324	-0.708
22514.7	1.602	1.162	1.060	0.430	-0.560	-0.757
23014.7	1.396	0.841	0.974	0.681	-0.844	-0.815
23514.7	1.124	0.611	0.840	0.818	-0.669	-0.882
24014.7	1.596	0.517	0.806	0.447	-0.047	-0.769
24514.7	1.479	0.355	1.022	0.572	-0.102	-0.785
25014.7	1.084	0.098	-	-	-0.141	-0.888

Table 6-6. Continued

Pressure	Temperature (^{o}F)					
(psia)	300	320	340	360	380	415
	Relative Error (%)					
514.7	5.929	5.578	5.224	4.881	4.537	3.944
1014.7	4.416	4.150	3.879	3.603	3.322	2.833
1514.7	3.044	2.856	2.652	2.446	2.229	1.843
2014.7	1.816	1.696	1.565	1.419	1.256	0.957
2514.7	0.744	0.683	0.608	0.511	0.405	0.181
3014.7	-0.162	-0.172	-0.208	-0.262	-0.331	-0.484
3514.7	-0.901	-0.883	-0.886	-0.903	-0.945	-1.047
4014.7	-1.484	-1.441	-1.422	-1.422	-1.438	-1.510
4514.7	-1.903	-1.834	-0.466	-1.821	-1.800	-1.929
5014.7	-1.785	-1.240	-0.914	-2.077	-1.965	-2.238
5514.7	-1.768	-1.241	-2.016	-2.248	-2.083	-2.297
6014.7	-1.580	-1.310	-2.296	-2.493	-2.520	-2.348
6514.7	-1.652	-1.478	-2.038	-2.183	-2.072	-2.665
7014.7	-1.360	-1.377	-1.607	-1.710	-1.927	-2.562
7514.7	-1.038	-1.239	-1.310	-1.732	-1.788	-2.490
8014.7	-0.861	-0.927	-1.323	-1.187	-1.680	-2.520
8514.7	-0.337	-0.677	-1.421	-2.010	-1.774	-2.206
9014.7	-0.530	-0.610	-1.903	-1.981	-1.696	-2.080
9514.7	-0.288	-0.378	-1.493	-1.718	-1.676	-1.829
10014.7	-0.178	-0.169	-1.295	-1.461	-1.308	-1.657
10514.7	0.135	-0.285	-1.281	-1.534	-1.318	-1.517
11014.7	0.451	-0.205	-1.233	-1.645	-0.887	-1.573
11514.7	0.576	-0.008	-1.011	-1.447	-0.798	-1.134
12014.7	-0.439	0.191	-1.066	-1.196	-0.794	-0.964
12514.7	-0.599	0.346	-1.120	-0.881	-0.670	-0.999
13014.7	-0.360	0.467	-1.150	-0.871	-0.717	-0.956
13514.7	-0.344	0.422	-1.022	-0.521	-0.649	-0.938
14014.7	-0.297	0.421	-1.110	-0.366	-0.582	-0.909

Table 6-6. Continued

Pressure	Temperature (^{o}F)					
(psia)	300	320	340	360	380	415
	Relative Error (%)					
14514.7	-0.036	0.347	-1.111	-0.242	-0.420	-0.750
15014.7	-0.172	0.239	-1.082	-0.283	-0.463	-0.583
15514.7	-0.244	-0.029	-1.388	-0.265	-0.322	-0.034
16014.7	-0.384	-0.113	-2.331	-0.349	-0.352	-0.079
16514.7	-0.705	-0.312	-2.043	-0.371	-0.370	0.132
17014.7	-0.583	-0.623	-1.973	-0.428	-0.438	-0.004
17514.7	-0.782	-0.547	-1.735	-0.439	-0.501	-0.014
18014.7	-0.952	-0.637	-2.536	-0.540	-0.507	-0.568
18514.7	-0.705	-1.192	-2.541	-0.873	-0.590	-0.245
19014.7	-0.860	-1.151	-2.491	-0.390	-0.568	-0.586
19514.7	-1.004	-0.896	-2.402	-0.533	-0.499	-0.231
20014.7	-1.073	-0.882	-2.091	-0.639	-0.410	-0.115
20514.7	-1.334	-0.877	-2.118	-0.642	-0.528	-0.302
21014.7	-1.187	-0.748	-1.998	0.146	-0.393	0.131
21514.7	-1.458	-1.038	-2.064	0.101	-0.113	0.456
22014.7	-1.629	-1.143	-1.794	0.224	-0.316	0.057
22514.7	-1.462	-1.355	-2.026	0.413	-0.444	0.511
23014.7	-1.629	-1.179	-1.665	0.589	-0.356	0.841
23514.7	-1.599	-1.502	-1.462	0.579	-0.078	0.678
24014.7	-1.932	-2.299	-1.139	0.580	-0.101	1.364
24514.7	-0.806	-2.384	-1.272	-0.544	-0.021	1.311
25014.7	-	-2.516	-1.206	-	-0.205	-

CHAPTER VII

CONCLUSIONS AND RECOMMENDATIONS

7.1 Conclusions

Upon the study we finished, following conclusions were made:

I. At high pressure, nitrogen viscosities from lab are lower than NIST values. The difference between lab data and NIST values increases as pressure increases.
II. At high pressure, methane viscosities from lab are higher than NIST values. The difference between lab data and NIST values increases as temperature decreases; this difference also increases as pressure increases.
III. New gas viscosity correlations derived in this study can be used to predict gas viscosity at HPHT confidently considering very high methane concentration in HPHT gas reservoirs.
IV. Existing gas viscosity correlations is inappropriate for gas with moderate to high nonhydrocarbon concentration.
V. A new nitrogen viscosity correlation based on our lab data was developed and can be used in HPHT reservoirs containing significant amount of nitrogen.

7.2 Recommendations

Further study should focus on

I. Measuring carbon dioxide viscosity at HPHT,
II. Measuring bi-component and tri-component mixtures viscosity,
III. Measuring viscosity of natural gas sampled from HPHT reservoirs,
IV. Deriving a new correlation basing on lab data covering low to high pressure and temperature.

NOMENCLATURE

Symbol	Description
atm	atmosphere
atms	atmospheres, pressure unit
A	area
A	a layer in fluid flow between two plates
AA	constant in friction factor equation
bar	pressure unit, 1 bar = 0.987 atms
B	buoyant force
B	a layer in fluid flow between two plates (higher velocity than layer A)
BB	constant in friction factor equation
cm	centimeter
cp	centipoise
CC	constant in friction factor equation
CO_2	carbon dioxide
^oC	Celsius temperature
d	difference
d_b	ball diameter
D	drag force
D_y	drag force in y dimension, or vertical direction
E_k	kinetic energy per unit volume
f	friction factor
f_d	driving force

Symbol	Description
f_f	friction force
ft	foot or feet
F	force
^{o}F	degree Fahrenheit
g	gravity acceleration factor
g	gram
g	gas
g_c	gravity constant
H_2S	hydrogen sulfide
HPHT	high pressure high temperature
in	inch
kg	kilogram
K	constant for viscosity from capillary viscometer
K	constant for viscosity correlation
Kpa	thousand Pascal
^{o}K	Kelvin temperature
l	length, distance
m	mass
m	meter
m_b	mass of ball or sphere
Mpa	million Pascal
M_w	molecular weight
n	number of moles
N	Newton, force unit

Symbol	Description
N_2	nitrogen
N_{Re}	Reynolds number
p	pressure
Δp	pressure change
p_1	pressure at inlet of pipe or tube
p_2	pressure at outlet of pipe or tube
p_i	initial pressure
p_c	critical pressure
p_{pc}	pseudocritical pressure
psi	gauge pressure
psia	absolute pressure
psig	gauge pressure
P	poise
Pa	Pascal
p_{pr}	pseudoreduced pressure
p_r	reduced pressure
r	distance from center of circle, tube, or pipe
R	radius of circle, tube, or pipe
R	universal gas constant
R_{gas}	universal gas constant
s	second
sec	second
SC	standard condition
t	time

Symbol	Description
T	temperature
T_c	critical temperature
T_{pc}	pseudocritical temperature
T_{pr}	pseudoreduced temperature
T_r	reduced temperature
u	velocity
u_x	velocity in x direction
u_y	velocity in y direction
v	velocity
v_{slip}	slip velocity
V	volume
V_1	volume above mercury in capillary tube
V_2	volume below mercury in capillary tube
V_b	volume of ball or sphere
$V_{elementary}$	elementary volume
W	weight
x	x direction or dimension
X	constant for viscosity correlation
y	y direction or dimension
y_{CO_2}	mole fraction of carbon dioxide in vapor
y_{H_2S}	mole fraction of hydrogen sulfide in vapor
y_{N_2}	mole fraction of nitrogen in vapor
$y_{N_2,\ CO_2,\ H_2S}$	mole fraction of the non-hydrocarbon component
Y	constant for viscosity correlation
z	z-factor

Greek

Symbol	Description
γ	shear rate
γ_g	gas specific gravity
μ	viscosity
μ_{1atm}	gas viscosity at 1 atmosphere
μ_g	gas viscosity
μ_{gSC}	gas viscosity at standard condition
υ	kinetic viscosity
ξ	constant for viscosity correlation
π	a mathematical constant whose value is the ratio of any circle's circumference to its diameter
ρ	density
ρ_b	ball or sphere density
ρ_f	fluid density
ρ_g	gas density
ρ_r	reduced density
τ	shear stress
ψ	sphericity
Δ	indicates difference

Subscripts

Symbol	Description
1	inlet of the tube or pipe
1	above the mercury in capillary tube viscometer
1atm	1 atmosphere

Symbol	Description
2	outlet of the tube or pipe
2	below the mercury in capillary tube viscometer
Avg	average
CO_2	carbon dioxide
g	gas
H_2S	hydrogen sulfide
i	initial
N_2	nitrogen
SC	low pressure condition
gSC	gas at low pressure condition
$_x$	x direction or dimension
$_y$	y direction or dimension

REFERENCES

Adzumi, H. 1937. Studies on the Flow of Gaseous Mixtures through Capillaries. I The Viscosity of Binary Gaseous Mixtures. *Bulletin of the Chemical Society of Japan*. **12**, (5): 199-226.

Assael, M.J. Dalaouti, N.K. and Vesovic, V. 2001. Viscosity of Natural-Gas Mixtures: Measurements and Prediction. *International Journal of Thermophysics*. **22**, (1): 61-71.

Audonnet, F. and Padua, A.A.H. 2004. Viscosity and Density of Mixtures of Methane and n-Decane from 298 to 393 K and up to 75 MPa. *Fluid Phase Equilibria*. **216**: 235-244.

Baron J.D. Roof, J.G. and Well, F.W. 1959. Viscosity of Nitrogen, Methane, Ethane, and Propane at Elevated Temperature. *Journal of Chemical and Engineering Data*. **4**: 283-288.

Barua, A.K. Afzal, M. Flynn, G.P. and Ross, J. 1964. Viscosities of Hydrogen, Deuterium, Methane, and Carbon Monoxide from -50^{o} to 150 ^{o}C below 200 Atmospheres. *The Journal of Chemical Physics*. **41**: 374-378.

Berwald, W.B. and Johnson, T.W. 1933. *Viscosity of Natural Gases*. U.S. Department of Commerce, Bureau of Mines, Technical Paper, 555.

Bicher, L.B. and Katz, D.L. 1943. Viscosity of Methane-Propane System. *Ind. Eng. Chem.* **35**: 754-761.

Blasius, H. 1913. Das Aehnlichkeitsgesetz bei Reibungsvorgängen in Flüssigkeiten. *Mitteilungen über Forschungsarbeiten auf dem Gebiete des Ingenieurwesens*. **131**: VDI-Verlag Berlin.

Boon, J.P. Legros, J.C. and Thomaes, G. 1967. On the Principle of Corresponding State for the Viscosity of Simple Liquids. *Physica*. **33**: 547-557.

Bourgoyne, T.A. Chenevert, E.M. Millhein, K.K. and Young, S.F. 1986. *Applied Drilling Engineering*. Richardson, Texas: Textbook Series, SPE.

Boyd, J. 1930. The Viscosity of Compressed Gases. *Physica Review*. **35**: 1284-1297.

Cambridge Viscosity Inc. 2010. Unpublished Paper. Viscous Drag in the Oscillating Piston Viscometer, Medford, Maryland: Cambridge Viscosity, Inc.

Canet, X. Baylaucq, A. and Boned, C. 2002. High-Pressure (up to 140 MPa) Dynamic Viscosity of the Methane+Decane System. *International Journal of Thermophysics*, **23**: 1469-1486.

Carmichael, L.T. Virginia, B. and Sage, B.H. 1965. Viscosities of Hydrocarbons. Methane. *Journal of Chemical and Engineering Data*. **10**: 57-61.

Carr, N.L. 1952. *The Viscosity of Gas Mixtures at High Pressures*. PhD thesis, Chicago, Illinois: Illinois Institute of Technology.

Carr, N.L. Kobayashi, R. and Burrows, D.B. 1954. Viscosity of Hydrocarbon Gases under Pressure. *Trans.* AIME. **201**: 264-272.

Castleman, R.A. 1926. The Resistance to the Steady Motion of Small Spheres in Fluids. National Advisory Committee for Aeronautics, Technical Note No. 231, Washington D.C., February.

Chan, R.K.Y. and Jackson, D.A. 1985. An Automated Falling-Cylinder High Pressure Laser-Doppler Viscometer. *J. Phys. E: Sci. Instrum*. **18**: 510-515.

Comings, E.W. and Egly, R.S. 1940. Viscosity of Gases and Vapors at High Pressures. *Industrial and Engineering Chemistry*. **32**: 714-718.

Comings, E.W. Mayland, B.J. and Egly, R.S. 1944. *The Viscosity of Gases at High Pressures.* Chicago, Illinois: University of Illinois Engineering Experiment Station Bulletin Series No. 354.

Dabir S.V. Tushar K. Ghosh D. Prasad, H.L. Nidamartyv. K. D. and Kalipatnapu Y.R. 2007. *Viscosity of Liquids-Theory, Estimation, Experiment, and Data*. Columbia, Missouri: University of Missouri.

Dempsey, J.R. 1965. Computer Routine Treats Gas Viscosity as a Variable. *Oil and Gas Journal*. 141-143, August 16.

Diehl, J. Gondouin, M. Houpeurt, A. Neoschil, J. Thelliez, M. Verrien, J.P. and Zurawsky, R. 1970. *Viscosity and Density of Light Paraffins, Nitrogen and Carbon Dioxide*. Technip, Paris, CREPS/Geopetrole.

Diller, D. E. 1980. Measurements of the Viscosity of Compressed Gases and Liquid Methane. *Physica*. **104A**: 417-426.

Diller, D. E. 1983. Measurements of the Viscosity of Compressed Gases and Liquid Nitrogen. *Physica*. **119A**: 92-100.
Dipippo R. Kestin, J. and Whitelaw, J.H. 1966. A High-Temperature Oscillating-Disk Viscometer. *Physica*. **32**: 2064-2080.

Earhart, R. F. 1916. The Ratio of Specific Heats and the Coefficient of Viscosity of Natural Gas from Typical Fields. *Trans. Am. Soc. Mech. Eng.* **38**: 983-994.

Ellis, C.P. and Raw, J.R. 1959. High Temperature Gas Viscosities. II. Nitrogen, Nitric Oxide, Boron Trifluoride, Silicon Tetrafluoride, and Sulfur Hexafluoride. *The Journal of Chemical Physics*. **30**(2): 574-576.

Elsharkawy, A.M. 2004. Efficient Methods for Calculations of Compressibility, Density, and Viscosity of Natural Gases, *Fluid Phase Equilibria*. **218**:1-13.

Florida Atlantic University. 2005. Falling Ball Viscometer. http://wise.fau.edu/~blarkin/Viscometer.html.

Flynn, G.P. Hanks, R.V. and Lemaire, N.A. 1963. Viscosities of Nitrogen, Helium, Neon, and Argon from -78.5^{o} to 100 ^{o}C below 200 Atmospheres. *The Journal of Chemical Physics*. **38**: 154-162.

Giddings, J.G. James, T.F. and Riki, K. 1966. Development of a High-Pressure Capillary-Tube Viscometer and Its Application to Methane, Propane, and Their Mixtures in the Gases and Liquid Regions. *The Journal of Chemical Physics*. **45**: 578-586.

Golubev, I.F. 1959. *Viscosity of Gases and Gas Mixtures, a Handbook*. This book is a translation from Russian by the National Technical Information Service. Alexandria, Virginia.

Gonzalez, M.H. Eakin, B.E. and Lee, A.L. 1970. *Viscosity of Natural Gases*. New York: Institute of Gas Technology (Chicago) Monograph on API Research Project 65.

Gonzalez, M.H. Richard, F.B. and Lee, A.L. 1966. The Viscosity of Methane. Paper SPE 1483 presented at the Annual Fall Meeting, Dallas, 2-5 Oct.

Grevendonk, W. Herreman, W. and De Bock, A. 1970. Measurements on the Viscosity of Liquid Nitrogen. *Physica*. **46**: 600-604.

Helleman, J.M. Kestin, J. and Ro, S.T. 1973. The Viscosity of Oxygen and Some of Its Mixtures with Other Gases, *Physica.* **65**: 362-375.

Helleman, J.M. Zink, H. and Van Paemel, O. 1970. The Viscosity of Liquid Argon and Liquid Methane along Isotherms as a Function of Pressure. *Physica*. **46**: 395-410.

Herbert, T. and Stokes, G.G. 1886. The Coefficient of Viscosity of Air. *Philosophical Transactions of the Royal Society of London*. **177**: 767-799.

Hongo, M. Yokoyama, C. and Takahashi, D. 1988. Viscosity of Methane-Chlorodifluoromethane (R22) Gaseous Mixtures in the Temperature Range from 298.15 to 373.15 ^{o}K and at pressures up to 5MP. *Journal of Chemical Engineering of Japan*. **21**: 632-639.

Huang, E.T.S. Swift, G.W. and Fred, K. 1966. Viscosities of Methane and Propane at Low Temperatures and High Pressure. *AIChE Journal*. **12**: 932-936.

Iwasaki, H. 1954. Measurement of Viscosity of Gases at High Pressure. II Viscosities of Nitrogen and Mixture of Nitrogen and Hydrogen. *The Chemical Research Institute of Non-Aqueous Solution*. 296-307.

Johnston, H.L. and McCloskey, K.E. 1940. Viscosities of Several Common Gases between 90°K and Room Temperature. *The Journal of Physical Chemistry*. **44**(9): 1038-1058.

Jossi, J.A. Stiel, L.I. and Thodos G. 1962. The Viscosity of Pure Substances in the Dense Gaseous and Liquid Phases. *AIChE Journal*. **8**(1): 59-62.

Kestin, J. and Leidenfrost, W. 1959. An Absolute Determination of the Viscosity of Eleven Gases over a Range of Pressures. *Physica*. **25**: 1033-1062.

Kestin, J. and Yata, J. 1968. Viscosity and Diffusion Coefficient of Six Binary Mixtures. *The Journal of Chemical Physics*. **49**: 4780-4791.

Klimeck, J. Kleinrahm, R. and Wagner, W. 1998. An Accurate Single-Sinker Densimeter and Measurement of the (p, ρ, T) Relation of Argon and Nitrogen in the Temperature Range from (235 to 520) K at Pressures up to 30 Mpa. *J. Chem. Thermodynamics*. **30**: 1571-1588.

Knapstad, B. Skjolsvik, P.A. and Oye, H.A. 1990. Viscosity of the n-Decane – Methane System in the Liquid Phase. *Ber. Bunsenges Phys. Chem.* **94**: 1156-1165.

Kuss, E. 1952. High pressure research II: the viscosity of compressed gases (in German). *Z. Angew. Phys.* **4**(6): 203-207.

Lambert, J.D. Cotton, K.J. Pailthorpe, M.W. Robinson, A.M. Scrivins, J. Vale, W.R.F. and Young, R.M. 1955. Transport Properties of Gaseous Hydrocarbons. *Proceedings of*

the Royal Society of London. Series A, Mathematical and Physical Sciences. **231**(1185): 280-290.

Latto, B., and Saunders, M.W. 1972. Viscosity of Nitrogen Gas at Low Temperatures Up to High Pressures: A New Appraisal. *Physica*. **46**: 600-604.

Lee, A.L. 1965. *Viscosity of Light Hydrocarbons*. New York: American Petroleum Institute, Monograph on API Research Project 65.

Lee, A.L. Gonzalez, M.H. and Eakin, B.E. 1966. The Viscosity of Natural Gases. Paper SPE 1340 presented at the 1966 Annual Technical Conference and Exhibition held in Shreveport, Louisiana, 11-12 November.

Lemmon, E.W. Huber, M.L. and McLinden, M.O. 2007. *NIST Reference Fluid Thermodynamic and Transport Properties—REFPROP Version 8.0, User's Guide*. Physical and Chemical Properties Division, National Institute of Standards and Technology, Boulder, Colorado.

Londono. F. 2001. New Correlations for Hydrocarbon Gas Viscosity and Gas Density. MS thesis, College Station, Texas: Texas A&M University,

Malaguti, D. and Suitter, R. 2010. Communication between Author and Cambridge Engineers. March.

Marsh, J. Zvandasara, T. Macgill, A. and Jenny, K. 2010. Material Selection for HP/HT Developments. Paper SPE 130716-MS presented at SPE International Conference on Oilfield Corrosion held in Aberdeen, United Kingdom, 24-25 May.

Meyer, O.E. 1866. Viskositiit Der Kolloide. *Pogg. Ann*. **127**: 263.

Michels A. and Gibson R.O. 1931. The Measurement of the Viscosity of Gases at High Pressures: The Viscosity of Nitrogen to 1000 Atms. *Proc. R. Soc. Lond. A*. **134**: 288-307.

National Institute of Science and Technology (NIST). 2010. Web-Book of Thermodynamic Properties of Fluids. http://webbook.nist.gov,chemisty/fluid.

Nowak, P. Kleinrahm, R. and Wagner, W. 1997a. Measurement and Correlation of the (p, ρ, T) Relation of Nitrogen I. The Homogeneous Gas and Liquid Regions in the Temperature Range from 55 K to 239 K at Pressures up to 12 MPa. *J. Chem. Thermodynamics*. **29**: 1137-1156.

Nowak, P. Kleinrahm, R. and Wagner, W. 1997b. Measurement and Correlation of the (p, ρ, T) Relation of Nitrogen II. Saturated Liquid and Saturated Vapor Densities and

Vapor Pressures along the Entire Coexistence Curve. *J. Chem. Thermodynamics*. **29**: 1157-1174.

Park, N.A. 1994. Apparatus and Method for Viscosity Measurements Using a Controlled Needle Viscometer. http://www.patentstorm.us/patents/5327778/claims.html.

Paul N. Gardner Company, Inc. 2010. Vibrational Viscometer Based on Tuning Fork Technology. http://www.gardco.com/pages/viscosity/viscometers/sv_10_100.html.

Rankine, A.O. 1910. On a Method of Determining the Viscosity of Gases, Especially Those Available only in Small Quantities. *Proc. Roy. Soc.* **83A**: 265-276.

Rankine, A.O. 1923. A Simple Viscometer for Gases. *J. Sci. Instr*. **1**: 105-111

Rudenko, N.S. and Schubnikow, L.W. 1934. The Viscosity of Liquid Nitrogen, Carbon Monoxide, Argon and Oxygen as a Function of Temperature. *Physikalische Zeitschrift Sowjetunion*. **6**: 470-477.

Ross, J. and Brown, G. 1957. Viscosity of Gases at High Pressures. *Ind. Eng. Chem.* **49**: 2026-2033.

Sage, B.H. and Lacey, W.N. 1938. Effect of Pressure upon Viscosity of Methane and Two Natural Gases. *Trans. Am. Inst. Mining Met. Engrs*. **127**: 118-134.

Schley, P. Jaeschke, M. Kuchenmeister, C. and Vogel E. 2004. Viscosity Measurements and Predictions for Natural Gas. *International Journal of Thermophysics*. **25**: 1623-1652.

Seibt, D. Vogel, E. Bich, E. Buttig, D. and Hassel, E. 2006. Viscosity Measurements on Nitrogen. *J. Chem. Eng. Data*. **51**: 526-533.

Setzmann, U. and Wagner, W. 1991. A New Equation of State and Tables of Thermodynamic Properties for Methane Covering the Range from the Melting Line to 625 K at Pressures up to 1000 MPa. *J. Phys. Chem. Ref. Data*. **20**(6): 1061-1155.

Smith, A.S. and Brown, G.G. 1943. Correlating Fluid Viscosity. *Ind. Eng. Chem.* **35**: 705-711.

Steffe, J.F. 1992. An Oscillating Sphere System for Creating Controlled Amplitude in Liquid, Rheological Methods in Food Process Engineering. Michigan, Illinois: Freeman Press.

Stephan, K. and Lucas, K. 1979. *Viscosity of Dense Fluids*. West Lafayette, Indiana: The Purdue Research Foundation.

Stewart, J.R. 1952. The Viscosity of Natural Gas Components at High Pressure. Master thesis, Chicago, Illinois: Illinois Institute of Technology.

Stokes, G.G. 1868. On the Communication of Vibration from a Vibrating Body to a Surrounding Gas. *Philosophical Transactions of the Royal Society of London*. **158**: 447-463.

Straty, G.C. and Diller, D.E. 1980. PVT of Saturated and Compressed Fluid Nitrogen. *J. Chem. Thermodynamics*. **12**: 927-936.

Sutton, R.P. 2005. Fundamental PVT Calculations for Associated and Gas/Condensate Natural-Gas Systems. Paper SPE 97099 presented at the SPE Annual Technical Conference and Exhibition, Dallas, Texas, 9–12 October.

Swift, G.W. Christy, J.A. and Kurata, F. 1959. Liquid Viscosities of Methane and Propane. *AIChE Journal*. **5**: 98-102.

Swift, G.W. Lorenz J. and Kurata, F. 1960. Liquid Viscosities above the Normal Boiling Point for Methane, Ethane, Propane, and n-Butane. *AIChE Journal*. **6**: 415-419.

Tomida, D. Kumagai, A. and Yokoyama, C. 2005. Viscosity Measurements and Correlation of the Squalane + CO2 Mixture. *International Journal of Thermophysics,* **28**(1): 133-145.

Trautz, M. and Zink, R. 1930. The Viscosity, Thermal Conductivity and Diffusion in Gas Mixtures. XII. Gas Viscosity at High Temperatures (in German). *Ann. Phys. (Leipzig)*. **7**: 427-452.

Van Der Gulik, P. S. Mostert, R. and Van Den Berg, H. R. 1988. The Viscosity of Methane at 25 ^{o}C up to 10 kbar. *Physica*. **151A**: 153-166.

Van Itterbeek, A. Hellemans, J. Zink, H. and Van Cauteren, M. 1966. Viscosity of Liquefied Gases at Pressures between 1 and 100 Atmosphere. *Physica*. **32**: 2171-2172.

Van Itterbeek A. Van Paemel, O. and Van Lierde, J. 1947. Measurements on the Viscosity of Gas Mixtures. *Physica XlII*. **1-3**: 88-96.

Viswanathan, A. 2007. Viscosities of Natural Gases at High Pressures and High Temperatures. Master thesis, College Station, Texas: Texas A&M University.

Viswanathan, A. and McCain Jr., W.D. 2005. Crisman Institute for Petroleum Research Monthly Report, April 2005. Department of Petroleum Engineering, College Station: Texas A&M University.

Viswanathan, A. McCain Jr. W.D., and Teodoriu, C. 2006. Crisman Institute for Petroleum Research Monthly Report, March to December 2006. Department of Petroleum Engineering, College Station: Texas A&M University.

Vogel, E. Wilhelm, J. Cornelia, K. and Manfred, J. 1999. High-Precision Viscosity Measurements on Methane. Presented at the 15th European Conference on Thermophysical Properties, Wurzburg, Germany, 5-9 September.

Wikipedia. 2009. Definition of Fanning Friction Factor. http://en.wikipedia.org/wiki/Fanning_friction factor.

Wikipedia. 2010. Viscosity. http://en.wikipedia.org/wiki/Viscosity.

Wilson, J. 1965. A Method of Predicting the Viscosities of Natural Gases for a Wide Range of Pressures and Temperatures. PhD dissertation, College Station, Texas: Texas A&M University.

Yen, K. 1919. LVIII. An Absolute Determination of the Coefficients of Viscosity of Hydrogen, Nitrogen, and Oxygen. *Philosophical Magazine Series 6*. Vol. **28**, Issue 227, Page 582-596.

Zhang, Zh. Fu, J. Lin, Y. Fan, H. Xia, B. and Zhang, J. 2010. The Mechanism of Pressure Control Problem in High H_2S/CO_2 Gas Wells. Paper SPE 130143-MS presented at CPS/SPE International Oil & Gas Conference and Exhibition in China held in Beijing, China, 8-10 June.

APPENDIX A

Comparison of Nitrogen Viscosity from This Study with NIST Values

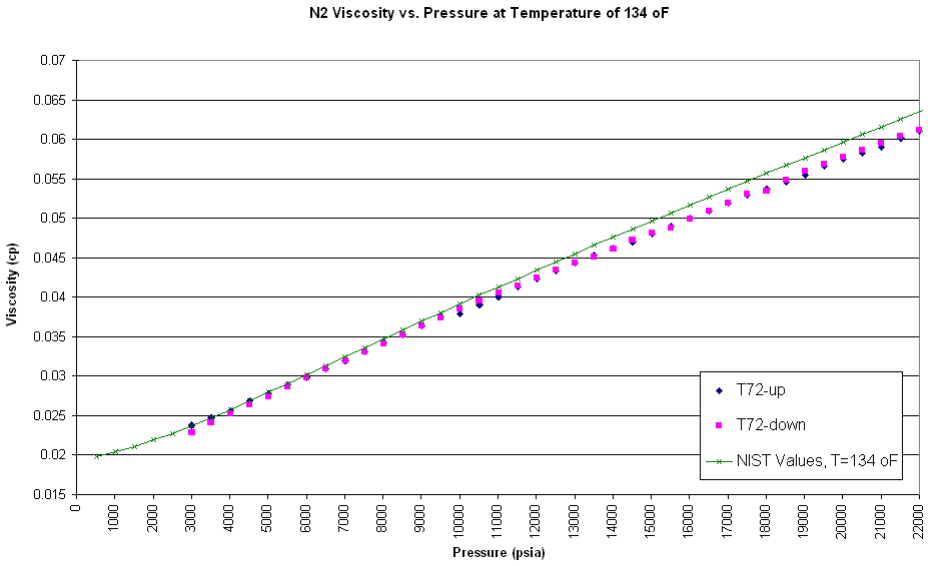

Figure A - 1. Nitrogen viscosity vs. pressure at 134 ^{o}F (Test 72)

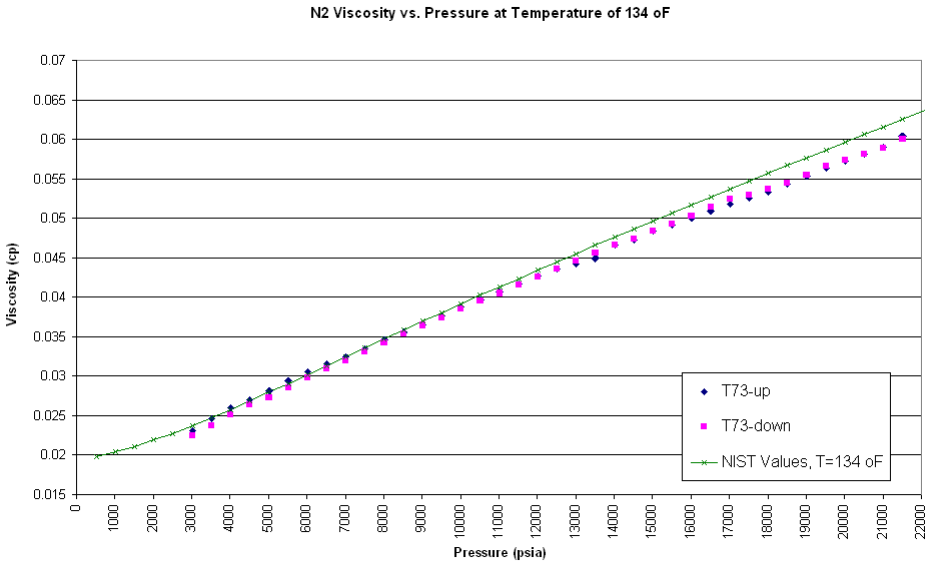

Figure A - 2. Nitrogen viscosity vs. pressure at 134 ^{o}F (Test 73)

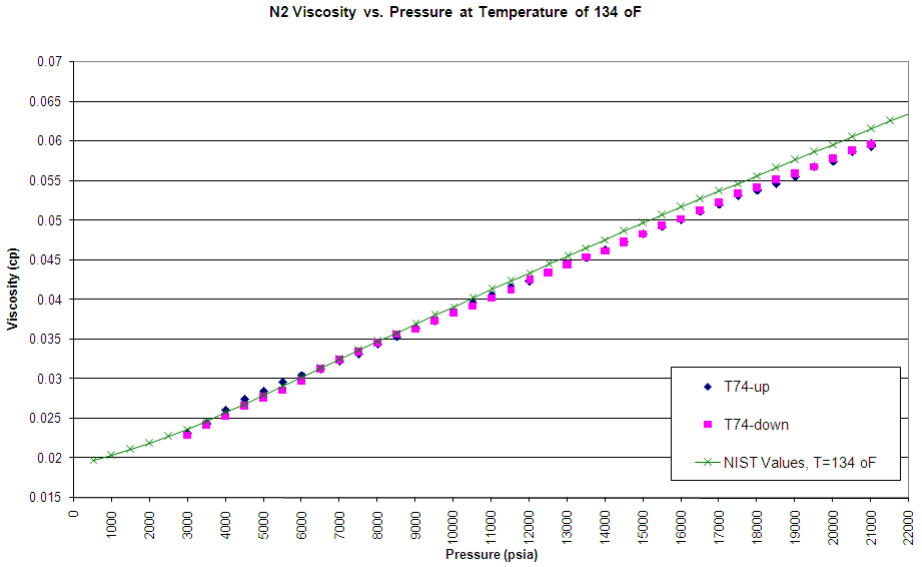

Figure A - 3. Nitrogen viscosity vs. pressure at 134 ^{o}F (Test74)

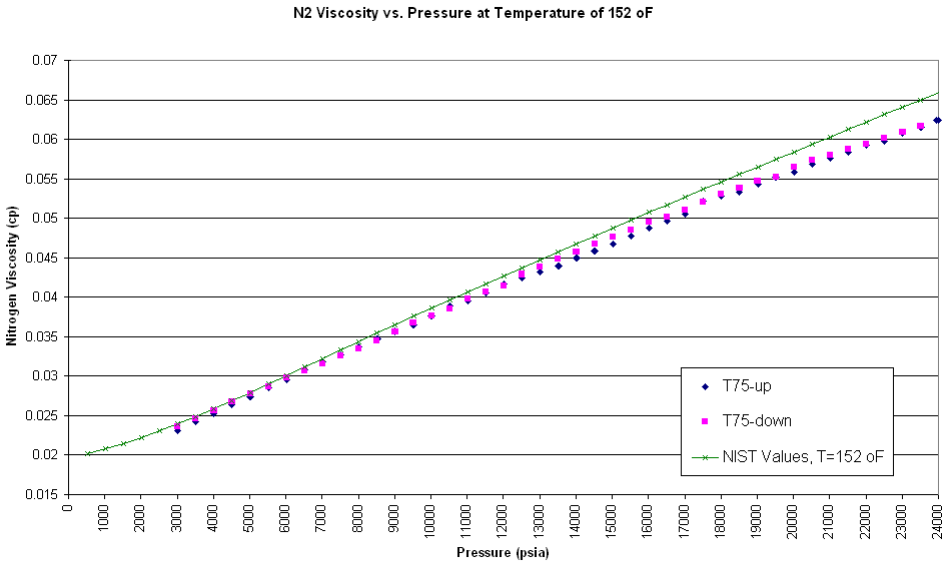

Figure A - 4. Nitrogen viscosity vs. pressure at 152 ^{o}F (Test 75)

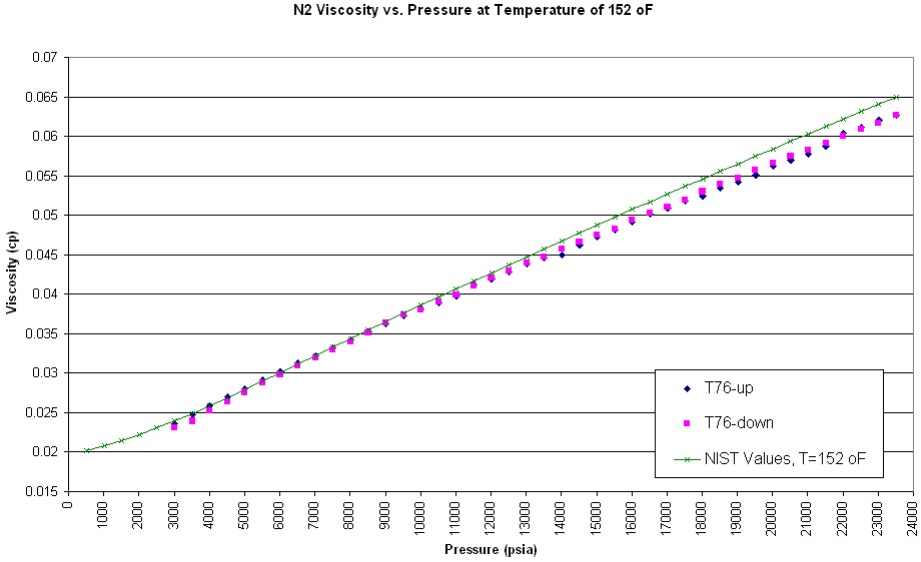

Figure A - 5. Nitrogen viscosity vs. pressure at 152 ^{o}F (Test 76)

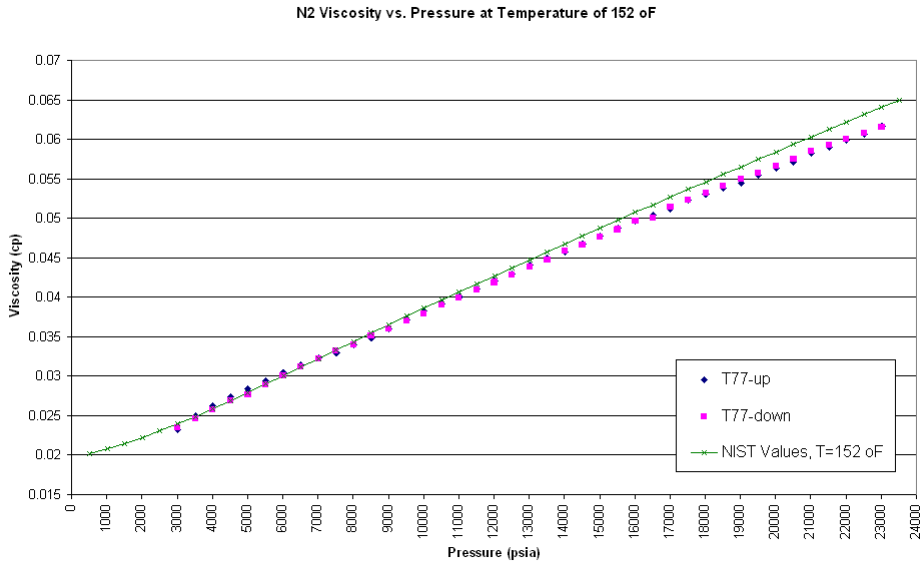

Figure A - 6. Nitrogen viscosity vs. pressure at 152 ^{o}F (Test 77)

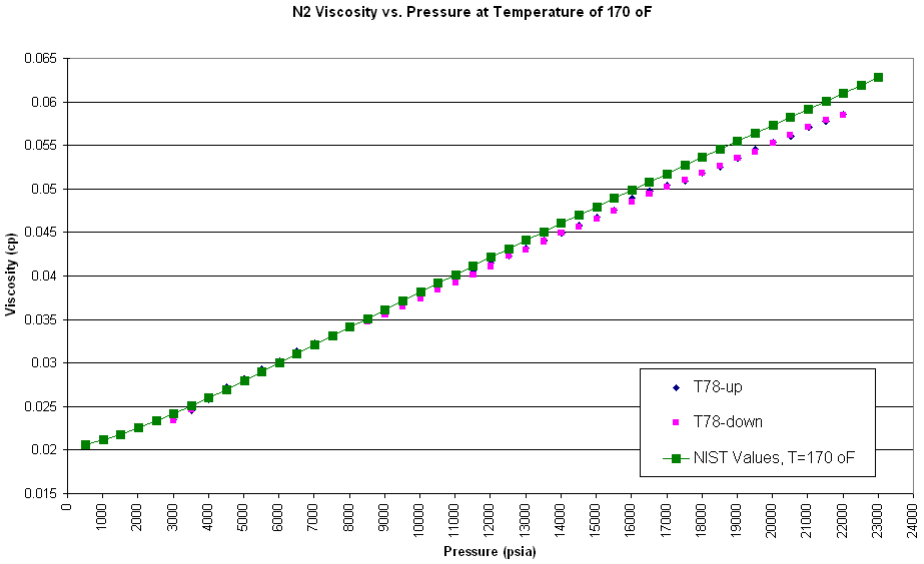

Figure A - 7. Nitrogen viscosity vs. pressure at 170 ^{o}F (Test 78)

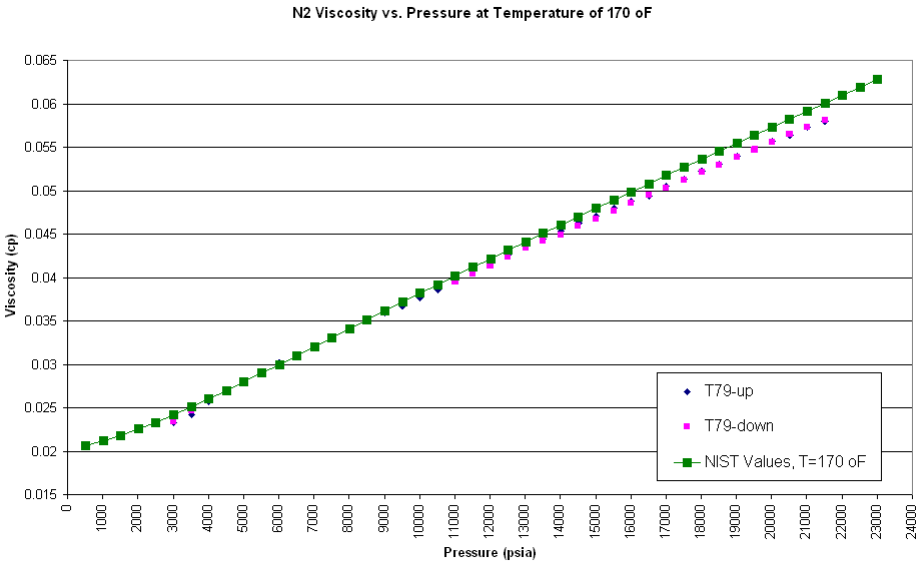

Figure A - 8. Nitrogen viscosity vs. pressure at 170 ^{o}F (Test 79)

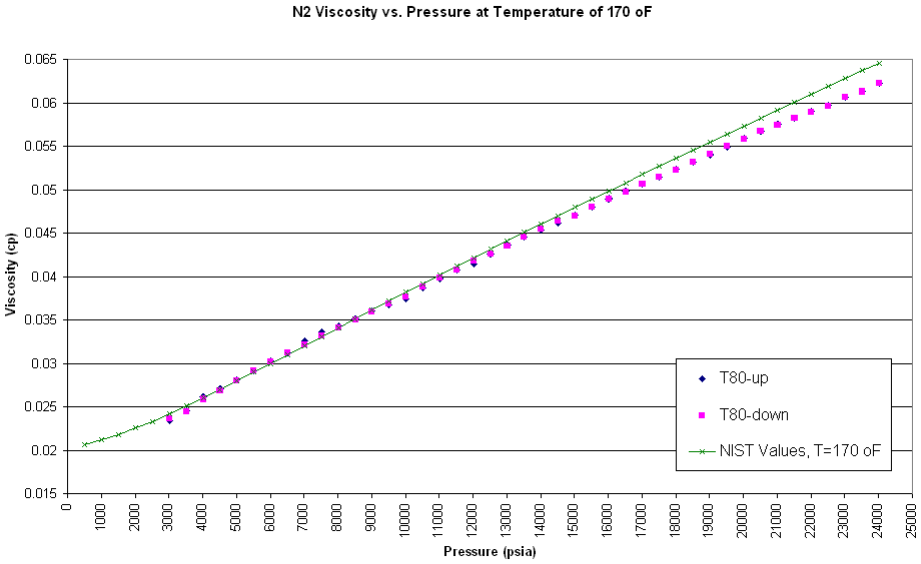

Figure A - 9. Nitrogen viscosity vs. pressure at 170 ^{o}F (Test 80)

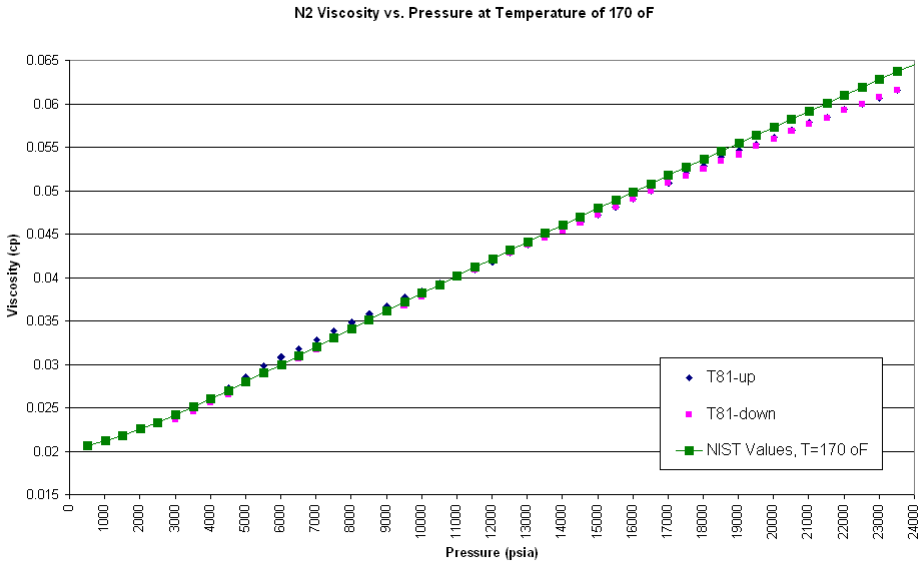

Figure A - 10. Nitrogen viscosity vs. pressure at 170 ^{o}F (Test 81)

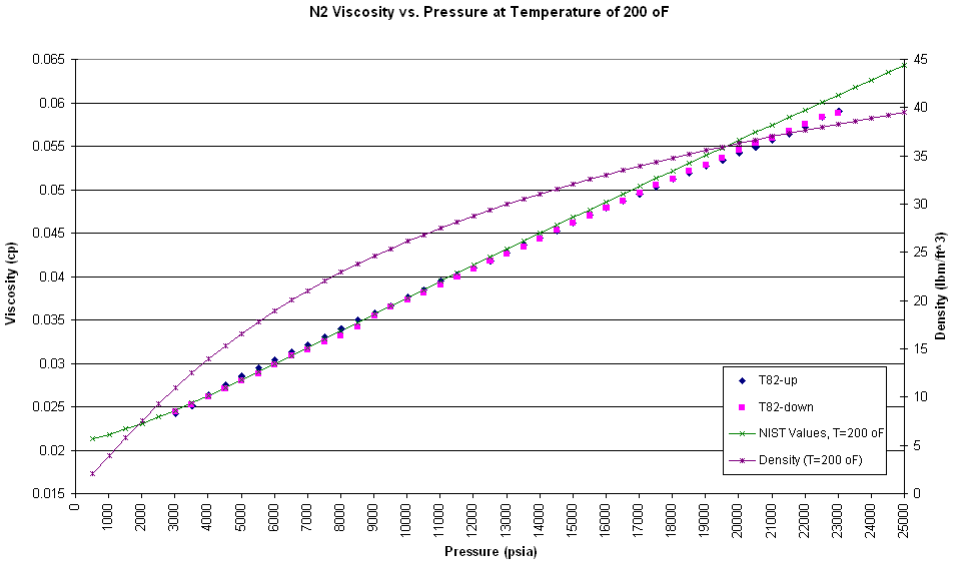

Figure A - 11. Nitrogen viscosity vs. pressure at 200 ^{o}F (Test 82)

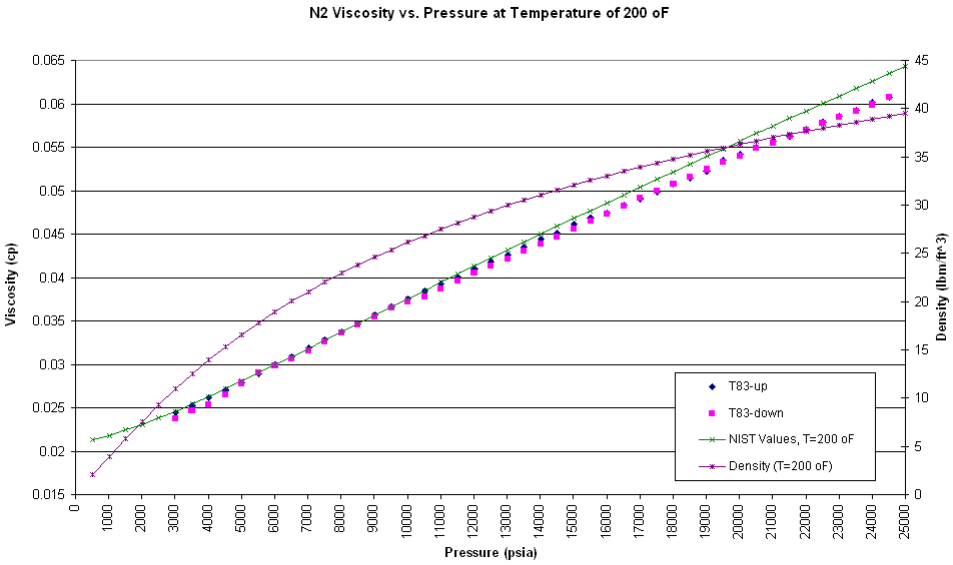

Figure A - 12. Nitrogen viscosity vs. pressure at 200 ^{o}F (Test 83)

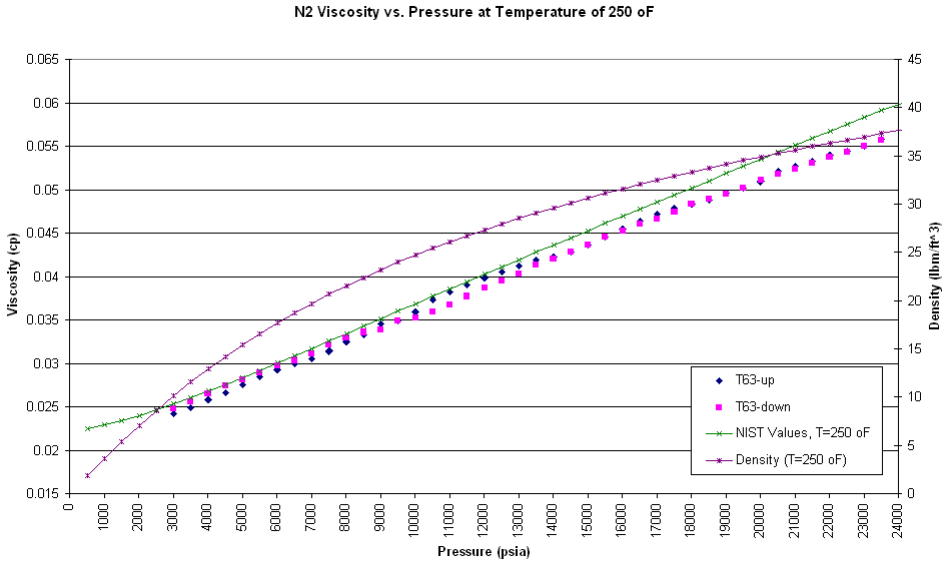

Figure A - 13. Nitrogen viscosity vs. pressure at 250 ^{o}F (Test 63)

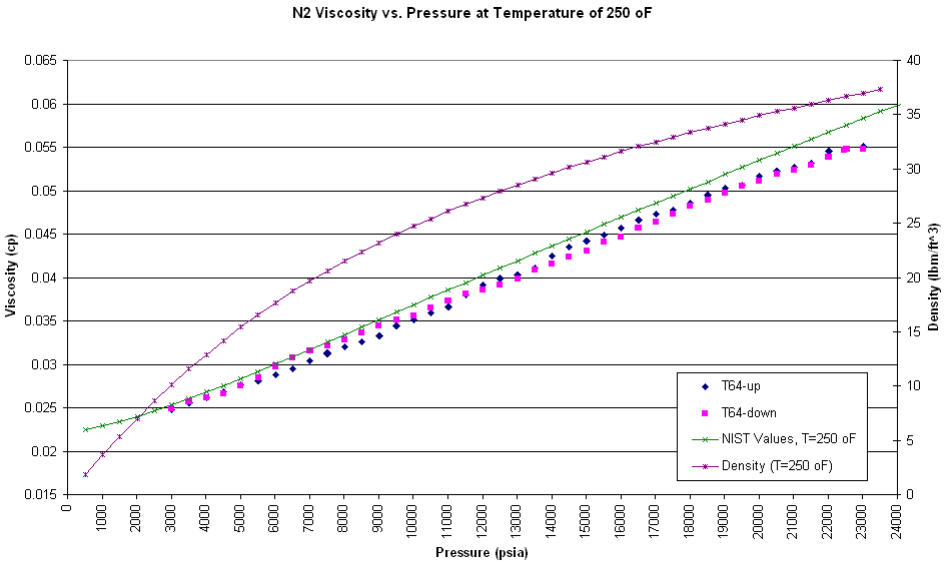

Figure A - 14. Nitrogen viscosity vs. pressure at 250 ^{o}F (Test 64)

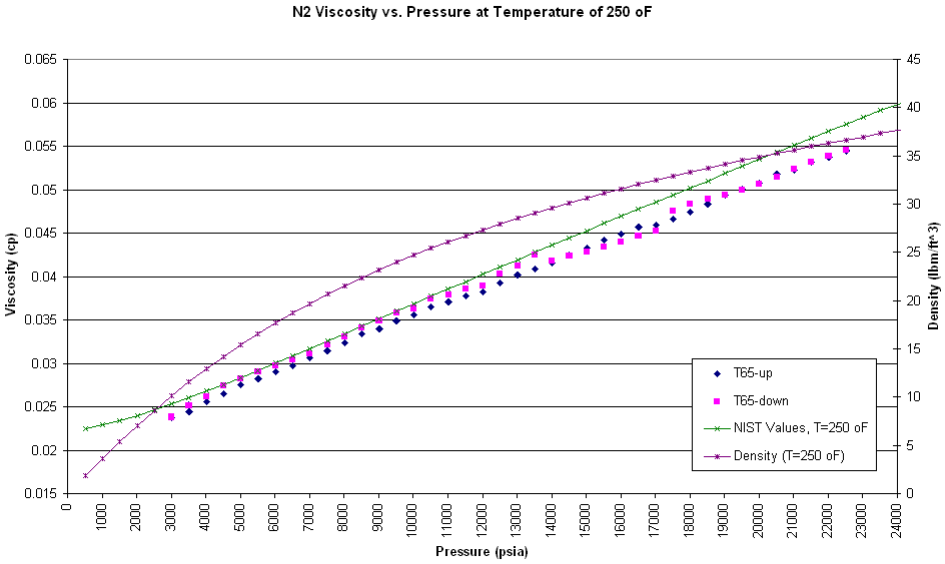

Figure A - 15. Nitrogen viscosity vs. pressure at 250 ^{o}F (Test 65)

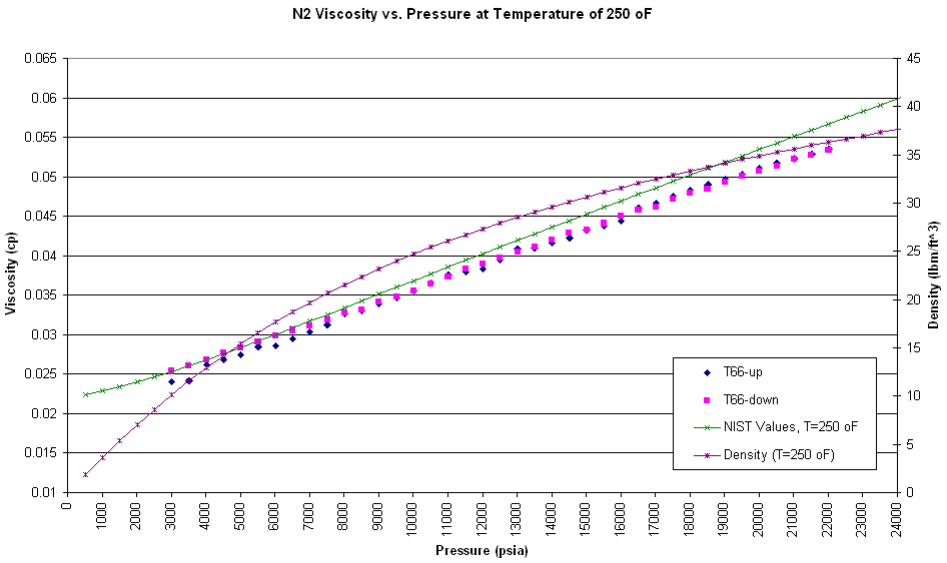

Figure A - 16. Nitrogen viscosity vs. pressure at 250 ^{o}F (Test 66)

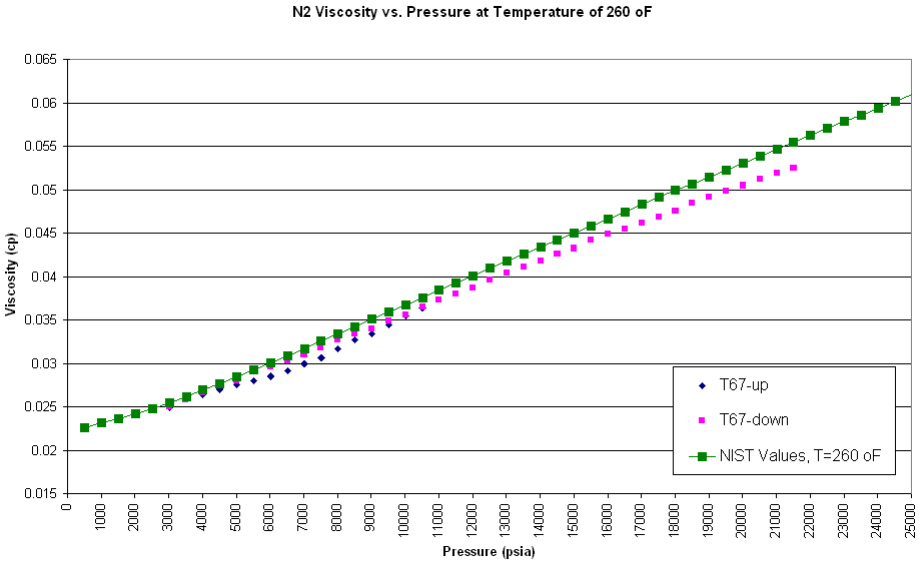

Figure A - 17. Nitrogen viscosity vs. pressure at 260 ^{o}F (Test 67)

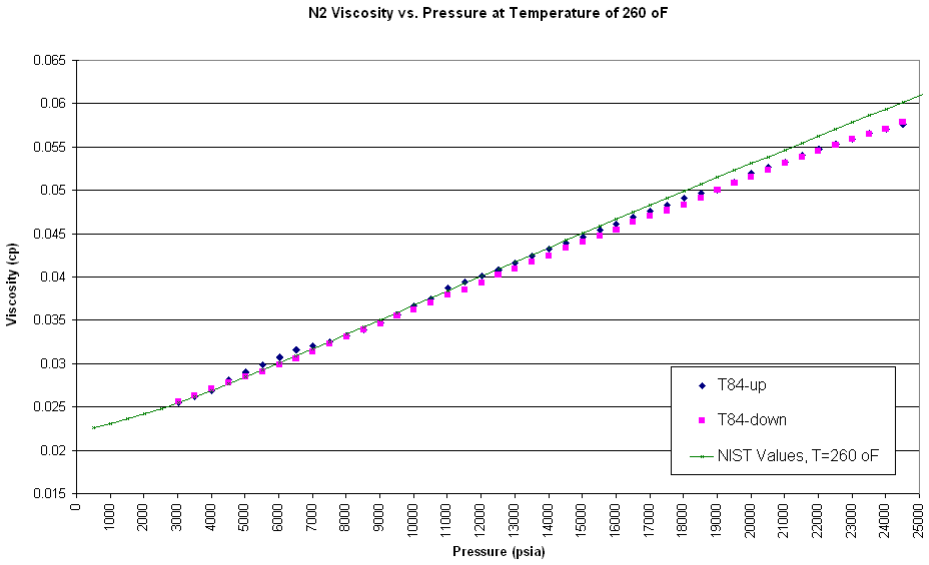

Figure A - 18. Nitrogen viscosity vs. pressure at 260 ^{o}F (Test 84)

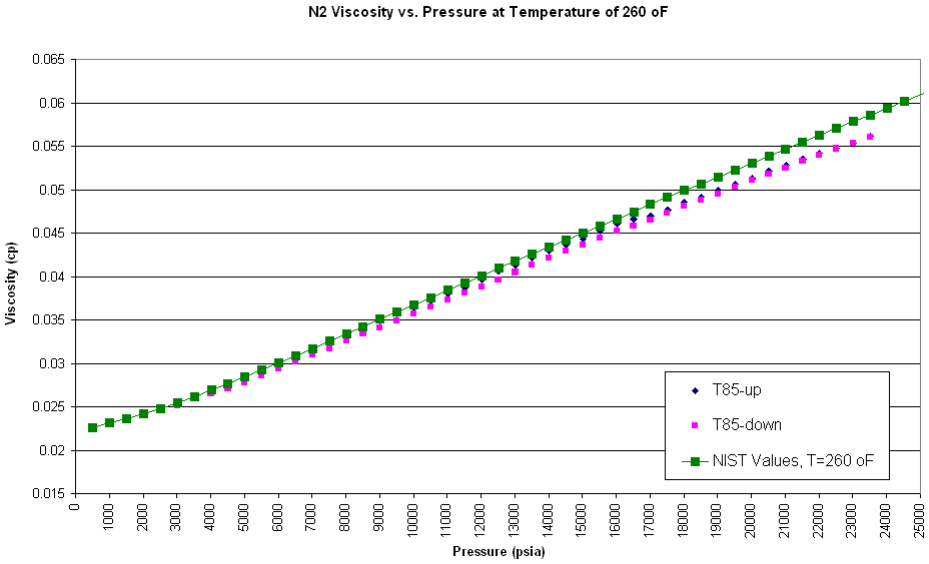

Figure A - 19. Nitrogen viscosity vs. pressure at 260 ^{o}F (Test 85)

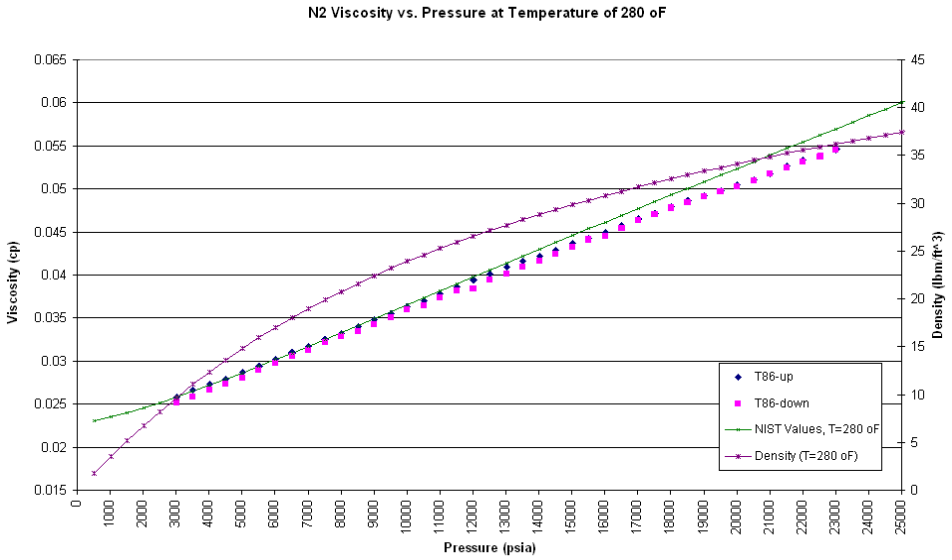

Figure A - 20. Nitrogen viscosity vs. pressure at 280 ^{o}F (Test 86)

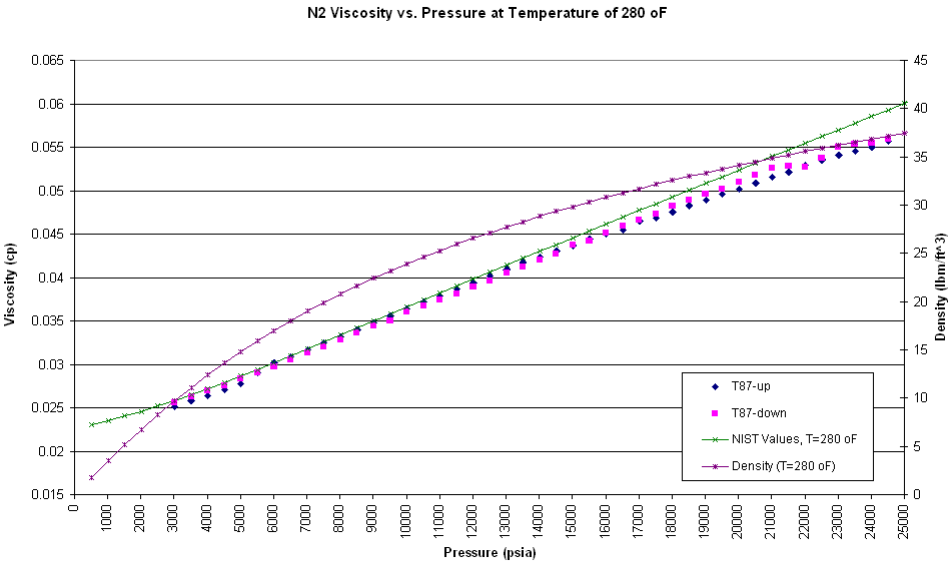

Figure A - 21. Nitrogen viscosity vs. pressure at 280 ^{o}F (Test 87)

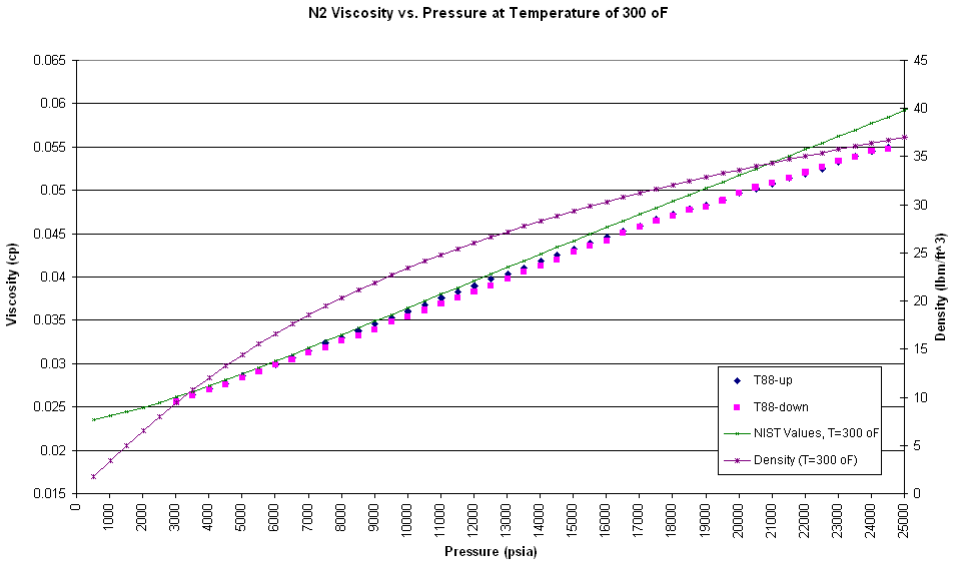

Figure A - 22. Nitrogen viscosity vs. pressure at 300 ^{o}F (Test 88)

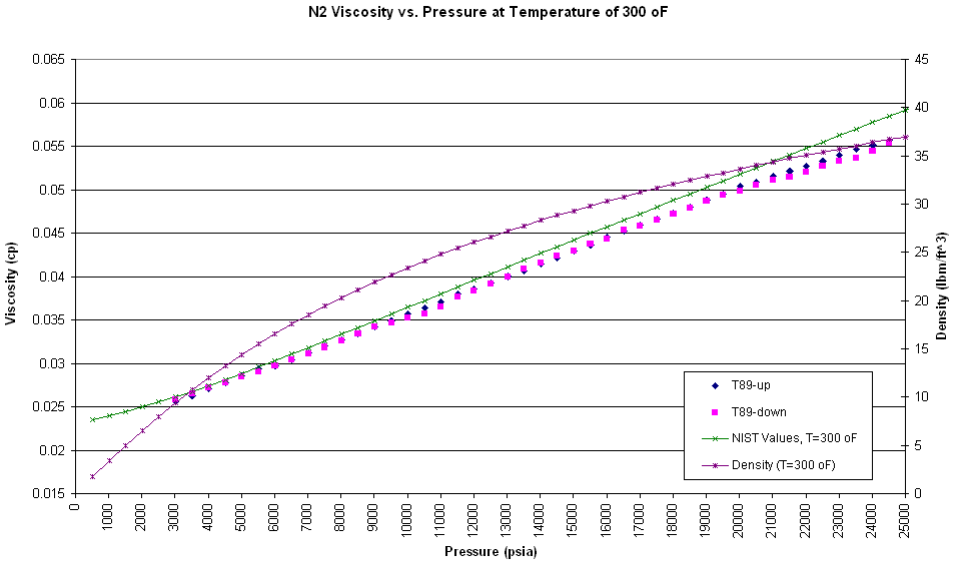

Figure A - 23. Nitrogen viscosity vs. pressure at 300 ^{o}F (Test 89)

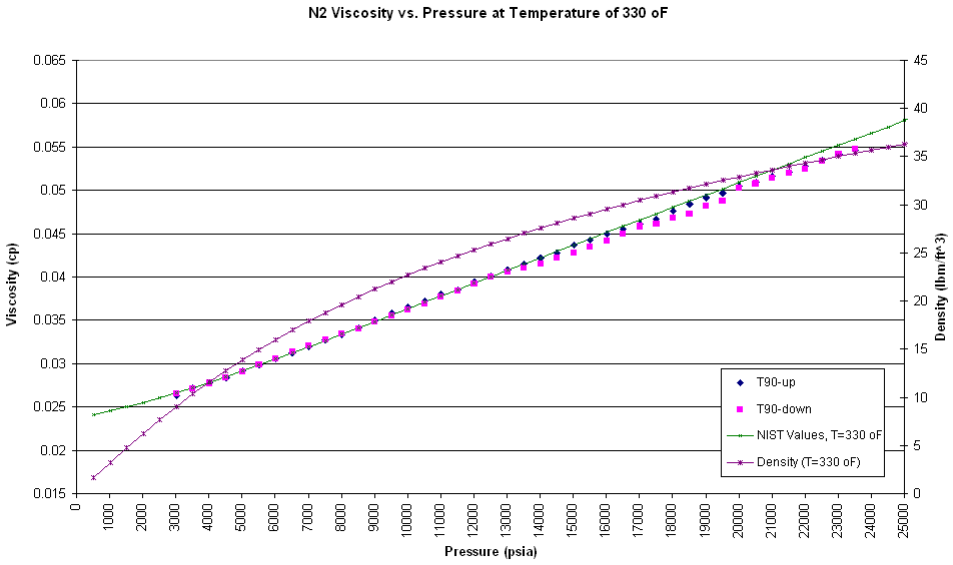

Figure A - 24. Nitrogen viscosity vs. pressure at 330 ^{o}F (Test 90)

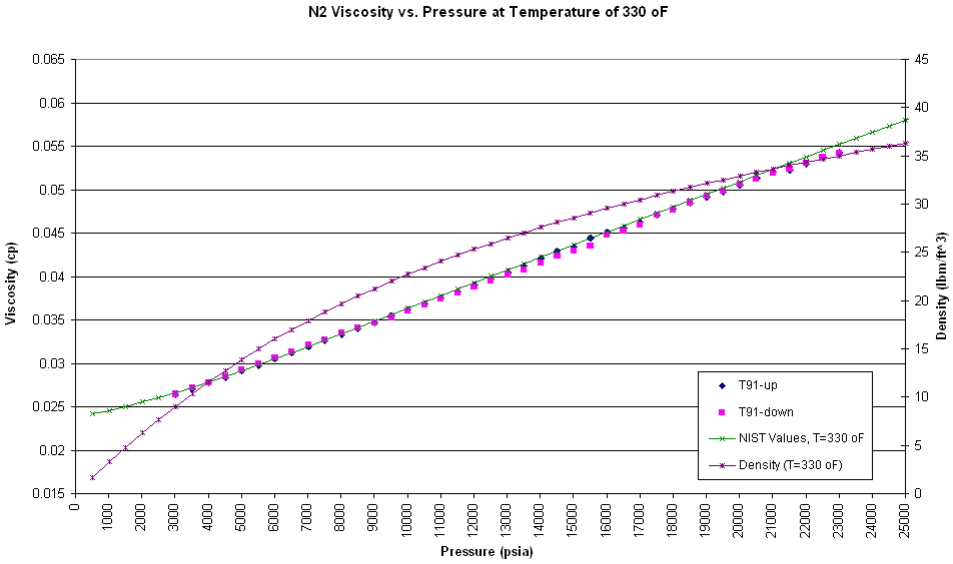

Figure A - 25. Nitrogen viscosity vs. pressure at 330 ^{o}F (Test 91)

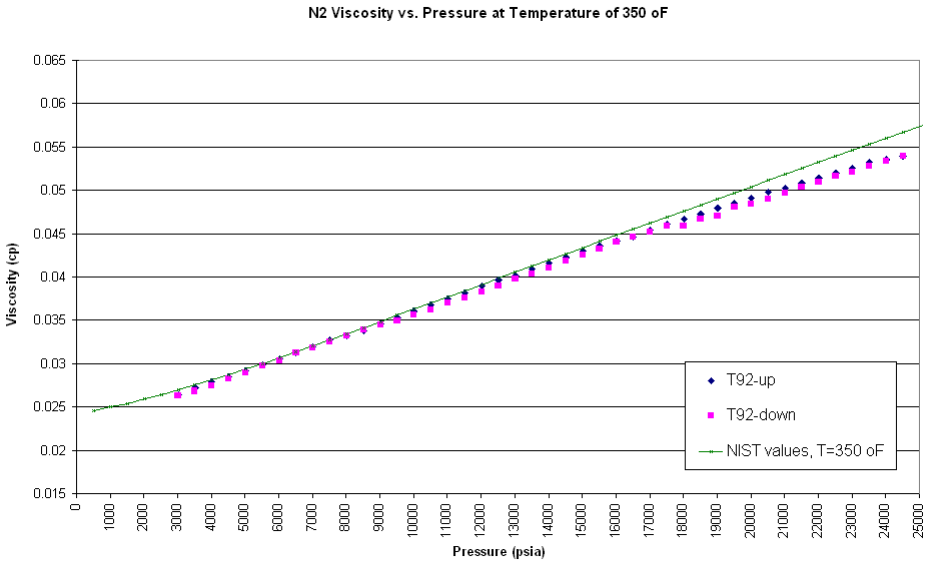

Figure A - 26. Nitrogen viscosity vs. pressure at 350 ^{o}F (Test 92)

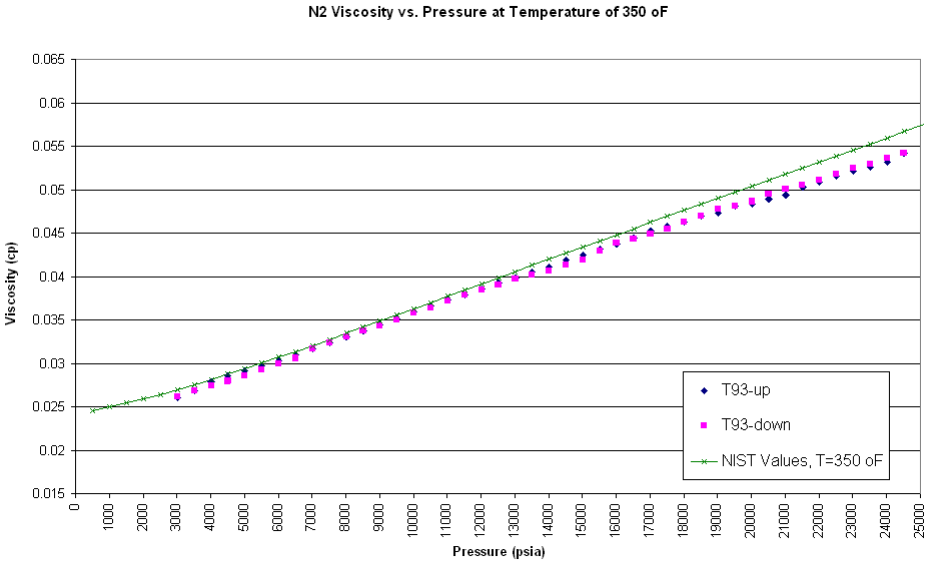

Figure A - 27. Nitrogen viscosity vs. pressure at 350 ^{o}F (Test 93)

APPENDIX B

Comparison of Methane Viscosity from This Study with NIST Value

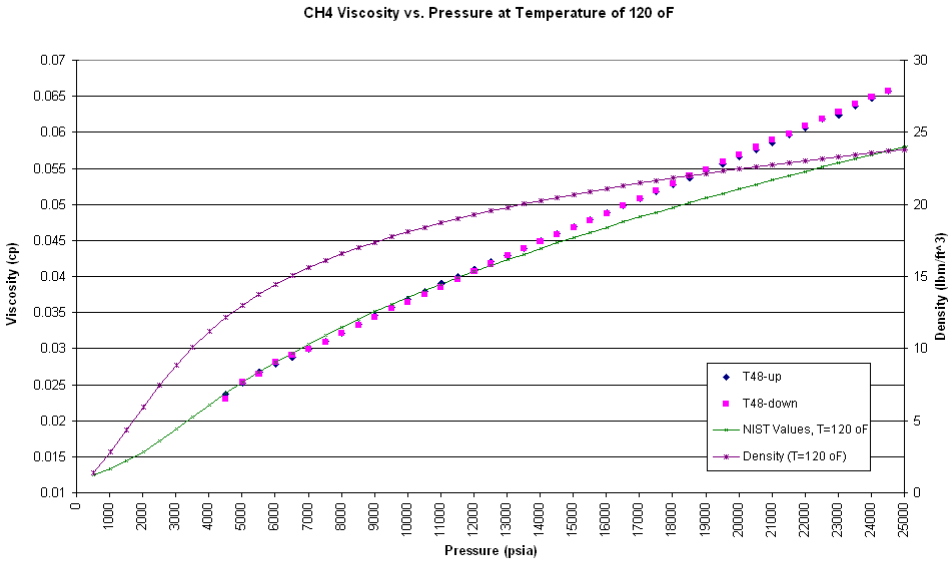

Figure B - 1. Methane viscosity vs. pressure at 120 ^{o}F (Test 48)

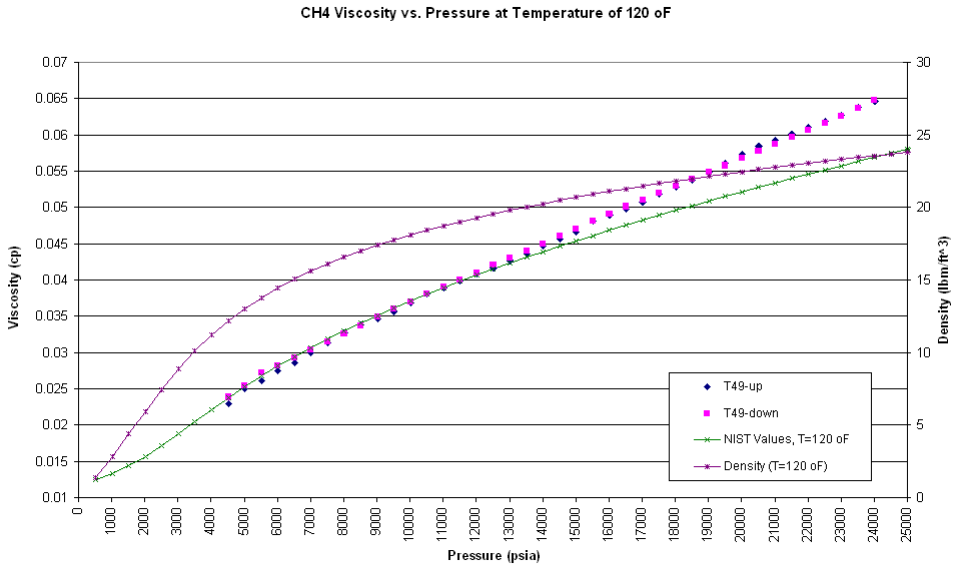

Figure B - 2. Methane viscosity vs. pressure at 120 ^{o}F (Test 49)

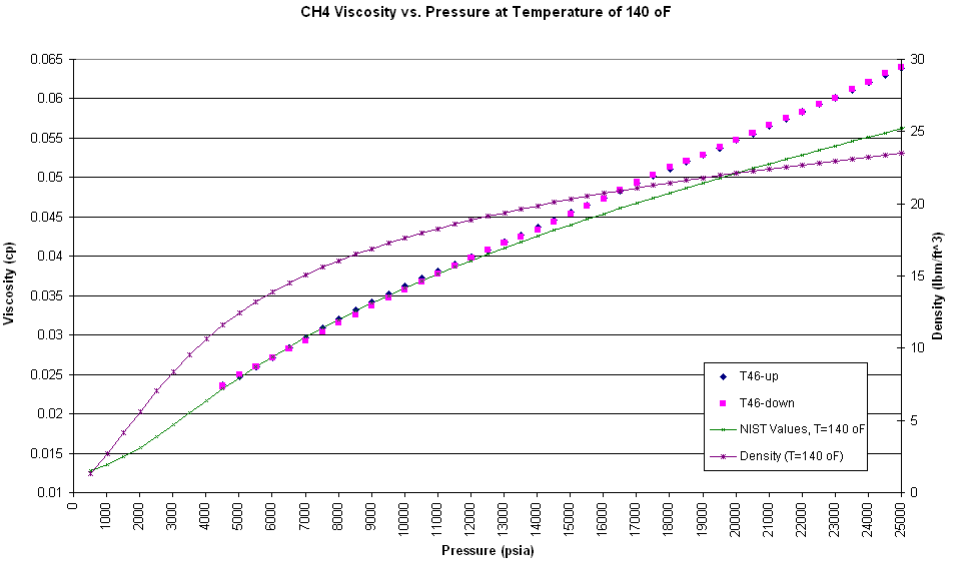

Figure B - 3. Methane viscosity vs. pressure at 140 ^{o}F (Test 46)

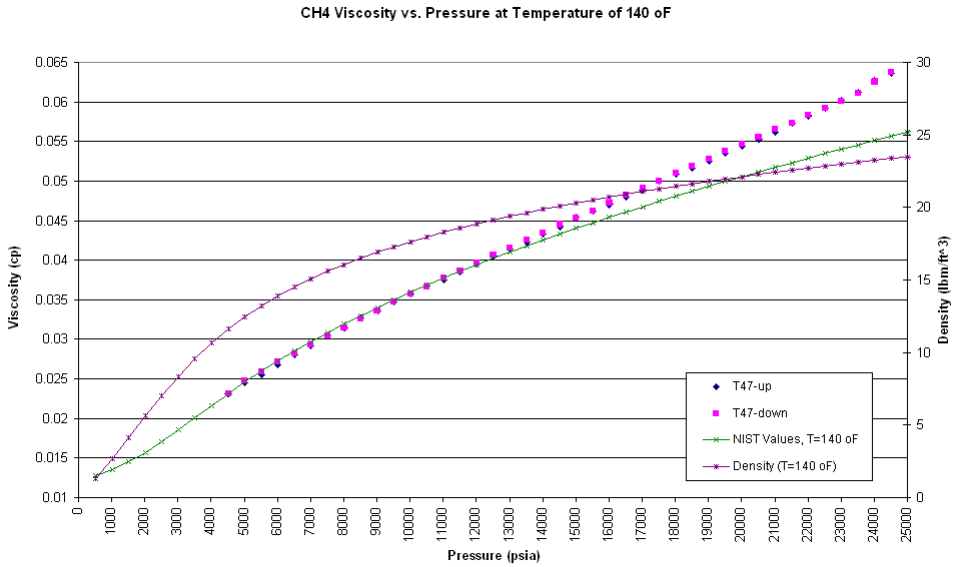

Figure B - 4. Methane viscosity vs. pressure at 140 ^{o}F (Test 47)

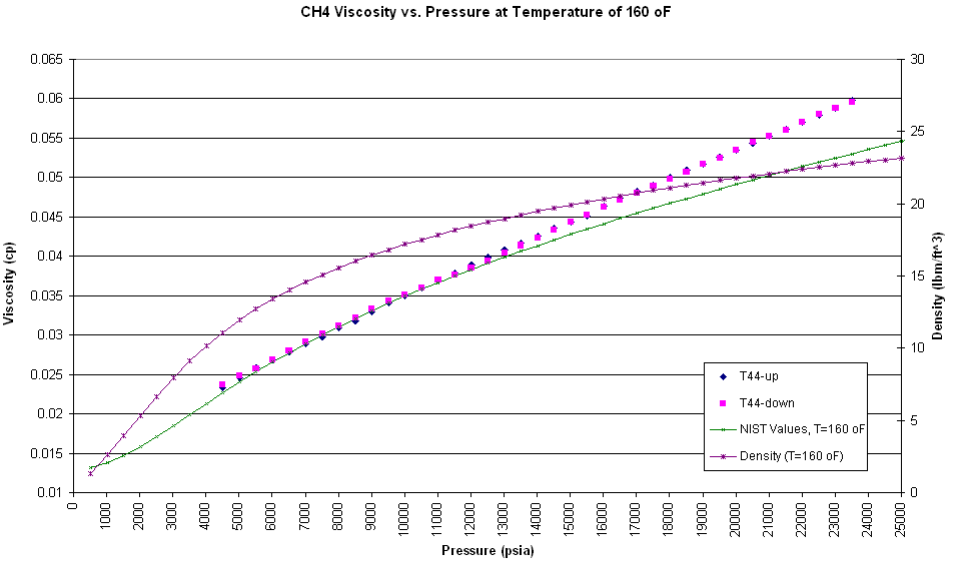

Figure B - 5. Methane viscosity vs. pressure at 160 ^{o}F (Test 44)

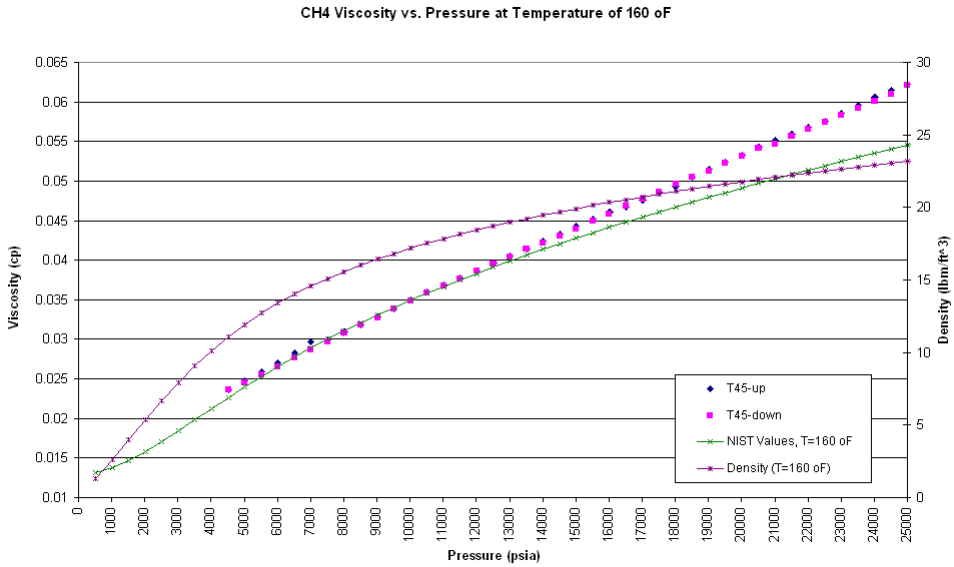

Figure B - 6. Methane viscosity vs. pressure at 160 ^{o}F (Test 45)

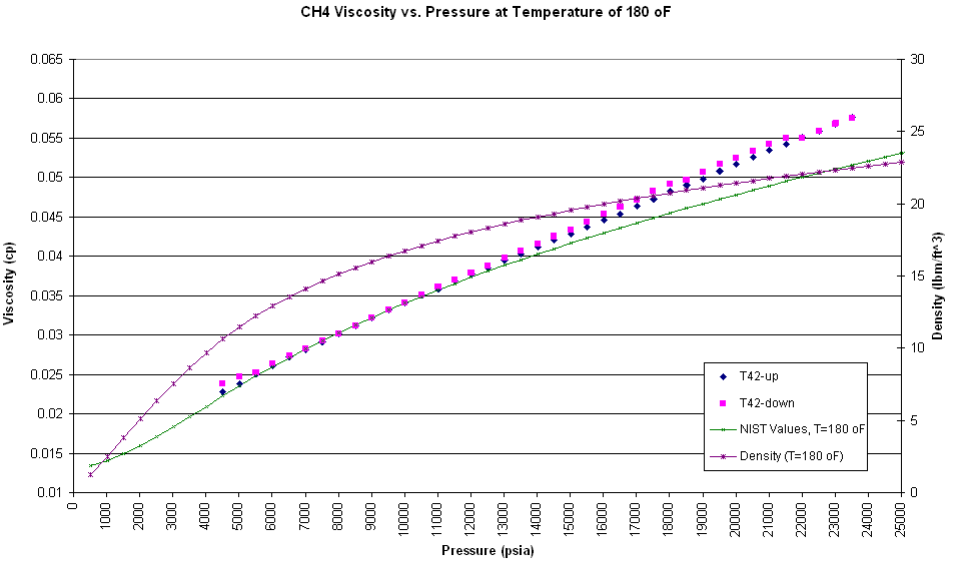

Figure B - 7. Methane viscosity vs. pressure at 180 ^{o}F (Test 42)

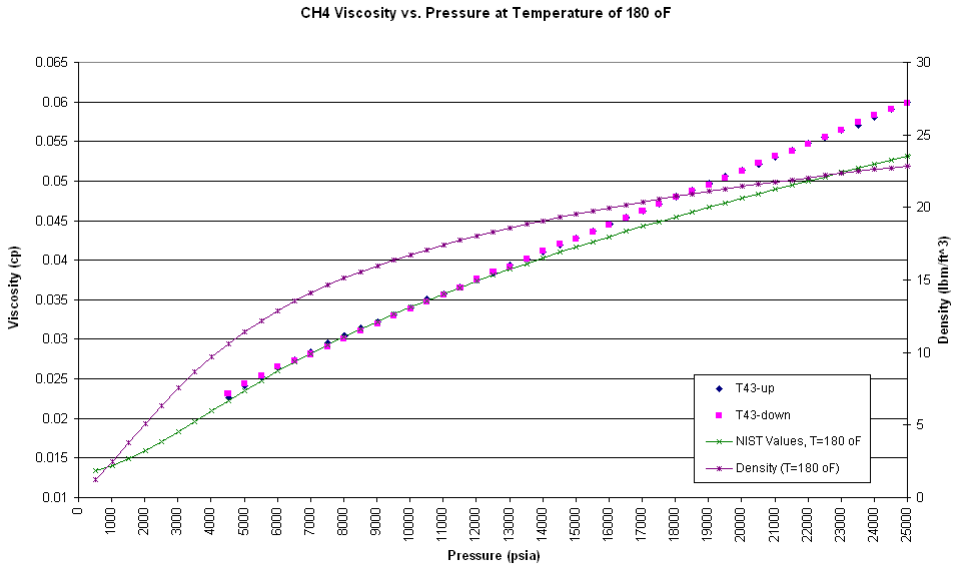

Figure B - 8. Methane viscosity vs. pressure at 180 ^{o}F (Test 43)

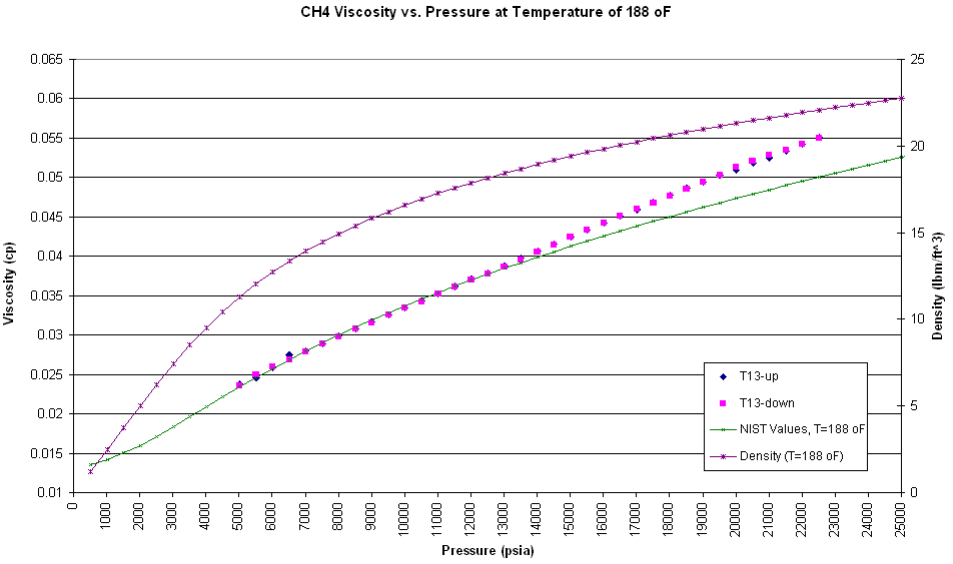

Figure B - 9. Methane viscosity vs. pressure at 188 ^{o}F (Test 13)

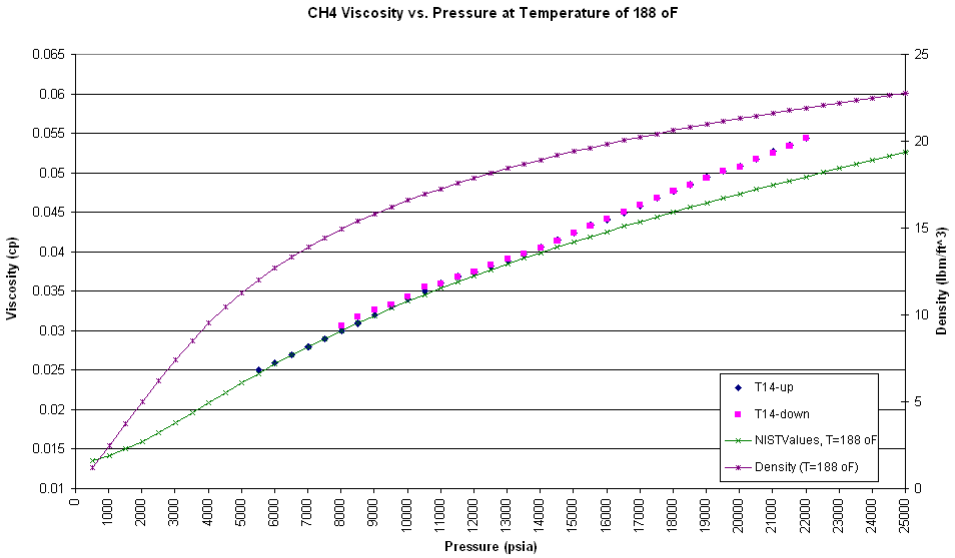

Figure B - 10. Methane viscosity vs. pressure at 188 ^{o}F (Test 14)

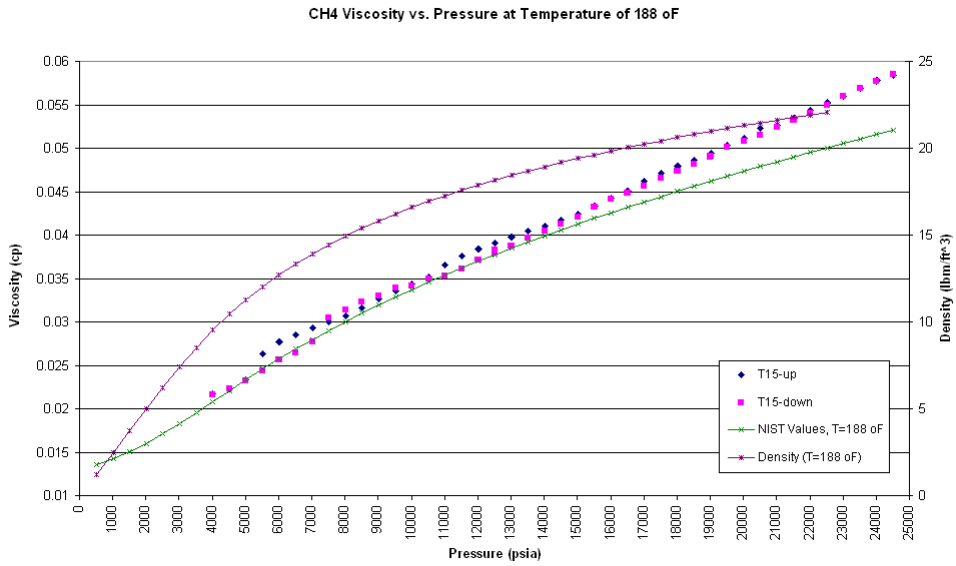

Figure B - 11. Methane viscosity vs. pressure at 188 ^{o}F (Test 15)

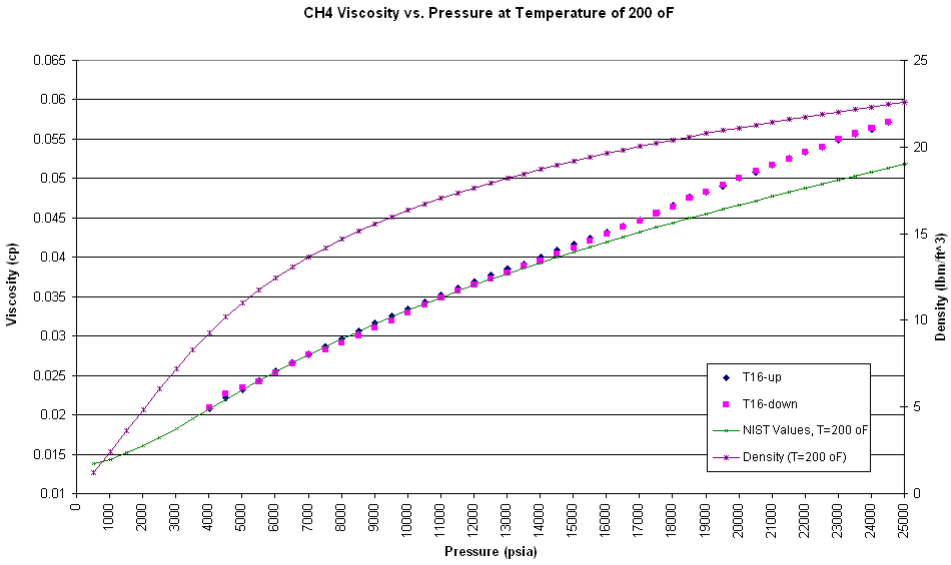

Figure B - 12. Methane viscosity vs. pressure at 200 ^{o}F (Test 16)

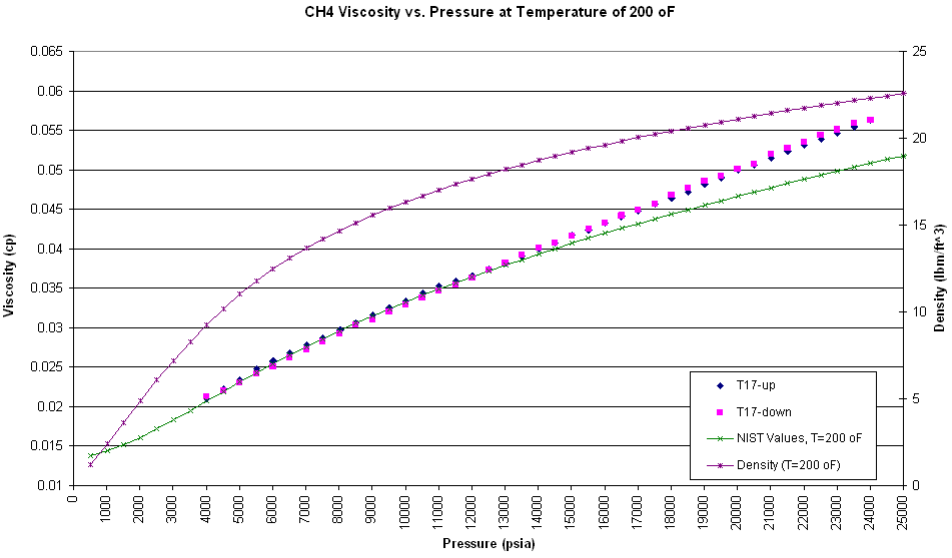

Figure B - 13. Methane viscosity vs. pressure at 200 ^{o}F (Test 17)

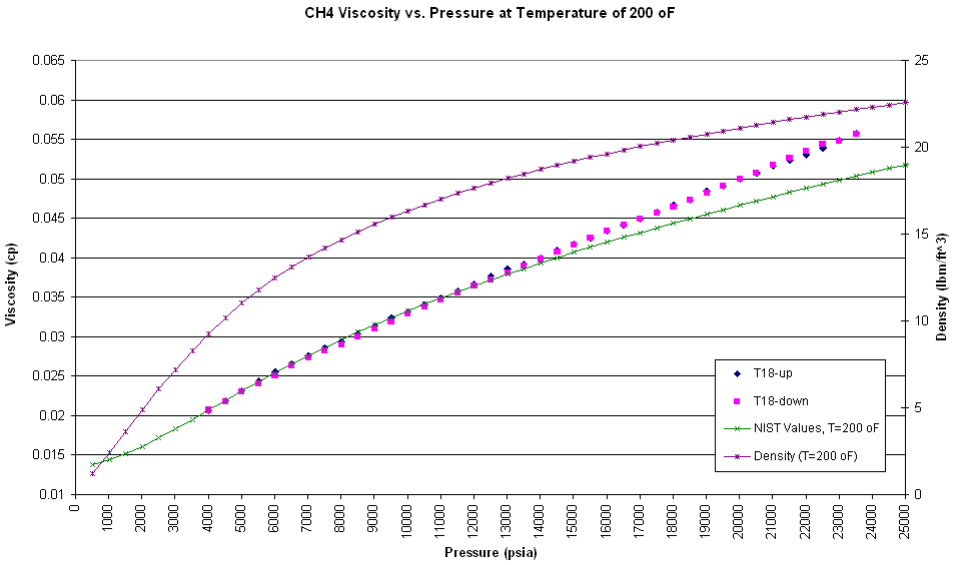

Figure B - 14. Methane viscosity vs. pressure at 200 ^{o}F (Test 18)

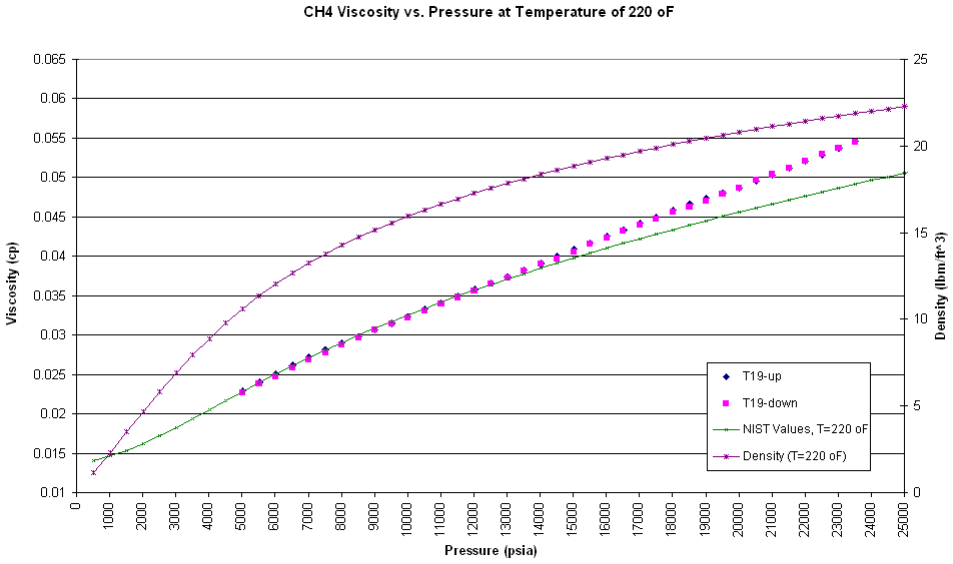

Figure B - 15. Methane viscosity vs. pressure at 220 ^{o}F (Test 19)

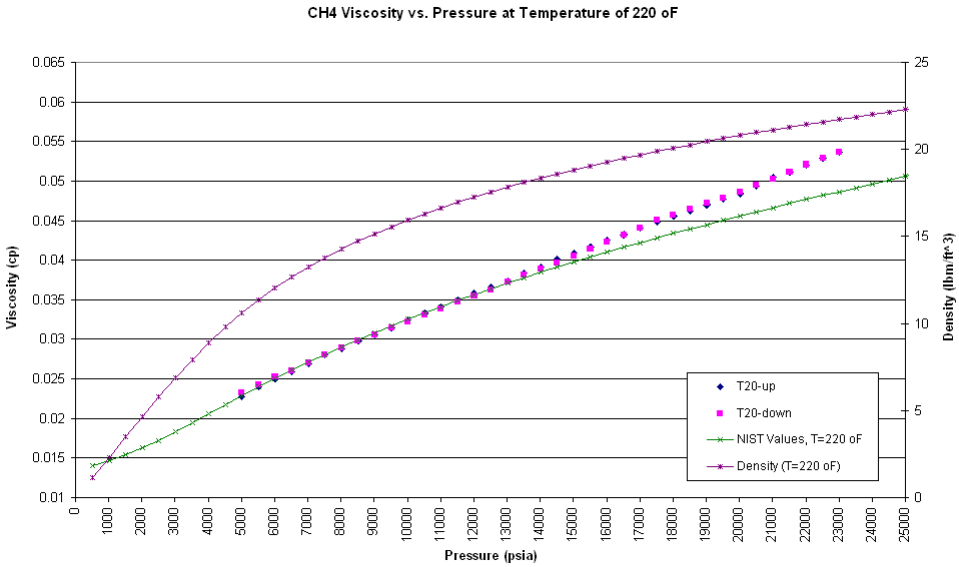

Figure B - 16. Methane viscosity vs. pressure at 220 ^{o}F (Test 20)

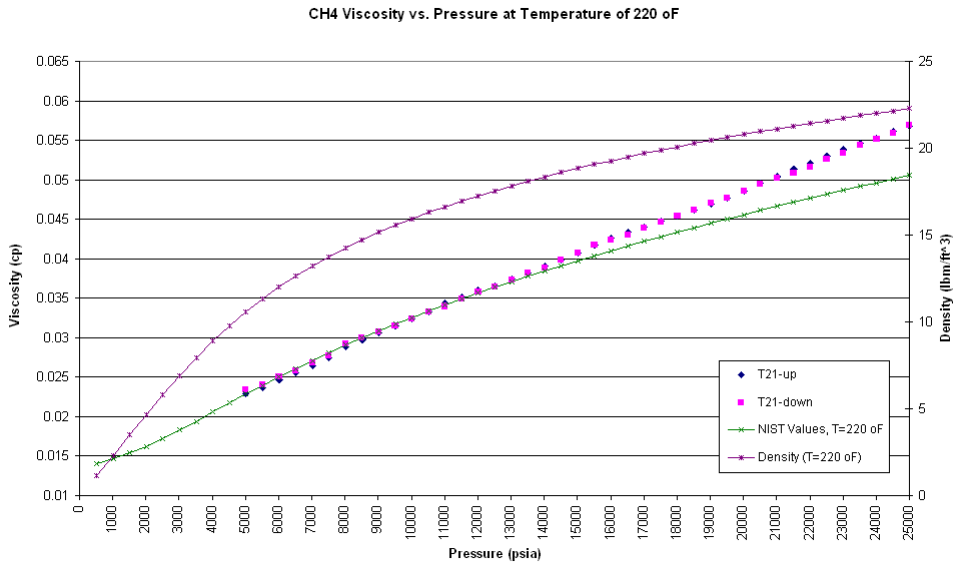

Figure B - 17. Methane viscosity vs. pressure at 220 ^{o}F (Test 21)

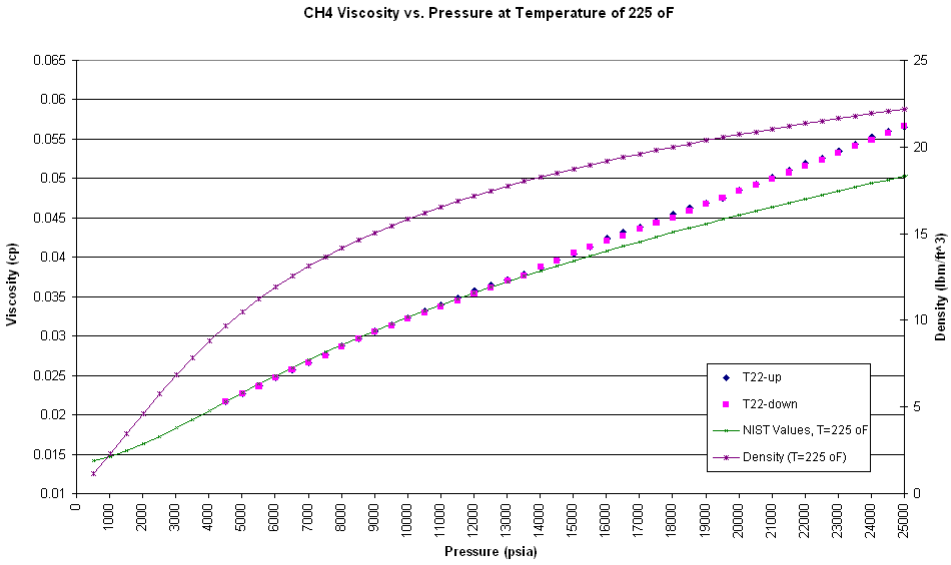

Figure B - 18. Methane viscosity vs. pressure at 225 ^{o}F (Test 22)

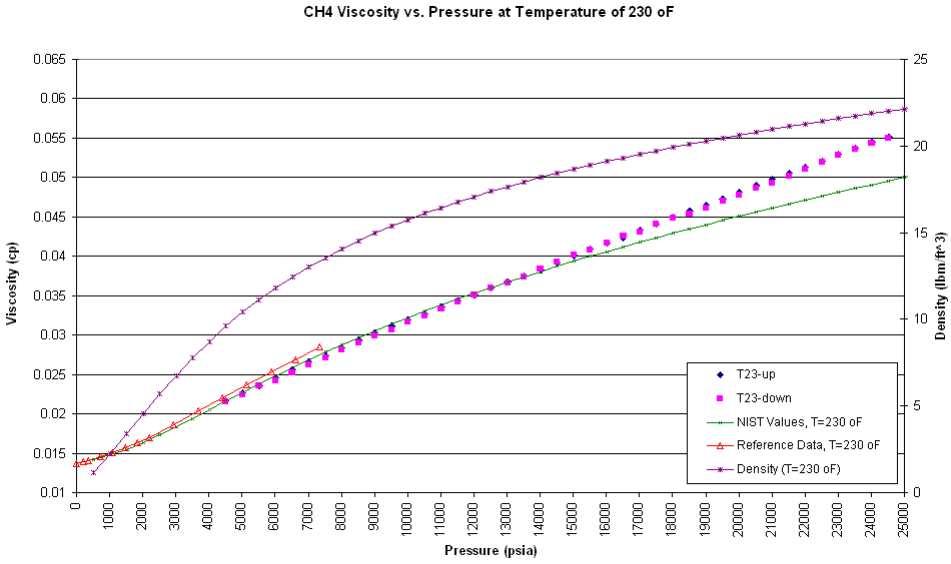

Figure B - 19. Methane viscosity vs. pressure at 230 ^{o}F (Test 23)

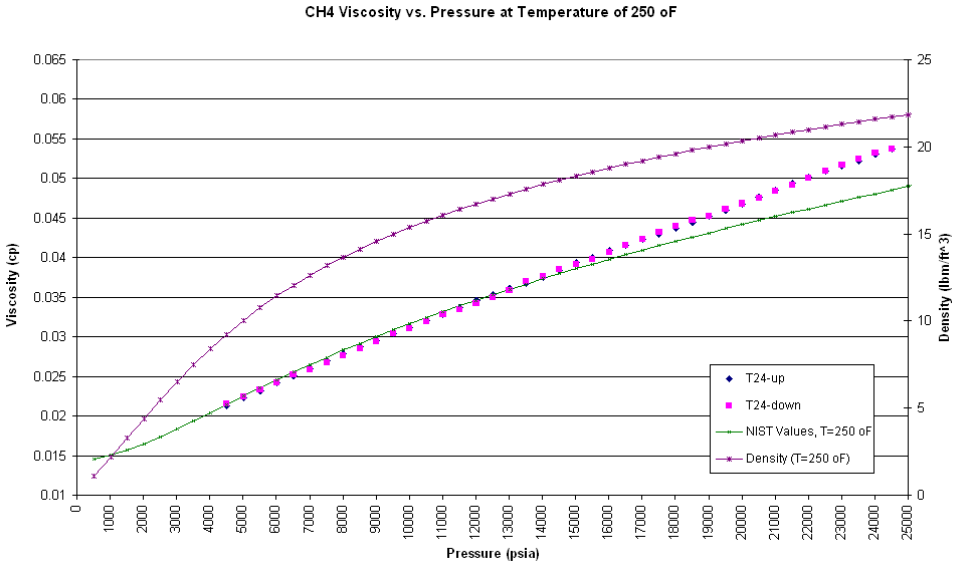

Figure B - 20. Methane viscosity vs. pressure at 250 ^{o}F (Test 24)

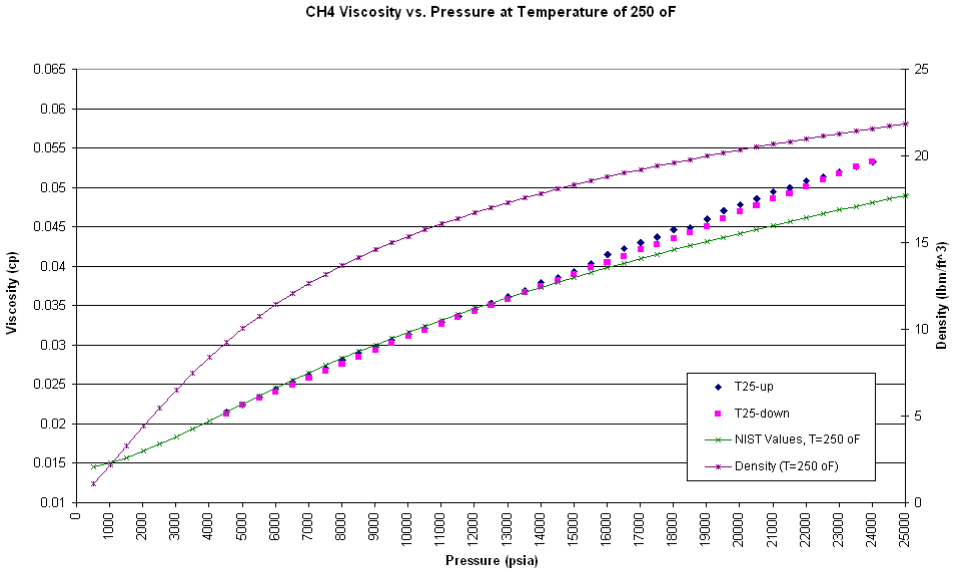

Figure B - 21. Methane viscosity vs. pressure at 250 ^{o}F (Test 25)

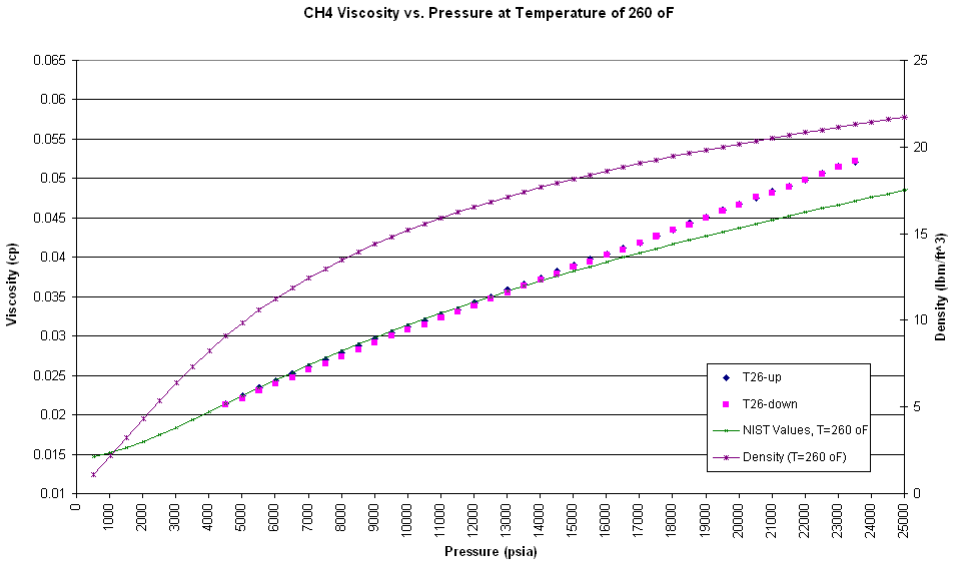

Figure B - 22. Methane viscosity vs. pressure at 260 ^{o}F (Test 26)

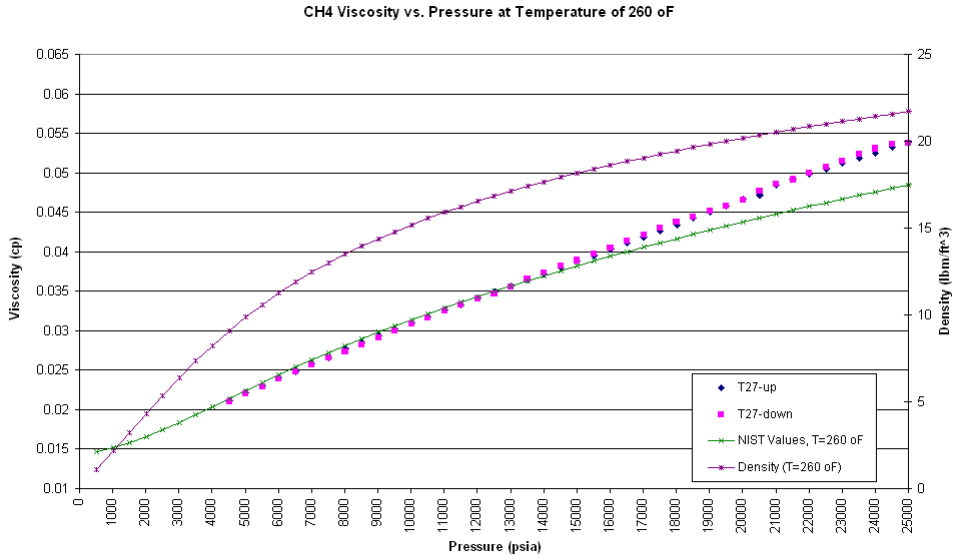

Figure B - 23. Methane viscosity vs. pressure at 260 ^{o}F (Test 27)

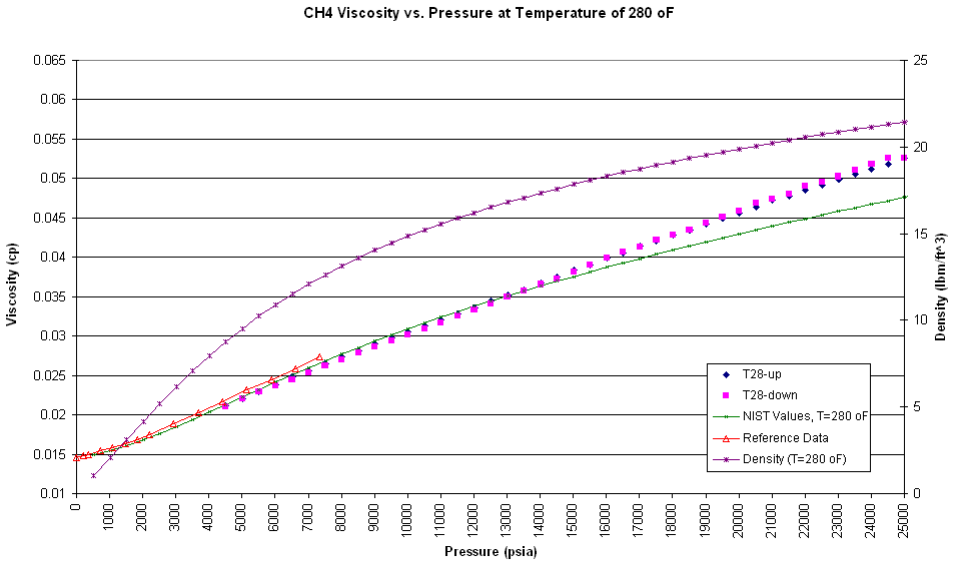

Figure B - 24. Methane viscosity vs. pressure at 280 ^{o}F (Test 28)

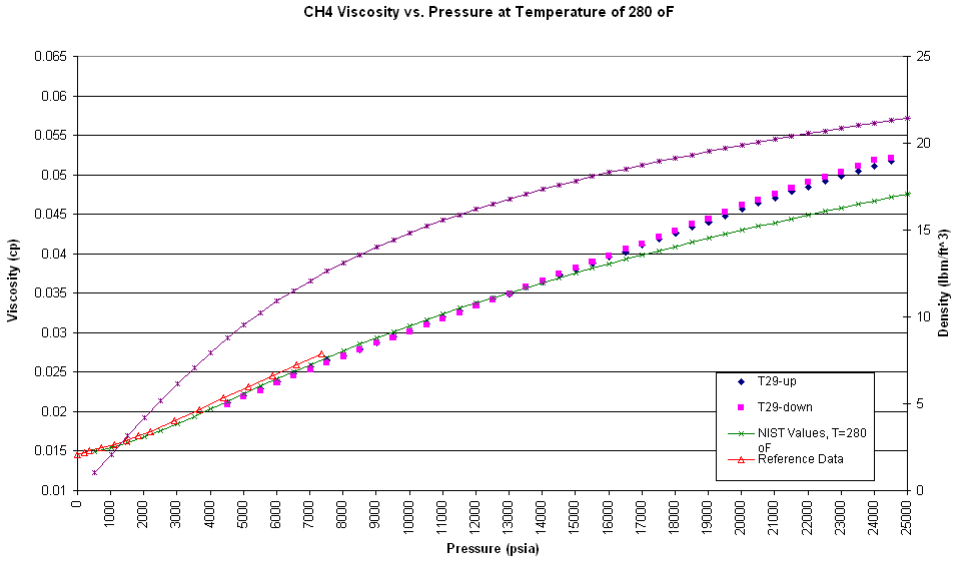

Figure B - 25. Methane viscosity vs. pressure at 280 ^{o}F (Test 29)

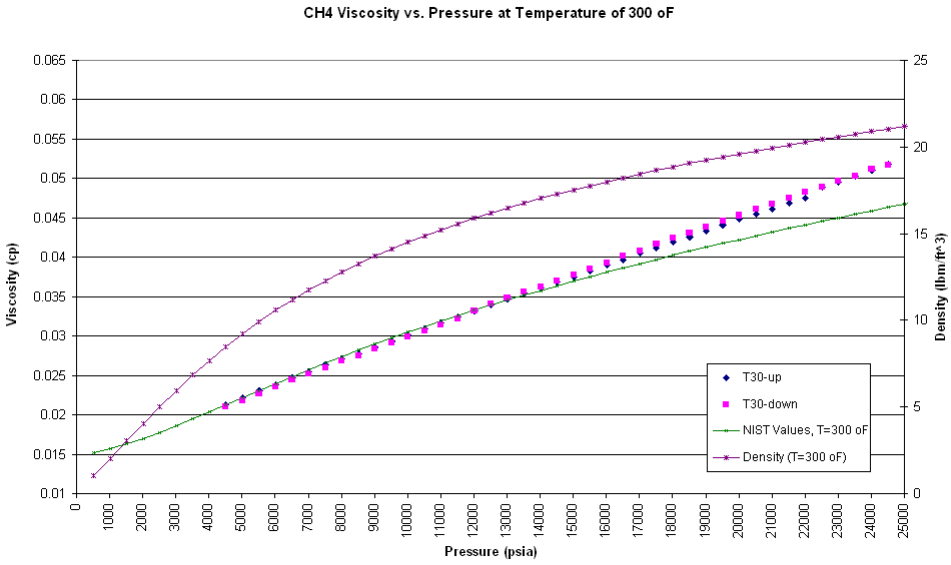

Figure B - 26. Methane viscosity vs. pressure at 300 ^{o}F (Test 30)

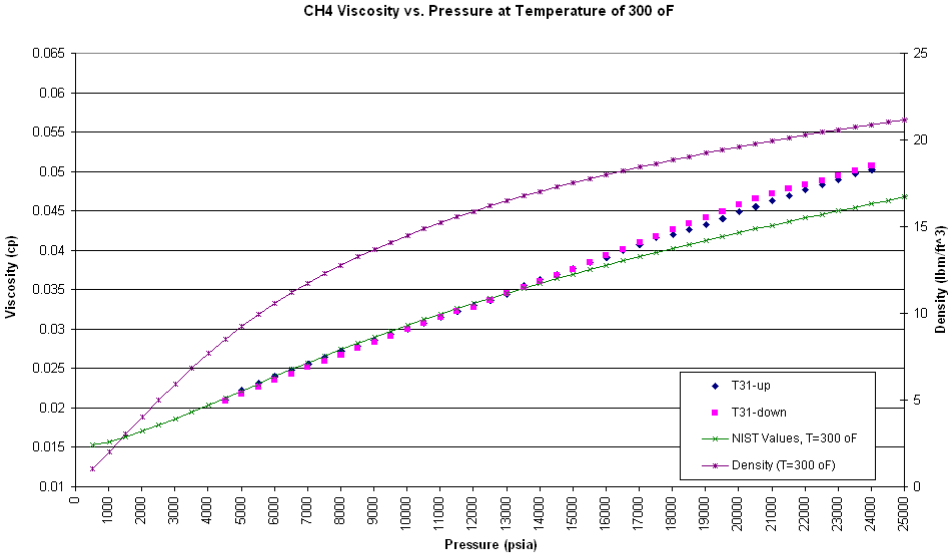

Figure B - 27. Methane viscosity vs. pressure at 300 ^{o}F (Test 31)

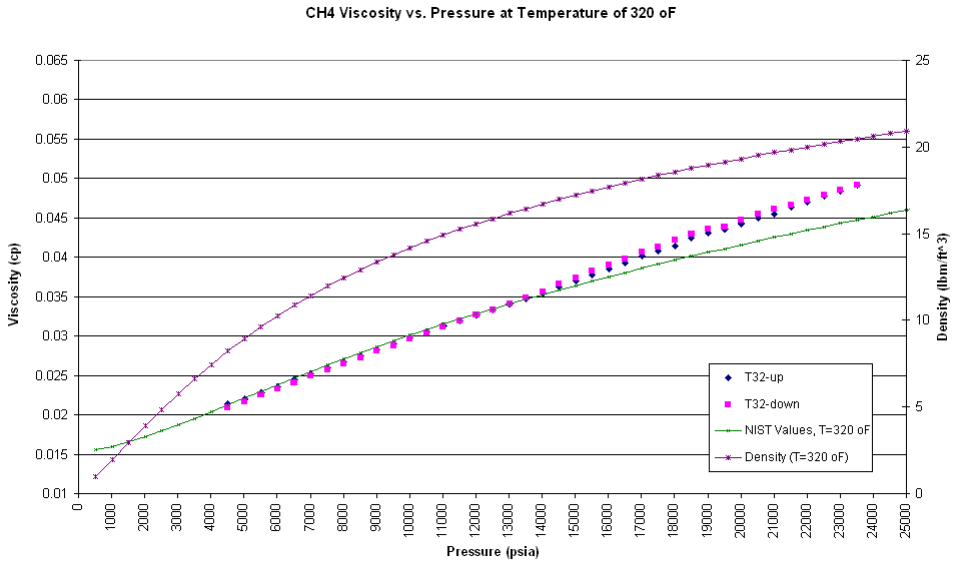

Figure B - 28. Methane viscosity vs. pressure at 320 ^{o}F (Test 32)

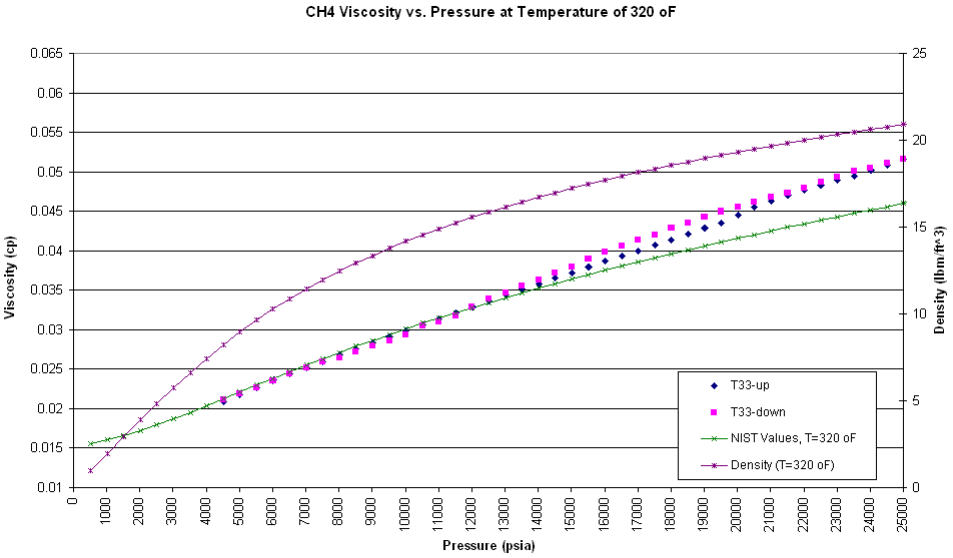

Figure B - 29. Methane viscosity vs. pressure at 320 ^{o}F (Test 33)

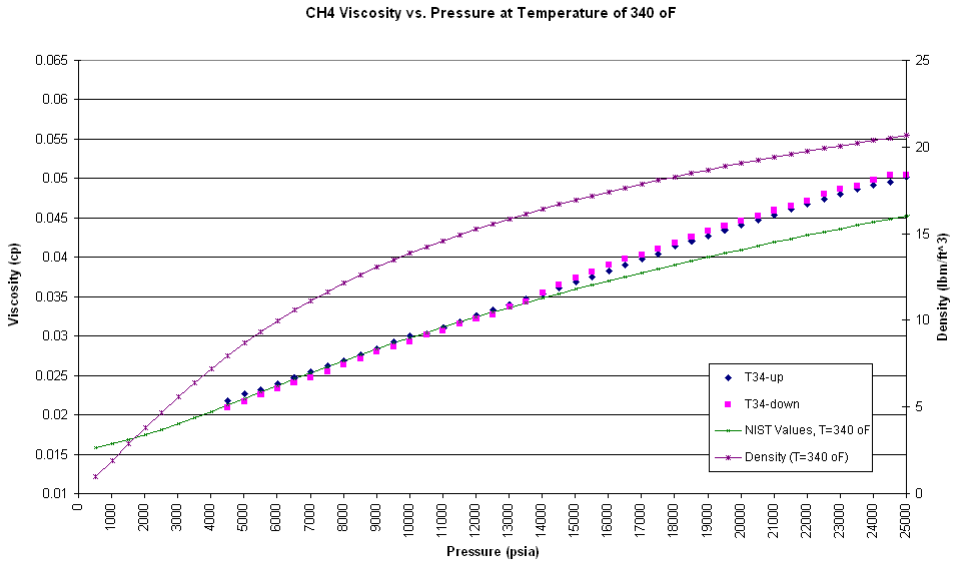

Figure B - 30. Methane viscosity vs. pressure at 340 ^{o}F (Test 34)

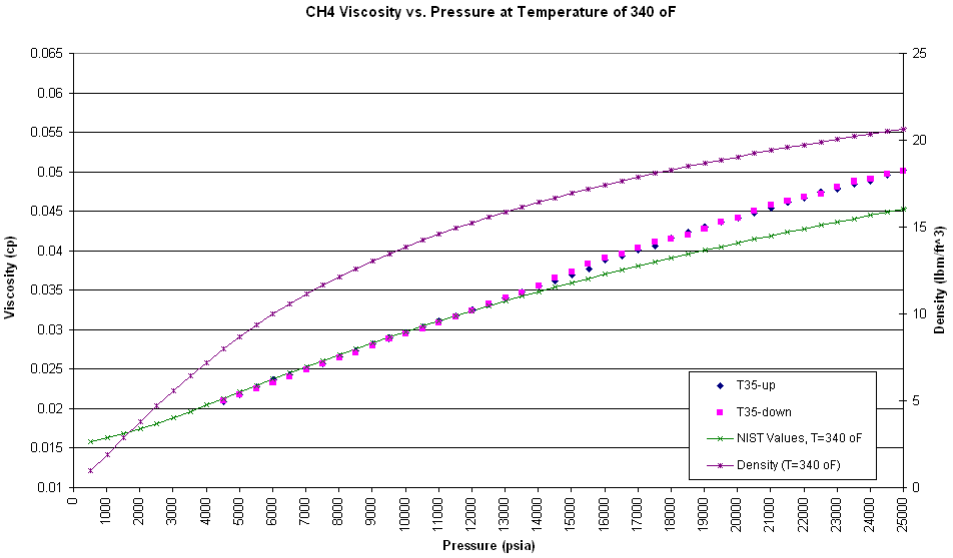

Figure B - 31. Methane viscosity vs. pressure at 340 ^{o}F (Test 35)

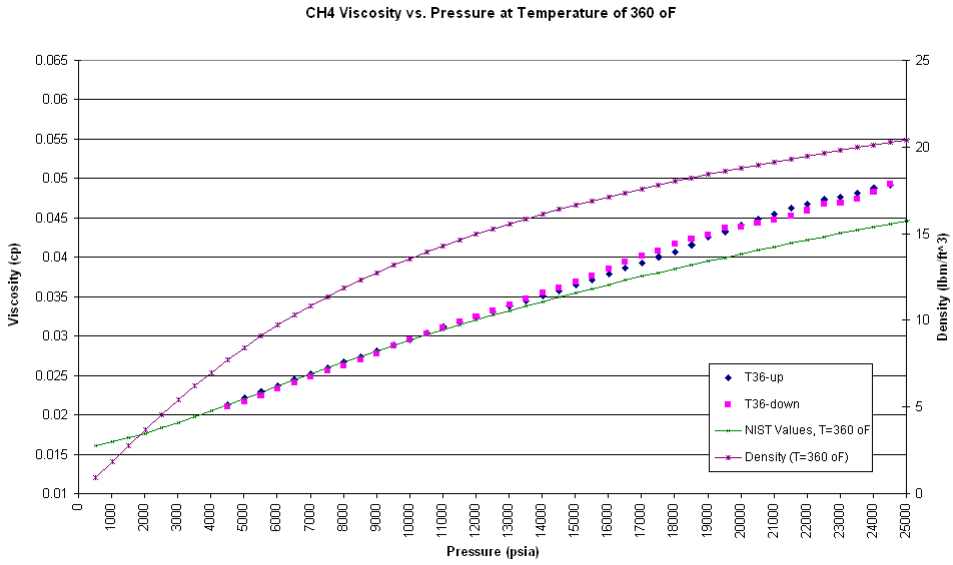

Figure B - 32. Methane viscosity vs. pressure at 360 ^{o}F (Test 36)

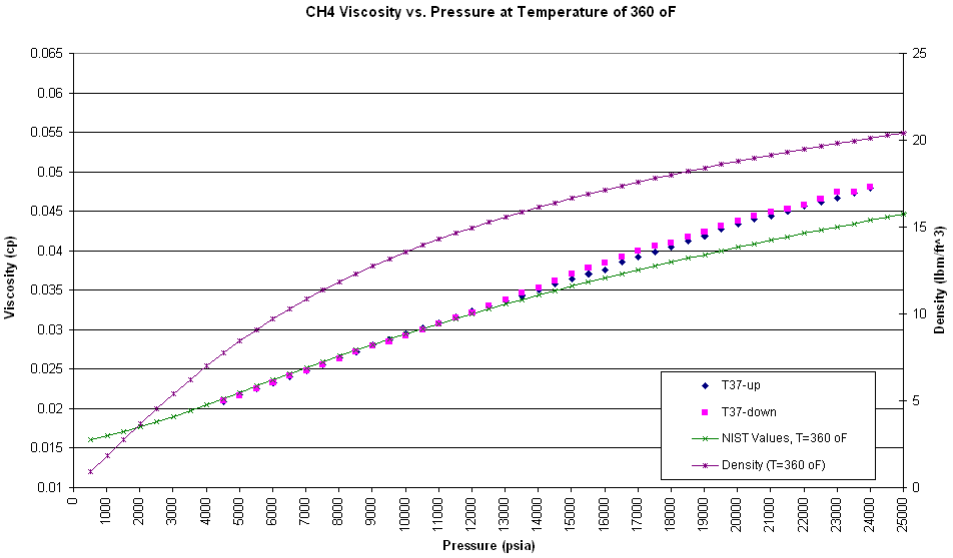

Figure B - 33. Methane viscosity vs. pressure at 360 ^{o}F (Test 37)

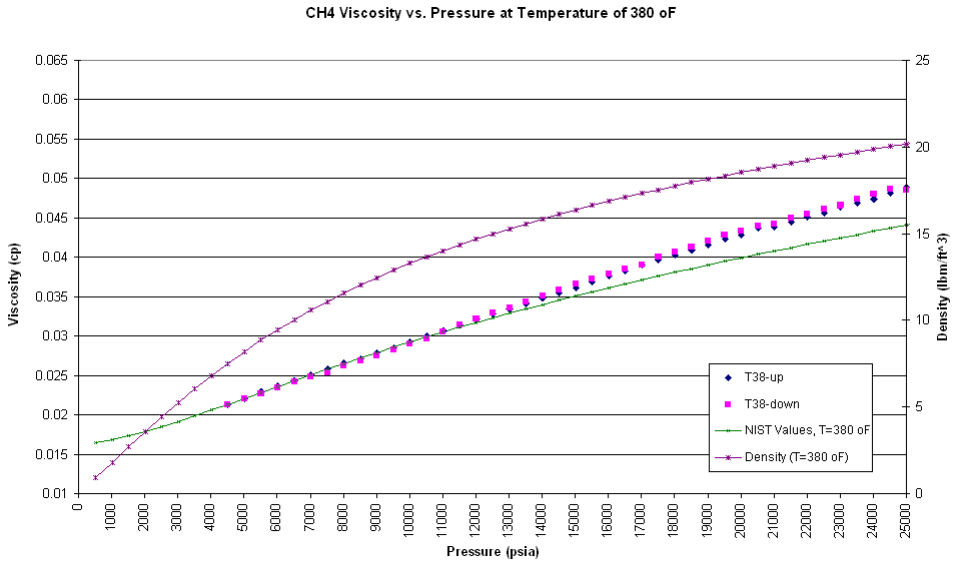

Figure B - 34. Methane viscosity vs. pressure at 380 ^{o}F (Test 38)

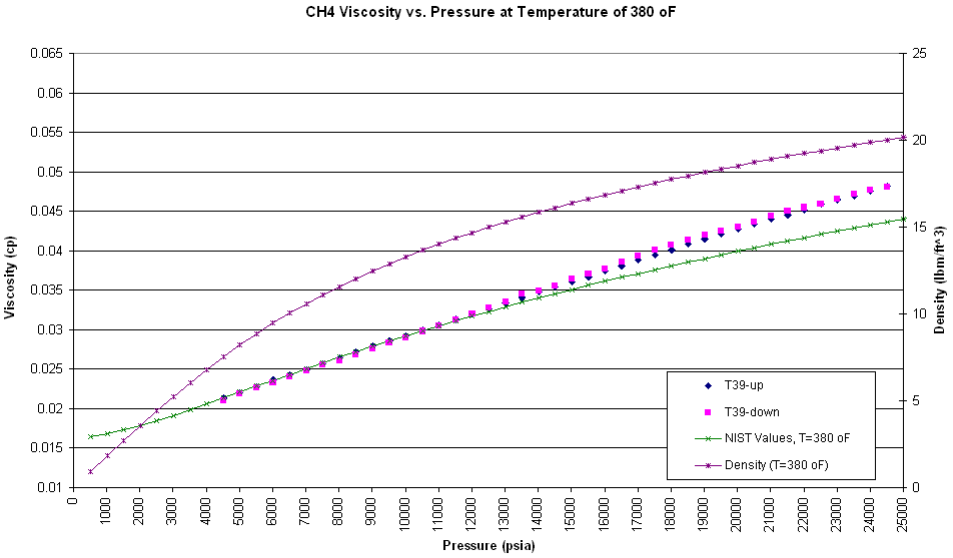

Figure B - 35. Methane viscosity vs. pressure at 380 ^{o}F (Test 39)

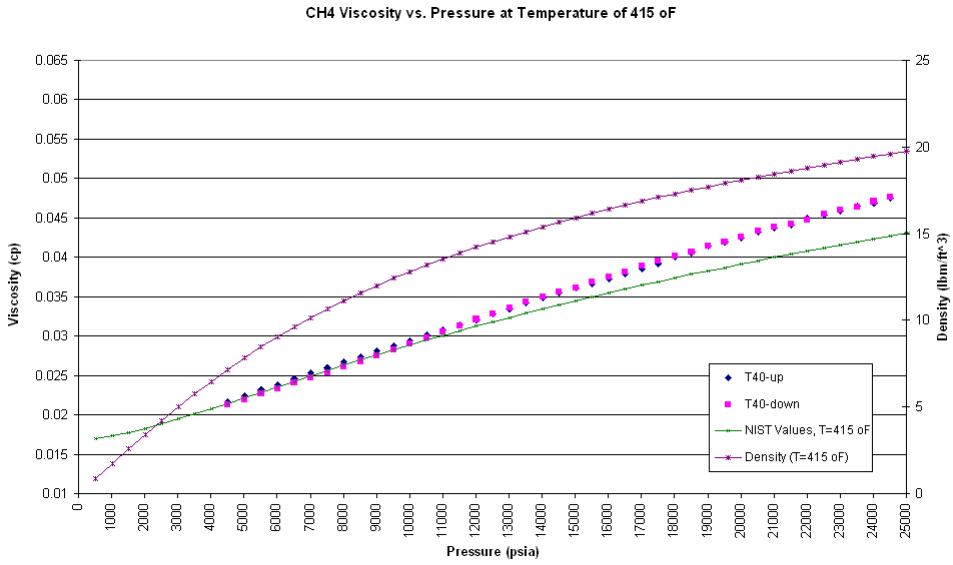

Figure B - 36. Methane viscosity vs. pressure at 415 ^{o}F (Test 40)

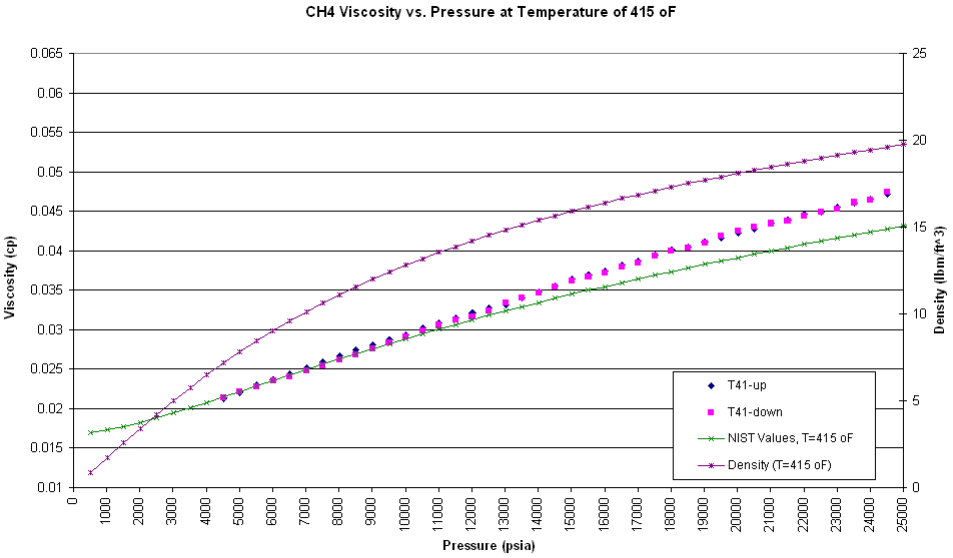

Figure B - 37. Methane viscosity vs. pressure at 415 ^{o}F (Test 41)

VITA

Name: Kegang Ling

Contact Information: Department of Petroleum Engineering
Texas A&M University
3116 TAMU Richardson Building
College Station, TX 77843-3116

Email Address: kegangling@yahoo.com

Education: M.S., Petroleum Engineering, University of Louisiana at Lafayette, 2006

B.S., Geology, China Petroleum University, 1995

Professional Affiliation: Society of Petroleum Engineers, Member